

Assessing the Efficacy of Magnetic Susceptibility as an Archaeological Characterization Tool within a Canadian Subarctic Context

By

James Steinberg

A thesis submitted in partial fulfilment of the requirements for the degree of
Masters of Archaeological Science

Department of Anthropology

Lakehead University

©James Steinberg 2024

Permission is hereby granted to the Lakehead University Library to reproduce single copies of this thesis and to lend or sell such copies for private, scholarly or scientific research purposes only. Where the thesis is converted to, or otherwise made available in digital form, Lakehead University will advise potential users of the thesis of these terms.

The author reserves all other publication and other rights in association with the copyright in the thesis and, except as herein before provided, neither the thesis nor any substantial portion thereof may be printed or otherwise reproduced in any material form whatsoever without the author's prior written permission.

Abstract

This thesis addresses experimental investigation of magnetic susceptibility and the utility of the Terraplus KT-10 magnetic susceptibility meter to characterize subarctic archaeological deposits. The Hogarth Tree Farm, outside of Thunder Bay, Ontario, was chosen as an experimental locale due to its relatively undisturbed and remote context. A grid was established, and preliminary test excavation done to assess the sediments and context. Using experimental firing events designed to reproduce the firing activities of precontact subarctic Indigenous people, natural sediments were heated, and the temperatures and fire duration were recorded. This sought to reveal how firing affected the sediment's magnetic susceptibility and whether its detection might have utility in documenting and interpreting what are often 'invisible' archaeological features.

This thesis addressed four research questions: 1) Did the experimental firing events enhance the magnetic susceptibility; 2) What was the minimum temperature needed to change the magnetic susceptibility signature of the natural soil/sediment; 3) What level of interpretation could be made from the magnetic susceptibility data; and 4) How effectively did the Terraplus KT-10 detect this change? Through my experiments, I found that the firing experiments performed were able to enhance the magnetic susceptibility of the sediments.

This study has research implications for archaeological investigations throughout much of the Canadian subarctic. Due to the generally acidic nature of boreal forest sediments, organic archaeological evidence is frequently destroyed over time, including bones, shells, charcoal and ash. The latter two types of evidence are generally important for identifying hearth/firing features during archaeological investigations, making them difficult to identify in the subarctic. Heating the sediments has demonstrated the ability to enhance the magnetic properties, including magnetic susceptibility, due to increased temperature triggering a reaction between different iron oxides (Dearing, 1999; Hodgetts, 2016; Schmidt, 2007, 2009; Tite, 1972; Tite and Mullins, 1971; Witten, 2014). With this chemical change occurring on the molecular level, these changes should be unaffected by the acidic soils. Further, the difficulties performing archaeological investigations within the subarctic mean requires that much of the geophysical

equipment used should be portable, require comparatively little electricity and robust enough to withstand field conditions. The Terraplus KT-10 magnetic susceptibility meter is a handheld device which may prove conducive for archaeogeophysical characterization since it generates immediate results when placed directly on the sedimentary surface. While the environmental and logistic realities of subarctic archaeological investigations confound some archaeological site prospection techniques, magnetic susceptibility has demonstrated potential to amplify archaeological insight when used concurrently with conventional archaeological methods.

Acknowledgements

I would like to express my gratitude to my supervisor, Dr. Scott Hamilton (Department of Anthropology, Lakehead University, Thunder Bay). His connections, the equipment and willingness to help throughout the experiment were essential for completing this program. His guidance throughout my university career set me on a path for success, both during and after the completion of my studies. His teachings in ethics, methodologies, and the passion for the value added when performing consulting archaeology have set me up for career in the industry.

I would like to thank the other members of my internal committee Dr. David Norris (Woodland Heritage Northwest, Adjunct Professor, Lakehead University, Thunder Bay) and Dr. Jill Taylor-Hollings (Research Associate, Lakehead University, Thunder Bay). Their mentorship, edits and comments have been appreciated throughout my archaeological career and continually make me a better archaeologist. I would also like to thank my external examiner, Dr. Krista Gilliland (Office Manager, Western Heritage, St. Albert) for her timely feedback on this experiment summary.

Additionally, I would like to thank Dr. Matt Boyd (Anthropology, Lakehead University, Thunder Bay). He provided the Terraplus KT-10 susceptibility meter central to performing the described experiments.

I would like to thank the Lakehead University Faculty of Natural Resource Management for allowing me to experiment on their Hogarth Tree Farm property. Their willingness to allow the firing experiment was essential for undertaking my experiments.

Thank you to Clarence Surette, Chris McEvoy, Dr. Taylor-Hollings and the Lakehead University Anthropology Association for their help with the pottery firing experiments as well as providing the vessels for firing.

I appreciate, acknowledge and am thankful for the financial support received from the MITACs research group.

I would like to thank my family, specifically my Mom and Dad, for encouraging me and helping me with the experiments whenever and however they could.

Lastly, I would like to express my gratitude towards my friends/unofficial editors, Jason Stephenson and Jackie Cannon-Wilvert, both of whom were integral to the completion of this project.

Table of Contents

Abstract	ii	
Acknowledgements	iv	
Table of Contents	vi	
List of Figures.....	ix	
List of Tables	xii	
Chapter 1	Introduction.....	1
1.1	Research Questions	3
1.2	Goals and Limitations	3
1.3	Methods.....	4
1.4	Study Location	4
1.5	Thesis Organization	6
Chapter 2	Geographical and Archaeological Background	8
2.1	Introduction	8
2.2	Geographic Conditions	8
2.2.1	The Landscape	8
2.2.2	Environmental Background	11
2.3	Archaeology of the Subarctic Region.....	14
2.3.1	Paleo-Period	14
2.3.2	The Shield Archaic/Middle Period	15
2.3.3	The Woodland Period	15
2.3.4	Post contact Period.....	18
2.3.5	Performing Archaeological Surveys in the Subarctic	19
2.4	Summary.....	19

Chapter 3	Archaeogeophysics	21
3.1	Archaeogeophysics Defined	21
3.2	Ground Penetrating Radar	22
3.3	Electrical Methods	24
3.3.1	Electrical Resistivity	24
3.3.2	Electromagnetic Induction.....	26
3.4	Magnetism	28
3.5	Magnetic Susceptibility.....	33
3.6	Statistics.....	36
3.7	Site Prospection vs Site Characterization	38
3.8	Summary.....	39
Chapter 4	Experiment Details.....	40
4.1	Introduction	40
4.2	Details about the Study Location.....	40
4.3	Purpose of Experiments.....	48
4.4	Equipment and Methods	48
4.4.1	Safety Measures and Equipment.....	49
4.4.2	Firing Experiments	50
4.5	Magnetic Susceptibility Data Collection	55
4.6	Summary.....	56
Chapter 5	Results	57
5.1	Firing Times.....	57
5.2	Temperature.....	57
5.3	Magnetic Susceptibility.....	62

5.3.1	Baseline.....	63
5.3.2	Experiment Data	66
5.4	Summary.....	70
Chapter 6	Discussion	72
6.1	Introduction	72
6.2	Did the experiments enhance the magnetic susceptibility of the sediments? .	72
6.3	What was the minimum firing intensity needed to change the magnetic susceptibility within the sedimentary matrix?.....	74
6.4	What level of interpretation could be made from the magnetic susceptibility data?	76
6.5	How effectively did the Terraplug KT-10 detect this change?	81
6.6	Temperature, and Magnetic Susceptibility.....	82
6.7	Limitations	82
6.8	Summary.....	85
Chapter 7	Conclusion	87
Chapter 8	References Cited.....	91
Appendices		96
	Appendix A: Temperature Data.....	96
	Appendix B: Magnetic Susceptibility Data.....	108

List of Figures

Figure 1.1 Location of Hogarth Tree Farm (H) relative to Thunder Bay, Ontario, Canada.	6
Figure 2.1 The northern regions of Ontario (taken from Hamilton 2013:78).....	9
Figure 2.2 Glacial Lakes Agassiz and Minong highlighting the various complexes associated with early peopling of Northwestern Ontario according to Ross (1995) (taken from Hamilton, 2013:85).	13
Figure 2.3 Evidence of selected Middle Woodland archaeological cultures, highlighting the huge expanse of Laurel composite sites and the diversification of pottery vessel types during the Middle Woodland (taken from Hamilton, 2013:90).	17
Figure 4.1 Location of Hogarth Tree Farm (H) relative to Thunder Bay, Ontario, Canada.	41
Figure 4.2 Zoomed in view of Hogarth Tree Farm location circa 2023. H denotes the gate used to enter the property. Grid location overlaid with grid.....	42
Figure 4.3 Study area conditions with the established grid area from the Southwestern corner of the grid. Corner closest to the camera is the 0N, 0E post facing Northeast.	43
Figure 4.4 Hogarth Tree Farm study area conditions, circa 2020, facing North. Water trough to extinguish fires.	44
Figure 4.5 This is the test pit excavated at -1N, 4E and facing North.	45
Figure 4.6 Test pit photo -1N, 4E plan view.....	46
Figure 4.7 Test pit sketch map and soil descriptions from fieldwork.	47
Figure 4.8 Thermocouple probes and thermometer in use during a long-term firing experiment.	51
Figure 4.9 Type and number of experiments performed at each location.....	53
Figure 4.10 Temperature requirements for pottery firing with resulting porosity (taken from Rice, 1987:5).....	54
Figure 4.11 Baseline magnetic susceptibility data collection locations for this study.....	55
Figure 5.1 Results of May 18th, 2021, with a one-hour firing event plus the associated cooldown.....	59
Figure 5.2 May 29, 2021, temperature results of one hour firing event, plus associated cooldown.....	60

Figure 5.3 September 16th, 2021, temperature data for one hour firing event plus associated cooldown.....	61
Figure 5.4 The Oct 25, 2021 temperature data of a five plus hour firing event plus associated cooldown.....	62
Figure 5.5 Frequency distribution of baseline magnetic susceptibility data. Bins are 0.0005k in size, starting at 0.0022k to 0.0107k. This data was collected throughout the experimental timeline.	64
Figure 5.6 Baseline magnetic susceptibility within a bell curve distribution. Each point on the graph is 1.0 baseline data point (collected throughout the experimental timeline).....	65
Figure 5.7 Baseline magnetic susceptibility data, taken from experimental fire pits, collected prior to the first experiment conducted within each location. Yellow and red measurements represent areas where the datapoint was one standard deviation above the mean or higher in value.	66
Figure 5.8 Fired magnetic susceptibility frequency distribution. Bins are sized 0.0005k from 0.0022k to 0.0107k. Collected throughout the experimental timeline.	68
Figure 5.9 Experimental fire magnetic susceptibility data collected from the experimental firing grid, throughout the full duration of the experiments.....	69
Figure 5.10 Magnetic susceptibility data taken from experimental fire pits collected on November 9 th , 2021. This data was collected after all firing experiments were completed. Yellow and red measurements represent areas where the datapoint was one standard deviation above the mean of higher in value.....	70
Figure 6.1 Frequency distributions for the baseline and fired magnetic susceptibility data collected throughout the experiment’s duration. Figures 5.5 and 5.8 were combined to place in the same bins for comparison. Bins are 0.0005k in size, between 0.0022k and 0.0107k.	73
Figure 6.2 Short-term vs long-term vs baseline magnetic susceptibility data frequency distribution.	75
Figure 6.3 Pre-firing experiment baseline data collection throughout the experimental timeline, within grid only. Yellow and red measurements represent areas where the datapoint was one standard deviation above the mean or higher in value.....	78

Figure 6.4 Last magnetic susceptibility data collection for this experiment, after last firing experiment performed days previously. Yellow and red measurements represent areas where the datapoint was one standard deviation above the mean or higher in value.79

Figure 6.5 Difference between initial, pre-experiment magnetic susceptibility and post-experiment measurements taken on November 9th, 2021.80

List of Tables

Table 5.1 Collected Magnetic Susceptibility Data	67
Table 6.1 P-Values comparing different magnetic susceptibility datasets. P value of 0.05 or less means the null hypothesis can be rejected.....	76

Chapter 1 Introduction

Due to the finite and fragile nature of archaeological resources, many archaeologists have shifted to less destructive investigative methods. This includes collection of information that is generally invisible using conventional excavation methods. Technological advances have facilitated application of non-invasive remote sensing techniques developed in other disciplines. This involves borrowing and redesigning methods to address archaeological situations, allowing insight through different informational filters (Campana, 2009; Clark, 2001; Dearing, 1999; Hodgetts et al., 2016; Kvamme, 2017; Liu et al., 2012; Oswin, 2009; Witten, 2014). Performing remote sensing surveys prior to conventional archaeological excavation supports more effective site prospection, contributes to stratified sampling designs, and generates data that is often overlooked (or even invisible) using traditional methods. These methods can also provide contextual information about both anthropogenic activities and environmental events in archaeological situations (Costa et al., 2022; Gibson, 1986; Hodgetts et al., 2016; Kvamme, 2017; Liu et al., 2012; Oswin, 2009; Rogers, 2011; Šindelář et al., 2021; Witten, 2014). Among these remote sensing methods are some that involve near-surface geophysical techniques.

Using near-surface geophysics in an archaeological context involves the identification of localities that exhibit characteristics that are anomalous from the earth's naturally occurring physical properties. These localized anomalous values may derive from anthropogenic modification, thereby enabling non-invasive archaeological site characterization that can be validated by strategic sampling to generate more representative excavation sampling (Costa et al., 2022; Dearing, 1999; Gibson, 1986; Hodgetts et al., 2016; Kvamme, 2017; Liu et al., 2012; Oswin, 2009; Piro, 2009; Rogers, 2011; Sala et al., 2012; Šindelář et al., 2021; Witten, 2014). This allows archaeologists to maximize the potential information recovery, much of which might not be readily detectable using conventional methods.

Geophysical remote sensing techniques have repeatedly demonstrated value in documenting archaeological features and environmental changes within the soil/sediments before or during archaeological excavations (Crowther & Barker, 1995; Dalan & Banerjee, 1998;

Dalan 2007; Dearing, 1999; Gaffney et al., 2002; Gibson, 1986; Hodgetts et al., 2016; Kvamme, 2001, 2003, 2017; Oswin, 2009; Rogers, 2011; Sala et al., 2012; Šindelář et al., 2021; Witten, 2014). These methods include ground penetrating radar (GPR), electrical resistivity and conductivity, magnetism and magnetic susceptibility (see Chapter 3 for an overview of these methods). After reviewing these methods, I chose to test magnetic susceptibility due to its ability to detect thermo-altered soils, and in consideration of the portability and ease of use of the available device. Only limited research has been conducted regarding the use of magnetic susceptibility within the boreal forest of central Canada. This research aims to determine if magnetic susceptibility is a viable tool within the environmental context and evaluate its efficacy for archaeological investigations.

Magnetic susceptibility is defined as an object's ability to accept magnetic enhancement. In the case of archaeological investigations, the soils and sediments associated with human occupation are of interest (Clark, 2001; Costa et al., 2022; Dalan, 2007; Dearing, 1999; Hodgetts et al., 2016; Liu et al., 2012; Rennie, 2019; Schmidt 2007, 2009; Šindelář et al., 2021; Tite & Mullins, 1971; Witten, 2014). This thesis evaluates magnetic susceptibility as a tool for archaeological remote sensing within a central Canadian subarctic context. It was not clear from a literature review as to how the subarctic soils would respond to magnetic enhancement, as there has been no research conducted to date. However, in other regions of the world, magnetic susceptibility is more common and has been used since the 1950s (Clark, 2001; Costa et al., 2022; Dalan, 2007; Dearing, 1999; Hodgetts et al., 2016; Liu et al., 2012; Šindelář et al., 2021; Tite, 1972; Tite & Mullins, 1971). Magnetic susceptibility survey has repeatedly demonstrated the capacity to detect hearths and other fire related archaeological features, organic decay within middens, and past shorelines (Clark, 2001; Dearing, 1999; Hodgetts et al., 2016; Schmidt, 2007, 2009; Šindelář et al., 2021; Tite, 1972; Tite & Mullins, 1971). Thus, this thesis specifically considered the use of magnetic susceptibility for archaeological investigation in Northwestern Ontario by first conducting controlled firing events under different conditions, then addressing when magnetic transformation occurred, the intensity of transformation, and whether a specific instrument could identify these transformations. It also became clear that

temperature recordings of firing events would be required to help determine how and when those changes occurred.

1.1 Research Questions

My main research questions derive from an opportunity to examine how magnetic susceptibility can be measured in subarctic contexts, and to contribute to the literature addressing its utility in other archaeological contexts (Clark, 2001; Hodgetts et al., 2016; Schmidt, 2007, 2009; Tite, 1972; Tite & Mullins, 1971). The project plan specifically addressed the following research questions:

- 1) Did the experimental firing events enhance the magnetic susceptibility?
- 2) What was the minimum temperature needed to change the magnetic susceptibility signature of the natural soil/sediment?
- 3) What level of interpretation can be made from the magnetic susceptibility data?
- 4) How effectively did the Terraplus KT-10 detect this change?

Using the experiments performed and summarized here, these four questions will be addressed in more detail in later sections of this thesis, as outlined in section 1.5.

1.2 Goals and Limitations

My primary research goals required testing whether the Terraplus KT-10 magnetic susceptibility meter (Terraplus, 2019) had archaeological utility in detecting generally overlooked features within a central Canadian subarctic context. This involved evaluation of the method (and the device) under controlled conditions. This simultaneously tested the assumption that subarctic soils behave similarly to those in other regions when heated in a hearth.

A series of controlled experiments were conducted to emulate pre-contact firing events to evaluate the effectiveness of the Terraplus KT-10 (Terraplus, 2019) in detecting simulated archaeological hearths, and the susceptibility response of the soil. I have also investigated the

surface and subsurface conditions of my study location to determine how that might affect the experiments and to ensure that I am not impacting an existing archaeological site.

The limitations encountered during this experiment were of three varieties; safety (injury potential, COVID-19 and equipment), weather (experiments fully weather dependant), and equipment (reset when batteries expired, limited measurement depth capability). Other limitations related to potential flaws in research design will be discussed in Chapter 6.

1.3 Methods

The instrument used for this research was the Terraplus KT-10 magnetic susceptibility meter (Terraplus, 2019). It is a handheld device that is capable of measuring, recording, and storing both volume-specific and mass-specific magnetic susceptibility measurements (Terraplus, 2019). While not as frequently used as other magnetic susceptibility equipment, the size and portability of the Terraplus KT-10 magnetic susceptibility meter (Terraplus, 2019) was deemed attractive for archaeological surveys conducted in remote geographical regions. These practical considerations were important given the portability and comparative low cost of equipment, the evaluative nature of most archaeological investigation in the region, and because of the leaching generally associated with subarctic podzolic soils.

To test the Terraplus KT-10 magnetic susceptibility meter (Terraplus, 2019), I established a control grid on a location near the City of Thunder Bay, Ontario with sediments that derive from glaciolacustrine subarctic conditions. I excavated two test pits to observe the sediment nature before undertaking my experiments. I then created eight experimental fire pits to simulate assumed expectations of Indigenous peoples' firepits. These hearths were then used to contain fires of different durations and intensity, with both magnetic susceptibility and temperature readings being collected. Further elaboration about the methods used can be found in Chapter 2.

1.4 Study Location

Central Canada's subarctic region is a large geographic area with considerable ecological and physiographic diversity, and a rich archaeological record that remains sparsely explored. It is characterized by conditions that range from low-lying water-saturated landscapes to heavily

eroded bedrock terrain, all of which are difficult to traverse and survey. The continental climate supports a conifer-dominated biome, that contributes to heavily leached acidic soils that often destroy most organic archaeological materials except limited amounts of carbonized residues and some dense bone fragments, or those preserved by permafrost conditions. This results in a narrower range of archaeological recoveries than some other areas with many anthropogenic features (i.e., hearths, storage features, refuse middens, etc.) being leached to the point that they are difficult to visually detect. While the geochemical remnants of such features might be detected through geophysical prospection methods, the vegetation cover and regional logistical challenges make it difficult to deploy the equipment.

The thesis study location is within the Hogarth Tree Farm, a semi-rural property approximately 13.8 kilometers southwest of the city center of Thunder Bay, Ontario, Canada (Figure 1.1). This location offered an undisturbed place where firing experiments could be done without safety concerns (i.e., starting a forest fire), and where the public would not interfere with the experiments or location. No known archaeological sites were reported or known to be there, with my preliminary test unit excavations revealing no material culture. This testing also enabled documentation of the general nature of the sediments (see Chapter 4 for a discussion about the results).

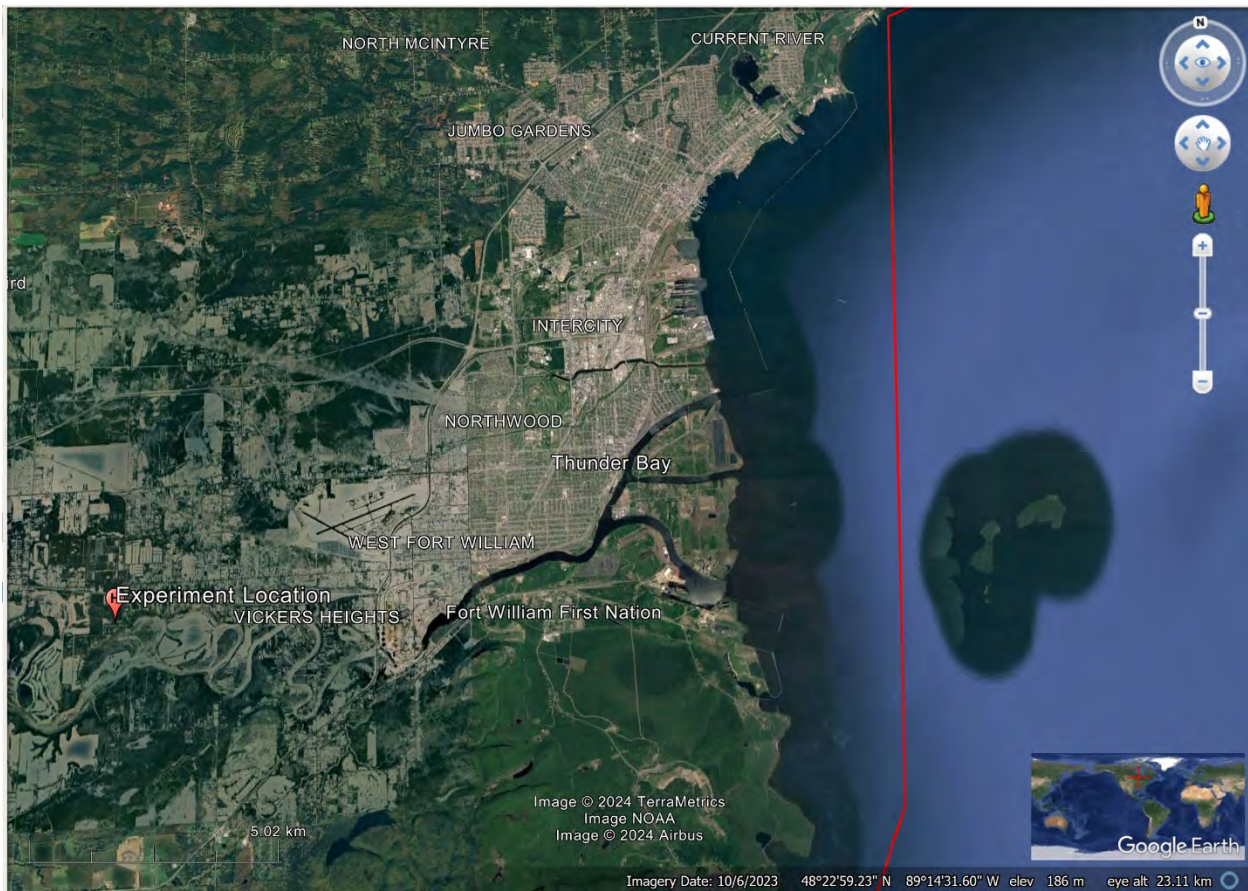


Figure 1.1 Location of Hogarth Tree Farm (H) relative to Thunder Bay, Ontario, Canada.

1.5 Thesis Organization

Following this introductory chapter, Chapter 2 offers the geographical, environmental, and archaeological culture history of the Thunder Bay region. This includes discussions about the difficulties often associated with archaeological investigation in the central Canadian subarctic and how geophysical surveys might serve to amplify this information. Chapter 3 describes archaeogeophysical method and theory, and the equipment frequently used to measure geophysical properties relevant for archaeological characterization. This includes examples of geophysical properties that have archaeological relevance, and how geophysical methodologies might be challenging within a central Canadian subarctic context. Other methods are described to clarify why I chose magnetic susceptibility for my study. The parameters, equipment and methods used during my experiments are described in Chapter 4. Chapter 5 presents the data that was collected during my experiments along with its statistical

characteristics. This will include temperature and magnetic susceptibility dataset summaries. Chapter 6 presents interpretations of the results, as well as their contribution to answering the questions posed. It also discusses the limitations of the experiment. Lastly, Chapter 7 presents the conclusions and recommendations for this thesis.

Chapter 2 Geographical and Archaeological Background

2.1 Introduction

The central Canadian subarctic is geographically massive, typically densely vegetated, and relatively sparsely populated. It is environmentally diverse with an intense Continental climate and a comparatively short frost-free season. Limited archaeological research has been conducted there because it is often difficult and expensive to access. However, archaeological evidence demonstrates that Indigenous populations have effectively occupied the landscape since the early Holocene (Boyd et al., 2012; Dawson, 1983; Hamilton, 2013; Norris, 2012, 2022; Taylor-Hollings, 2017; Winterhalder, 1983; Wright, 1972, 1995). This chapter reviews Northwestern Ontario's subarctic area, specifically the conditions that affect archaeological investigations and ultimately my experiments in that area.

2.2 Geographic Conditions

Archaeological investigations in subarctic Northwestern Ontario are conditioned by a series of interrelated factors that include its physical and ecological nature, its Quaternary geological history, the intensely seasonal climate, and the nature of human history within the area. Most of the 10,000-year human history of this region involved only Indigenous cultures inhabiting this area (Dawson, 1983; Gibson, 2017; Hamilton, 2013; Norris, 2022; Taylor-Hollings, 2017; Wright, 1995).

2.2.1 The Landscape

Ontario's subarctic landscape is physiologically diverse and dominated by the bedrock of the Canadian Shield and the flat Hudson Bay Lowlands to the North (Hamilton, 2013) (Figure 2.1). The Canadian Shield contains some of the oldest rock on earth, dating to almost two billion years ago (e.g., Hollings et al., 2010). This bedrock consists of ancient mountain belts worn down by millions of years of erosion. The Hudson Bay Lowlands encompass low-lying Paleozoic era bedrock mantled with till deposits and post-glacial marine sediment, much of which are still water saturated. Although the lowlands are located far from the Thunder Bay area, they do figure strongly in the lithic raw materials found in glacial till deposited there (e.g., Hudson Bay Lowland chert).

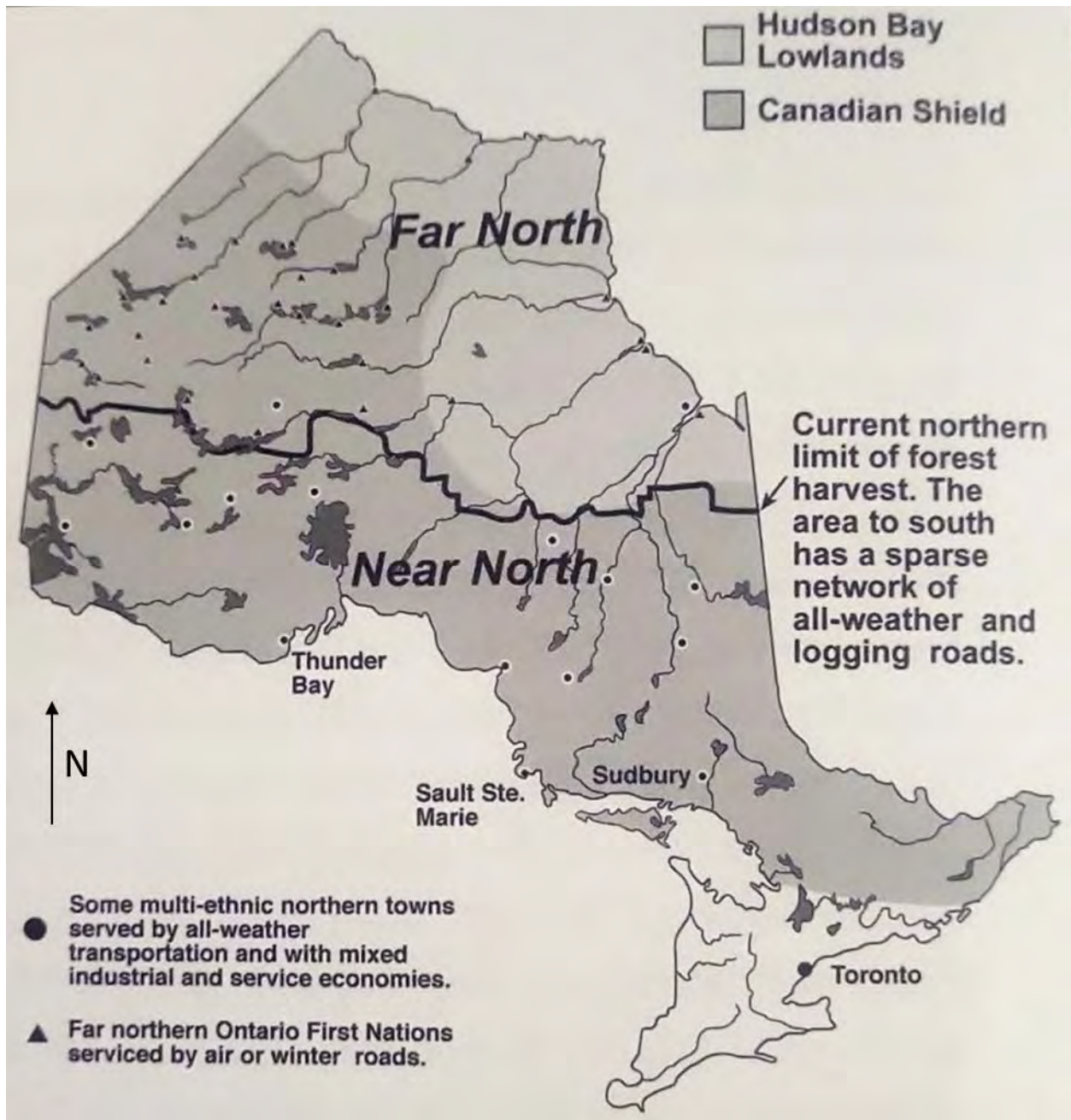


Figure 2.1 The northern regions of Ontario (taken from Hamilton 2013:78).

Landscapes in Northwestern Ontario are mantled with complex water systems and extensive forests, with the more southerly area overlaid with predominately coniferous forest with some deciduous trees. The far north consists extensive fens and muskeg that grade from taiga to a narrow northern fringe of tundra along the coast of Hudson and James Bays

(Hamilton, 2013). This area has been extensively modified by both Pleistocene glaciation and Holocene deglaciation processes. The most important modern consideration here is glacial scouring of bedrock uplands and lowland accumulation of ground moraine or glacio-fluvial and glacio-lacustrine sediments. This results in considerable natural sedimentological variability that might impact the testing of magnetic susceptibility/geophysical methods. That is, it might be difficult to differentiate the consequences of anthropogenic modification in the context of natural variability found within such sediments. To this end, I deliberately selected a test area with comparatively uniform sediments that were laid down through glacio-lacustrine processes, which will be addressed in more detail below.

Vegetation within Northwestern Ontario is dictated by the topography, minimal soil development and drainage/hydrology of the region (Gibson, 2017; Hamilton, 2013; Norris, 2022; Taylor-Hollings, 2017; Winterhalder, 1983). On exposed bedrock plateaus, moss, balsam fir, and jack pine dominate the drier uplands of this area. The saturated bogs, swamps and valleys of the region provide diverse habitats for species such as black spruce, poplars, birch, lichen, sedges, and Labrador tea (Winterhalder, 1983). These diverse landscapes and vegetation communities result in mixed upland forests or wetlands observed through exploratory surveys and aerial imagery. Further complexity derives from the subarctic climate and weather patterns that result in extreme high and low annual temperatures, precipitation and extreme weather-related events. Also important are forest fires and other forest damage from wind and insect infestation (Hinshelwood, 1996; Winterhalder, 1983). This vegetative diversity supports a wide variety of terrestrial and aquatic herbivores and carnivores, plus a range of insect, fish and bird species (Hamilton, 2013; Winterhalder, 1983).

In large measure because of the coniferous forest cover, subarctic sediments can be quite acidic, resulting in rapid degradation of organic matter, and severe leaching down the soil profile (Hamilton, 2013; Hinshelwood, 1996). This results in the destruction of most organic archaeological evidence, particularly in the chemically active upper parts of the soil profile. Further complicating the environmental picture, forest fires regularly occur, enabling vegetative regeneration at a lower trophic level that sustains denser and more diverse plant and animal

life. This combination of destruction and renewal can significantly affect the underlying soils and archaeological deposition within them (Hinshelwood, 1996).

Further complicating the environmental landscape are modern resource extraction activities that include mining, forestry, fishing, agriculture and renewable energy production that have permanently altered some of the landscape. Also, road building and herbicide spraying have also affected the original landscapes in Northwestern Ontario. Despite these impediments, many Indigenous peoples in Northwestern Ontario continue to hunt, trap, and gather plants, both using traditional and more modern methods (Taylor-Hollings, 2017).

The Ontario subarctic area is massive, measuring approximately 900,000 square kilometers and representing over 80% of the province's landmass, but with only a relatively small percent of the population (Woodrow, 2002). Much of this area is accessible only by air or winter ice roads, with limited all-weather infrastructure. A sparse population density and sometimes limited economic development profoundly impacts both the nature and intensity of archaeological investigation, resulting in little more than a cursory understanding of the nature and timing of human occupations. Also, the patterned distribution of archaeological sites across this diverse landscape is not well understood (Hamilton, 2000). In part, this reflects a void deriving from limited research addressing the 10,000 year-long human history in Northwestern Ontario.

2.2.2 Environmental Background

The defining characteristic of subarctic Indigenous occupation involves millennia of dynamic adaptation to frequently changing climatic, topographic, physiographic, hydrological, and vegetative conditions. Further complexity derives from seasonality, localized sediment and moisture conditions and ecological succession, all of which contributes to distinctive lifestyles throughout the subarctic region. Clearly, Indigenous peoples have been highly successfully adapting for many millennia to these everchanging conditions in the boreal forest.

During much of the Pleistocene epoch, the subarctic region was covered by the Laurentide Ice Sheet (Figure 2.2) that contained vast quantities of ice and clasts, which ranged from boulders to tiny pieces ground down to clay sized particles. Upon deglaciation, beginning

approximately 14,000 yBP, rock material of all sizes including sand, silt and clay were gradually released from the ice and deposited or transported by glacial meltwater (Boyd et al., 2012). This resulted in complex sedimentary situations with mixed till deposits interspaced with water-sorted fine sediments (both alluvial and lacustrine) and with some wind-blown loess deposition (Loope, 2006). With deglaciation, glacial meltwater lakes of various sizes formed in lower-lying areas. These meltwater accumulations could be quite transitory and are largely undocumented throughout the subarctic, with only the largest and most being well known (i.e. Glacial Lakes Minong and Agassiz) (Boyd et al., 2012; Hamilton, 2013; Loope, 2006). As these lakes developed, transformed, and eventually drained into the ocean, they significantly impacted ocean levels, temperature gradients, biological capacity and salinity, all of which had global-scale climatic and environmental implications. One such post-glacial period of warmer and drier conditions is called the Hypsithermal (Boyd et al., 2012; Loope, 2006). During this time, hydrological systems were significantly transformed, particularly when coupled with ongoing isostatic uplift that dramatically transformed drainage gradients and continues to affect the Hudson Bay Lowlands (Loope, 2006). These complicated processes are incompletely understood, so their full impacts upon the ecological system and to human occupation in Northwestern Ontario are not fully documented. These transformations continued throughout the Holocene with a series of less dramatic climatic events through to present day climate change (Boyd et al., 2012; Hamilton, 2013; Loope, 2006). Sedimentary conditions in the boreal forest are constantly transforming due to intense seasonality and chronic vegetative disturbance through fire, snow, wind damage and disease. This all contributes to complex archaeological site formation processes within the Ontario subarctic area (Hamilton, 2013; Hinshelwood, 1996).

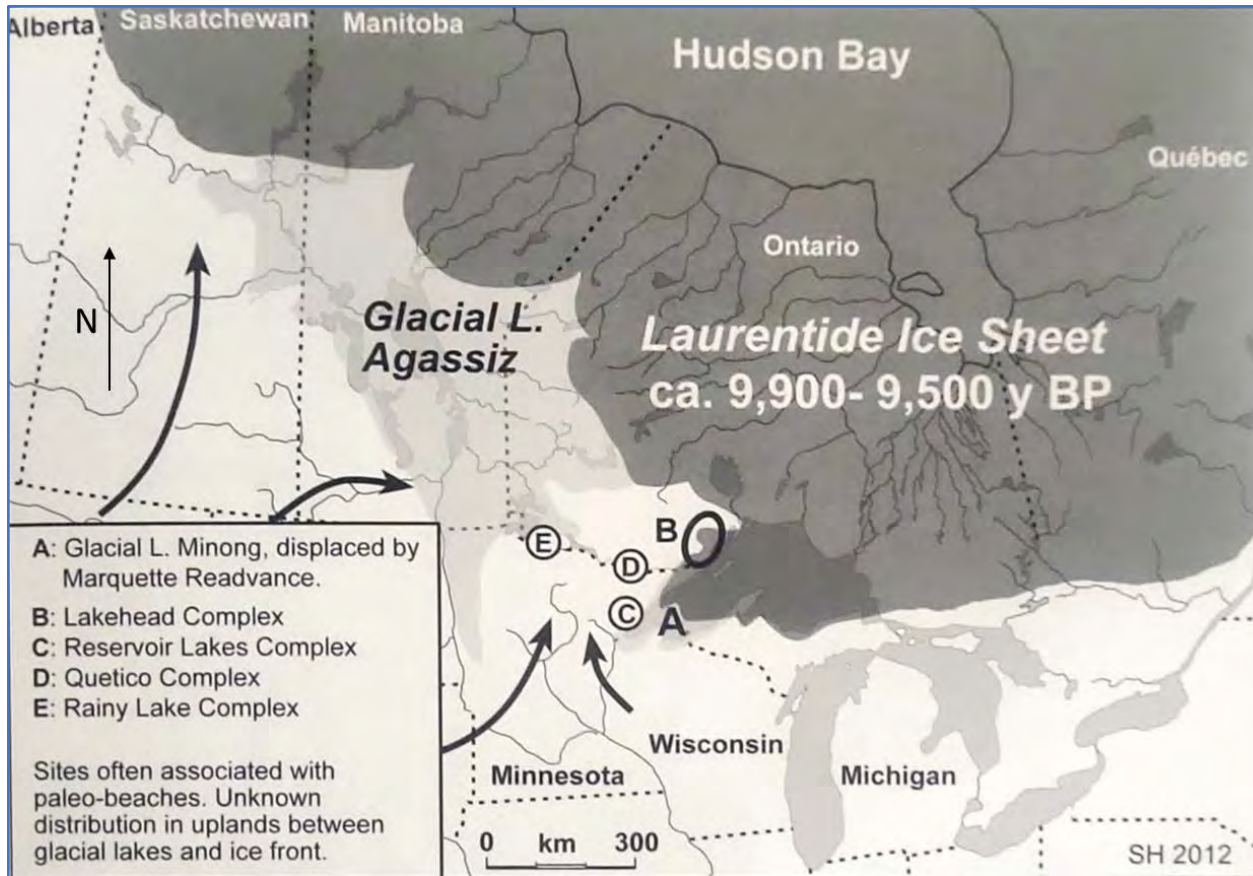


Figure 2.2 Glacial Lakes Agassiz and Minong highlighting the various complexes associated with early peopling of Northwestern Ontario according to Ross (1995) (taken from Hamilton, 2013:85).

By adapting to seasonal resource availability, nomadic subarctic Indigenous populations are thought to have had a strong orientation towards shorelines but also harvested inland zones. This likely resulted in many repeatedly used habitation sites being established along previous and modern waterways. This assumption profoundly affects archaeological perceptions of past settlement patterns and how archaeologists focus their efforts (Dawson, 1983; Hamilton, 2013; Wright, 1972, 1995). Little organic material dating from the Early/Paleo period is evident, likely due to acidic soil conditions. Using ethnographic analogies of Northwestern Ontario Indigenous people, it is assumed that large ungulates such as moose and caribou were numerous and highly valued food sources, seasonally supplemented with smaller mammals, fish, migratory waterfowl and edible plants. Such subsistence flexibility was structured around seasonal cycles of abundance, and it also enabled people to readily cope

with periodic scarcities (Winterhalder, 1983). Variations on this seasonal foraging system persisted throughout the Holocene epoch as people adapted to changing environmental conditions. The increased density of archaeological sites dating to the late Holocene is thought to indicate growth in human population levels, with people developing new procurement technologies. High mobility and seasonal strategies of population aggregation and dispersal enabled long term habitation of the subarctic (Dawson, 1983; Hamilton, 2013; Wright, 1995).

2.3 Archaeology of the Subarctic Region

The peopling of subarctic Ontario likely occurred within a few hundred years following deglaciation and biological recovery. This process of deglaciation is time-transgressive (south to north), with some regions becoming deglaciated as early as ca. 12,000 yBP, but for much of northern Ontario, this likely occurred between about 10,000 and 7,000 years ago (Dawson, 1983; Gibson, 2017; Hamilton, 2013; Norris, 2022; Taylor-Hollings, 2017; Wright, 1995). Temporal estimates offered here represent uncalibrated dates (yBP) unless specifically referenced as radiocarbon calibrated dates (cal yBP). Details about ancient Indigenous people are relatively unknown, but likely reflect a succession of hunter-gatherer cultures that are archaeologically defined by distinctive technologies. This sequence of cultural adaptations is briefly described to contextualize the kinds of archaeological features sought through the experiments described in this thesis.

2.3.1 Paleo-Period

The earliest habitation recorded by archaeologists within subarctic Ontario occurred during the Paleo period (ca. 10,000 to 8,500 yBP), which is archaeologically defined by relatively large, flaked lithic tool assemblages, with the most diagnostic tool form being finely flaked lanceolate spear points (Fagan, 2005; Gibson, 2017; Hamilton, 2013; Julig, 1984; Norris, 2012, 2022; Wright, 1995). It is thought that these early occupants entered the region from the south or west in wake of deglaciation and biological recovery (Hamilton, 2013; Norris, 2022). The Paleo period occupation is thought to have been quite sparse and characterized by small nomadic forager groups attracted northwards into the early post glacial landscape in pursuit of arctic-adapted animals. Since the early Holocene period is a time of rapid environmental

change, it is likely that the Early Period populations practiced a highly flexible economy and settlement system. Ross (1995) has proposed the Lakehead composite and a series of four complexes (the Lakehead complex, Lake of the Woods/Rainy River complex, Quetico Superior complex, and Reservoir Lakes complex) in relation to this period (Figure 2.2) (Hamilton, 2013; Norris, 2022; Ross, 1995; Taylor-Hollings, 2017).

2.3.2 The Shield Archaic/Middle Period

The Middle period, or Shield Archaic period, of subarctic culture history is the longest interval (ca. 7,000 to ca 2,200 yBP), which is thought to involve broad-spectrum foraging by highly mobile Indigenous groups organized around the extended family (Hamilton, 2013; Wright, 1972). The most diagnostic technology of this long-time interval is defined by the change to medium sized dart projectile points that often feature stems, corner or side notching to facilitate hafting on to spear or atlatl dart shafts (Dawson, 1983; Fagan, 2005; Hamilton, 2013; Pilon & Dalla Bona, 2004; Wright, 1972, 1995). These stone tool assemblages also included a variety of ground stone tools that are thought to have been used in woodworking and fishing activities (Dawson, 1983; Hamilton, 2013; Pilon & Dalla Bona, 2004; Wright, 1972, 1995). Also, of regional importance during the Middle period is the mining and processing of Native copper to produce a wide range of utilitarian and decorative items (Dawson, 1983; Hamilton, 2013; Taylor-Hollings, 2017; Wright, 1972, 1995). Through a process of heating, hammering and annealing, copper nuggets were shaped into a range of tools that include projectile tips, awls, knives, adzes, and sometimes a range of personal ornaments (Dawson, 1983; Hamilton, 2013; Pilon & Dalla Bona, 2004; Wright, 1972, 1995). Using these methods, copper metal working in the Lake Superior basin is the oldest metallurgy in the world.

2.3.3 The Woodland Period

Beginning approximately 3,000 years ago, technological and cultural influences from the south and west spread into the eastern subarctic that generally define the Woodland period. The most archaeologically visible of these transformations include the northward diffusion of fired terracotta or earthenware cooking vessels and the appearance of bow and arrow technology featuring small projectile tips. In some areas along the southern flank of the boreal forest in central Canada, burial ceremonialism involving burial mound construction also

occurred, which is a practice more widely observed in southern Canada and the eastern United States (Boyd et al., 2014; Boyd & Hamilton, 2018; Dawson, 1983; Fagan, 2005; Hamilton, 2013; Taylor-Hollings, 2017).

There is also growing evidence of consumption (and perhaps also the production) of domesticated plants such as maize, beans and squash in addition to the use of wild plant foods, most notably wild rice, all of which could be readily stored for later consumption (Boyd et al., 2014; Boyd & Hamilton, 2018; Hamilton, 2013; Taylor-Hollings, 2017). While perhaps reflecting the enhanced visibility of late pre-contact sites due to the presence of well-preserved pottery, it is generally thought that the Woodland period is also characterized by higher population density than was the case in the earlier periods (Hamilton, 2013; Taylor-Hollings, 2017).

The Woodland period is divided into Early, Middle (2,200 – 750 yBP) and Late Woodland (1,250 – 150 yBP) timeframes. Early Woodland pottery has not been found in Northwestern Ontario but has been identified in Northern Minnesota and Southern Ontario (Taylor-Hollings, 2017). Laurel composite is the most widespread Middle Woodland cultural entity evident in Northwestern Ontario and into other provinces and Minnesota; it is known for pottery with conical shapes, smoothed surface finishes, with distinctive stamped decorations (Hamilton, 2013; Taylor-Hollings, 2017) (Figure 2.3).

In the Late Woodland period, pottery wares are more diagnostic than the small side-notched and triangular arrow heads that people made throughout the Woodland period (Taylor-Hollings, 2017). Blackduck (ca. 1,450 to 950 yBP), Selkirk (ca. 950 to 150 yBP), and Sandy Lake (ca. 950 – 150 yBP), wares are the main types of Late Woodland pottery that have been found in central, subarctic Canada (Figure 2.4) (Hamilton, 2013; Taylor-Hollings, 2017). They are grouped within larger cultural units such as composites. The most recent precontact Winnipeg Fabric-impressed ware, included in the larger Selkirk composite grouping of occupations, has been found all over the central Canadian Shield in Alberta, Saskatchewan, Manitoba, Ontario and Quebec plus Minnesota and Michigan; however, the composite is better understood to the west of the area (Taylor-Hollings, 2017). Sandy Lake ware is also later dating and indicates

influences from the Plains, however, coming up through the region from the southwest (Taylor-Hollings, 2017).

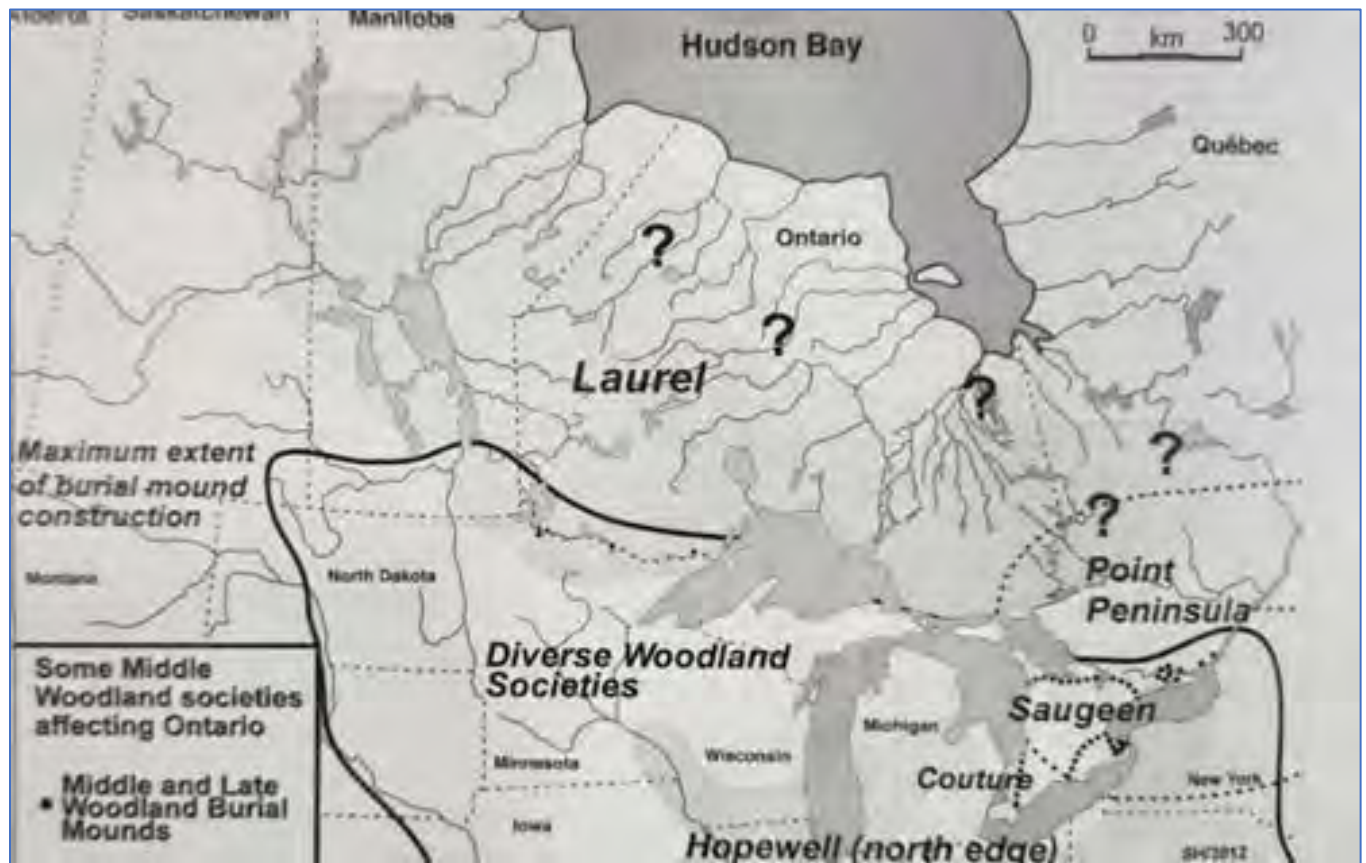


Figure 2.3 Evidence of selected Middle Woodland archaeological cultures, highlighting the huge expanse of Laurel composite sites and the diversification of pottery vessel types during the Middle Woodland (taken from Hamilton, 2013:90).

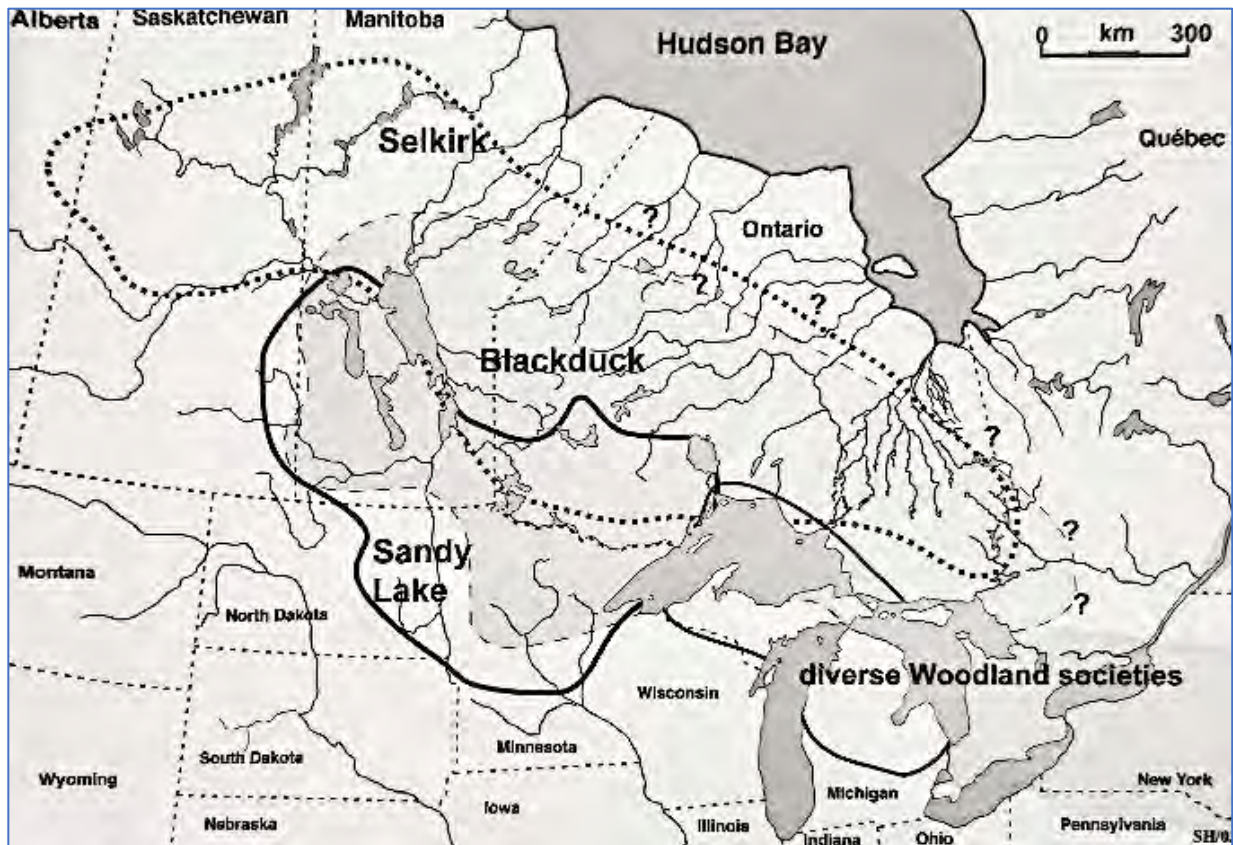


Figure 2.4. Evidence of selected Late Woodland archaeological cultures, highlighting the huge expanse and the diversification of pottery wares during the Late Woodland (taken from Hamilton, 2013:95).

2.3.4 Post contact Period

With colonial expansion of Europeans to Canada beginning about 400 years ago, most Indigenous societies underwent transformation and adaptation through interaction with colonial agencies and the fur trade. Often involving the integration of foreign technologies such as metal edged tools and cooking vessels, textiles, beads, firearms, etc., there was a gradual transformation or abandonment of traditional technologies by most Indigenous peoples. While this significantly transformed the material culture of Indigenous societies over the post-contact period, they continued to practise mobile hunting and gathering within comparatively small family groups (Hamilton, 2013; Rogers, 1983). However, the ecological consequences of the fur trade (new technologies, materials), coupled with continued westward expansion of European-derived settlement and natural resource extraction economies, meant that mobile foraging faced mounting pressure to change. This culminated with the continued colonial expansion

across northern North America. The formulation of the modern nation of Canada, and an era of treaty-making that ultimately also resulted in many Indigenous nations becoming geographically confined to reserves and becoming more subject to the colonial governance of modern Canada (Hamilton, 2013; Rogers, 1983).

2.3.5 Performing Archaeological Surveys in the Subarctic

Archaeological research in the central Canadian boreal forest requires methodologies designed for the field conditions and environmental challenges. Equipment portability is often essential due to transportation difficulties across difficult landscapes characterized by dense vegetation, isolated population centres, and inconsistent or no road access. Also problematic is the limited thematic and cartographic mapping throughout much of the region that makes it difficult to identify landforms thought to be associated with human usage. These issues can have significant logistical impacts upon archaeological investigations and the technologies that can be effectively utilized.

The acidification of boreal forest soils can destroy organic evidence, including that which is associated with hearths. Further compounding problems with sedimentary interpretations are transformation processes common within the subarctic biome. Wildlife, vegetation roots systems, forest fires, wind-toppled trees and modern land modification activities can alter the archaeological record. Due to the shallow depositional context of most subarctic archaeological sites, these disturbance processes can be chronic and quite severe. These complex issues have incompletely understood implications upon archaeological site interpretation and speak to the importance of experimental investigations such as those addressed here.

2.4 Summary

Indigenous peoples occupied all Northwestern Ontario as deglaciation and biotic recovery was sufficiently advanced. It is thought that they adapted to the subarctic by living in mobile family-based bands who flourished despite the central continental climate and fluctuating ecology of the area. While considerable variability across space and through time is expected, it can be generalized that this settlement system was built around extended families who formed the primary unit, with an annual cycle of population aggregation and dispersal

conditioned by the passing of the seasons (Dawson, 1983; Hamilton, 2013; Rogers, 1983; Taylor-Hollings, 2017; Wright, 1972, 1995).

These gathering places enabled consolidation of loosely allied families into larger ethnolinguistic units and fostered trade, exchange, spiritual and diplomatic interaction. Such gatherings would likely occur within times and places of predictable resource plenty that would sustain the larger group, but with the passing of the season of plenty, individual families would again disperse across vast homelands to sustain themselves on the available resources. This has led to the generalization that archaeological sites and their distribution will likely reflect the patterned distribution of people across vast landscapes, with large, repeatedly used aggregation sites in some areas, but with much smaller and temporary encampments also distributed more broadly (Dawson, 1983; Hamilton, 2013; Rogers, 1983; Wright, 1972, 1995). These sites are deposited within acidic soils that result in the rapid destruction of most organic materials, and with chronic forest disturbance and the freeze-thaw cycle resulting in the upper part of the sediment profile being subjected to constant transformation. This cumulatively results in a small proportion of the original material culture surviving in the archaeological assemblage and with the chemically active soil resulting in severe leaching of many indications of human habitations (Dawson, 1983; Hamilton, 2013; Winterhalder, 1983). These processes pose significant archaeological interpretative challenges, leading to my study of exploring new geophysical site documentation methods.

Chapter 3 Archaeogeophysics

Early archaeological experimentation with remote sensing methods began as a strategy to optimize sampling and interpretation (Kvamme, 2017; Oswin, 2009; Rogers, 2011; Witten, 2014). Such investigations should be complemented with a range of mapping methods designed to maximize thematic information capture to better guide investigation and interpretation. This can include conventional, sketch and topographical mapping, aerial photography, satellite imagery, and thermal imaging (Gaffney et al., 2002; Gibson, 1986; Kvamme, 2017; Oswin, 2009; Rogers, 2011; Witten, 2014). It can also involve mapping variability in soil chemistry and near-surface geophysical properties. These methods are non-invasive or marginally invasive remote sensing methodologies that archaeologists have borrowed from other disciplines such as physics and geology.

Archaeological geophysical prospection involves applying laws of physics to characterize changes in the earth's character that might derive from human intervention (Kvamme, 2017; Rennie, 2019; Witten, 2014). Archaeologists began experimenting with geophysics as a prospection and characterization tool in the early 20th century. This chapter describes common geophysical prospection and its relevance to archaeology, with particular attention to possible applicability to subarctic site conditions. This chapter focuses on ground penetrating radar (GPR), electrical methods, magnetism, and magnetic susceptibility as a means of explaining why I chose the latter to investigate.

3.1 Archaeogeophysics Defined

Archaeogeophysics represents a subset of remote sensing methods that involve measuring of geophysical properties to aid archaeological interpretation (Clark, 2001; Kvamme, 2001, 2017; Oswin, 2009; Witten, 2014). To plan excavations more effectively, archaeologists began using geophysical survey methods to differentiate between natural sedimentary contexts and distinct archaeological features and to refine sampling strategies (Gaffney et al., 2002; Kvamme, 2001, 2003, 2017; Oswin, 2009; Rogers, 2011; Witten, 2014). Archaeogeophysical survey methods can be either active (insertion of probes for direct interaction with the soil) or passive, with no direct interaction with soils (Clark, 2001; Kvamme, 2017; Oswin, 2009). A

literature review reveals a range of experiments conducted to test the efficacy of GPR, electrical methods, magnetism, magnetic susceptibility, gravitational measurements, and audio measurements. While not all these methods were archaeologically efficient, the first four have repeatedly demonstrated capacity to identify often-intangible aspects of an archaeological site (Clark, 2001; Kvamme, 2003, 2017; Oswin, 2009; Piro, 2009; Rogers, 2011; Schmidt, 2007, 2009; Witten, 2014). Knowing this, I was inspired to study magnetic susceptibility as an archaeological remote sensing technique within a subarctic context, but I will explain the other methods to help explain their strengths and shortcomings to better understand why they are not often used within subarctic contexts.

3.2 Ground Penetrating Radar

Ground penetrating radar (GPR) has become a widely used archaeogeophysical method to detect archaeological features prior to conducting archaeological excavations. It involves directing electromagnetic waves at different frequencies into the ground and then measuring the time required for a portion of that wave to reflect back towards the surface to be detected by the equipment (Clark, 2001; Kvamme, 2017; Oswin, 2009; Witten, 2014). This timed interval offers a means to measure the depth of the object or sedimentary strata causing the reflection. Specifically, electromagnetic waves transmitted into the ground undertake a consistent interaction with a sediment/soil until the sedimentary matrix changes, at which point a new 'interaction' occurs (Clark, 2001; Kvamme, 2001; Oswin, 2009; Piro, 2009; Rogers, 2011; Witten, 2014). It is these changes in interaction that cause the 'reflection' back to the surface. Some unconformities completely reflect the wave back to the GPR equipment. Other sedimentary contexts allow some of the electromagnetic wave to pass through while reflecting some of it back to be detected by the antenna (Piro, 2009; Sala et al., 2012; Witten, 2014). Still other sediments will completely absorb the wave, allowing no 'return' reflection. Clearly, the effectiveness of GPR survey depends heavily upon the nature and moisture content of the sediments, and constituent materials within it. When GPR surveys are performed systematically across an archaeological site, detected anomalies that may be of archaeological interest are plotted three dimensionally in cartesian space to enable further investigation.

The primary application of GPR investigation is in earth science and civil engineering, with methodologies requiring significant adjustment when applied to archaeological prospection and characterization. GPR application to geology involves characterization of large and often deeply buried unconformities. Similarly, civil engineering and construction applications involve the search for buried infrastructure that have strong and distinctive reflections. In contrast, archaeological features are generally quite small, ephemeral and difficult to characterize (Campana, 2009; Kvamme, 2017; Oswin, 2009; Piro, 2009; Witten, 2014). This requires selection of antennae and survey sampling designs appropriate for the kinds of unconformities being sought.

Selection of the appropriate GPR antenna (emitting specific frequencies of the electromagnetic waves) is driven by the objectives of the survey, the data resolution required, and the optimal depth of signal penetration sought (Kvamme, 2001, 2017; Witten, 2014). While GPR equipment can produce wave frequencies in excess of 2500 Megahertz (MHz), the range that archaeologists typically use is between 100 and 400 MHz, due to the size of the sought-after anomalies (Kvamme, 2017; Piro, 2009; Witten, 2014). Another important consideration when selecting antenna frequency is the nature of the sedimentary context, including soil texture and moisture (Kvamme, 2017; Oswin, 2009; Piro, 2009; Witten, 2014).

GPR investigation allows archaeologists to focus their excavations towards “high potential” areas to maximize archaeological recoveries, or to more appropriately stratify archaeological sampling to gain more comprehensive interpretative insight in a less consumptive way (Kvamme, 2001, 2017; Piro, 2009). A distinct advantage that GPR has over other archaeogeophysical methods is the ability to produce three dimensional models of the subsurface. Using equations associated with electromagnetic waves, the depth distance within the soil can be calculated. When plotted in cartesian space, this creates a three-dimensional perspective of the buried features (Clark, 2001; Kvamme, 2017; Piro, 2009; Witten, 2014).

While use of GPR has generally demonstrated success, the subarctic sedimentary, environmental and archaeological contexts are not ideal for this methodology. The sedimentary context is typically challenging, with shallow soil development on top of till deposits or bedrock.

Glacially compacted clay C-horizons beneath a thin weathered soil zone may absorb much of the electromagnetic energy, while the frequent clasts found in ground moraine may also cause considerable signal interference (Hamilton, 2013; Hinshelwood, 2004; Oswin, 2009; Piro, 2009; Witten, 2014). The irregular landscape, coupled with dense vegetation cover, also hinders the use of GPR in boreal forest contexts (Witten, 2014).

In summary, under certain conditions, GPR is a reliable archaeogeophysical method useful for archaeological prospection. The ability of GPR to produce a 3D model of the subsurface and to differentiate between natural stratigraphic and archaeological layers makes a useful tool. However, the undulating landscape, typically shallow sedimentary contexts, and dense vegetation of the subarctic, Canadian Shield region significantly limits GPR's archaeological applications.

3.3 Electrical Methods

Electrical archaeogeophysical surveys have demonstrated effectiveness in detecting archaeological features (Kvamme, 2001, 2017; Oswin, 2009; Piro, 2009; Schmidt, 2009; Witten, 2014). Electrical laws and properties underlying these methods are well established with early experiments attempting to explain light, electricity and the movement of electrons (Oswin, 2009; Schmidt, 2009; Witten, 2014). Geophysicists have used electrical methodologies to locate geological anomalies and by construction/civil engineering applications to detect underground utilities (Oswin, 2009). The two primary electrical remote sensing survey methods used by archaeologists involve measurement of Electrical Resistivity and Electromagnetic Induction (Kvamme, 2017; Oswin, 2009; Piro, 2009; Schmidt, 2009; Witten, 2014).

3.3.1 Electrical Resistivity

Electrical Resistivity meters encompass an active archaeogeophysical remote sensing method that involves projecting an electric current from a probe into the ground and measuring the resistance the current experiences while travelling to an adjacent probe (Clark, 2001; Kvamme, 2001; Oswin, 2009; Piro, 2009). This methodology centres around three electrical properties, resistance (R in ohms), current (I in amperes), voltage (V in volts), and Ohm's Law, which dictates the relationship between the three (Clark, 2001; Oswin, 2009;

Rennie, 2019). Ohm's Law states, "at constant temperature, the electric current flowing in a conducting material is directly proportional to the applied voltage, and inversely proportional to the Resistance" (Rennie, 2019:418). While Ohm's law is the theoretical basis of resistivity archaeological surveys, it requires two assumptions to be made: 1) consistent soil temperature; and 2) consistency of the material providing the resistance (Clark, 2001; Oswin, 2009; Schmidt, 2009). In archaeological situations, these assumptions are difficult to meet since soil temperature varies and the sedimentary matrix is of highly variable consistency. Sediment matrixes often contain minerals, ions or ions which will allow the electric current to travel freely within in it (Clark, 2001; Oswin, 2009; Schmidt, 2009). This becomes archaeologically useful since some of the sedimentary factors affecting the conductivity or resistance of electricity through the ground reflect anthropogenic influence.

In an archaeological context, resistivity measures the voltage and amperage between the transmitting probe(s) and the probe(s) receiving the electric signal. Based on how the current travels through the soil and the change in voltages, the resistance encountered by the flowing electricity can be determined (Clark, 2001; Kvamme, 2017; Oswin, 2009; Piro, 2009). When systematically collected and plotted in a cartesian grid, the size, shape, and orientation of subsurface features can be delimited subject to the chemical composition, moisture content, particle size and soil temperature of both natural and anthropogenic sediment (Clark, 2001; Oswin, 2009; Schmidt, 2009).

Due to the numeric data collected during resistivity surveys, statistical analysis of the detected anomalies can aid interpretation of potential human features (Clark, 2001). Electrical resistivity has demonstrated ability to detect archaeological features such as building foundations, cemeteries, midden features, and recent experiments have led to attempts to 3D model a burial mound (Kvamme, 2017).

Several underlying assumptions about resistivity as an archaeogeophysical survey technique require consideration in reference to the difficulties of the subarctic landscape before its viability can be addressed. As resistivity surveys are affected by soil moisture, this can play an unintentional but crucial role. The subarctic region consists of an unusually high number

of lakes, rivers, creeks, swamps, and bogs interspersed throughout the landscape. Over-saturation can cause the electric current to become too free flowing, while dry sedimentary conditions can inhibit the current entirely, both of which can cause problems with the performance and interpretation of this type of archaeogeophysical survey (Clark, 2001; Kvamme, 2017; Oswin, 2009; Witten, 2014). The dense network of vegetative roots common to boreal forest may also affect soil moisture content, thereby affecting the efficacy of electrical resistivity survey. These shallow root systems consist of dense, intertwined, small tendril roots and thick tree roots, all of which are carrying nutrients and water to the tree. While there has been limited evidence to suggest that root moisture can affect resistivity archaeogeophysical surveys, archaeologists should familiarize themselves with the type of vegetation in the survey area. Similar to ground penetrating radar, resistivity equipment requires ground clearance and soil depth to optimally measure the subsurface conditions. Ground clearance is required to be able to maneuver the equipment and to insert the probes into the subsurface. Due to the limited soil development in large portions of the region, the resistivity current may penetrate deep enough into the sedimentary profile to register the subsoil as one massive anomaly (Kvamme, 2017; Oswin, 2009). Lastly, another problem with performing resistivity surveys is the kind of anomalies the methodology is best at detecting, resistivity surveys work best when there are physical barriers (e.g., foundation walls) and drastic moisture changes such as in a midden (Kvamme, 2017).

In summary, while electrical resistivity has repeatedly demonstrated its viability as an archaeogeophysical survey methodology under specific circumstances, its analytic value remains controlled by the two crucial assumptions addressed above. Resistivity is most effective in adequately moist, consistent soil conditions and has demonstrated its capability to detect a variety of archaeological features affiliated with moisture, density or physical changes within the survey area. However, the subarctic landscape and boreal forest vegetation may not meet the conditions needed for an effective archaeogeophysical survey with this method.

3.3.2 Electromagnetic Induction

While relatively new to the archaeogeophysics toolbox, Electromagnetic Induction (EMI) is gaining in popularity (Bigman, 2012; Kvamme, 2001, 2017; Witten, 2014). EMI can also be

referred to as a conductivity survey, as the equipment measures the conductivity of the soil, or how readily the soil accepts an electric current, which is the opposite of resistance (Bigman, 2012; Kvamme, 2017; Rennie, 2019; Rogers, 2011; Witten, 2014). As with other geophysical methods, conductivity surveys are capable of generating numeric data useful for determining what the natural conditions are in a study area, thereby enabling identification of statistically significant anomalies that might be of archaeological interest.

Conductivity archaeogeophysical surveys can be performed with a variety of instruments, either active or passive equipment (Bigman, 2012; Kvamme, 2001; Witten, 2014). The equipment produces a time-varying magnetic field using coiled copper wire and an electric current, which when exposed to a conductive subsurface material, causes that material to acquire an induced time-varying (AC) electric current that flows as a loop within the conductive material (Witten, 2014). Active EMI archaeogeophysical equipment require a probe to be inserted into the ground to collect numeric level data. The probe consists of central piston which emits the electromagnetic field, receivers which capture the conductivity data and a cylinder which stores this portion of the equipment in between uses (Witten, 2014). Passive EMI instruments are either held by a strap or handheld devices which do not require direct contact with the sedimentary context to obtain the same numeric level data. The secondary field within the soil is proportional in size and shape to the primary field, depending on the size, shape, and orientation of the anomaly (Witten, 2014).

An additional advantage to conductivity archaeogeophysical surveys, is the relationship between electricity and magnetism. Conductivity instruments perform their surveys in two phases: quadrature phase and the in-phase (Kvamme, 2017; Witten, 2014). The quadrature phase collects conductivity data while the in-phase collects magnetic susceptibility data (Kvamme, 2017; Rogers, 2011; Witten, 2014). Magnetic susceptibility is a geophysical property that has repeatedly and reliably demonstrated its capability to detect anthropogenic/archaeological and natural firing features, environmental changes within the soil and land use surveys (Clark, 2001; Rogers, 2011; Schmidt 2007, 2009; Tite & Mullins, 1972; Witten, 2014). While magnetic susceptibility will be covered in further detail in Chapter 3.5, it was important to briefly mention because of the distinct advantage given to conductivity

surveys by its ability to collect two distinct datasets, both of which can identify archaeological anomalies within the soil.

While the versatility of electromagnetic instruments seems like it would offer a potential methodology for archaeogeophysical surveys in the subarctic region, the reality of the situation is less optimistic. Electromagnetic Induction surveys are also at the mercy of moisture content within the soil, meaning that tree roots, swamps, muskegs, bogs, even heavily saturated soils have the potential to affect survey results. Conductivity surveys require consistent orientation and ground clearance which is not easily achieved within most subarctic Canadian Shield contexts. Lastly, as conductivity is a new archaeogeophysical remote sensing tool, archaeologists experimenting with it repeatedly mention how difficult it is to understand the theoretical knowledge required to enhance the understanding of the survey results due to its more complicated nature (Kvamme, 2001, 2017; Oswin, 2009; Witten, 2014). Combined, these reasons are enough to dissuade archaeologists from using electromagnetic surveys within a subarctic context.

To summarize, EMI remote sensing surveys can reliably, repeatedly detect archaeological features within either of its dual collected data sets, offering archaeogeophysicists multiple, distinct views into the same subsurface area. Within a subarctic context, there are several challenges that must be taken into consideration, which have typically barred archaeologists from experimenting with this type of archaeogeophysical methods including relative inexperience when compared to other methods, moisture content and preparation needed for the survey.

3.4 Magnetism

Magnetic remote sensing methods have been widely used by archaeologists since mid-twentieth century (Clark, 2001; Gibson, 1986; Kvamme, 2017; Schmidt, 2007, 2009; Witten, 2014). They are routinely used as a prospection tool to aid planning of European archaeological investigations (Kvamme, 2017; Schmidt, 2007, 2009). Magnetic surveys rely on the geophysical theory addressing the relationships between the earth and its magnetic field. A working

knowledge of theory is required to properly apply magnetic remote sensing surveys in any archaeological context.

The earth's magnetic field derives from its iron-rich chemical composition, and the movement of the earth's cores and protects the planet from solar radiation (Clark, 2001; Kvamme, 2017; Schmidt, 2007, 2009; Witten, 2014). This magnetic field exhibits relative consistency in direction and strength on a global scale, while spatial and temporal variation have occurred (Rennie, 2019). Given that magnetic variation of anthropogenic origin can be comparatively subtle, controlling for natural variation due to local sediment/bedrock conditions, modern magnetic fields, or atmospheric fluctuations is essential when undertaking archaeological prospection. These issues aside, archaeologists have been experimenting with magnetism as a tool for remote sensing (Clark, 2001; Gibson, 1986; Kvamme, 2017; Schmidt, 2007, 2009; Witten, 2014).

Magnetic archaeogeophysical surveys aim to find localized anomalies within the soil that may have been caused by anthropogenic changes (Gibson, 1986; Kvamme, 2001, 2003, 2017; Oswin, 2009; Schmidt, 2007, 2009; Witten, 2014). The chemical composition of the natural sediment dictates its relationship with the earth's magnetic field. Chemical elements and compounds (iron and its associated oxides, such as hematite, magnetite and maghemite) more readily accept influence from the magnetic field (Clark, 2001; Gaffney et al., 2002; Tite, 1972; Tite and Mullins, 1971; Witten, 2014). Previous and modern human activities may have permanently changed the magnetic properties of the soil, thereby offering considerable application for archaeological prospection (Clark, 2001; Gaffney et al., 2002; Gibson, 1986; Hodgetts et al., 2016; Kvamme, 2001, 2017; Oswin, 2009; Schmidt, 2007, 2009; Tite, 1972; Tite and Mullins, 1971; Witten, 2014).

There are five main pathways that the magnetic properties of soils can be enhanced or minimized due to anthropogenic activities (Schmidt, 2007; Tite, 1972; Tite & Mullins 1971). The first pathway of anthropogenic magnetic modification relates to deliberate heating of the soil through domestic heating and lighting, food preparation, waste disposal, industrial functions, and so on. Once soil is heated past a certain temperature, the magnetic minerals within the

sediments re-align with the earth's magnetic field conditions at the time of heating (Clark, 2001; Gibson, 1986; Hodgetts et al., 2016; Kvamme, 2017; Oswin, 2009; Rogers, 2011; Schmidt, 2007, 2009; Witten, 2014). This temperature is known as the Curie Temperature (Clark, 2001; Tite & Mullins, 1971; Witten, 2014). As the fire is extinguished and the soil cools, the 'new' soil magnetic alignment "freezes" to reflect that time when the fire exceeded the Curie temperature (Clark, 2001; Kvamme, 2017; Oswin, 2009; Rogers, 2011; Schmidt, 2007, 2009). This results in the fired soil exhibiting a magnetic field that is anomalous to the surrounding sediments that were unaffected by the heating and therefore still reflect the natural magnetic profile.

The second pathway of magnetic enhancement involves the breakdown of organic material with the resulting bacterial action altering the magnetic signal within the soil, thereby signalling the location of anthropogenic features such as middens (Hodgetts et al., 2016; Schmidt, 2007, 2009; Tite, 1972; Tite & Mullins, 1971). Depending upon the nature of the parent soil material, this organic decomposition creates an anaerobic environment that typically allows for a variety of bacteria to thrive. This bacterium continues to break down the deposited organic material, thereby changing the chemical composition of the soil and thus changing the natural magnetic properties (Schmidt, 2007, 2009; Tite, 1972; Tite & Mullins, 1971). Again, the anthropogenic feature (midden) will emit a magnetic field anomalous to the surrounding natural magnetic character of the sediment.

A third known process occurs when bacteria produce crystalline magnetite within their cellular structure that align consistently with the natural magnetic field existing at that time. When the bacteria die, these structures and their associated iron particles remain intact, causing a potential avenue for magnetic alteration (Schmidt, 2009). These so-called 'Magnetotactic bacteria' thrive in bogs and similar wet anaerobic environments (Schmidt, 2009). So, while not an anthropogenic modification, this third magnetic enhancement pathway can be important when considering the environmental context for the potential magnetic survey.

The fourth pathway of magnetic enhancement is also associated with anthropogenic firing, but with the firing of artifacts (such as metal, fire cracked rock or pottery objects) rather than more general habitation type activities. Due to their metallic content or thermally altered magnetic fields, these objects may have magnetic fields that are sufficiently strong to appear anomalous to surrounding sedimentary matrix (Kvamme, 2017; Schmidt, 2007, 2009). While individual fired artifacts may not produce a strong enough magnetic field to produce an anomaly, large clusters of artifacts have been proven to have this ability (Schmidt, 2007, 2009).

The fifth pathway of magnetic alteration can be created by soil formation processes and the anthropogenic removal of the soil (Gibson, 1986; Hodgetts et al., 2016; Kvamme, 2017; Schmidt, 2007, 2009). As soil forms through the weathering processes, it begins to take on natural magnetic properties based on its natural chemical composition and the earth's magnetic properties at that time. Such weathered surfaces might be eroded away, or buried by further sedimentary accumulation, resulting in the creation of a succession of weathered surfaces, the older of which are buried to form 'paleosols'. Each of the created soil horizons maintains its own magnetic properties that are dependent on the natural environment, and the magnetic field at the time the sedimentary contexts are created, as well as the natural soil composition (Dalan, 2007; Hodgetts et al., 2016; Schmidt, 2009).

The objective of magnetic surveys is to measure the magnetic force acting at a specific point (Kvamme, 2001, 2017; Oswin, 2009). Within an archaeogeophysical context, magnetic surveys demonstrate the magnetic force acting over an entire survey area (Kvamme, 2001, 2017; Oswin, 2009; Schmidt, 2007). Once anomalies are identified and the size and intensity of said anomalies are considered, interpretations can be made to determine whether the anomalies are anthropogenic or natural (Kvamme, 2001,2017; Oswin, 2009). These interpretations should undergo testing or validation.

As with other archaeogeophysical techniques, the geophysical imprint left by anthropogenic activities are minor compared to that left by natural anomalies (Clark, 2001; Kvamme, 2017). Due to the presence of the earth's magnetic field, modern interference, bedrock-controlled landscapes, and atmospheric conditions, the relatively minor anomalies left

by anthropogenic/archaeological features can be masked when a single magnetometer is used (Clark, 2001; Gibson, 1986; Hodgetts et al., 2016; Kvamme, 2001, 2017; Witten, 2014).

Gradiometers consisting of two magnetometers positioned at two different elevations above the ground surface, compensate for this by simultaneously measuring the magnetic intensity at a specific location from two different heights above the ground surface (Kvamme, 2001, 2017; Piro, 2009; Witten, 2014). Since the strength of magnetic fields declines at a known rate depending upon distance from its source, gradiometers are effective for detection of weak and localized magnetic fields that more commonly derive from anthropogenic sources.

Magnetic remote sensing surveys can be a great benefit to subarctic archaeological investigations, as demonstrated with the archaeogeophysical investigations at the Martin-Bird site in 2009 and 2010 (Boyd & Hamilton, 2018). Located west of Thunder Bay Ontario, the Martin-Bird site is predominantly Blackduck with other pre-contact pottery recoveries including Laurel, Sandy Lake, Selkirk wares and other vessels (Boyd & Hamilton, 2018). Two burial mounds are located on the same island where this site is located. Originally investigated in the 1970, Ken Dawson noted that there was the large number of features within the encampment areas removed from the burial mound (Boyd & Hamilton, 2018). Before the site was re-excavated, Dr. Terry Gibson lent his expertise and equipment in archaeogeophysics to help plan the investigations. Using a gradiometer, several anomalies were identified, which were then investigated to reveal heating features, containing large quantities of fire broken rock (Boyd & Hamilton, 2018). This example proves the utility of archaeogeophysical surveys in the subarctic, but they do require careful site preparation, including extensive vegetation clearing.

Magnetic surveys have repeatedly demonstrated an ability to find archaeological features and environmental events (Gibson, 1986; Kvamme, 2001, 2017; Oswin, 2009; Schmidt, 2007, 2009; Witten, 2014). In addition to being able to detect features associated with the previously mentioned magnetic enhancement pathways, these surveys can reliably detect changes within the sedimentary matrix due to anthropogenic and natural means (Kvamme, 2001, 2017; Oswin, 2009; Schmidt, 2007, 2009; Witten, 2014).

Being able to measure the total magnetic forces acting within a survey area has benefitted archaeologists and their excavations no matter what area of the world they are studying. The consistent manner that anthropogenic activities modify the natural magnetism of the sedimentary context has been well documented, and archaeologists have been able to use magnetometers and gradiometers to find these features. This has allowed archaeologists to better focus their investigations and aid in their interpretations of an archaeological site. As previously highlighted, magnetic surveys can aid archaeologists working within the subarctic area to identify potential features, but it still requires a high amount of site preparation to perform these surveys within that context.

3.5 Magnetic Susceptibility

Magnetic susceptibility is defined as “the dimensionless quantity describing the contribution made by a substance when subjected to a magnetic field to the total magnetic flux density present” (Rennie, 2019:603). Archaeologically, this means how readily the sedimentary matrix will accept a change to its magnetic properties, whether due to anthropogenic or natural forces, when an external magnetic force is applied (Costa et al., 2022; Dearing, 1999; Liu et al., 2012; Schmidt, 2009; Oswin, 2009; Witten, 2014). Though a dimensionless quantity (denoted k), magnetic susceptibility can be measured, resulting in numeric datapoints.

The first pathway of magnetic enhancement as discussed in section 3.4, is the heating of soils. This primary action enhances the magnetic susceptibility, in addition to the previously discussed total magnetic field (Clark, 2001; Costa et al., 2022; Hodgetts et al., 2016; Kvamme, 2017; Liu et al., 2012; Oswin, 2009; Schmidt, 2009; Šindelář et al., 2021; Witten, 2014). Total magnetic surveys are effective at detecting remnant (permanent, emanating) magnetic anomalies while magnetic susceptibility detects the induced portion of these anomalies (Clark, 2001; Schmidt, 2007, 2009; Witten, 2014). Induced magnetic features are only evident in the presence of an external magnetic field, and magnetic susceptibility meters measure how readily the anomaly will accept the induced field (Clark, 2001; Hodgetts et al., 2016; Rogers, 2011; Schmidt, 2007, 2009; Tite, 1972; Tite & Mullins, 1971).

The chemical reduction of hematite ($\alpha\text{-Fe}_2\text{O}_3$), into magnetite (Fe_3O_4) through heating and ensuing cooldown resulting in maghaemite ($\gamma\text{-Fe}_2\text{O}_3$) allow for susceptibility enhancement to be observed around hearths. Hematite is an anti-ferromagnetic iron oxide that is abundant in natural, organic rich soils (Dalan, 2007; Dearing, 1999; Schmidt, 2007, 2009; Tite, 1972; Tite & Mullins, 1971). Anti-ferromagnetic means that the hematite is generally not susceptible to magnetic changes due to the magnetic ions being rather 'disordered' in their alignment but equal in strength, and therefore displaying limited or no magnetic properties (Dalan, 2007; Schmidt, 2007, 2009; Tite, 1972; Tite & Mullins, 1971). Magnetite and maghaemite are iron oxides that also occur naturally in the soil. Magnetite is a ferromagnetic material (net magnetization due the presence of an additional iron ion), while maghaemite is a ferrimagnetic material, similarly 'disordered' as anti-ferromagnetic, but the magnetic ions are unequal in strength, resulting in net magnetic enhancement (Dalan & Banerjee, 1998; Dalan, 2007; Schmidt, 2007). When hematite experiences heating past its Curie temperature (between 650 and 750 degrees Celsius), it begins to convert to magnetite. Once a heat source is removed and the sediment cools, further chemical change ensues that converts the magnetite into maghaemite (Dalan, 2007; Dearing, 1999; Schmidt, 2007, 2009; Tite, 1972; Tite & Mullins, 1971). Maghaemite has a similar chemical composition to hematite, but maghaemite retains the magnetic properties more similar to magnetite. This conversion results in an enhancement of the magnetic susceptibility of the sedimentary context (Schmidt, 2007; Tite, 1972; Tite & Mullins, 1971). Archaeologically, this means that there is potential for magnetic susceptibility surveys to detect anthropogenic firing events (Crowther & Barker, 1995; Dalan, 2007, 2009; Dearing, 1999; Rogers, 2011; Schmidt, 2007; Šindelář et al. 2021; Tite, 1972; Tite & Mullins, 1971). Other metal compounds and archaeological materials may also be detected by conducting a magnetic susceptibility survey (Tite, 1972; Tite & Mullins, 1971). Lastly, re-deposition of soils through ditch excavation, modern stripping and construction, previously buried utilities and agricultural activities have all been detected using magnetic susceptibility (Hodgetts et al., 2016; Šindelář et al., 2021; Tite, 1972; Tite & Mullins, 1971).

Magnetic susceptibility surveys can be carried out using a variety of instruments that include use of active or passive methods and can be employed before or during archaeological

investigations (Costa et al., 2022; Crowther & Baker, 1995; Dalan & Banerjee, 1998; Dalan, 2007; Dearing, 1999). The electromagnetic field inducing coil discussed in section 3.3.2 is the same equipment that is used to measure magnetic susceptibility. Usually electrical conductivity/magnetic susceptibility meters are contained in a single unit, capable of measuring both dataset types, by inducing the sedimentary context with an electromagnetic field. Offering a wide variety of instrumentation, the equipment size and capability are dependent on the number of wire coils and where its receiver is. The Barington MS-2 and MS-3 are devices that used probes to gather information (Costa et al., 2022; Dearing, 1999; Hodgetts et al., 2016). In order to collect a measurement, the probe is inserted into the soil, the handle/wire transmits the data to the processing unit, which stores the data until such a time the data can be uploaded and interpreted (Dearing, 1999; Schmidt, 2009). The size of the collection probe is dependent on the specific Barington unit (Dearing, 1999). Field generating units include the EMS series of conductivity meters, which are single unit devices comprised of five components. The generating coil is located at the front of the unit, with wires connecting it to a centrally located battery. Next to the battery is the data storage which receives the data from the conductivity meter located at the back end of the equipment (Witten, 2014). Handheld magnetic susceptibility meters, such as the Terraplus magnetic susceptibility meters, allow for the user to take measurements directly on whatever surface they desire. The Terraplus company offers a range of handheld magnetic susceptibility/conductivity meters which have demonstrated potential in detecting archaeological features (Costa et al., 2022; Hodgetts et al., 2016; Terraplus, 2019), particularly since anthropogenic enhancement of magnetic susceptibility typically reflects statistically significant levels of change (Dalan & Banerjee, 1998; Dalan, 2007).

Magnetic susceptibility has repeatedly demonstrated success locating anthropogenic features and natural anomalies occurring within a variety of sedimentary contexts. Particularly important is the detection of widespread burning, middens, storage pits, excavated ditches and foundations (Clark, 2001; Costa et al., 2022; Dalan & Banerjee, 1998; Dearing, 1999; Hodgetts et al., 2016; Rogers, 2011; Schmidt, 2007, 2009; Šindelář et al., 2021; Tite, 1972; Tite & Mullins, 1971). Magnetic susceptibility has also been used to find large ore bodies and evidence of

natural sediment movements (landslide, alluvial vs. fluvial sedimentary deposits) in other environmental surveys. Adding to the utility of magnetic susceptibility is the variety of instruments which can be used to complete this type of archaeological remote sensing (Clark, 2001; Costa et al., 2022; Dalan & Banerjee, 1998, 2007; Dearing, 1999; Hodgetts et al., 2016; Rogers, 2011; Schmidt, 2007, 2009; Šindelář et al., 2021; Witten, 2014).

3.6 Statistics

A working knowledge of statistics is necessary to generate meaningful insight from archaeogeophysical survey results. Since the experimental results yielded a ratio-scale dataset, descriptive statistical analysis used here address mean (average of a dataset), median (central value or values of a dataset) and mode (most frequently occurring value in a dataset) to provide measures of central tendency (Lane et al., 2003). Once the dataset is described this way, further statistical tests are applied to the numeric archaeogeophysical data to document the data distribution around the central tendency.

Data evaluation begins by examining the frequency distribution of values using a series of 'bins' that aggregate the data distribution into a series of same-sized data ranges (Lane et al., 2003). This offers a visual representation of the data distribution, readily identifying how the data is distributed around the mean, median and mode, and drawing attention to data outliers. This visual data summary also reveals whether the data appears 'normally' distributed on each side of the mean, median, mode, or whether it is skewed higher or lower than the measures central tendency.

If the data sufficiently reflects the assumption of a normal distribution, then statistical tools such as standard deviation can be used to numerically characterize the dispersal of datapoints around the mean (Lane et al., 2003). One standard deviation represents approximately 68% of the variance observed within the sample, with 1.96 (often rounded to two) standard deviations representing approximately 95%, and three standard deviations accounting for 99.7% of the sample variance (Lane et al., 2003; Oswin, 2009; Witten, 2014). This allows an approach to visualizing how tightly (or not) the data clusters around the mean. Other statistical tests can contribute to determination whether similarities or differences observed

between (or within) data samples (control versus experimental data) are statistically significant. This is important for evaluating the null hypothesis (Lane et al., 2003). Statistical tests generate a probability value or, p-value, that determines whether two sets of data are sufficiently different to statistically demonstrate that they represent two discrete populations or reflect variation within the range expected of the same sample population. In this case, are there statistically significant differences in magnetic susceptibility readings between the control sample (pre-firing baseline data) versus the post-firing readings from the experimental hearths. If there are statistically significant differences, then it indicates that the experimental firing was sufficient to transform the magnetic character of the sediments. If the results are not statistically significant, then they challenge the efficacy of magnetic susceptibility as an archaeological site characterisation method within the subarctic region. Similar evaluations might offer insight whether repeated firings or those of greater duration and intensity further enhance magnetic susceptibility (at a statistically significant level). This determination will be made by comparing the calculated p-values with the alpha-value, the commonly accepted value for determining if the null hypothesis can be rejected, of 0.05 (Lane et al., 2003). Within Excel, statistical T-tests can be used within one dataset (Paired), two equally sized datasets (Equal Variance) or two samples with unequal size and variances (Unequal Variance), as well as one – or two tailed tests. One tailed T-tests examine a single portion of the distribution, while two tailed tests examine two sections of a distribution, depending on how normally, or skewed, the dataset is distributed (Lane et al., 2003).

Archaeogeophysical surveys rely on the collected dataset approximating a normal distribution pattern and displaying consistency across the survey location. By filtering the data to identify sample values falling beyond of 1 standard deviation from the central value, the analyst can identify areas yielding anomalous values that can be more closely examined to assess whether they are of anthropogenic origin, or to aid in post-excavation interpretation of the archaeological recoveries (Kvamme, 2017; Witten, 2014).

When used as a site prospection and characterization method, the process involves statistical analysis to identify values that fall outside of -1 and 1 standard deviation and then plotting the spatial distribution of these statistical outliers in search of patterns that might be

archaeologically informative. Data processing and examination using Geographic Information Systems can enable multi-iterative data presentation after filtering it to remove patterns that are not of archaeological interest in this case (e.g., plough marks). Ideally, such spatial plotting of anomalous values (of anthropogenic origin) will appear non-random or patterned in ways inconsistent with expectations of non-anthropogenic sediments (Clark, 2001; Kvamme, 2017; Witten, 2014). This thesis anticipates eventual application of this approach by summarizing experiments conducted under controlled conditions to determine how soil heating affects soil magnetic susceptibility. In the case of these experiments, the physical locations of the firing features are known, and the focus of attention is whether (and under what conditions) the heating caused a significant transformation of the naturally occurring levels of magnetic susceptibility.

3.7 Site Prospection vs Site Characterization

Most archaeogeophysical and remote sensing methods are used for archaeological prospection: to locate and distinguish potential archaeological features prior to excavation. This thematic site information enables sample stratification to aid in generating more representative samples. Using the detected anomalies to inform subsurface sampling, archaeologists can focus investigations on subareas reflecting differing characteristics in order to generate a more comprehensive sense of the nature, function and extent of activity areas, and to generate a more representative material culture sample.

In addition to prospection, archaeological remote sensing can be a tool for site characterization. In acidic soil conditions where visible evidence of many features may be obscured or destroyed, anthropogenic modifications may be detectable using geochemical or geophysical methods. By systematically collecting geophysical information as part of routine excavation, such techniques may reveal otherwise invisible evidence to supplement conventionally recovered archaeological information. Given the challenges associated with generally shallow subarctic archaeological sites due to its active environmental character (acidity, bioturbation, cryo-turbation and animal disturbance), such methods have considerable potential to aid archaeological interpretation, particularly in the identification of hearth

features. It is proposed that magnetic susceptibility evaluation might have its greatest utility as a site characterization tool.

3.8 Summary

This chapter introduces a variety of geophysical methods used by archaeologists since their application began in the early 20th century. Using electric, magnetic and wave properties, archaeologists have been able to guide, inform and enhance information recovery, whether the remote sensing surveys are completed during, before or after excavation. However, these methods have been infrequently used in the subarctic and Northwestern Ontario, requiring controlled experimentation to assess the efficacy of the selected method.

Chapter 4 Experiment Details

4.1 Introduction

I tested the efficacy of magnetic susceptibility as an archaeological prospection and characterization tool by conducting a series of firing experiments within a test site at the Hogarth Tree Farm near Thunder Bay, Northwestern Ontario (Figures 4.1, 4.2, 4.3, 4.4). After reviewing in Chapter 3 the different archaeogeophysical methods, I chose to evaluate magnetic susceptibility effectiveness in a subarctic context, using a Terraplus KT-10 magnetic susceptibility meter recently purchased by the Lakehead University Department of Anthropology. This required testing, under controlled conditions in an appropriate locale, minimized independent variables that might affect results and mitigated potential hazards of outdoor firing. The test location exhibits sediments of uniform texture, moisture content and with limited disturbances (see below for detailed discussion about the test units). This location is currently mantled with mixed grass and low woody shrubs, with little or no nearby foot traffic as it is fenced off from the public. While it is probable that mixed forest covered the locality for much of the post-glacial past the locality is now a tree farm with much of it covered with mature conifers. No trees are currently found within 50 metres of the test area. The lack of forest vegetation associated with the test area, coupled with emergency water stored near at hand mitigated fire risk.

The specific firing methods guiding these experiments are described in this chapter. This includes the tools used to perform the experiments and to collect the data. This chapter also describes how the experiments were carried out, as well as the safety precautions taken.

4.2 Details about the Study Location

The study location is within the Hogarth Tree Farm, a property owned and managed by Lakehead University's Faculty of Natural Resource Management (Figures 4.1-4.4). It is located within the city limits of Thunder Bay, Ontario, but exhibits comparatively undisturbed sediments and likely was covered with boreal forest vegetation for much of the post-glacial period. Other considerations affecting my locale choice included fire safety, security, convenient access, and the realities of initiating research during the COVID-19 pandemic. These

experiments occurred during the warmer seasons to enable excavation of the test holes and to be able to accurately measure the firing temperatures without first controlling for air and soil temperature. These issues all delayed the start of the firing experiments.

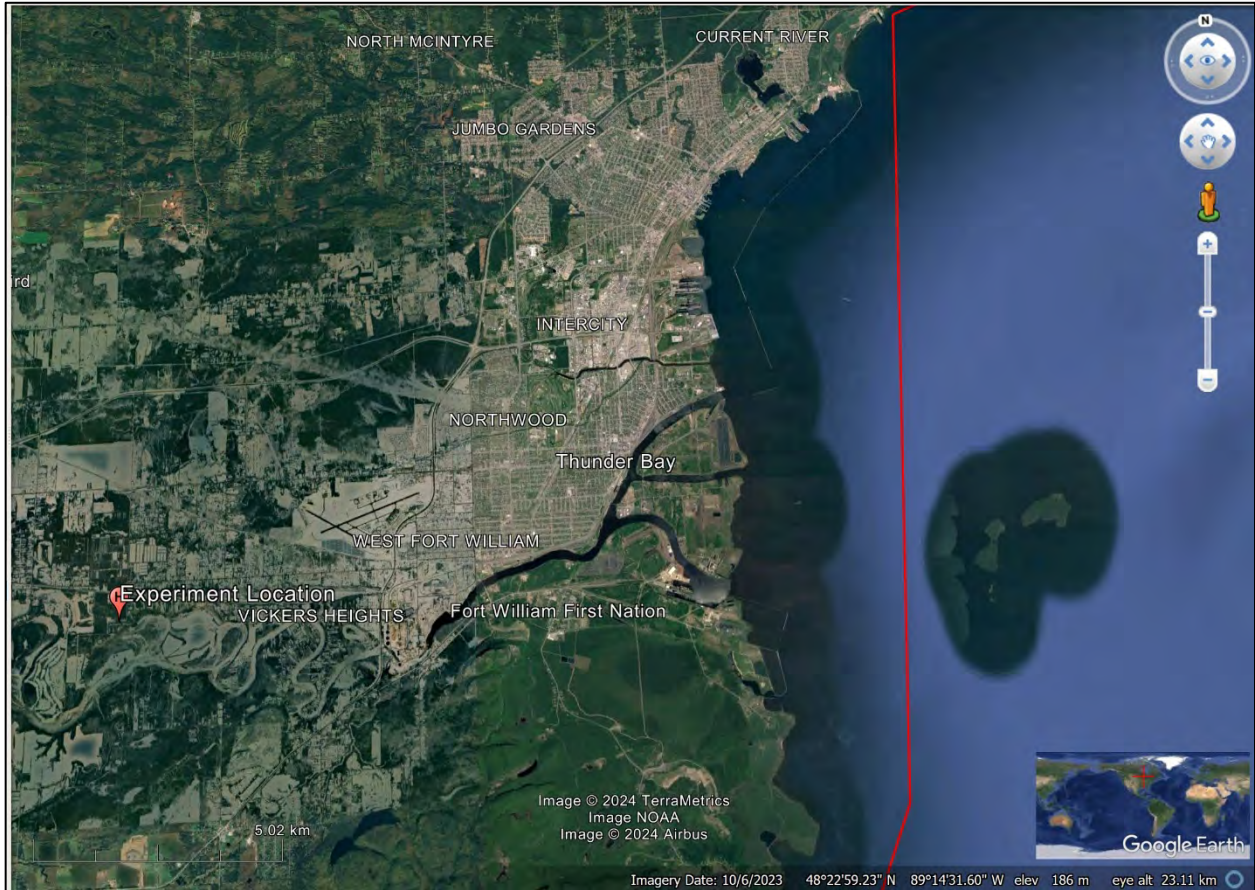


Figure 4.1 Location of Hogarth Tree Farm (H) relative to Thunder Bay, Ontario, Canada.

The Hogarth Tree Farm is a semi-rural property approximately 13.8 kilometers southwest of the main centre of the City of Thunder Bay, Ontario, Canada. It is named after Dr. R. W. Hogarth, the man who donated the property to Lakehead University. The southern portion is currently clear of trees (Figure 4.2), presumably to maintain a firebreak to protect nearby homes. Within this clearing a 5-meter square grid was established using a compass and a 60 meter tape (Figure 4.2 – 4.4). The grid was created to capture and record discrete firing events. Figure 4.2 offers an aerial view of the property with the gated access (H, Figure 4.2) and the approximate location of the experimental grid. The most southwesterly stake was identified as location 0N, 0E and the most north-easterly stake was 5N, 5 E (see Figure 4.3).

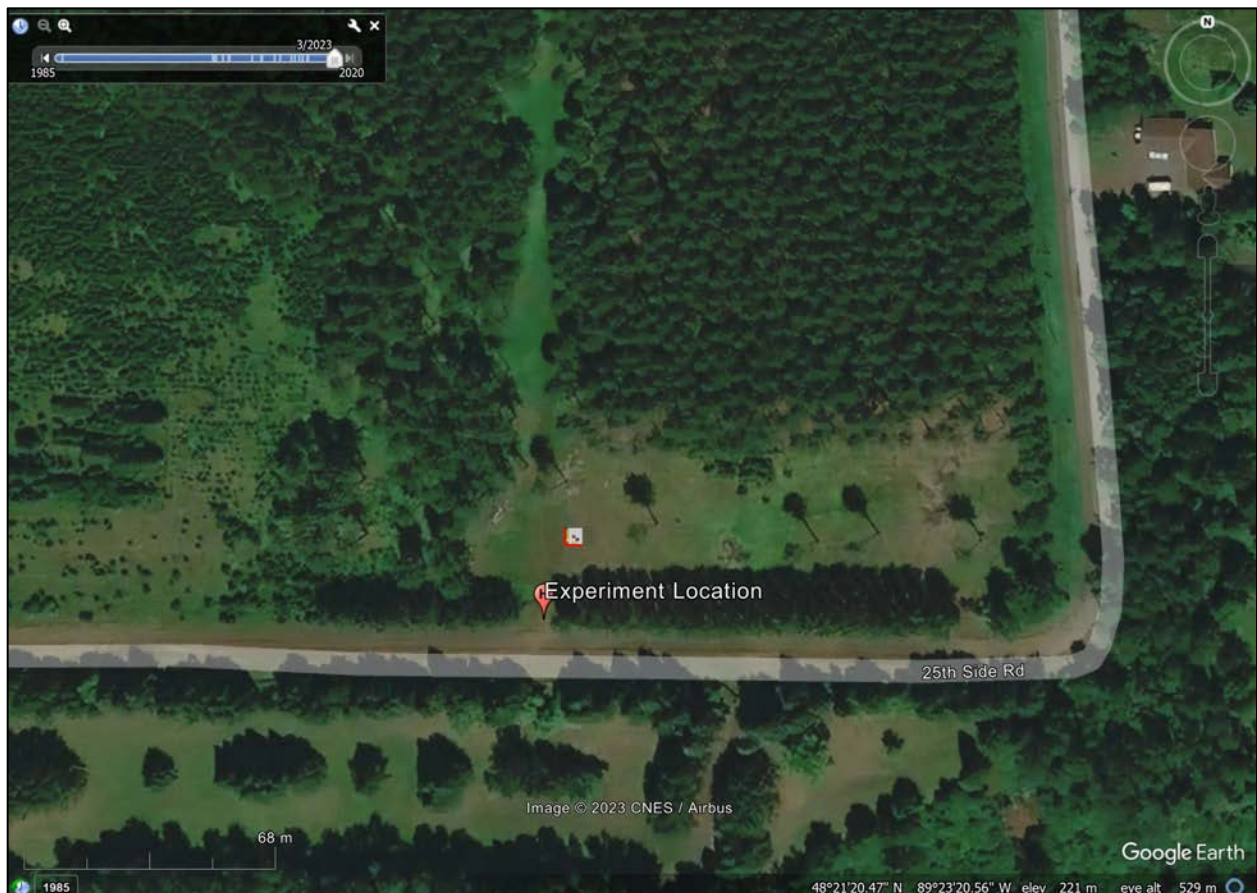


Figure 4.2 Zoomed in view of Hogarth Tree Farm location circa 2023. H denotes the gate used to enter the property. Grid location overlaid with grid.

The southern cleared portion of the property is mantled with grasses, shrubs and other regenerative growth (Figures 4.3 and 4.4). This vegetation was manually cleared around and within the grid prior to any experiments. To the north of the grid, rows of planted coniferous trees extend to the northern edge of the property with walking trails meandering through the forest. Additionally, there is an off-road trail extending north through the gate.



Figure 4.3 Study area conditions with the established grid area from the Southwestern corner of the grid. Corner closest to the camera is the ON, OE post facing Northeast.



Figure 4.4 Hogarth Tree Farm study area conditions, circa 2020, facing North. Water trough to extinguish fires.

The sedimentary context for the experimental area was examined by excavating two test trenches (50 cm by 1 m) to the north (5N, 0E) and east (-1N, 4E) (Figures 4.5, 4.6). Visual inspection of these trenches revealed a thin organic layer (0-10 cm) of dark orange-brown weathered sandy loam topsoil containing moderate amounts of organic material, which covers a compacted reddish-brown sandy silty sand down to at least 40 cm of depth. The apparent parent material is light brownish-grey silty sand that extends to at least 90 cm below surface. These uniform fine sediments are consistent with expectations of the Kaministiquia River delta. This delta originally developed at the mouth of a major glacial outwash channel into glacial Lake Minong and was flooded by at least two early Holocene events culminating in the Nipissing Transgression (Boyd et al., 2012). Periodic seasonal floods likely resulted in further sediment accumulation throughout its history. The sedimentary profile reveals what is interpreted to be a

uniform glacio-lacustrine depositional history, with no sedimentary particles larger than sand, and with no large clasts or cobbles that might affect the magnetic susceptibility experiments (Figures 4.6, 4.7).



Figure 4.5 This is the test pit excavated at -1N, 4E and facing North.



Figure 4.6 Test pit photo -1N, 4E plan view.

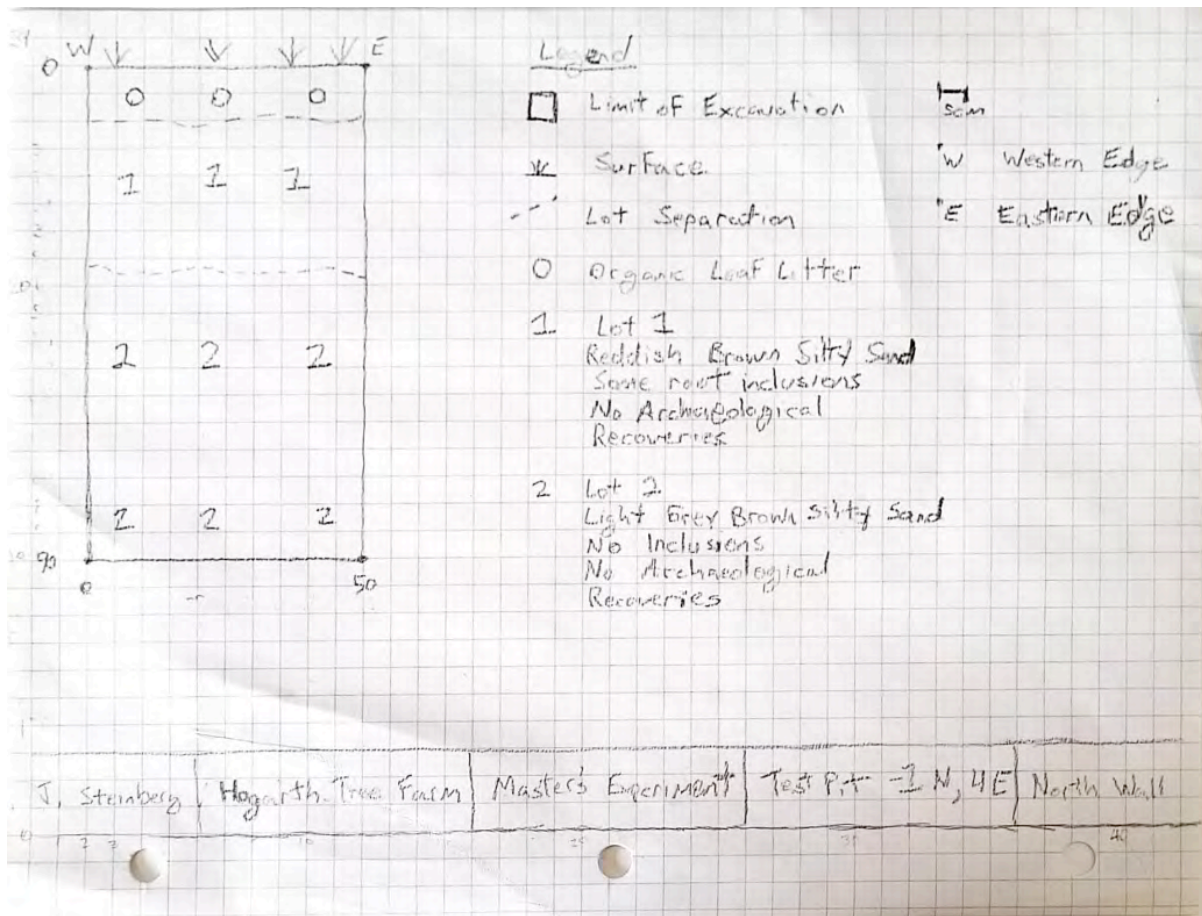


Figure 4.7 Test pit sketch map and soil descriptions from fieldwork.

When establishing a new firepit, the long tape was stretched between perimeter grid stakes to identify and delimit the 1 square meter unit that was to contain it; two measuring tapes were used to triangulate the 1 m squares. All experiments were conducted within the established grid area, except for the preliminary excavation test trench.

Conducting these experiments on relatively uniform glacio-lacustrine sediments found within the Kaministiquia River delta was calculated to ensure some degree of analytic consistency for the experiments. While this does not reflect the diversity of circumstances found in either the area or throughout the general subarctic bioregion, it does help minimize the number of natural variables that might be affecting geo-physical character of the sediments within the test area. Also, it helps to render the experimental heating as the primary dependent variable. This was deemed necessary to address the viability of magnetic susceptibility as an

archaeogeophysical methodology. Also, it helped to understand where all of the experiments were taking place in this small, restricted area.

4.3 Purpose of Experiments

The experiments were conducted to assess the utility of magnetic susceptibility for archaeological characterization, specifically whether and under what conditions hearths might be detected in the typical subarctic podzolic soils (Gibson, 2017; Hamilton, 2000). It is already established that chemical changes in the soil occur through anthropogenic burning and can be detected using magnetic susceptibility meters (Clark, 2001; Costa et al., 2022; Hodgetts et al., 2016; Kvamme, 2017; Liu et al., 2012; Oswin, 2009; Schmidt, 2009; Šindelář et al., 2021; Tite & Mullins, 1971; Witten, 2014). At issue is whether such alterations are sufficiently distinctive from those caused by repeated forest fires and under what conditions we might expect domestic hearths to transform the soil character to a detectable level. The testing also sought to specifically evaluate the effectiveness of the Terraplus KT-10 magnetic susceptibility meter (Terraplus, 2019) in documenting soil transformation. Also, I wanted to address whether its portability and versatility offered value in subarctic archaeogeophysical characterization.

4.4 Equipment and Methods

The Terraplus KT-10 unit, provided by Dr. Matthew Boyd, requires direct contact with the mineral sediment matrix to collect magnetic susceptibility data and is unable to measure characteristics more than one centimeter below the measurement surface (Terraplus, 2019). This requires removal of vegetative overburden and excavation to the desired depths before testing, which is consistent with the situation apparent during archaeological excavations that exposes mineral soil through removal of successive layers. Additionally, excavation allowed for a visually uniform sedimentary matrix to be exposed in the hope for consistent results. That renders the instrument ideal for measuring patterns of magnetic susceptibility variation across horizontal surfaces or at successive depths down vertical profiles during archaeological excavation. In this sense, the experiments anticipated utility in geophysical characterization during excavation rather than as an archaeological prospection tool. The acidic nature of subarctic sediments often destroys the organic archaeological recoveries (bone, charcoal, ash,

wood, etc.), often removing this line of evidence from archaeological interpretations. Luckily, magnetic susceptibility surveys have the potential to locate hearth features within a sedimentary context due to the first pathway of magnetic enhancement, discussed previously.

To address my objectives, a series of firing experiments were designed and performed to heat the soil in a fashion like that expected of hearths used by pre-contact hunter-gatherers. Small, open air firing experiments took place in shallowly excavated fire pits using two time intervals (short and long term, discussed in section 4.4.2). While the time interval between experimental firing and data collection is only a matter of a few days or months (as opposed to decades, centuries or more, expected when addressing archaeological deposits), these experiments provided a proof-of-concept as to whether the Terraplus KT-10 magnetic susceptibility meter (Terraplus, 2019) offered practical application to subarctic archaeological prospection and site characterization.

Throughout the duration of the experiment, three main variables were considered: 1) temperature achieved; 2) time duration since ignition; and 3) magnetic susceptibility 'response'. Temperature data was collected to see if a consistent temperature profile for each experiment duration could be achieved. Firing duration sought to address whether minimum thresholds of temperature and duration were required to enhance the magnetic susceptibility to the point that a statistically significant anomaly would be generated.

4.4.1 Safety Measures and Equipment

Given the potential hazards associated with the firing experiments, two 100-gallon water tanks were placed near the established grid on wooden pallets to maximize slope and make it easier to pour the water onto the grid zone if necessary. Once filled with water, garden hoses were attached to enable emergency fire suppression. Four 5-gallon water containers and a fire extinguisher were also brought to the site for each experiment to have on hand for extra safety. Municipal fire laws and bans were obeyed throughout the duration of the experiments and whenever drought conditions were present.

The experiments were complicated by several uncontrollable circumstances due to the COVID-19 pandemic. Consistent with guidelines issued by the province of Ontario and Lakehead

University's COVID-19 social distancing guidelines, only the author and his supervisor were onsite during most of the experiments. As the pandemic conditions eased, experiments that required more than two people became feasible and I enlisted assistance from the Lakehead University Department of Anthropology Technicians, a Postdoctoral Fellow, and fellow graduate students.

During my project, chopping firewood, creating kindling, igniting a fire, and maintaining the firing experiments were all identified as potential hazards. These hazards were mitigated by wearing steel-toed boots, safety glasses and gloves. Thick leather welding gloves were also worn, when working near the fire to minimize risk. I usually worked at the project site with a partner to ensure emergency assistance was available in case of an accident or a fire.

4.4.2 Firing Experiments

The equipment needed included wood cutting and splitting equipment (axe, hand saw and hatchet), fuel for the firing events (wood, bark), a lighter, a shovel, a thermometer and thermocouple probes, an Apple iPad, as well as the previously mentioned safety equipment. Most of the equipment initially listed was used to prepare and perform the experiments, while the thermometers, probes, iPad, and Terraplus KT-10 unit (Terraplus, 2019) were recording devices for the experiment results.

The project experiments were designed to document the effects of changing two dependent variables: 1) duration of firing (controlled); and 2) temperature achieved (partially controlled). This section outlines the specific equipment used, how it was utilized to monitor the variables and how the firing experiments were conducted.

Recording devices were used to track the temperature and firing duration variables. Temperature monitoring was conducted using the 88598 4ch K SD Logger thermocouple thermometer. This device measured temperature from four individual type K thermocouple probes and the information was recorded onto an SD memory card. Two types of thermocouple probes were used (Figure 4.7). One was rated to measure temperatures up to 1200° C and it was placed within the fire pit itself to record the hottest temperatures. The second probe type was a wire probe that measured the temperatures achieved around the margins of the

excavated fire pit. The device can record a temperature value every five seconds, but for these experiments it was set to record the temperature at each probe once per minute (see Appendix A for those results). These measurements were collected until the device was turned off at the end of each experiment. The measurements were saved in a .txt file format on a 64GB SD card. The thermometer was used as a secondary timekeeper, as it collected temperature data every minute. Experiment timing was also measured with a cellular phone and an Apple iPad, which also doubled as the main camera.



Figure 4.8 Thermocouple probes and thermometer in use during a long-term firing experiment.

Each experimental fire pit was located within a specific one-meter square on the grid (Figure 4.3, 4.8). A level firepit floor was excavated down 10-15 centimeters through the A-horizon to avoid the impact of more modern natural events, and to ensure direct heating of the unweathered parent material. After the firepit was excavated, baseline magnetic susceptibility

measurements were taken at the fire pit base and recorded for later reference. The next step involved placement of the thermocouple probes. For each firing event, a 1200° C rated probe was placed in the east, south and west walls of each fire pit, with the exposed temperature gathering points oriented towards the center of the hearth feature. The insulated wire portion of the probe was protected from the intense heat by burying it slightly in the fire pit. The wire probe was placed in the southern wall. This was deemed the ideal orientation due to the length of the probe's wires (1 meter) and how close the thermometer could be to the fire itself without damaging the device. The 1200° C probes recorded data on channels 1, 3, and 4 in the thermometer. The wire probe recorded on channel 2 and was placed in the southern wall above the 1200° C probe, to measure heat radiating from the margins of the fire. Placing kindling and wood in perpendicular directions within the firepit allowed fire ignition with birch bark, wood shavings and a lighter.

Each experiment occurred over a pre-determined time limit over portions of two warm weather field seasons in 2020 and 2021. Based upon presumed firing activities at archaeological sites, three types of firing experiments were performed: short term (one hour); long term (five+ hours); and pottery firing. For the timed firing events, fuel was added to the fire for the set time limit at the author's discretion. Once the time had expired, the firing event was allowed to burn itself out until only ashes were left, usually 1.5-2 hours after the last piece of wood was added. The purpose of having more than one type of firing event was to determine what fire intensity/duration was sufficient to alter the magnetic susceptibility signature of the soil and the maximum amount of enhancement that could be achieved through each experiment.

Most of the short-term experiment locations were used repeatedly to determine the cumulative effect of repeated firing events within a single firepit. Long term firing events were performed in three locations in an effort to produce the most intense magnetic enhancement possible. The number of firing events performed during each short-term experiment location is reported below (Figure 4.8). Time durations were not mixed between the different firing locations.

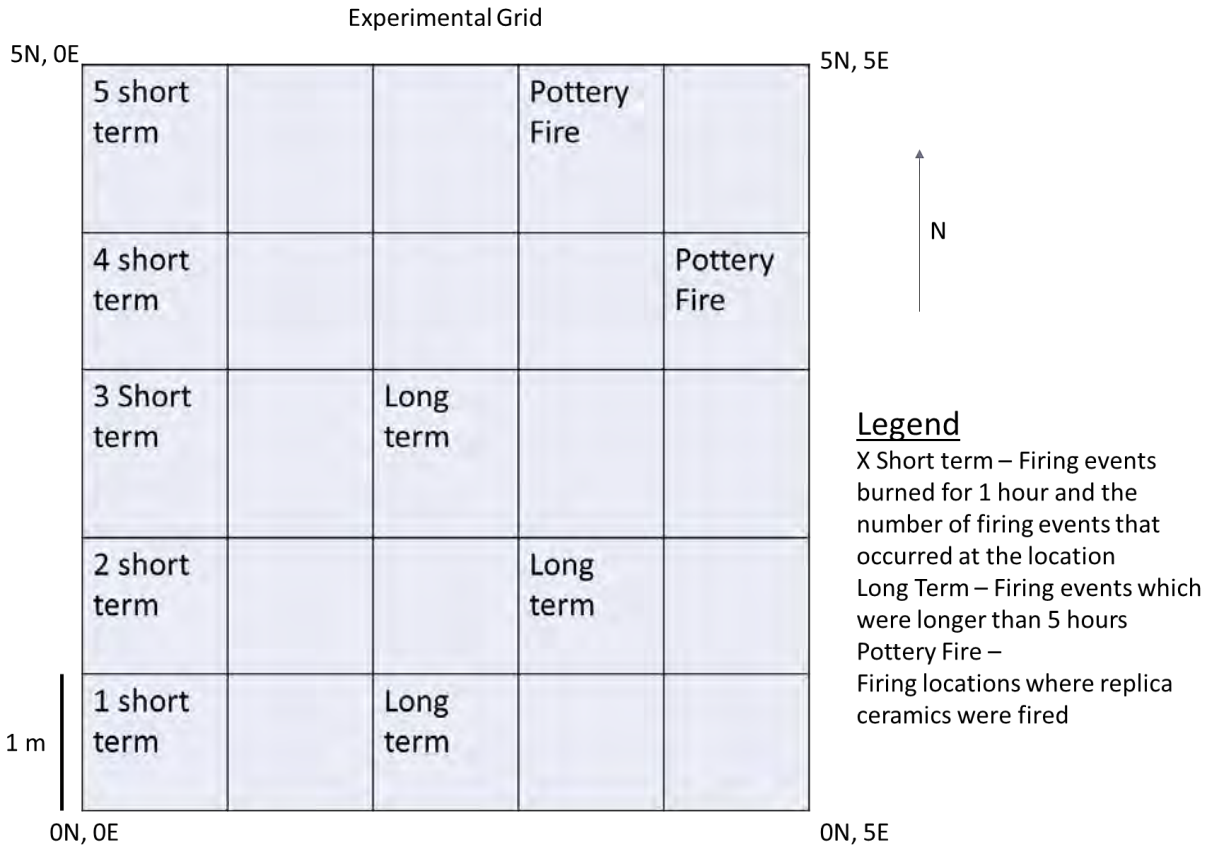


Figure 4.9 Type and number of experiments performed at each location.

The only firing event not constrained by a time limit involved a replica pottery firing experiment. It involved pre-contact pottery replicas prepared by Dr. Jill Taylor-Hollings, Clarence Surette, and various students within Lakehead University’s Department of Anthropology. The replicas were constructed from locally gathered clay using methods replicating pre-contact Indigenous pottery production methods. After days of air drying, the pots were fired using procedures deriving from ethnoarchaeological experiments previously conducted by others (e.g., Goltz, 2019). This experimentation demonstrated the importance of establishing a bed of coals prior to pottery firing, ensuring that the vessels were fully dry before firing, and to ensure ‘base temperatures’ were achieved (i.e., heated coals) before the clay vessels are placed in the fire (Goltz, 2019). During the time required for the fire to create a bed of coals, the unfired vessels were placed around the edge of the firepit to complete the drying process. Once ready, the vessels were placed with the open mouth facing down on top of the bed of coals, with smaller brush and sticks placed around the vessels until the pot could not be

seen through the added fuel (e.g., Goltz, 2019). This fuel was allowed to burn as hot as possible for about a half an hour to an hour and a half. After the added fuel burned, the vessels were allowed to cool for a short time, and then were slowly removed from the coals and ash, either intact or in fractured pieces.

The development of pottery vessels during the Woodland period revolutionized food storage and preparation for the North American Indigenous people. Since vessel firing is a specific firing activity, the hypothesis was that this might produce a different, distinct, susceptibility response. While such fires were tested, there was not enough magnetic susceptibility datapoints collected to enable statistical analysis suitable for inclusion within this thesis. Several pots were successfully fired, and the recorded temperature data and duration will assist in designing future firing experiments. It was particularly enlightening to see the maximum temperature achieved under that day's conditions and to see if the terracotta stage of had been achieved (Figure 4.9) (e.g., Rice, 1987).

Type	Firing Temp. (°C)	Porosity
Terracotta	Below 900	30% or more
Earthenware	900-1200	10-25%
Stoneware (high Fe content – red to brown)	1200-1350	0.5–2.0%
China (white, vitrified)	1100-1200	Less than 1%
Porcelain (fairly pure kaolin clays)	Above 1300	Usually 0%

Figure 4.10 Temperature requirements for pottery firing with resulting porosity (taken from Rice, 1987:5).

4.5 Magnetic Susceptibility Data Collection

Baseline magnetic susceptibility measurements for each fire location was collected before each firing event and consisted of 4-5 measurements per location as previously outlined. It was soon realized that this would generate insufficient data to meaningfully represent the area's natural magnetic susceptibility. To mitigate this, 30 cm diameter test pits were excavated (10-15cm below the surface) at 1-meter intervals extending five meters north and east from the established outer-edge gridlines (Figure 4.9). Approximately 300 baseline magnetic susceptibility measurements were then taken from these test pits, prior to any firing experiment within the grid. In each of these small pits, control data was collected at the depth corresponding approximately with the depth of the prepared firepits.

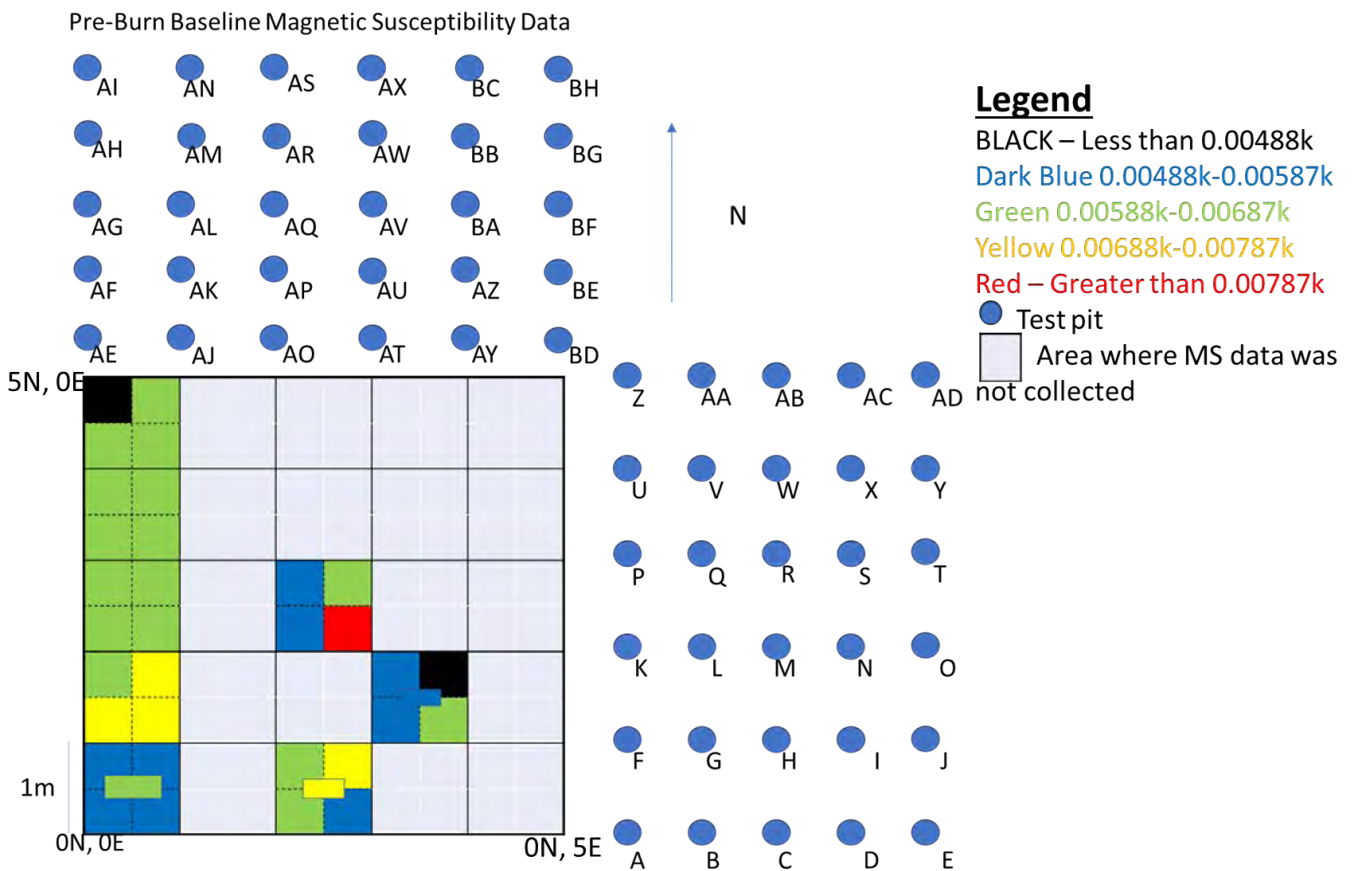


Figure 4.11 Baseline magnetic susceptibility data collection locations for this study.

Post-fire data collection was performed after the firepit had been left for at least 24 hours after each firing experiment was completed. This allowed for the sediments to cool down

after each firing event, an important consideration since the cooling process continues the chemical reaction that results in magnetic susceptibility enhancement. Additionally, this was done to ensure my safety and to prevent damage to the geophysical equipment. The measurements were collected from the center of each quadrant (NW, NE, SE, SW) and later (April 2021) a measurement from the center of the firepit was added to maximize information recovery. This magnetic susceptibility data was recorded digitally within the Terraplus KT-10 unit (Terraplus, 2019) and written down in a notebook. The digital data was transferred to a computer and uploaded into a Microsoft Excel file, sorted by grid location and number of times burned.

For each subsequent firing experiment, a measurement was taken before the start of the next experiment, to help meet the pre-determined cooling period time, though this often resulting in longer times between burns, due to poor weather and other unavoidable occurrences. The measurements were collected in the same manner as previously described to keep data collection consistent. On November 9, 2021, magnetic susceptibility data was collected from the experiment locations without the addition of further firing experiments being performed, allowing for a before and after experiment comparison of the study area. Approximately 200 measurements were taking from heated soils.

4.6 Summary

My experiments were designed to simulate expected hearth firing activities practised by precontact subarctic forager groups, in order to determine the degree that magnetic susceptibility was enhanced, and to document the conditions causing these enhancements. I also sought to assess whether the Terraplus KT-10 magnetic susceptibility meter (Terraplus, 2019) had the capability of detecting the anomalies produced by anthropogenic burning. In the next chapter the results of these experiments are discussed.

Chapter 5 Results

This chapter discusses and summarizes the dataset collected during the experimental firing events at the Hogarth Tree Farm using the methods presented in the last chapter. The numeric data collected from each firing experiment (i.e., date, time, temperature, and magnetic susceptibility) are listed in Appendix A. It also details the experiments used to test run the Terraplus KT-10 magnetic susceptibility meter, the 88598 4ch K SD Logger thermocouple, and thermocouple probes at this location in a number of spots and different times in the warm seasons.

5.1 Firing Times

As discussed in Chapter 4, the firing time duration was the only variable that could be directly controlled. Most of the firing experiments sought to simulate comparatively short-term firing events of one hour duration. This sought to reflect what I imagine to be a short-term cooking event. At the end of that one-hour interval, the fire was allowed to burn down and go out. Other fires were maintained for five-plus hour intervals to reflect sustained heating events. Since the experimental fires were allowed to cool down naturally, the experimental heat data was collected for a longer period to allow the thermocouple to characterize the cool down periods in degrees Celsius at one minute time intervals. When multiple firing experiments were being performed at once in multiple grid locations, the thermocouple and associated probes were connected to the short-term experiment being conducted, and then they were also left in the firing pit to record the fire burning out. This sought to create a temperature profile for the entire process of heating through to final cool down (Figures 5.1, 5.2, 5.3 and Appendix A).

5.2 Temperature

Achieving and maintaining stable temperatures during the firing experiments was challenging given the breadth of factors outside of the researcher's control affecting the process. Maintaining the temperature was thought to have been important to keep the chemical change continuing as long as possible, to reduce inter-experiment variability, and to better understand the thermal dynamics of such hearth fires. Firing temperature was controlled by the amount and timing of wood added during the experiments, the condition of said fuel,

and the wind, humidity, and ambient temperature during each day, which were recorded in a project notebook. The conditions were tracked in a notebook maintained by the author to describe each experiment. Appendix A contains the temperature data collected throughout the experimental timeline, but three specific examples will be discussed.

Although many steps of this project involved determining how best to test the equipment types in the boreal forest setting, some interesting results were recorded that reflect the internal dynamics of combustion and heating within small hearths. For example, the temperature results from a one-hour burn conducted on May 18th, 2021, indicated that each of the three 1200°C rated thermocouple probes demonstrated similar patterns reflecting an initial steep temperature increase after initial ignition and fuel addition (Figure 5.1). This was an important step to understand how each of the probes were functioning. While the eastern probe did not experience this initial uptick, it was likely due to a wood piece being inadvertently placed on the probe, insulating it from the temperature increase. Once this piece burned away, the eastern probe achieved temperatures similar to the other two probes and exhibited a subsequent downward trend associated with the cool down of the soil. The wire probe did not display this pattern, and instead revealed two localized maximums. One was approximately 300°C at 137 minutes into the firing period and the other hovered below 500°C between 206-224 minutes until a drastic drop as the soil reached the end of its cool down period (Figure 5.1). This might have reflected subtle changes in wind direction that redirected heat emanating from the nearby central fire. The maximum temperature experienced during this firing event was 744.7°C, being registered on the western probe. This result was hot enough to alter dried clay items to a fully transformed terracotta state (e.g., Rice, 1987), which is typical for precontact pottery in this area; this fired clay would still be somewhat porous but if the clay was part of a pottery vessel it would not return to its original state. Additionally, this means that the Curie temperature for Hematite was reached.

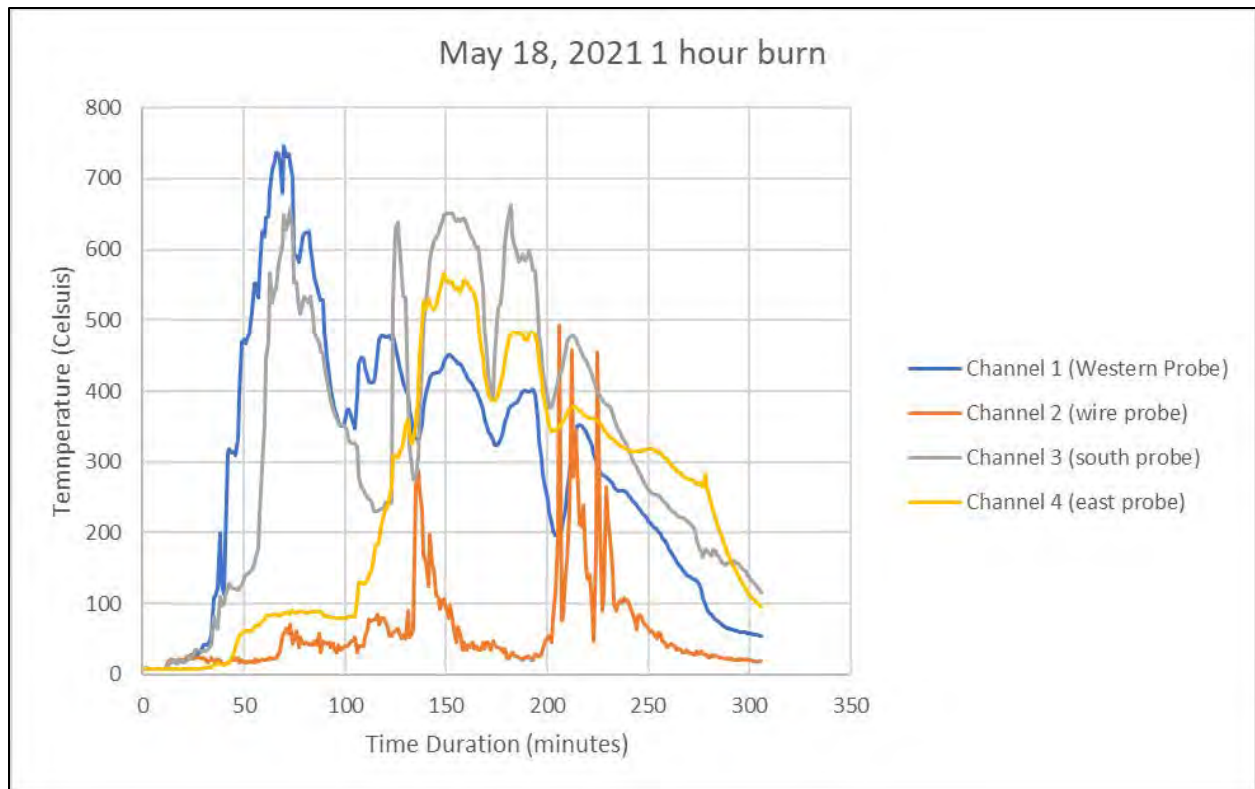


Figure 5.1 Results of May 18th, 2021, with a one-hour firing event plus the associated cooldown.

The temperature profile from May 18, 2021 (Figure 5.1) revealed a dramatically different temperature profile from the May 29, 2021, experiment (Figure 5.2). While the data from May 18th revealed a general consistency between the probes, temperature data from May 29th (Figure 5.2) is devoid of any such pattern. Only the south probe appeared to consistently track the temperature of this firing event throughout, experiencing a maximum temperature of 708.2°C. The wire probe experienced inconsistent temperature measurements, peaking at 668.8°C, however, it usually hovered below 100°C. Once again, the irregularities experienced by the probes could potentially have been from wood falling on the probes and insulating them.

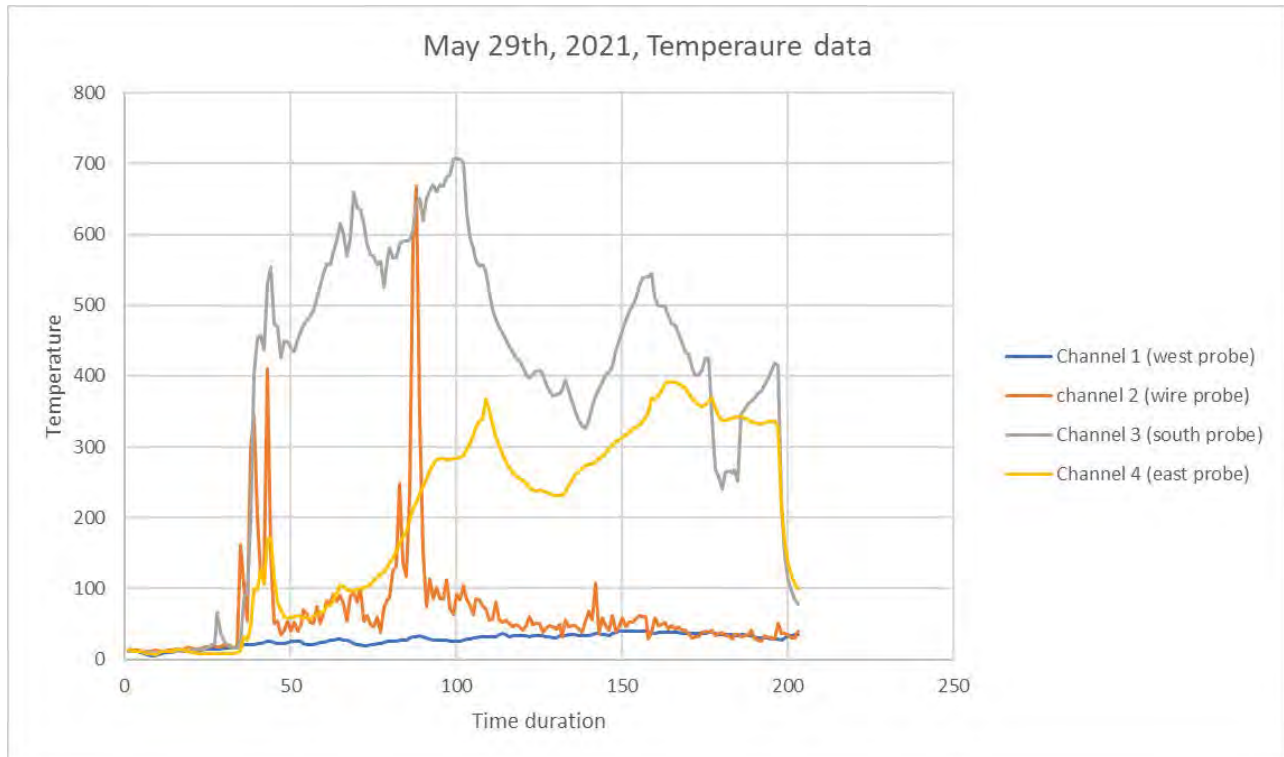


Figure 5.2 May 29, 2021, temperature results of one hour firing event, plus associated cooldown.

The temperature data illustrated in Figure 5.2 highlights the difficulty in attempting to consistently recreate temperature profiles during open pit firing events. While factors affecting firing heat and duration were usually controlled, sometimes environmental factors such as air temperature, rain, wind direction and speed intervened to affect the experiments. Though the actual wind speed was unknown, it was noted as ‘brisk’ and consistently coming from an SSE direction, which directly affected the temperature readings from the eastern, southern and wire probes. Although there was variation, this would also be consistent with conditions in the ancient past.

The temperature data from a third firing event on September 16, 2021, was recorded (Figure 5.3). Similar to Figure 5.2, ambiguous temperature patterns were recorded by the probes during this short-term firing event. Only the southern probe registered sustained heat for the duration of the fire when wood was added, reaching a maximum of 713.8°C. The east probe and wire probe evinced some heating but not until almost a full hour after the final piece of wood was added to the firing experiment. The eastern probe experienced about 100 minutes

of gradual temperature increase followed by a short-duration peak of approximately 240°C. The wire probe did the reverse of this, peaking quickly at 539.9°C then gradually diminishing until the fire was extinguished. The western probe recorded minimal increase, registering temperatures below 100°C for the duration of the firing experiment, perhaps reflecting instrument error or an insulation effect due to unburned wood blocking heat to the sensor.

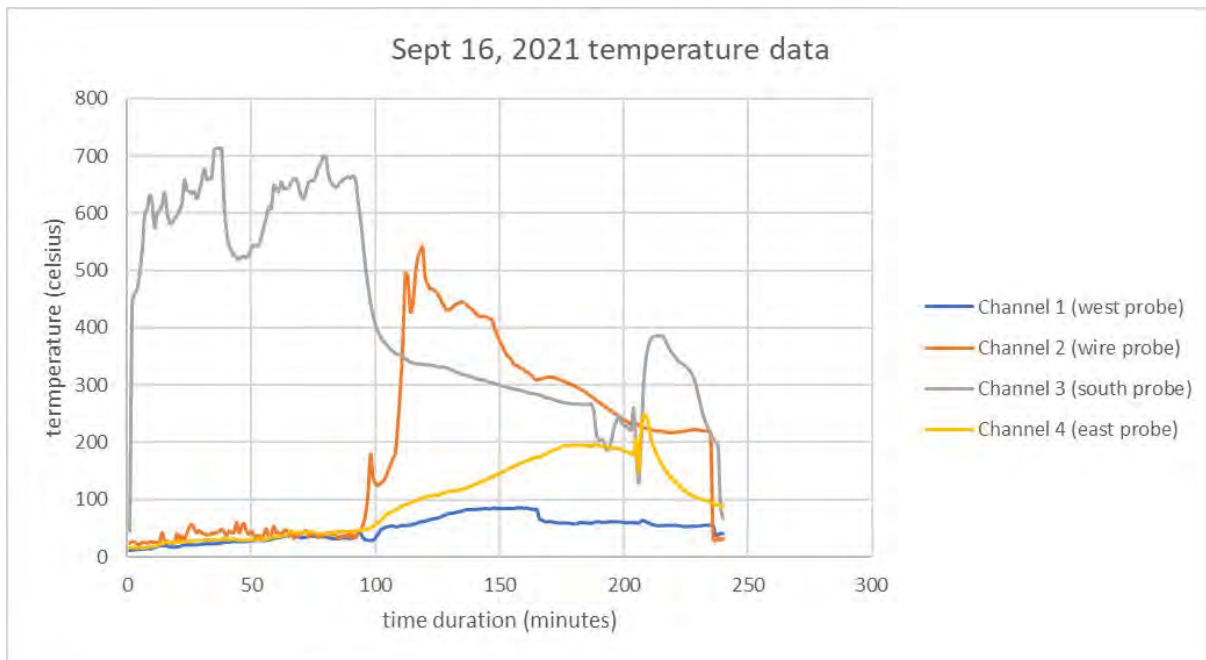


Figure 5.3 September 16th, 2021, temperature data for one hour firing event plus associated cooldown.

Lastly, the temperatures were recorded by the probes during a long-term firing performed in late October 2021 (Figure 5.4). Over 6.5 hours (400 minutes) in duration, each of the four probes briefly reached over 800°C, the highest temperature of 832.5°C being recorded on the wire probe. All the 1200°C probes experienced the same pattern of heating: a sharp increase between 0 and 120 minutes, a leveling out until about 210 minutes, and then a gradual decline associated with a curtailment of new fuel.

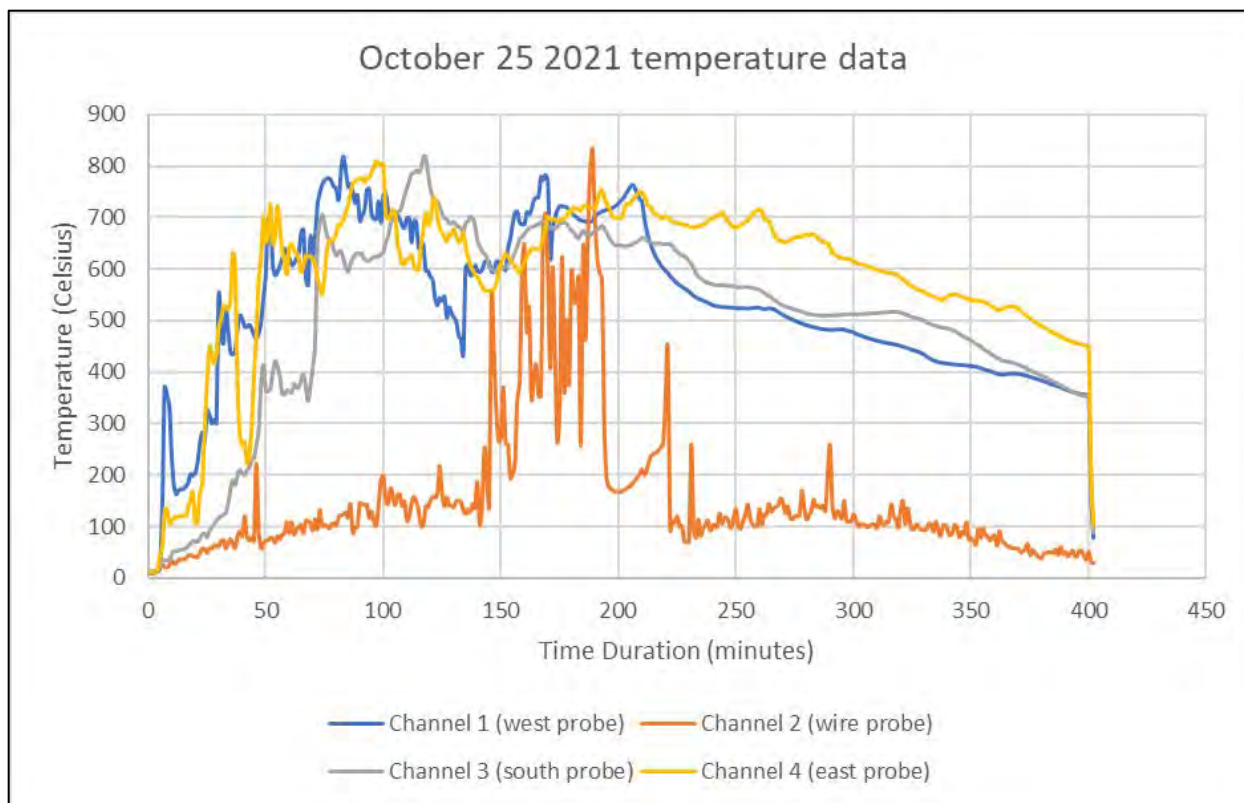


Figure 5.4 The Oct 25, 2021 temperature data of a five plus hour firing event plus associated cooldown.

These temperature graphs reveal that a consistent temperature profile was not achieved (Figures 5.1-5.4). However, the temperature data revealed that even short-term firing events could exceed 700°C, easily surpassing the Curie temperature for hematite. This means that even short-term fires were hot enough to start the chemical transformation to magnetite and maghaemite to enhance the magnetic susceptibility and achieved sufficient heat to allow transformation of clay to the terracotta stage (Rice, 1987).

5.3 Magnetic Susceptibility

The magnetic susceptibility experimental data was collected throughout the spring and summer of 2020 and 2021, culminating with the last data gathered on November 9th, 2021. A total of 571 susceptibility measurements were recorded by the Terraplus KT-10 magnetic susceptibility meter to address the experimental objectives. These data are discussed here in terms of the context of their collection: baseline versus post-fire. Every magnetic susceptibility

measurement was collected using the Standard Unit (SI), denoted by k. Magnetic susceptibility data was uploaded to and organized in Microsoft Excel for analysis.

5.3.1 Baseline

A total of 368 baseline magnetic susceptibility data points were collected using the test pits outside of the grid and the pre-burn firing data gathered from within the grid whenever a new firepit was established. Collected from the locations outlined above (Figure 4.9), the baseline measurements represent the natural magnetic susceptibility of the study area. The mean of the baseline data is 0.00577k with a standard deviation of 0.00111k. Between 0.00952k and 0.0022k was the range of this dataset. A full list of the baseline magnetic susceptibility measurements is included in Appendix B.

The frequency distribution of this data revealed a 'near perfect' normal distribution (Figure 5.5). One standard deviation from the mean (contained in bin 8) ranges from .00459 to .00681 (Bin 5 to 10), while two standard deviations range from .00348 to .00792 (Bin 3 to Bin 12). Statistical extremes beyond 2.0 standard deviations represent a small part of the range of variation in the baseline data. No readily evident explanation for these extreme values were noted during data collection. The 1.0 and 2.0 standard deviation limits are treated as references to evaluate the strength/direction of magnetic susceptibility response to the experimental firing, discussed in more detail below.

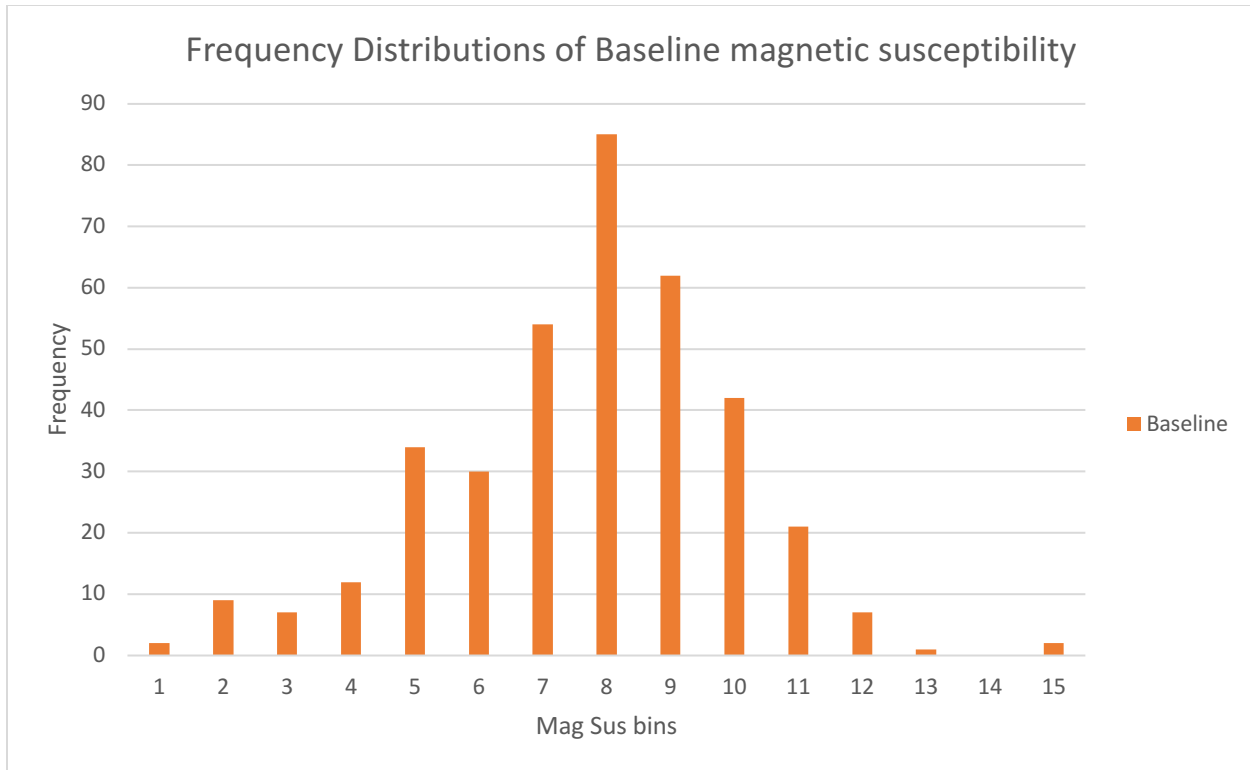


Figure 5.5 Frequency distribution of baseline magnetic susceptibility data. Bins are 0.0005k in size, starting at 0.0022k to 0.0107k. This data was collected throughout the experimental timeline.

The frequency distribution of the baseline magnetic susceptibility data suggests a normal distribution, indicating only variation that might be expected deriving from natural sources within the baseline data. Due to the lack of spatial patterning, the six higher values observed in Figures 4.9 and 5.7, are considered to reflect natural variation, though the exact cause is unknown. When fired, these higher values would ideally result in further enhancement, however, these locations could also demonstrate susceptibility reduction. This will be more fully explored in section 6.4. Approximately 68.7% (253/368) of the baseline magnetic susceptibility data falls within one standard deviation of the mean, closely aligning with the expected 68% usually observed within 1 sigma. Similarly, 94.8% (349/368) of the values fall within two standard deviations of the mean, with the expectation for normal distributions being 95%. Both percentages provided reassurance that the gathered magnetic susceptibility data is normally distributed.

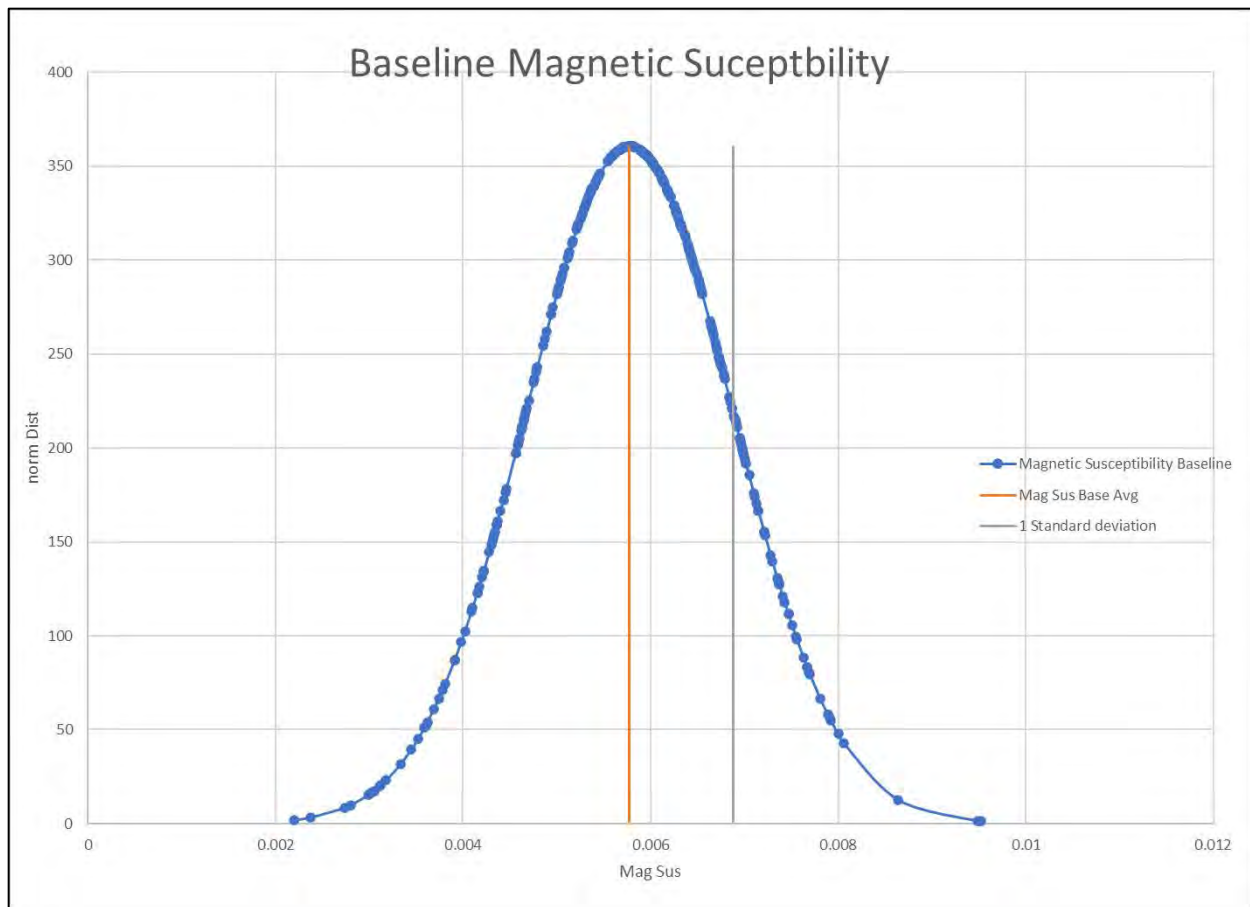


Figure 5.6 Baseline magnetic susceptibility within a bell curve distribution. Each point on the graph is 1.0 baseline data point (collected throughout the experimental timeline).

Also under consideration is the overall change of the magnetic susceptibility within each experimental firepit throughout the timeline. Comparing the natural magnetic susceptibility data to that after the firing experiments was important to document notable variability in the baseline data that might hinder the interpretation of the post-firing results. The location of baseline data values relative to the statistical distribution of those values, and six measurements within the experimental grid are reported to be more than one standard deviation above the 'baseline' mean (Figure 5.7). The mean of the baseline data is the lower limit of the green data labels, while the lower limit of the adjacent colours (blue and yellow) represents one standard deviation away from the mean in both positive and negative directions. While the remaining colours (black and red) represent two standard deviations

above and below the mean. As discussed earlier, the results from the six higher value measurements (highlighted below in yellow and red), will be discussed in section 6.4.

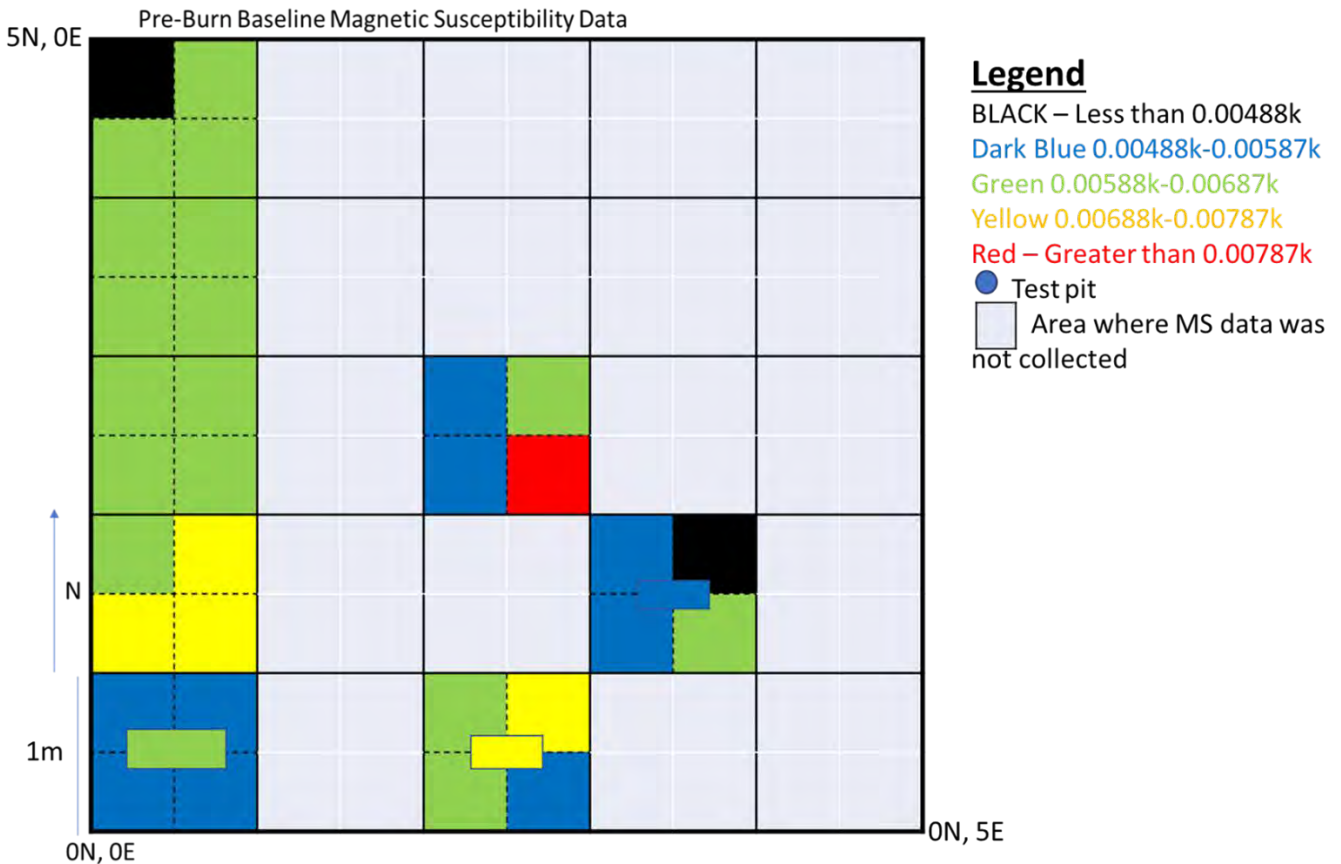


Figure 5.7 Baseline magnetic susceptibility data, taken from experimental fire pits, collected prior to the first experiment conducted within each location. Yellow and red measurements represent areas where the datapoint was one standard deviation above the mean or higher in value.

5.3.2 Experiment Data

During this study, 203 magnetic susceptibility datapoints were collected as/after firing experiments occurred. Results generated from within each experiment fire pit reveal an average magnetic susceptibility of 0.00681k with a standard deviation of 0.00127k (Table 5.1). The raw magnetic susceptibility measurements from the fire pit locations were collected throughout the experiment timeframe, as the Terraplus KT-10 device displays and saves the measurements as scientific notation. To make the data easier to interpret, it was translated to

numeric notations to make it easier to subject to statistical analysis. Appendix B also contains the fired magnetic susceptibility data as a part of the full list of collected experimental data.

Table 5.1 Collected Magnetic Susceptibility Data

Northing	Easting	Location of m	Pre-burn mea	Pre-burn mea	Post Burn 1 M	Post Burn 1 M	Post Burn 2	Post Burn 2	Post Burn 3	Post Burn 3	post burn 4	post burn 4	Post burn 4	Post burn 4	August 6th m	August 6th m	October 15 m	October 15 m	November 9	November 9
4		0NWQ	4.45*10 ⁻³	0.0045	4.87*10 ⁻³	0.00487	5.14*10 ⁻³	0.00514	4.93*10 ⁻³	0.00493	5.12*10 ⁻³	0.00512	4.75*10 ⁻³	0.00475	4.17*10 ⁻³	0.00417	7.11*10 ⁻³	0.00711		0.00711
4		0NEQ	6.15*10 ⁻³	0.00615	5.81*10 ⁻³	0.00581	4.66*10 ⁻³	0.00466	6.13*10 ⁻³	0.00613	4.15*10 ⁻³	0.00415	5.55*10 ⁻³	0.00555	5.26*10 ⁻³	0.00526	7.02*10 ⁻³	0.00702		0.00702
4		0SEQ	6.49*10 ⁻³	0.00649	6.86*10 ⁻³	0.00686	5.10*10 ⁻³	0.0051	6.56*10 ⁻³	0.00656	4.93*10 ⁻³	0.00493	6.27*10 ⁻³	0.00627	5.15*10 ⁻³	0.00515	6.37*10 ⁻³	0.00637		0.00637
4		0SWQ	6.87*10 ⁻³	0.00687	5.11*10 ⁻³	0.00511	5.50*10 ⁻³	0.0055	5.49*10 ⁻³	0.00549	5.01*10 ⁻³	0.00501	6.14*10 ⁻³	0.00614	6.03*10 ⁻³	0.00603	7.87*10 ⁻³	0.00787		0.00787
4		0Center									4.93*10 ⁻³	0.00493	6.88*10 ⁻³	0.00688	7.26*10 ⁻³	0.00726	6.79*10 ⁻³	0.00679		0.00679
3		0NWQ	6.48*10 ⁻³	0.00648	6.28*10 ⁻³	0.00628	6.89*10 ⁻³	0.00689			6.11*10 ⁻³	0.00611	6.75*10 ⁻³	0.00675	6.61*10 ⁻³	0.00661	6.58*10 ⁻³	0.00658		0.00658
3		0NEQ	5.71*10 ⁻³	0.00571	6.41*10 ⁻³	0.00641	6.83*10 ⁻³	0.00683			5.52*10 ⁻³	0.00552	7.64*10 ⁻³	0.00764	6.63*10 ⁻³	0.00663	7.44*10 ⁻³	0.00744		0.00744
3		0SEQ	6.36*10 ⁻³	0.00636	6.55*10 ⁻³	0.00655	7.29*10 ⁻³	0.00729			5.91*10 ⁻³	0.00591	8.09*10 ⁻³	0.00809	8.40*10 ⁻³	0.0084	8.90*10 ⁻³	0.0089		0.0089
3		0SWQ	5.96*10 ⁻³	0.00596	6.27*10 ⁻³	0.00627	10.2*10 ⁻³	0.0102			5.73*10 ⁻³	0.00573	6.97*10 ⁻³	0.00697	7.08*10 ⁻³	0.00708	7.73*10 ⁻³	0.00773		0.00773
		0Center									5.73*10 ⁻³	0.00573	7.90*10 ⁻³	0.0079	6.21*10 ⁻³	0.00621	7.23*10 ⁻³	0.00723		0.00723
2		0NWQ	6.30*10 ⁻³	0.0063	7.09*10 ⁻³	0.00709	5.84*10 ⁻³	0.00584	6.89*10 ⁻³	0.00689					7.10*10 ⁻³	0.0071	7.52*10 ⁻³	0.00752		0.00752
2		0NEQ	6.41*10 ⁻³	0.00641	6.27*10 ⁻³	0.00627	4.23*10 ⁻³	0.00423	5.23*10 ⁻³	0.00523					6.47*10 ⁻³	0.00647	8.04*10 ⁻³	0.00804		0.00804
2		0SEQ	6.55*10 ⁻³	0.00655	5.08*10 ⁻³	0.00508	4.86*10 ⁻³	0.00486	2.42*10 ⁻³	0.00242					6.04*10 ⁻³	0.00604	6.58*10 ⁻³	0.00658		0.00658
2		0SWQ	6.27*10 ⁻³	0.00627	6.75*10 ⁻³	0.00675	6.69*10 ⁻³	0.00669	7.33*10 ⁻³	0.00733					6.35*10 ⁻³	0.00635	6.22*10 ⁻³	0.00622		0.00622
		0Center									7.84*10 ⁻³	0.00784			8.57*10 ⁻³	0.00857	8.60*10 ⁻³	0.0086		0.0086
1		0NWQ	6.66*10 ⁻³	0.00666	6.75*10 ⁻³	0.00675									5.14*10 ⁻³	0.00514	6.23*10 ⁻³	0.00623		0.00623
1		0NEQ	7.47*10 ⁻³	0.00747	6.38*10 ⁻³	0.00638									5.60*10 ⁻³	0.0056	6.23*10 ⁻³	0.00623		0.00623
1		0SEQ	7.81*10 ⁻³	0.00781	4.95*10 ⁻³	0.00495									7.28*10 ⁻³	0.00728	7.39*10 ⁻³	0.00739		0.00739
1		0SWQ	7.28*10 ⁻³	0.00728	7.03*10 ⁻³	0.00703									7.94*10 ⁻³	0.00794	7.09*10 ⁻³	0.00709		0.00709
		0Center			7.05*10 ⁻³	0.00705									8.31*10 ⁻³	0.00831	7.19*10 ⁻³	0.00719		0.00719
0		0NWQ	5.05*10 ⁻³	0.00505	7.18*10 ⁻³	0.00718									7.38*10 ⁻³	0.00738	6.73*10 ⁻³	0.00673		0.00673
0		0NEQ	5.71*10 ⁻³	0.00571	7.43*10 ⁻³	0.00743									7.07*10 ⁻³	0.00707	8.36*10 ⁻³	0.00836		0.00836
0		0SEQ	5.95*10 ⁻³	0.00595	4.99*10 ⁻³	0.00499									5.86*10 ⁻³	0.00586	6.43*10 ⁻³	0.00643		0.00643
0		0SWQ	5.88*10 ⁻³	0.00588	7.03*10 ⁻³	0.00703									7.03*10 ⁻³	0.00703	7.16*10 ⁻³	0.00716		0.00716
0		0Center			6.72*10 ⁻³	0.00672									8.35*10 ⁻³	0.00835	7.41*10 ⁻³	0.00741		0.00741
1		0NWQ	6.32*10 ⁻³	0.00632	7.01*10 ⁻³	0.00701					4.19*10 ⁻³	0.00419			8.23*10 ⁻³	0.00823	6.60*10 ⁻³	0.0066		0.0066
1		0NEQ	5.81*10 ⁻³	0.00581	7.01*10 ⁻³	0.00701					4.98*10 ⁻³	0.00498			6.62*10 ⁻³	0.00662	7.01*10 ⁻³	0.00701		0.00701
1		0SEQ	5.97*10 ⁻³	0.00597	5.97*10 ⁻³	0.00597					6.06*10 ⁻³	0.00606			5.82*10 ⁻³	0.00582	6.16*10 ⁻³	0.00616		0.00616
1		0SWQ	5.36*10 ⁻³	0.00536	7.66*10 ⁻³	0.00766					4.47*10 ⁻³	0.00447			6.86*10 ⁻³	0.00686	6.90*10 ⁻³	0.0069		0.0069
		0Center			5.96*10 ⁻³	0.00596	6.21*10 ⁻³	0.00621			4.45*10 ⁻³	0.00445			6.00*10 ⁻³	0.006	6.51*10 ⁻³	0.00651		0.00651
2		0NWQ	5.83*10 ⁻³	0.00583	6.45*10 ⁻³	0.00645	6.76*10 ⁻³	0.00676	7.77*10 ⁻³	0.00777					6.27*10 ⁻³	0.00627	7.23*10 ⁻³	0.00723		0.00723
2		0NEQ	6.28*10 ⁻³	0.00628	7.05*10 ⁻³	0.00705	6.30*10 ⁻³	0.0063	9.29*10 ⁻³	0.00929					10.1*10 ⁻³	0.0101	7.99*10 ⁻³	0.00799		0.00799
2		0SEQ	9.49*10 ⁻³	0.00949	7.54*10 ⁻³	0.00754	6.17*10 ⁻³	0.00617	9.74*10 ⁻³	0.00974					8.88*10 ⁻³	0.00888	7.15*10 ⁻³	0.00715		0.00715
2		0SWQ	5.58*10 ⁻³	0.00558	7.76*10 ⁻³	0.00776	6.17*10 ⁻³	0.00617	8.76*10 ⁻³	0.00876					10.2*10 ⁻³	0.0102	6.98*10 ⁻³	0.00698		0.00698
2		0Center			6.90*10 ⁻³	0.0069	8.08*10 ⁻³	0.00808	7.05*10 ⁻³	0.00705					9.48*10 ⁻³	0.00948	7.50*10 ⁻³	0.0075		0.0075
0		0NWQ	7.37*10 ⁻³	0.00737											6.81*10 ⁻³	0.00681				0.00681
0		0NEQ	8.64*10 ⁻³	0.00864											6.21*10 ⁻³	0.00621				0.00621
0		0SEQ	5.29*10 ⁻³	0.00529											7.83*10 ⁻³	0.00783				0.00783
0		0SWQ	6.96*10 ⁻³	0.00696											6.99*10 ⁻³	0.00699				0.00699
0		0Center			7.67*10 ⁻³	0.00767									6.51*10 ⁻³	0.00651				0.00651

Using the same frequency distribution ‘bins’ as the baseline data in Figure 5.5, Figure 5.8 summarizes the experimental data gathered from fire locations. Using the same sorting increments allowed a visual comparison between the data in the discussion. As can be seen in Figure 5.6, the fired magnetic susceptibility data centralized around bin 10, slightly higher than the baseline data. Further, bins 2 and 3 do not contain data points, which may contribute to a distortion of the bell curve. The absence of data points in these bins will be discussed further in the following chapter, however, the singular data point in bin 1 was kept in the survey because this point was still within the range established by the baseline dataset.

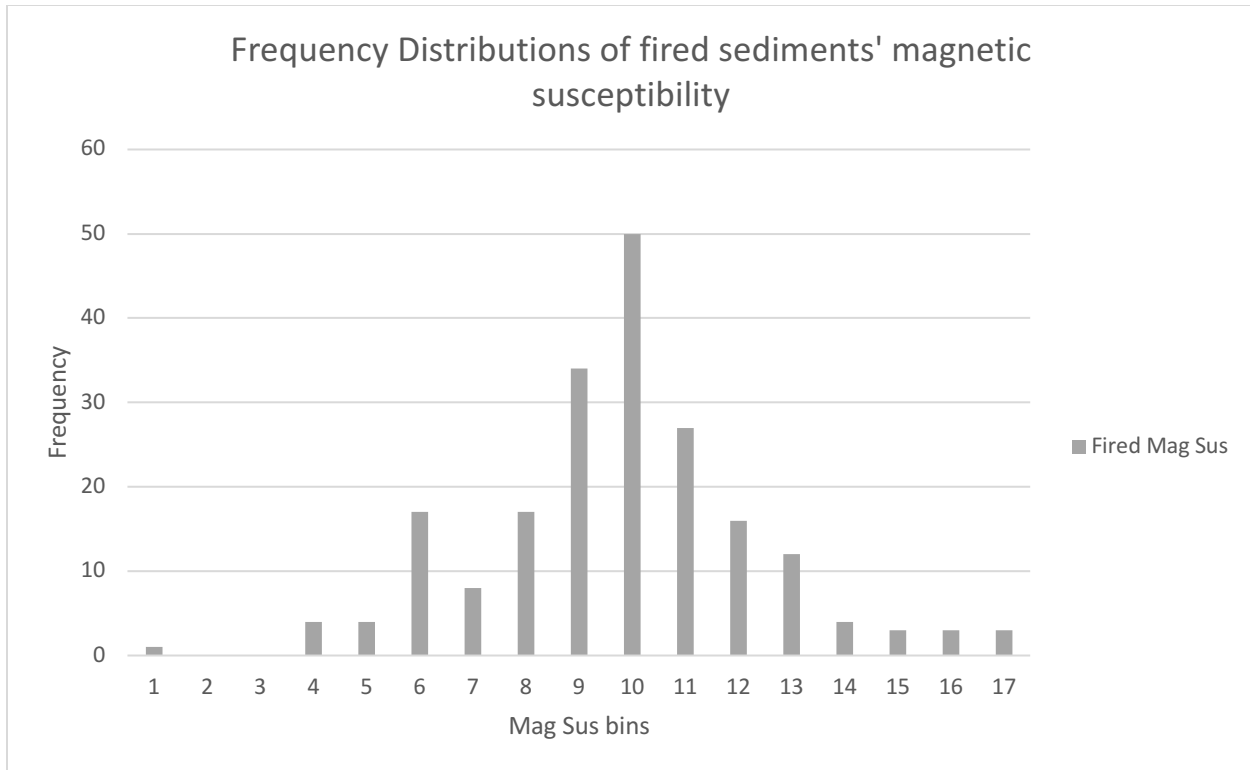


Figure 5.8 Fired magnetic susceptibility frequency distribution. Bins are sized 0.0005k from 0.0022k to 0.0107k. Collected throughout the experimental timeline.

To further confirm the normalcy of the fired magnetic susceptibility data, they were placed into a frequency distribution, which did conform to a bell curve (Figure 5.9). This demonstrates that most of the data falls within the expected shape of a normal distribution, the tails are different shapes due to the low measurements previously discussed. While it causes a slight distortion in the curve, since the data point occurs within the range of the natural dataset, it was kept within the dataset to be statistically valid. Approximately, 71.9% (146/203) of the measurements fall within one standard deviation from the mean, which is higher than what would be expected in a normal distribution, 93.1% (189/203) of the data falls within two standard deviations from the mean, slightly lower than the expected percentage (95%) in a normal distribution of data. As can be seen below, the fired experimental data does not exhibit the expected symmetry seen in other normal distributions (Figure 5.9). This could reflect the anthropogenic modification of the mineral matrix that occurred during the experiments.

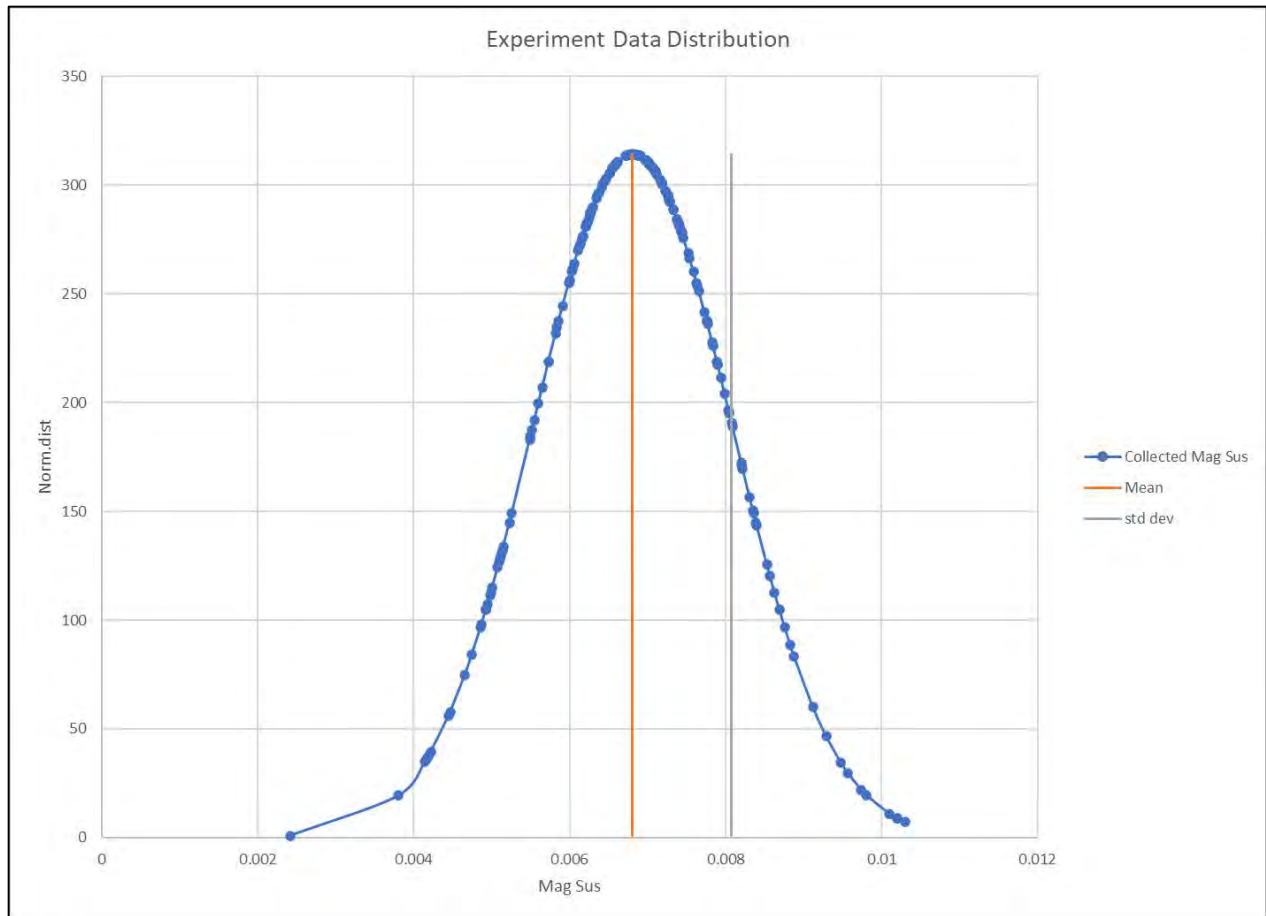


Figure 5.9 Experimental fire magnetic susceptibility data collected from the experimental firing grid, throughout the full duration of the experiments.

In an attempt to determine the overall magnetic susceptibility changes caused by the firing events, the final fired magnetic susceptibility data gathered from the fire pits was plotted in its location of collection (Figure 5.10). These 41 measurements were collected on November 9th, 2021. The numeric scale was produced by creating a dataset that encompassed the baseline data, and the fired data collected on November 9th, 2021. Comparing the November 9th dataset to the baseline allowed the total effect of the culminative firing experiments to natural sedimentary susceptibility response. The scale in the figure below was produced similarly to the baseline figure above (Figure 5.7), however the numeric values have been altered to include the susceptibility data collected on November 9th, 2021.

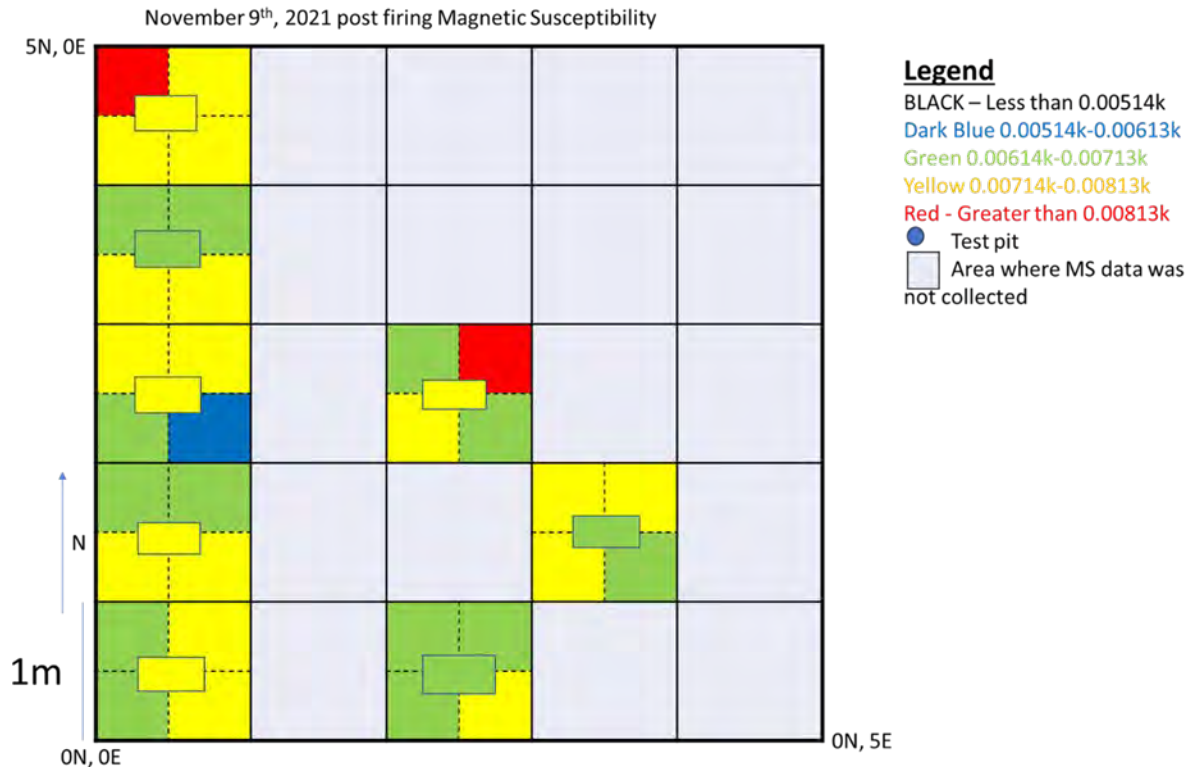


Figure 5.10 Magnetic susceptibility data taken from experimental fire pits collected on November 9th, 2021. This data was collected after all firing experiments were completed. Yellow and red measurements represent areas where the datapoint was one standard deviation above the mean of higher in value.

5.4 Summary

This chapter summarized the temperature and magnetic susceptibility data collected as a baseline prior to firing (Figure 5.5) and the heated soil data (Figure 5.8). Both data sets were considered using simple frequency distributions and normalized distributions to assess the naturally occurring variability and the statistical strength of the post-fire transformations. Initial evaluation suggested that the experiments sufficiently heated the soils to induce the chemical changes necessary to increase the magnetic susceptibility, although no discernable patterns were noted that suggested cumulative susceptibility change from repeated firing.

The main objective of the experiments was to understand the pre-firing ‘baseline’ nature of magnetic susceptibility in the sediments, and then examine what, if any, changes were observed under different firing conditions. I also evaluated the Terraplus KT-10, the 88598 4ch K SD Logger thermocouple, and thermometer under field experimental conditions. The

temperature data collected demonstrated the implications of uncontrollable variables evident in the outdoor field trials, most notably with highly variable ambient temperature, humidity, and wind pattern effects. The investigation demonstrated that the open-hearth fires expected of subarctic hunter-gatherers could readily achieve temperatures hot enough to initiate the chemical reactions required to transform magnetic susceptibility and to fire pottery vessels.

Chapter 6 Discussion

6.1 Introduction

This chapter discusses and interprets the results presented in Chapter 5. Four main research questions were addressed during this project:

- 1) Did the experimental firing events enhance the magnetic susceptibility of sediments?
- 2) What was the minimum temperature needed to change the magnetic susceptibility signature of the natural soil/sediment?
- 3) What level of interpretation could be made from the magnetic susceptibility data and
- 4) How effectively did the Terraplus KT-10 detect this change?

Each of these research questions are discussed in the following sections.

6.2 Did the experiments enhance the magnetic susceptibility of the sediments?

To determine if the sediments subjected to experimental burning experienced magnetic susceptibility enhancement, the previously shown baseline frequency distribution (Figure 5.5) was compared to results after firing (Figure 5.8). The distributions of both data sets were examined using the same bin sizes to visually represent the impact of firing events upon magnetic susceptibility (Figure 6.1). Results presented here show that the baseline dataset is centralized from bins 6 to 11 with the highest frequency falling in bin 8 (0.0057-0.0062k). Bin 8 also contained the baseline mean value, with the 1.0 standard deviation range including bins 6 to 11. This represented 66.7% of the variance from the mean. The fired magnetic susceptibility data was distributed further to the right on the horizontal axis, with the most frequent firing score being in bin #10 (which also contains the mean). The bins associated with 1.0 standard deviation range from bin 7 to 12, demonstrated the maintenance of a normal distribution. The data also revealed that the upper end of the range in the fired data was higher than the baseline susceptibility measurements, and with fewer data points occupying the bins at the lower range limit (Figure 6.1). The comparative from the data sets shows that the firing experiments did indeed enhance the magnetic susceptibility of the natural soils.

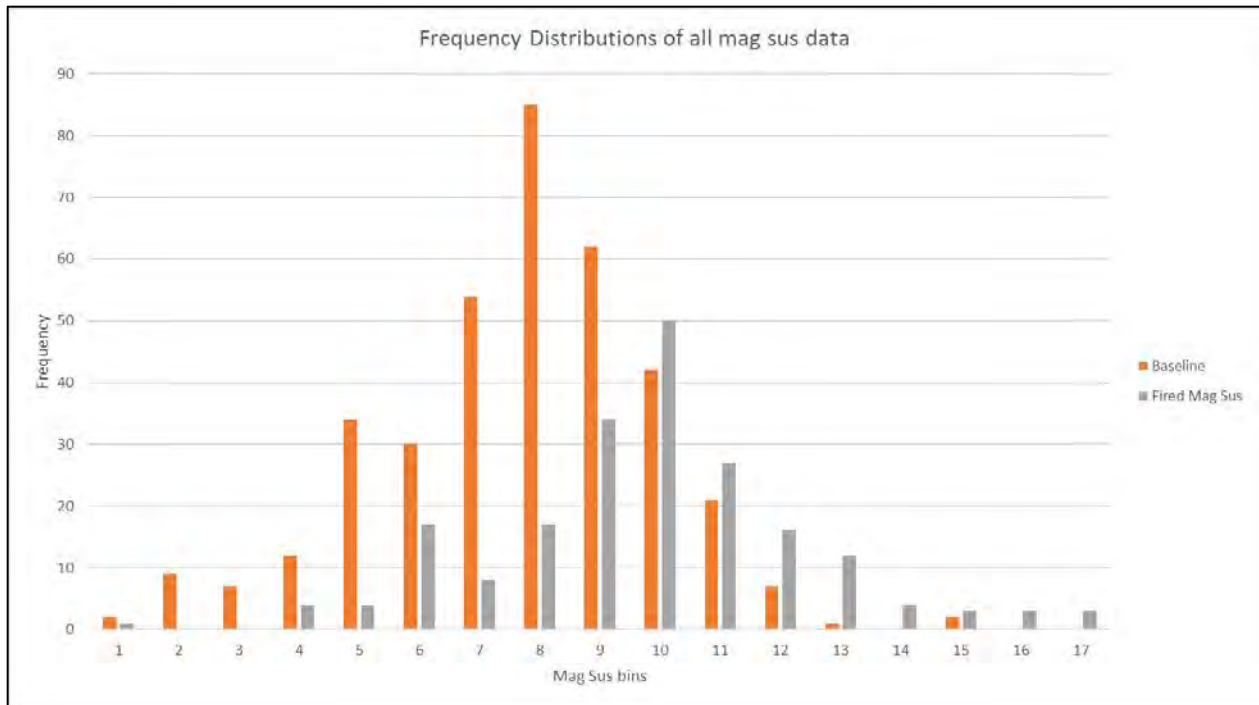


Figure 6.1 Frequency distributions for the baseline and fired magnetic susceptibility data collected throughout the experiment's duration. Figures 5.5 and 5.8 were combined to place in the same bins for comparison. Bins are 0.0005k in size, between 0.0022k and 0.0107k.

To test the statistical strength of the difference between the baseline and fired magnetic susceptibility, an unequal variance, two-tailed T-test was performed to compare the two datasets. The null hypothesis being tested was that the firing experiments did not change the magnetic susceptibility of the sedimentary matrix to a statistically significant extent. This parametric test was selected since both data sets approximate a normal distribution, but the baseline and fired datasets are of unequal size (368 and 203 measurements, respectively) and variance ($1.26 \cdot 10^{-6}$ and $1.60 \cdot 10^{-6}$, respectively). In this circumstance, the null hypothesis is that firing did not affect the magnetic susceptibility of the sediments, while the alternate hypothesis proposes that such transformation occurred to a statistically significant extent. The data sets show that transformation occurred, while the T test assessed whether this transformation was statistically significant (Figure 6.1). In this case if the p-value was lower than the threshold of significance (i.e., $p < 0.05$) then the difference between the samples was not deemed to be due to chance and the null hypothesis would be false. The T-test generated a p-value of 6.73644

$*10^{-20}$, well below the 0.05 value, thereby confirming that the difference between fired and baseline magnetic susceptibility was statistically significant.

The comparison of the frequency distributions demonstrated the viability of magnetic susceptibility as an archaeogeophysical characterization technique within a subarctic context (Figure 6.1). It also demonstrated that the subarctic sediments react similarly to sediments in other regions when heated through an open pit firing process (Kvamme, 2017; Tite and Mullins, 1972; Witten, 2014).

6.3 What was the minimum firing intensity needed to change the magnetic susceptibility within the sedimentary matrix?

To determine the minimum firing intensity and duration needed to enhance the magnetic susceptibility, frequency distributions were created to demonstrate variations between the baseline and the firing experiments of short versus long-term duration. Also considered were how the number of firing events in each hearth affected the degree of susceptibility enhancement. The frequency distribution illustrated in Figure 6.2 included the baseline data (gray bars) compared to the distribution of values associated with the short-term (blue) versus long-term (orange) firing events. Of note, the frequency distributions demonstrated the mean values for the three datasets demonstrate a change to higher magnetic susceptibility values. The baseline average was 0.00577k, the short-term average was 0.00665k and long-term average was 0.00714k. This indicated that firing length affects the overall magnetic susceptibility but that the degree of enhancement associated with longer-term firing may not be readily differentiated from the short-term firings. It was evident since the peak values for both short and long-term firing occurred in the same frequency distribution bin, and that the variance strongly overlapped (Figure 6.2). Indeed, the short and long-term firing data mimicked each other in their distribution across the frequency distribution bins (Figure 6.2).

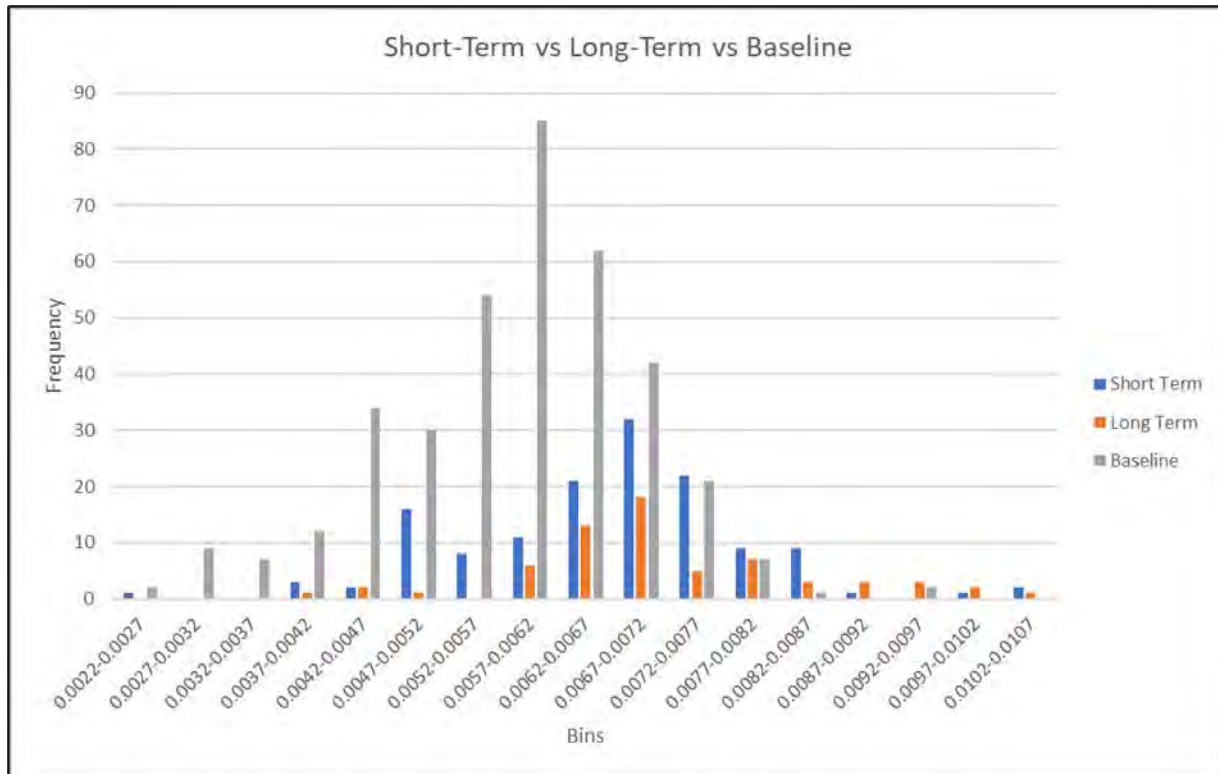


Figure 6.2 Short-term vs long-term vs baseline magnetic susceptibility data frequency distribution.

To test the statistical strength of distinctions between long-term and short-term firing events, T-tests were performed to compare both experiment types to the baseline and to each other. When comparing the baseline to experimental data, the null hypothesis is that the firing events do not affect the susceptibility data. When comparing the short- and long-term firing events the null hypothesis is that the longer firing period do not further enhance the magnetic susceptibility. P-values comparing the baseline to short-term (9.74×10^{-12}) and long-term experiments (2.51×10^{-12}) are both below 0.05, suggested that both experiment types yielded statistically significant differences from the baseline (Table 6.1). This leads to rejection of the null hypothesis and acceptance of the alternate hypothesis. That is, that firing enhances magnetic susceptibility to a statistically significant level. When the two experimental datasets (reflecting different firing durations) were compared, the resulting p-value is 0.00805 (Table 6.1). This value is also below the critical 0.05 value, indicating rejection of the null hypothesis. Given the visual overlap in frequency distributions apparent in Figure 6.2, this was surprising but does indicate that longer firing duration caused a statistically significant increase in

magnetic susceptibility values. I believe that these results might be affected by the small sample size, and further experimentation is needed to confirm this pattern.

Table 6.1 P-Values comparing different magnetic susceptibility datasets. P value of 0.05 or less means the null hypothesis can be rejected.

Firing Event type	Compared to	p value
All Fires Magnetic Susceptibility Data	Baseline	$6.73644 * 10^{-20}$
Long-Term Fires Magnetic Susceptibility Data	Baseline	$2.51 * 10^{-12}$
Short-Term Fires Magnetic Susceptibility Data	Baseline	$9.74 * 10^{-12}$
Short-Term Fires Magnetic Susceptibility Data	Long-Term Magnetic Susceptibility Data	0.00805

The visible shifts in the magnetic susceptibility data between the natural and the fired dataset demonstrated that firing significantly enhanced magnetic susceptibility. Furthermore, the *p* values comparing the baseline, long- and short-term magnetic susceptibility data are all lower than 0.05 threshold and confirm that the null hypotheses were false. The *p* value does not indicate the strength of the difference between datasets, but it does indicate that they exhibit statistically significant differences. This confirms that the conducted firing experiments were able to enhance the magnetic susceptibility of sedimentary matrix within the grid locations, and that some degree of enhanced magnetic susceptibility occurred with long-term firing.

6.4 What level of interpretation could be made from the magnetic susceptibility data?

Given that there was no readily apparent pattern in enhancement of magnetic susceptibility distinguishable between the number and types of firing events, I then explored whether these data exhibited any spatial patterns within the survey area.

The spatial distribution of magnetic susceptibility values deriving from the experimental hearths was collected at the end of the experiment period (Figure 6.4) and assessed in comparison to the natural magnetic susceptibility data for the same locations that were collected prior to firing (Figure 6.3). The baseline data revealed localized zones with magnetic susceptibility values higher than one standard deviation (yellow and red), with the balance being within one standard deviation or lower than the mean. This suggests naturally occurring variability in magnetic susceptibility can be quite substantial, creating complexity for data interpretation. While the magnetic susceptibility data presented to this point reflects data that was collected after each discrete firing experiment, the November 9th, 2021, dataset represents cumulative magnetic susceptibility recorded at the end of the experiment. This reflected the full extent of enhancement of magnetic susceptibility achieved in each experimental hearth location.

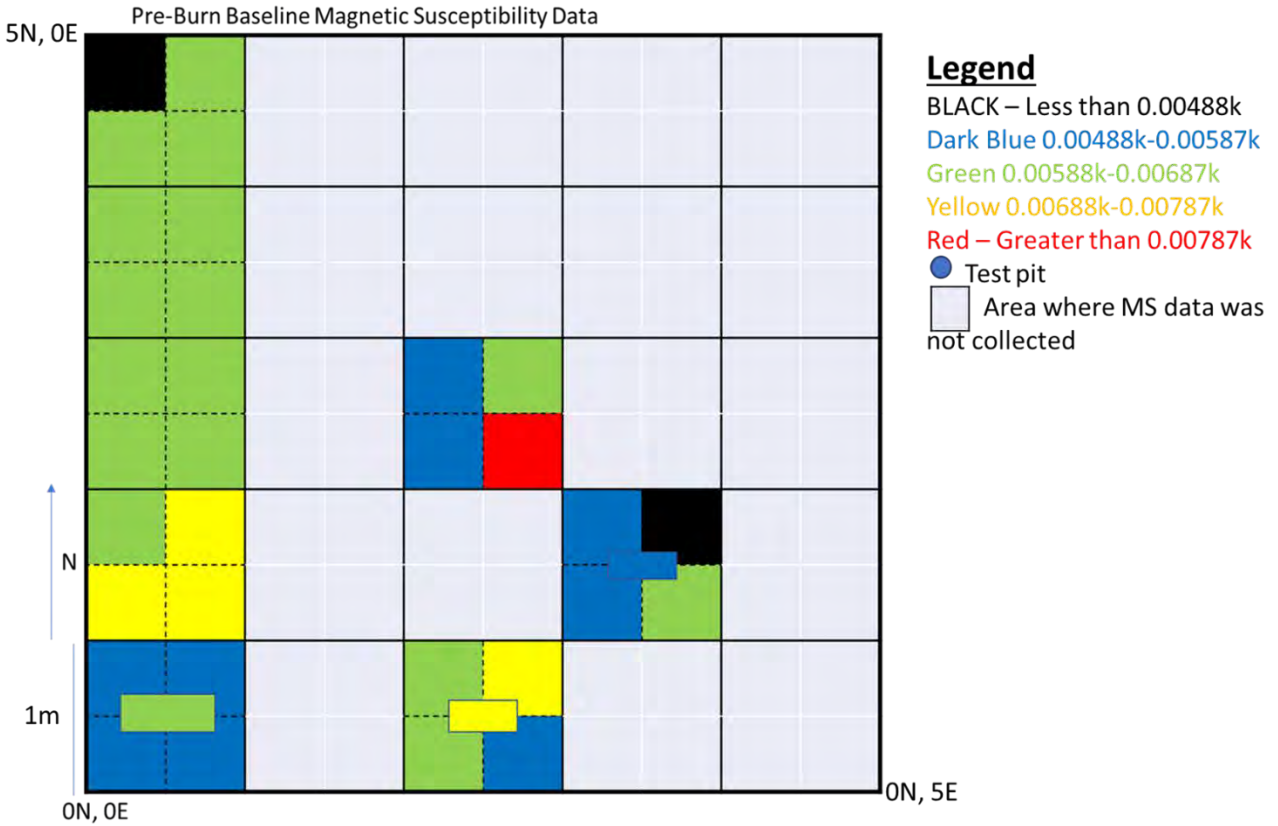


Figure 6.3 Pre-firing experiment baseline data collection throughout the experimental timeline, within grid only. Yellow and red measurements represent areas where the datapoint was one standard deviation above the mean or higher in value.

Blank units within the area represent places where experiments were not conducted, and magnetic susceptibility data was not collected (Figure 6.3). Locations where experiments occurred are colour coded to reflect the statistical distribution of magnetic susceptibility measurements. Except for six locations coded yellow and red (1N, 0E NEQ, SEQ, SWQ, 0N, 2E center, NEQ, 2N, 2E SEQ), the baseline data was devoid of values more than 1 standard deviation of the mean. Perhaps these localized anomalous values reflect intense burning from a forest fire, agricultural processes dating to the first half of the twentieth century, or by the undocumented mineralogical composition of the sediment. This localized variability within the baseline data points to a serious flaw in research design that will be addressed more fully below.

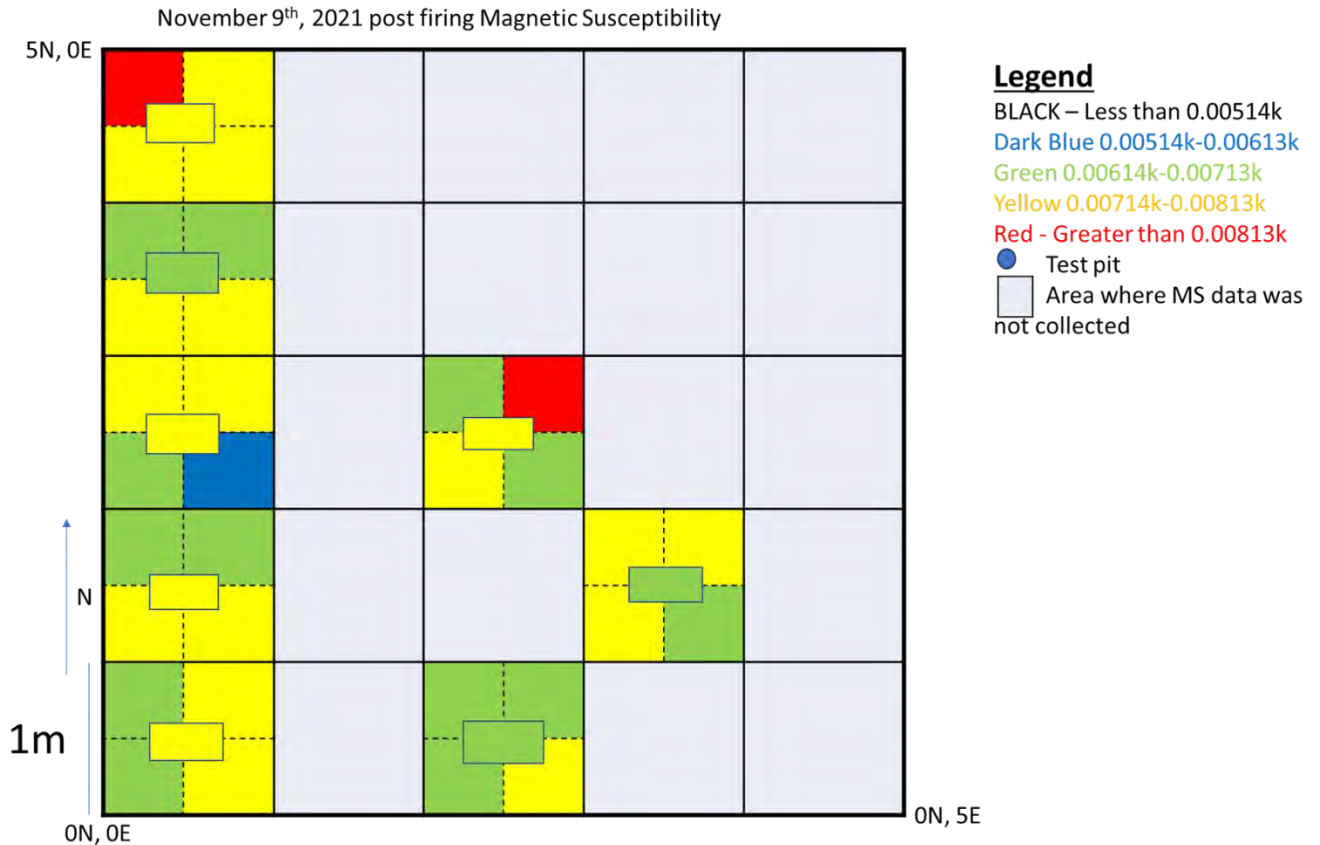


Figure 6.4 Last magnetic susceptibility data collection for this experiment, after last firing experiment performed days previously. Yellow and red measurements represent areas where the datapoint was one standard deviation above the mean or higher in value.

When compared to the baseline presented in Figure 6.3, data presented in Figure 6.4 revealed that enhanced levels of magnetic susceptibility were present, but sometimes this increase was marginal, and in a few locations, there is a reported decline in magnetic susceptibility (Figure 6.5). The latter was unexpected and may reflect the consequences of uncontrolled variables such as unexpected (and unmeasured) heterogeneity in the mineralogical content of the sediment. That is, slight differences in sensor placement upon the sediment surface might have resulted in numbers reflecting interception of different concentrations of ferric minerals. Despite these complications, the experimental hearths coincided with enhanced magnetic susceptibility readings, sometimes more than the one standard deviation above the mean increase.

The overall difference in magnetic susceptibility between the beginning and the end of the experiments was then calculated (Figure 6.5). Unlike the previous grid figures, the colour coordination in Figure 6.5 was not related to the mean or standard deviation of the data, rather the changes between the start of the experiments through the last date of data collection, November 9th, 2021. This was produced to demonstrate if there was a consistent, overall enhancement within the experimental fire pits. As the figure below demonstrates, the individual firepits generally experienced susceptibility enhancement but that the enhancement was not consistent. This could be due to the presence of microscopic minerals within the soil, inconsistent heating experienced by the sediments or user error.

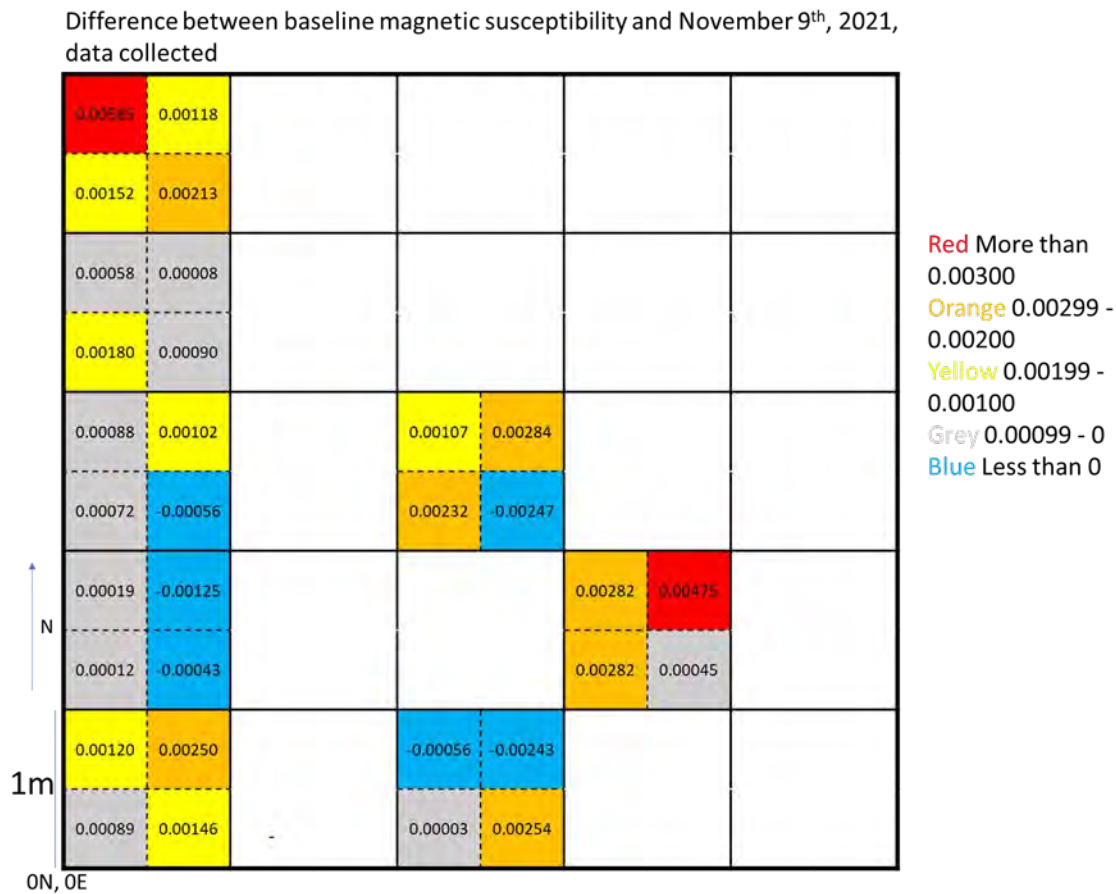


Figure 6.5 Difference between initial, pre-experiment magnetic susceptibility and post-experiment measurements taken on November 9th, 2021.

The geophysical data offered some indications of the location of experimental hearth features, but some data remains rather ambiguous. While the data demonstrated that the

experimental hearths generally enhanced the magnetic susceptibility (Figure 6.5), it also indicated that the spatial distribution of values does not reveal a consistent and unequivocal pattern. Half of the quadrants (16/32) exhibit change in magnetic susceptibility over 0.00100k, with eight measurements presenting change over 0.00200k. The remaining balance of the fire pits exhibited only marginal positive enhancement (10/32 with less than 0.00100k) and six (6/32) measurements demonstrated decreased susceptibility after the experiments were completed. Of these six measurements, four of the decreased values coincided with areas identified with higher value baseline measurements prior to the firing experiments. Each of the experimental firepits exhibited at least one anomalous measurement compared to the baseline data, but that these variations are not sufficiently distinctive from the naturally occurring variability apparent in the baseline data. Hindsight now indicates that the unknown mineralogical makeup of the archaeological sediments is likely a confounding uncontrolled variable affecting the insight gained from the Terraplus KT-10 magnetic susceptibility meter. But those results do indicate that more experiments are required and that other users of this instrument need to know about those variables.

Originally, there were discussions with my supervisor about trying to find a pattern to distinguish between a single versus repeated short-term firing events taking place in one location. This was not possible in the limited data gathered within that specific context and should be explored further with new experiments.

6.5 How effectively did the Terraplus KT-10 detect this change?

The Terraplus KT-10 magnetic susceptibility meter reliably performed the tasks thereby arguing for its inclusion in the archaeologist's toolkit. Being a handheld unit, combined with the intuitive use and reasonable battery life made the unit ideal for field use within a subarctic context. The data storage capability of the device allowed for mass information collection, which the device internally stores by date. Once connected to a computer, the data could be uploaded from the device easily, still sorted by the date the information was gathered. A concern was that when the battery within the device dies, the internal clock and date settings automatically reset, meaning that data had the potential to be registered to a date several years wrong from the date that the data was actually collected. The recording of the magnetic

susceptibility data within a notebook mitigated the minor issues that arose and is recommended.

6.6 Temperature, and Magnetic Susceptibility

Though temperatures were tracked throughout these experiments, there is not enough evidence within this dataset to comment whether a higher firing temperature resulted in a higher magnetic susceptibility measurement. That was beyond the scope of an already large project. As previously discussed (Chapter 3.4, 3.5), sedimentary minerals being heated past the Curie temperature of hematite is what causes the chemical reaction that results in an increase of the sediment's reaction when exposed to an external magnetic field. The temperature data collected (section 5.2) demonstrated that short term firing events can result in temperatures exceeding the Curie temperature of hematite, as well as the temperature required to fire replica pre-contact pottery. Though the experiments conducted are insufficient to fully explore the relationship between the heating temperature and magnetic susceptibility, they revealed that both long- and short-term firing events can produce the necessary temperature to change the magnetic properties of the sedimentary matrix.

6.7 Limitations

While conducting these experiments, and with subsequent analysis of the output, several key ambiguities and limitations became apparent that hindered the effectiveness of both experiments and their interpretation. These limitations can be divided into 1) sedimentary, 2) equipment or 3) human caused constraints.

A key assumption made throughout the experiments was the uniformity of the sedimentary matrix within the experimental grid. Microscopic mineralogical and geochemical variability likely exerted an unmeasured effect on magnetic susceptibility beyond the impact of firing. Determining the chemical composition of the sedimentary matrix, specifically the ratios between the amount of hematite, magnetite and maghaemite, would have aided in defining the amount of susceptibility enhancement possible from the firing experiments. This might have identified chemicals and minerals that interfered or enhanced the chemical reactions caused by the heating of the sediments. Measuring magnetic susceptibility of sediment samples

within a lab context after field measurements would also have allowed sediment preparation by sifting, drying and the removal of rocks, roots, vegetation and other materials. This, of course, would have aided interpretative resolution of the data, but would have constrained evaluation of the Terraplus KT-10 as a tool for rapid field evaluation and data collection. By solely relying on visual inspection to infer sedimentological uniformity, the interpretation of the collected data cannot explicitly demonstrate that the only factor causing the magnetic susceptibility enhancement was the heating of the soils. However, that would have added exponentially to the time, complexity and equipment costs of the project that was designed to be a field-based evaluation.

At issue here is that the experiment design failed to address all of the independent variables affecting the clarity of the results, though this was not unexpected. I suspect that an important unmeasured variable affecting magnetic susceptibility in the baseline data, with subsequent impact upon the firing experiment, was related to the mineralogical content of the fine lacustrine sediments of the test area. These sediments formed part of the Kaministiquia River delta and were likely laid down as glacial outwash deposits into Glacial Lake Minong. As such, the fine well-sorted sediments likely derived from fine glacial outwash deriving from diverse mineralogical sources. While of uniform texture and composition at a macroscopic scale, I suspect that the sediments exhibit localized variability in ferric mineral concentration that might have contributed to the test results. This ends up in a situation whereby the firing experiments generally enhanced magnetic susceptibility to a statistically significant level, but that the uncontrolled variables in the experiment complicated data interpretation. This was not unexpected, since this sedimentological diversity is commonplace in an archaeological context, and with the comparatively subtle shifts in magnetic susceptibility that might derive from anthropogenic transformation, it may be difficult to apply this method as an archaeological prospection and characterization tool to have perfect results. Though a more thorough examination of the excavated test pit sedimentary matrix following previously established soil characterization methods after the field readings could have aided interpretations of the magnetic susceptibility data.

Another possible experimental limitation is the equipment used to measure the magnetic susceptibility. The Terraplus KT-10 device was utilized considering its portability, ideally suited for subarctic archaeological surveys, and it was available through Lakehead University's Department of Anthropology. While the device requires direct contact with the sedimentary matrix, it is only useful for measuring magnetic susceptibility at that point of contact. Other magnetic susceptibility meters, such as Barington and Geonics devices, offer advantages by allowing measurements to greater depths below the surface, so are more widely used in archaeological excavations and feature more efficient data collection. A possible avenue for future research might involve comparison of two or more instruments to measure the same sediment sample under controlled situations.

Further equipment limitations were caused by the digital thermometer and the Type K thermocouple probes. The digital thermometer experienced two shutdowns, one due to power failure and the other being high temperature exposure. The prolonged high temperatures experienced by the type K probes resulted in several of the probes malfunctioning (melting) and requiring replacement throughout the experiment.

As with any experimentation with new methodologies, there is a learning curve associated with applying a new technique. The Terraplus KT-10 was easy and practical to use for field data collection, but processing and analysis was more problematic. When the magnetic susceptibility data was transferred from the device to the computer via USB port, it would seemingly disappear within the software. It was later learned that the computer program saved the magnetic susceptibility data by the date it was collected, as measured by the Terraplus KT-10 device. At one point, I discovered that the device's internal clock was set for 2017 rather than the experimental timeline. While the device was capable of internal digital data storage, care was taken to generate redundant data by manual data recording in a field notebook. The written data was used to cross-check and correct the digital output within Microsoft Excel, and I used that database throughout analysis.

Additionally, my initial inexperience with using the Terraplus KT-10 may have led to inconsistent placement of the data collection point within the center and quadrants in the

firepits, when collecting the geophysical data. This might have been mitigated by repeated measurement at the same location after each firing experiment to assess the degree of variability that might derive from the instrument or how the author handled the instrument. Such evaluation during the baseline data collection might have provided additional information with which to assess the experimental results. Finally, the COVID-19 pandemic resulted in limitations previously discussed in section 4.4.1.

6.8 Summary

Analyzing the magnetic susceptibility data collected throughout experiments led to three conclusions. Firstly, the magnetic susceptibility characteristics of subarctic acidic and organic-rich sediments were consistent with results reported about other sediment types tested in other biomes. That is, when exposed to anthropogenic heating, the sediments experience enhanced magnetic susceptibility. The firing experiments were able to enhance the sediment's susceptibility within the fire pits, regardless of the fire duration or repetition. The frequency distributions (Figure 6.2) demonstrate that after the sediments were fired, the magnetic susceptibility generally increased to a statistically significant degree. Indeed, the mean associated with the fired data nearly exceeds the 1.0 standard deviation interval observed in the baseline data.

With repeated experimental firing events within the same firepit location, however, a cumulative increase in magnetic susceptibility was not as readily evident in the data. Figure 6.5 demonstrates that the repeated short term firing events and the long-term firing events did not exhibit readily interpretable susceptibility enhancement beyond that at the short-term firing locations with fewer fires performed. Contrary to the expectations, this result suggested that the number of firing events and the duration of firing event did not cause the magnetic susceptibility to become further enhanced. While the t-test comparing the short- and long-term firing experiments still produced a p-value (0.00805) that suggests the null hypothesis can be rejected (Table 6.1), further research, as well as more data collection are necessary to determine the extent and interpretability of this difference.

Since some spatial variability in magnetic susceptibility was observed in the baseline data, the experimental firing events did not offer a readily interpretable spatial pattern that indicated the location of the fire pits. When the spatial context of the eight experimental fire pits was considered, some degree of magnetic susceptibility enhancement was observed. However, the pattern was insufficiently robust to unequivocally demonstrate that firing sufficiently explained the enhancement.

The Terraplus KT-10 magnetic susceptibility meter met the expectations required to be an effective field data collection tool. It was portable, easily used, with built in redundancies for collecting data. This geophysical device detected the susceptibility changes occurring within the sedimentary context caused by the experimental firing events. Though post-experiment processing was a challenge due to the software and battery resetting issues, these problems were easily mitigated due to built-in abilities of the program and back up data collection using a notebook. I believe that interpretative difficulties deriving from the experiment reflect as-yet undiscovered independent variable(s) that are affecting the degree and consistency of fire-induced enhancement of magnetic susceptibility.

This experiment serves as a starting point for the use of magnetic susceptibility as an archaeogeophysical site characterization technique within a subarctic context. Using firing experiments meant to simulate the open hearths utilized by Indigenous people during the precontact period, the Terraplus KT-10 was used to measure the magnetic susceptibility enhancement within the heated sedimentary matrix. By confirming that the sedimentary contexts of the Canadian subarctic react similarly to sediments in location where they have been tested (Clark, 2001; Tite & Mullins, 1971; Witten, 2014), it can be surmised that magnetic susceptibility has potential as an archaeogeophysical tool to augment archaeological excavations in the subarctic.

Chapter 7 Conclusion

This thesis outlines firing experiments that addressed the efficacy of magnetic susceptibility as an archaeological site characterization method, specifically to detect the geophysical signature of precontact hearths expected in subarctic hunter-gatherer sites. The study area was at the Hogarth Tree Farm located near Thunder Bay, Ontario. This involved establishment of a control grid, the collection of baseline control data, conducting test hearth firing in controlled conditions, and then post-fire measurements to document the degree of geophysical transformation.

Four specific research questions were addressed that are designed to assess the viability of magnetic susceptibility as an archaeogeophysical characterization tool: 1) Did the experimental firing events enhance the magnetic susceptibility; 2) What was the minimum temperature needed to change the magnetic susceptibility signature of the natural soil/sediment; 3) What level of interpretation can be made from the magnetic susceptibility data; and 4) How effectively did the Terraplug KT-10 detect this change? I sought to determine whether the naturally occurring magnetic susceptibility of the sediments would be enhanced because of a single short-term burn, over a succession of short burns, and as a consequence of long-term firing. Additionally, the experiments evaluated the capability and utility of the handheld Terraplug KT-10 magnetic susceptibility meter under conventional field conditions. Validity testing of this method was important since it would offer a non-destructive site characterization method, and it would enable documentation of archaeological information that is otherwise unavailable using conventional testing methods.

The time and the temperatures reached during firing experiments were documented as part of measuring magnetic susceptibility response in the sediments within the experimental hearths, and whether such responses occurred at a statistically significant level. An appreciable difference in magnetic susceptibility between the baseline and fired sediments was observed with the frequency distributions (Figures 6.1 and 6.2), which T-test evaluation demonstrated were statistically significant (Table 6.1). This confirms that the sediments encountered within

the northern Ontario subarctic behave similarly to other area's sediments when they are heated.

When the results from the firing experiments are considered collectively, short-term firing events (Figure 6.2) have the capacity to enhance the magnetic susceptibility, often as much as a long-term firing event within a boreal forest context (Figures 6.2, 6.5). However, examination of the firing data compared to the baseline demonstrated that it was not possible to differentiate between the number and type of experimental firing events in each fire pit, or type of firing event conducted. However, it is possible to detect a firing event, which may not be visible macroscopically.

When the specific magnetic susceptibility response of each hearth location was reconsidered as a discrete unit of analysis, the impact of firing was not clearcut. This involved comparison of the magnetic susceptibility readings from each hearth zone before the firing (Figure 6.3) to the readings collected at the end of the experiments on November 9, 2021 (Figure 6.4). The difference in readings observed in each quadrant making up the hearth location (Figure 6.5) reveals little that would reflect amplification of magnetic susceptibility response with increased number and intensity of firings. While the data in Figure 6.8 reveals a net increase in magnetic susceptibility, sometimes this increase is quite modest, and in a few cases, there was a slight decline in magnetic susceptibility. In general, a single short-term fire was sufficient to enhance susceptibility, with only modest further enhancement with repeated short-term fires.

Indeed, in a few locations (grid locations 2N, 0E SWQ, 2N, 2E SWQ, 1N, 0E NWQ, SWQ, 0N, 2E NEQ, NWQ), there was a modest decline in the measurements. These latter results were unexpected and difficult to interpret. On the one hand, when the data is aggregated, there was a consistent enhancement in magnetic susceptibility with firing, but the effect is not appreciably cumulative with repeated or with sustained firing. More surprising, in a few cases, the net outcome of firing suggested a lower magnetic susceptibility value than the baseline reading from specific portions of the hearths. I do not have a clear explanation for these unexpected results. On the one hand, there was a statistically robust trend demonstrating that

firing tends to enhance magnetic susceptibility, but there was no clear correlation how fire repetition and duration affect enhancement. When considering each hearth independently, no clear enhancement pattern is evident. This suggests that other unmeasured variables were affecting how fire affects magnetic susceptibility. One possibility is that even within these (macroscopically) uniform, lacustrine sediments there was an uneven distribution of ferric minerals (i.e., hematite, magnetite, maghaemite) that are the basis of the geochemical transformations underlying anthropogenic modification of magnetic susceptibility. If this speculation is correct, perhaps mineralogical characterization of the sedimentary parent material underlying archaeological deposits is a necessary precondition before applying magnetic susceptibility as an archaeological prospection and characterization tool.

This study has research implications for archaeological investigations throughout much of the Canadian subarctic, where acidic sediments often degrade or destroy organic materials and promote severe leaching of archaeological features. Such deposits are also compromised by other taphonomic processes, such as frost heaving, periodic intense wildfires, and bioturbation (plant and animal disturbance). The very nature of archaeological investigation also impacts organic materials. Thus, there is a growing appeal in non-invasive investigative methods, including geophysical prospection, to detect evidence of past human activities. Such site characterization is useful to help characterize the sediments exposed during excavations. This might amplify interpretative capacity by considering vertical change in magnetic susceptibility down the soil profile, and what relationship it might have with the vertical distribution of material culture. This might aid in refining interpretation of repeated human occupation. In the challenging context of subarctic archaeology, detection and delineation of otherwise 'invisible' features using magnetic susceptibility might aid in interpreting intra-site use of space. While the environmental and logistic realities of subarctic archaeological investigations confound some archaeological site prospection techniques, magnetic susceptibility has the demonstrated potential to amplify archaeological insight when used concurrently with conventional archaeological methods.

In conclusion, magnetic susceptibility is a viable geophysical property to detect anthropogenic changes within a Canadian subarctic archaeological context, but with some

important considerations that became apparent after conducting the experiments. Open pit firing experiments were found to sufficiently heat the underlying sediments to cause enhancement of magnetic susceptibility beyond that present in the natural sediments. The Terraplus KT-10 magnetic susceptibility meter demonstrated its potential as an archaeological site characterizations technique, enabling ready data collection needed for the statistical analysis to demonstrate the difference between natural and fired sediments. Frequency distributions and statistical tests were used to demonstrate the observed ranges of the baseline and fired sediments susceptibility, as well as the statistical significance between the two. Though some of the results were unexpected, these experiments can serve as a starting point for future magnetic susceptibility experiments and surveys within the Canadian subarctic.

Chapter 8 References Cited

- Bigman, D. P. (2012). The Use of Electromagnetic Induction in Locating Graves and Mapping Cemeteries: An Example from Native North America. *Archaeological Prospection*, 19, 31-39. Wiley Online Library.
- Boyd, M., & Hamilton, S. (2018). The Martin-Bird Site Revisited. *Ontario Archaeology*, 98, 35-47.
- Boyd, M., Surette, C., Lints, A., & Hamilton, S. (2014). Wild rice (*Zizania* spp.), The Three Sisters, and the Woodland tradition in Western and Central Canada. In *Reassessing the Timing, Rate, and Adoption Trajectories of Domesticated Use in the Midwest and Great Lakes*, (Maria E. Raviele and William A. Lovis, eds.), pp. 7-32.
- Boyd, M., Teller, J. T., Yang, Z., Kingsmill, L., & Shultis, C. (2012). An 8,900-year-old Forest Drowned by Lake Superior: Hydrological and Paleoecological Implications. *Journal of Paleolimnology*, 47, 339-355.
- Campana, S., (2009). Archaeological Site Detection and Mapping: Some Thoughts on Differing Scales of Detail and Archaeological 'Non-Visibility'. In *Seeing the unseen. Geophysics and landscape archaeology* (pp. 31-52). London, UK: CRC press.
- Campana, S., & Piro, S. (Eds.). (2009). *Seeing the unseen. Geophysics and landscape archaeology*. London, UK: CRC press.
- Clark, A. (2001). *Seeing Beneath the Soil: Prospecting Methods in Archaeology* (New Edition). New York: Routledge.
- Costa, H. D. S., Licht, O. A. B., Ferreira, F. J. F., Vasconcellos, E. M. G., & da Costa, A. C. S. (2022). Validation of the Use of Portable Equipment for Magnetic Characterization of Soils, State of Paraná, Brazil. *Brazilian Journal of Geology*. 52 (4):e2022011. Electronic resource.
<https://www.scielo.br/j/bjgeo/a/kxBP3hDbh8mHqXjdYzJ7p9h/?format=pdf&lang=en>, accessed December 15, 2023.
- Crowther, J., & Barker, P. (1995). Magnetic Susceptibility: Distinguishing Anthropogenic Effects from the Natural. *Archaeological Prospection*, 2(4), 207-215.
- Dalan, R. A., & Banerjee, S. K. (1998). Solving Archaeological Problems Using Techniques of Soil Magnetism. *Geoarchaeology: An International Journal*, 13(1), 3-36.
- Dalan, R. A. (2007). A Review of the role of Magnetic Susceptibility in Archaeogeophysical Studies in the USA: Recent Developments and Prospects. *Archaeological Prospection*, 15(1), 1-31.

- Dawson, K. C. (1983). Prehistory of the Interior Forest of Northern Ontario. In *Boreal Forest adaptations: The Northern Algonkians*, (A. T. Steemann, Jr., ed.), pp. 55-84. New York: Plenum Press.
- Dearing, J. (1999). Environmental Magnetic Susceptibility: Using the Bartington MS2 System, 2nd edition ed., Chi Publishing, Kenilworth.
- Fagan, B. M. (2005). *Ancient North America: the Archaeology of a Continent*. (Fourth Edition). London: Thames and Hudson.
- Gaffney, C. F., Gater, J., & Ovenden, S. (2002). *The Use of Geophysical Techniques in Archaeological Evaluations* (Vol. 6). Reading: Institute of Field Archaeologists.
- Gibson, T. H. (1986). Magnetic Prospection on Prehistoric Sites in Western Canada. *Geophysics*, 51(3), 553-560.
- Gibson, T. (2017). Stage 4 Archaeological Excavation of the Mackenzie River 1 site DdJf-9. PIF # P330-009-2011. Report completed by Western Heritage and submitted to the Ontario Ministry of Transportation, Thunder Bay, Ontario.
- Goltz, G. (2019). Grant Goltz: Rethinking Blackduck Pottery Video. Lakeland PBS. <https://www.youtube.com/watch?v=Gf9UioBtmsl>.
- Hamilton, S. (2013). A World Apart? Ontario's Canadian shield. In *Before Ontario: the archaeology of a province*, (eds. Marit K. Munson and Susan M. Jamieson), pp.72, 77-95. Montreal: McGill-Queen's University Press.
- Hamilton, S. (2012). 2011 Recoveries of Human Remains from the Bug River Site (FkJm-1), Big Trout Lake: (Stage 4a recovery). Unpublished report prepared for the Cemeteries Regulation Unit, Ontario Ministry of Consumer Services and Kitchenuhmaykoosib Inninuwug First Nation.
- Hamilton, S. (2004). Early Holocene Human Burials at Wapekeka (FlJj-1), Northern Ontario. The Late Palaeo-Indian Great Lakes: Geological and Archaeological Investigations of Late Pleistocene and Early Holocene Environments. Mercury Series Archaeology Paper, 165, 337-368.
- Hamilton, S. (2000). Archaeological Predictive Modelling in the Boreal Forest: No Easy Answers. *Canadian Journal of Archaeology/Journal Canadien d'Archéologie*, 41-76.
- Hinshelwood, A. (2004). Archaic Reoccupation of Late Palaeo-Indian Sites in Northwestern Ontario. In *The Late Palaeo-Indian Great Lakes: Geological and Archaeological Investigations of Late Pleistocene and Early Holocene environments*. (L.J. Jackson, and A.

- Hinshelwood, Eds.). pp. 225-250. Mercury Series, Mercury Archaeology Paper 165. Gatineau, Quebec: Canadian Museum of History.
- Hinshelwood, A. (1996). Boreal Forest Fire Ecology and Archaeological Site Formation: An Example from Northern Ontario. *Ontario Archaeology*, 62, 63-92.
- Hodgetts, L., Millaire, J. F., Eastaugh, E., & Chapdelaine, C. (2016). The Untapped Potential of Magnetic Survey in the Identification of Precontact Archaeological Sites in Wooded Areas. *Advances in Archaeological Practice*, 4(1), 41-54.
- Hollings, P., Smyk, M., Heaman, L. M., & Halls, H. (2010). The Geochemistry, Geochronology and Paleomagnetism of Dikes and Sills Associated with the Mesoproterozoic Midcontinent Rift near Thunder Bay, Ontario, Canada. *Precambrian Research*, 183(3), 553-571.
- Julig, P. J. (1984). Cummins Paleo-Indian Site and its Paleoenvironment, Thunder Bay, Canada. *Archaeology of Eastern North America*, Vol. 12. 192-209. Eastern States Archaeological Federation.
- Kvamme, K. L. (2001). Current Practices in Archaeogeophysics. In Paul Goldberg, Vance T. Holliday, C. Reid Ferring (Eds), *Earth sciences and archaeology* (pp. 353-384). Boston, MA; Springer.
- Kvamme, K. L. (2003). Geophysical Surveys as Landscape Archaeology. *American Antiquity*, 68(3), 435-457.
- Kvamme K. (2017). Geophysical Prospecting in Archaeology. Lecture. Youtube. https://www.youtube.com/watch?v=ZkTL_JQ7NMk&t=3170s.
- Lane, D., Scott, D., Hebl, M., Guerra, R., Osherson, D., & Zimmer, H. (2003). *Introduction to statistics*. Online Edition. David Lane. <https://citeseerx.ist.psu.edu/document?repid=rep1&type=pdf&doi=a8182909e4e95c530f4849ba75f74c7c633651b0>
- Liu, Q., Roberts, A. P., Larrasoana, J. C., Banerjee, S. K., Guyodo, Y., Tauxe, L., & Oldfield, F. (2012). Environmental Magnetism: Principles and Applications. *Reviews of Geophysics*, 50(4).
- Loope, H. M. (2006). Deglacial Chronology and Glacial Stratigraphy of the Western Thunder Bay Lowland, Northwest Ontario, Canada. Unpublished PhD dissertation, Department of Geology, University of Toledo.
- Norris, D. (2022). 3D Morphometric Analysis of Late Paleoindigenous Projectile Points from the Mackenzie I Site, Northwestern Ontario, and Surrounding Regions. Unpublished PhD

- dissertation, Department of Anthropology, University of Western Ontario, London, Ontario.
- Norris, D. (2012). Current Archaeological Investigations in Ontario: the Discovery of and Preliminary Information Regarding Several Paleoindian Sites East of Thunder Bay. *Minnesota Archaeologist*, 71, 45-59.
- Oswin, J. (2009). A Field guide to Geophysics in Archaeology. Chichester, United Kingdom: Springer Science & Business Media.
- Pilon, J. L., & Dalla Bona, L. (2004). Insights into the Early Peopling of Northwestern Ontario as Documented at the Allen Site (EcJs-1), Sioux Lookout District, Ontario. *The Late Palaeo-Indian Great Lakes: Geological and Archaeological investigations of late Pleistocene and early Holocene environments*. (L. J. Jackson, and A. Hinshelwood, Eds.), pp. 315-335. Mercury Series, Mercury Archaeology Paper 165. Gatineau, Quebec: Canadian Museum of History.
- Piro, S. (2009). Introduction to Geophysics for Archaeology. In *Seeing the unseen. Geophysics and landscape archaeology* (pp. 53-92). London, UK: CRC Press.
- Rice, P. M. (1987). *Pottery Analysis: A Sourcebook*. Chicago: The University of Chicago Press.
- Richard, R. (ed.) (2019). *Dictionary of Physics*. Eighth Edition. Oxford University Press. New York, NY.
- Rogers, M. (2011). Chapter 8: Archaeological Geophysics: Seeing Deeper with Technology to Compliment Digging. In Matthew Seddon, Heidi Roberts, and Richard V.N. Ahlstrom (Eds.), *Archaeology in 3D: Deciphering Buried Sites in the Western U.S. Society* (pp. 114-137). Washington, DC: American Archaeology Press.
- Rogers, E. S. (1983). Cultural Adaptations: the Northern Ojibwa of the Boreal Forest 1670–1980. In *Boreal Forest Adaptations: The Northern Algonkians*, (A. T. Steemann, Jr., ed.), pp. 55-84. New York: Plenum Press.
- Ross, W. (1995). The Interlakes Composite: A Re-Definition of the Initial Settlement of the Agassiz-Minong Peninsula. *The Wisconsin Archeologist* 76(3-4):244-268.
- Sala, R., Garcia, E., & Tamba, R. (2012). Archaeological Geophysics—from Basics to New Perspectives. In Ollich-Castanyer, I. (Ed.). *Archaeology, New Approaches in Theory and Techniques. Archaeology: New Approaches in Theory and Techniques*. pp133-166. Rijeka, Croatia: InTech.

- Schmidt, A. (2007). Archeology, Magnetic Methods. In Gubbins, D., & Herrero-Bervera, E. (Eds) *Encyclopedia of Geomagnetism and Paleomagnetism*. (pp. 23-31). Springer Science & Business Media. Dordrecht, The Netherlands: Springer.
- Schmidt, A. (2009). Electrical and Magnetic Methods in Archaeological Prospection. In *Seeing the Unseen. Geophysics and Landscape Archaeology* (pp. 93-108). London, UK: CRC Press.
- Šindelář, J., Mazuch M., Hladík, M. (2021). Measuring Magnetic Susceptibility to Determine Desposits in Field Archaeological Research at the MIKULČICE SITE. *GeoScience Engineering* 67(4):176-186.
- Taylor-Hollings, J. S. (2017). "People Lived There a Long Time Ago": Archaeology, Ethnohistory, and Traditional Use of the Miskweyaabizibee (Bloodvein River) in Northwestern Ontario. Unpublished PhD dissertation, Department of Anthropology, University of Alberta, Edmonton.
- Terraplus (2019). *Magnetic Susceptibility Conductivity Meters - Terraplus*. Electronic document, retrieved January 2019, from <https://terraplus.ca/wp-content/uploads/terraplus-Brochures-English/KT-10-Magnetic-Susceptibility-Conductivity-Meters.pdf>.
- Tite, M. S. (1972). The Influence of Geology on the Magnetic Susceptibility of Soils on Archaeological Sites. *Archaeometry*, 14(2), 229-236.
- Tite, M. S., & Mullins, C. (1971). Enhancement of the Magnetic Susceptibility of Soils on Archaeological Sites. *Archaeometry*, 13(2), 209-219.
- Winterhalder, B. (1983). History and Ecology of the Boreal Zone in Ontario. In *Boreal Forest Adaptations: The Northern Algonkians*, (A. T. Steemann, Jr., ed.), pp. 55-84. New York: Plenum Press.
- Witten, A. (2014). *Handbook of Geophysics and Archaeology*. New York: Routledge.
- Woodrow, M. (2002). *Challenges to Sustainability in Northern Ontario*. Maureen Woodrow, Institute of the Environment, University of Ottawa.
- Wright, J. V. (1972). *The Shield Archaic*. Bulletin No. 206. Ottawa: National Museums of Ottawa.
- Wright, J. V. (1995). *A History of the Native People of Canada. Volume 1 (10,000-1000B.C.)*. Mercury Series, Archaeological Survey of Canada, Paper 152, Hull, Quebec: Canadian Museum of Civilization.

Appendices

Appendix A: Temperature Data

Legend

MN – Temperature maintenance.

AT – Temperature Measurement.

date – Date Collected (note: instrument did not allow correct date).

time – Time collected (note: instrument did not allow correct time).

int – Measurement intervals (one minute).

1ch – Channel 1 (western probe)

2ch – Channel 2 (wire probe)

3ch – Channel 3 (southern probe)

4ch – Channel 4 (eastern probe)

unit – Unit of temperature measurement

April 27, 2021, Long Term Firing Event

MN/AT	date	time	int	1ch	2ch	3ch	4ch	unit	
AT	2011-01-01	00:18:46	1m	7.8	43.7	214.3	10.4	C	
AT	2011-01-01	00:11:46	1m	5.5	6.7	9.2	13.6	C	AT 2011-01-01 00:19:46 1m 7.3 32.6 364.5 11.2 C
AT	2011-01-01	00:12:46	1m	7.7	6.6	9.2	10.2	C	AT 2011-01-01 00:20:46 1m 6.9 27.2 378.9 11.8 C
AT	2011-01-01	00:13:46	1m	7.7	9.9	16.8	9.9	C	AT 2011-01-01 00:21:46 1m 6.8 40.9 384.9 12.6 C
AT	2011-01-01	00:14:46	1m	7.7	18.9	42.4	9.8	C	AT 2011-01-01 00:22:46 1m 7.6 33.2 459.8 13.7 C
AT	2011-01-01	00:15:46	1m	7.2	35.1	64.2	9.7	C	AT 2011-01-01 00:23:46 1m 8.3 41.4 492.7 15.2 C
AT	2011-01-01	00:16:46	1m	7.6	37.8	263.2	9.9	C	
AT	2011-01-01	00:17:46	1m	7.4	45.6	242.7	10.1	C	

April 27, 2021, Long Term Firing Event

MN/AT	date	time	int	1ch	2ch	3ch	4ch	unit
AT	2011-01-01	00:24:46	1m	8.6	40.5	520.9	16.9	C
AT	2011-01-01	00:25:46	1m	8.8	43.2	474.4	18.8	C
AT	2011-01-01	00:26:46	1m	10.7	45.5	463.3	20.5	C
AT	2011-01-01	00:27:46	1m	12.6	58.1	457.6	21.8	C
AT	2011-01-01	00:28:46	1m	17.9	52.6	488.1	22.9	C
AT	2011-01-01	00:29:46	1m	21.6	49.7	488.5	23.6	C
AT	2011-01-01	00:30:46	1m	30.7	57.2	454.1	24.4	C
AT	2011-01-01	00:31:46	1m	31.1	57.6	452.6	25.3	C
AT	2011-01-01	00:32:46	1m	36.4	56.6	478.6	28.0	C
AT	2011-01-01	00:33:46	1m	30.8	50.2	508.3	29.9	C
AT	2011-01-01	00:34:46	1m	31.7	64.2	536.4	30.7	C
AT	2011-01-01	00:35:46	1m	32.6	65.5	525.1	31.3	C
AT	2011-01-01	00:36:46	1m	34.5	72.4	522.4	31.9	C
AT	2011-01-01	00:37:46	1m	37.8	75.0	562.7	32.2	C
AT	2011-01-01	00:38:46	1m	40.2	96.3	520.9	36.4	C
AT	2011-01-01	00:39:46	1m	48.3	62.3	562.3	32.8	C
AT	2011-01-01	00:40:46	1m	58.6	61.4	570.7	32.9	C
AT	2011-01-01	00:41:46	1m	60.4	50.4	592.1	33.5	C
AT	2011-01-01	00:42:46	1m	60.5	50.9	706.1	35.2	C
AT	2011-01-01	00:43:46	1m	67.8	88.7	716.4	41.7	C
AT	2011-01-01	00:44:46	1m	76.3	87.6	727.3	49.2	C
AT	2011-01-01	00:45:46	1m	80.9	94.8	718.7	51.0	C
AT	2011-01-01	00:46:46	1m	75.9	87.4	742.6	51.6	C
AT	2011-01-01	00:47:46	1m	83.0	91.8	747.0	53.9	C
AT	2011-01-01	00:48:46	1m	88.2	103.1	762.4	59.2	C
AT	2011-01-01	00:49:46	1m	110.8	140.8	843.7	65.8	C
AT	2011-01-01	00:50:46	1m	127.1	159.4	832.4	71.1	C
AT	2011-01-01	00:51:46	1m	131.2	131.1	833.9	80.0	C
AT	2011-01-01	00:52:46	1m	145.4	150.2	807.2	84.4	C
AT	2011-01-01	00:53:46	1m	197.9	163.6	790.8	82.1	C
AT	2011-01-01	00:54:46	1m	236.1	160.7	766.1	80.7	C
AT	2011-01-01	00:55:46	1m	268.8	202.1	794.5	82.7	C
AT	2011-01-01	00:56:46	1m	291.5	186.4	761.8	82.6	C
AT	2011-01-01	00:57:46	1m	318.1	139.6	738.3	85.5	C
AT	2011-01-01	00:58:46	1m	305.9	148.6	770.5	87.4	C
AT	2011-01-01	00:59:46	1m	312.9	155.2	800.6	88.4	C
AT	2011-01-01	01:00:46	1m	336.3	188.4	799.6	87.6	C
AT	2011-01-01	01:01:46	1m	320.2	169.4	786.2	89.5	C
AT	2011-01-01	01:02:46	1m	332.8	163.3	774.3	92.1	C
AT	2011-01-01	01:03:46	1m	397.4	159.6	804.0	97.4	C
AT	2011-01-01	01:04:46	1m	398.8	138.3	831.9	105.3	C
AT	2011-01-01	01:05:46	1m	440.8	171.3	808.6	135.8	C
AT	2011-01-01	01:06:46	1m	470.1	146.4	731.8	153.0	C
AT	2011-01-01	01:07:46	1m	462.9	240.7	677.2	125.0	C
AT	2011-01-01	01:08:46	1m	418.9	146.8	688.6	109.7	C
AT	2011-01-01	01:09:46	1m	409.1	148.6	686.9	106.3	C
AT	2011-01-01	01:10:46	1m	390.4	167.8	718.0	110.3	C
AT	2011-01-01	01:11:46	1m	417.2	170.9	749.6	114.6	C
AT	2011-01-01	01:12:46	1m	400.6	182.5	736.9	120.4	C
AT	2011-01-01	01:13:46	1m	469.8	227.1	662.5	128.6	C
AT	2011-01-01	01:14:46	1m	447.8	216.4	663.6	139.1	C

April 27, 2021, Long Term Firing Event

MN/AT	date	time	int	1ch	2ch	3ch	4ch	unit
								AT 2011-01-01 01:41:46 1m 378.0 183.4 614.4 439.8 C
AT	2011-01-01	01:15:46	1m	439.7	215.1	662.1	148.0	C
AT	2011-01-01	01:16:46	1m	502.7	226.2	656.4	156.7	C
AT	2011-01-01	01:17:46	1m	584.0	225.5	654.1	151.4	C
AT	2011-01-01	01:18:46	1m	512.4	186.8	641.7	152.3	C
AT	2011-01-01	01:19:46	1m	468.5	178.1	640.1	160.6	C
AT	2011-01-01	01:20:46	1m	462.6	183.2	635.9	174.0	C
AT	2011-01-01	01:21:46	1m	450.9	207.9	621.2	175.9	C
AT	2011-01-01	01:22:46	1m	520.7	208.5	601.4	178.6	C
AT	2011-01-01	01:23:46	1m	559.1	196.3	642.7	198.3	C
AT	2011-01-01	01:24:46	1m	563.2	194.2	628.4	222.6	C
AT	2011-01-01	01:25:46	1m	607.7	197.3	616.1	236.9	C
AT	2011-01-01	01:26:46	1m	671.0	193.7	614.9	239.8	C
AT	2011-01-01	01:27:46	1m	706.7	213.2	632.8	233.7	C
AT	2011-01-01	01:28:46	1m	723.4	199.7	609.9	232.9	C
AT	2011-01-01	01:29:46	1m	713.9	205.9	616.4	234.4	C
AT	2011-01-01	01:30:46	1m	667.1	194.3	596.8	244.3	C
AT	2011-01-01	01:31:46	1m	712.7	141.2	582.1	260.9	C
AT	2011-01-01	01:32:46	1m	711.3	136.3	582.5	301.7	C
AT	2011-01-01	01:33:46	1m	665.3	164.8	572.8	364.2	C
AT	2011-01-01	01:34:46	1m	641.3	143.7	562.7	407.1	C
AT	2011-01-01	01:35:46	1m	591.4	198.4	628.0	433.7	C
AT	2011-01-01	01:36:46	1m	532.1	175.2	644.1	416.2	C
AT	2011-01-01	01:37:46	1m	486.2	176.1	641.4	410.4	C
AT	2011-01-01	01:38:46	1m	450.2	172.1	631.9	418.9	C
AT	2011-01-01	01:39:46	1m	418.8	156.2	628.7	426.5	C
AT	2011-01-01	01:40:46	1m	395.3	167.2	611.8	432.1	C
								AT 2011-01-01 01:42:46 1m 359.1 170.3 611.5 452.6 C
								AT 2011-01-01 01:43:46 1m 345.7 188.1 605.2 455.4 C
								AT 2011-01-01 01:44:46 1m 334.2 176.1 613.9 457.0 C
								AT 2011-01-01 01:45:46 1m 322.7 206.1 619.1 455.4 C
								AT 2011-01-01 01:46:46 1m 312.9 183.8 594.9 464.2 C
								AT 2011-01-01 01:47:46 1m 304.1 195.9 618.8 472.8 C
								AT 2011-01-01 01:48:46 1m 296.6 199.4 623.9 482.7 C
								AT 2011-01-01 01:49:46 1m 289.6 233.8 623.9 494.9 C
								AT 2011-01-01 01:50:46 1m 283.7 295.9 625.9 510.8 C
								AT 2011-01-01 01:51:46 1m 277.4 268.3 607.7 525.1 C
								AT 2011-01-01 01:52:46 1m 275.5 213.2 604.9 530.4 C
								AT 2011-01-01 01:53:46 1m 275.7 209.8 596.3 543.2 C
								AT 2011-01-01 01:54:46 1m 277.6 226.2 622.2 544.9 C
								AT 2011-01-01 01:55:46 1m 281.3 237.1 621.0 546.9 C
								AT 2011-01-01 01:56:46 1m 281.3 213.6 623.2 560.0 C
								AT 2011-01-01 01:57:46 1m 285.8 250.2 658.3 584.1 C
								AT 2011-01-01 01:58:46 1m 287.9 231.7 644.4 585.3 C
								AT 2011-01-01 01:59:46 1m 285.8 223.1 679.0 586.3 C
								AT 2011-01-01 02:00:46 1m 283.9 218.7 683.2 586.9 C
								AT 2011-01-01 02:01:46 1m 280.2 176.6 744.9 589.1 C
								AT 2011-01-01 02:02:46 1m 276.9 214.8 781.7 588.7 C
								AT 2011-01-01 02:03:46 1m 277.4 233.7 783.0 594.1 C
								AT 2011-01-01 02:04:46 1m 276.7 226.8 771.6 593.0 C
								AT 2011-01-01 02:05:46 1m 278.2 229.8 771.2 600.6 C

April 27, 2021, Long Term Firing Event

MN/AT	date	time	int	1ch	2ch	3ch	4ch	unit
AT	2011-01-01	02:06:46	1m	276.1	184.3	798.8	600.3	C
AT	2011-01-01	02:07:46	1m	279.8	199.6	813.4	607.2	C
AT	2011-01-01	02:08:46	1m	281.6	186.9	815.2	617.8	C
AT	2011-01-01	02:09:46	1m	282.7	229.9	806.7	615.9	C
AT	2011-01-01	02:10:46	1m	285.1	209.2	782.4	606.2	C
AT	2011-01-01	02:11:46	1m	286.8	202.5	803.8	610.1	C
AT	2011-01-01	02:12:46	1m	288.9	258.3	786.1	625.8	C
AT	2011-01-01	02:13:46	1m	292.1	210.3	776.2	598.8	C
AT	2011-01-01	02:14:46	1m	296.2	210.7	781.4	571.4	C
AT	2011-01-01	02:15:46	1m	297.4	206.3	775.7	547.4	C
AT	2011-01-01	02:16:46	1m	299.2	204.9	773.1	528.4	C
AT	2011-01-01	02:17:46	1m	302.1	220.0	784.2	512.7	C
AT	2011-01-01	02:18:46	1m	303.5	192.5	780.6	499.3	C
AT	2011-01-01	02:19:46	1m	307.1	202.2	795.6	488.9	C
AT	2011-01-01	02:20:46	1m	310.5	214.9	798.2	479.4	C
AT	2011-01-01	02:21:46	1m	312.7	204.7	801.3	471.1	C
AT	2011-01-01	02:22:46	1m	310.4	202.2	802.8	460.9	C
AT	2011-01-01	02:23:46	1m	308.6	151.6	786.9	456.2	C
AT	2011-01-01	02:24:46	1m	308.8	204.3	800.0	451.9	C
AT	2011-01-01	02:25:46	1m	311.3	190.6	794.4	448.7	C
AT	2011-01-01	02:26:46	1m	314.8	199.9	797.6	448.9	C
AT	2011-01-01	02:27:46	1m	317.6	181.0	795.4	448.2	C
AT	2011-01-01	02:28:46	1m	316.8	178.2	783.1	445.4	C
AT	2011-01-01	02:29:46	1m	319.1	189.0	784.2	444.5	C
AT	2011-01-01	02:30:46	1m	319.4	234.3	780.5	442.2	C
AT	2011-01-01	02:31:46	1m	317.2	208.4	771.6	434.7	C
AT	2011-01-01	02:32:46	1m	316.7	206.7	769.9	426.7	C

AT	2011-01-01	02:33:46	1m	314.1	219.6	776.7	421.3	C
AT	2011-01-01	02:34:46	1m	310.8	230.8	774.9	415.9	C
AT	2011-01-01	02:35:46	1m	309.1	215.8	769.4	411.8	C
AT	2011-01-01	02:36:46	1m	308.6	207.9	757.8	406.2	C
AT	2011-01-01	02:37:46	1m	305.9	207.0	764.4	401.3	C
AT	2011-01-01	02:38:46	1m	306.7	222.3	757.9	396.2	C
AT	2011-01-01	02:39:46	1m	305.3	218.9	741.3	393.2	C
AT	2011-01-01	02:40:46	1m	303.1	219.5	775.4	387.2	C
AT	2011-01-01	02:41:46	1m	303.8	269.7	756.6	383.8	C
AT	2011-01-01	02:42:46	1m	304.4	324.2	748.4	382.4	C
AT	2011-01-01	02:43:46	1m	305.3	310.2	741.8	384.2	C
AT	2011-01-01	02:44:46	1m	311.3	319.9	728.3	389.8	C
AT	2011-01-01	02:45:46	1m	316.1	260.0	736.6	394.0	C
AT	2011-01-01	02:46:46	1m	320.1	302.6	742.8	397.8	C
AT	2011-01-01	02:47:46	1m	322.5	282.2	764.8	396.3	C
AT	2011-01-01	02:48:46	1m	323.0	248.4	743.1	394.5	C
AT	2011-01-01	02:49:46	1m	327.1	259.3	736.7	400.6	C
AT	2011-01-01	02:50:46	1m	329.1	250.0	742.4	401.8	C
AT	2011-01-01	02:51:46	1m	332.1	267.4	740.7	404.8	C
AT	2011-01-01	02:52:46	1m	333.1	269.4	744.3	405.1	C
AT	2011-01-01	02:53:46	1m	332.4	263.3	744.5	404.4	C
AT	2011-01-01	02:54:46	1m	330.9	280.7	753.7	404.2	C
AT	2011-01-01	02:55:46	1m	329.2	274.7	743.7	404.4	C

April 27, 2021, Long Term Firing Event

MN/AT	date	time	int	1ch	2ch	3ch	4ch	unit
								AT 2011-01-01 03:23:46 1m 338.3 286.3 696.0 378.9 C
AT	2011-01-01	02:56:46	1m	329.7	267.0	737.3	409.8	C
								AT 2011-01-01 03:24:46 1m 339.4 361.4 694.6 379.1 C
AT	2011-01-01	02:57:46	1m	331.7	243.8	736.6	418.5	C
								AT 2011-01-01 03:25:46 1m 341.1 259.4 698.5 381.6 C
AT	2011-01-01	02:58:46	1m	335.7	257.8	726.9	430.2	C
								AT 2011-01-01 03:26:46 1m 341.1 287.2 702.1 380.5 C
AT	2011-01-01	02:59:46	1m	338.7	228.6	713.7	437.2	C
								AT 2011-01-01 03:27:46 1m 341.3 301.4 701.3 381.6 C
AT	2011-01-01	03:00:46	1m	345.6	172.9	741.1	436.2	C
								AT 2011-01-01 03:28:46 1m 341.6 609.6 706.9 379.1 C
AT	2011-01-01	03:01:46	1m	345.4	164.4	739.8	429.9	C
								AT 2011-01-01 03:29:46 1m 343.7 669.8 698.5 377.7 C
AT	2011-01-01	03:02:46	1m	344.8	201.6	727.9	423.1	C
								AT 2011-01-01 03:30:46 1m 339.6 567.6 690.4 377.3 C
AT	2011-01-01	03:03:46	1m	341.9	217.7	719.3	415.9	C
								AT 2011-01-01 03:31:46 1m 338.4 560.1 679.5 374.4 C
AT	2011-01-01	03:04:46	1m	341.6	528.4	723.2	415.8	C
								AT 2011-01-01 03:32:46 1m 337.1 551.0 667.3 372.3 C
AT	2011-01-01	03:05:46	1m	340.6	280.6	708.3	417.7	C
								AT 2011-01-01 03:33:46 1m 337.9 544.2 656.3 371.8 C
AT	2011-01-01	03:06:46	1m	338.1	388.4	682.7	416.3	C
								AT 2011-01-01 03:34:46 1m 338.6 540.9 646.5 371.1 C
AT	2011-01-01	03:07:46	1m	336.2	383.0	683.4	408.6	C
								AT 2011-01-01 03:35:46 1m 336.6 537.8 639.0 369.6 C
AT	2011-01-01	03:08:46	1m	332.9	343.1	684.3	403.4	C
								AT 2011-01-01 03:36:46 1m 334.3 532.9 634.1 366.8 C
AT	2011-01-01	03:09:46	1m	330.3	392.6	686.3	396.9	C
								AT 2011-01-01 03:37:46 1m 331.7 528.2 632.6 363.9 C
AT	2011-01-01	03:10:46	1m	329.8	312.7	683.2	393.9	C
								AT 2011-01-01 03:38:46 1m 327.9 522.8 629.0 361.6 C
AT	2011-01-01	03:11:46	1m	329.7	323.1	672.5	391.7	C
								AT 2011-01-01 03:39:46 1m 325.6 519.7 626.3 357.9 C
AT	2011-01-01	03:12:46	1m	331.4	301.8	666.6	389.3	C
								AT 2011-01-01 03:40:46 1m 323.4 517.9 626.6 354.0 C
AT	2011-01-01	03:13:46	1m	332.7	297.2	666.2	387.0	C
								AT 2011-01-01 03:41:46 1m 321.4 517.8 624.1 350.4 C
AT	2011-01-01	03:14:46	1m	332.4	316.4	669.4	386.3	C
								AT 2011-01-01 03:42:46 1m 317.9 517.5 622.7 345.7 C
AT	2011-01-01	03:15:46	1m	331.9	273.3	670.9	382.3	C
								AT 2011-01-01 03:43:46 1m 315.2 515.7 622.0 341.3 C
AT	2011-01-01	03:16:46	1m	331.1	269.7	673.1	380.9	C
								AT 2011-01-01 03:44:46 1m 311.7 513.8 620.8 337.2 C
AT	2011-01-01	03:17:46	1m	331.7	303.6	668.7	379.8	C
								AT 2011-01-01 03:45:46 1m 308.8 512.1 618.7 333.7 C
AT	2011-01-01	03:18:46	1m	334.3	278.6	663.9	380.8	C
								AT 2011-01-01 03:46:46 1m 305.2 512.8 616.8 330.8 C
AT	2011-01-01	03:19:46	1m	336.9	292.2	663.7	381.2	C
AT	2011-01-01	03:20:46	1m	338.2	254.7	669.8	378.7	C
AT	2011-01-01	03:21:46	1m	336.5	242.8	688.2	376.9	C
AT	2011-01-01	03:22:46	1m	337.0	250.4	693.1	379.2	C

April 27, 2021, Long Term Firing Event

MN/AT	date	time	int	1ch	2ch	3ch	4ch	unit
								AT 2011-01-01 04:14:46 1m 317.7 528.4 597.1 315.8 C
AT	2011-01-01	03:47:46	1m	301.4	513.1	615.6	328.3	C
								AT 2011-01-01 04:15:46 1m 318.4 524.5 597.7 316.6 C
AT	2011-01-01	03:48:46	1m	297.2	513.7	618.3	325.7	C
								AT 2011-01-01 04:16:46 1m 320.7 521.4 598.3 317.7 C
AT	2011-01-01	03:49:46	1m	295.1	512.6	618.3	322.2	C
								AT 2011-01-01 04:17:46 1m 321.6 518.8 598.7 318.7 C
AT	2011-01-01	03:50:46	1m	293.4	511.4	613.2	319.3	C
								AT 2011-01-01 04:18:46 1m 323.4 516.4 600.2 318.7 C
AT	2011-01-01	03:51:46	1m	291.8	512.1	610.8	316.8	C
								AT 2011-01-01 04:19:46 1m 323.1 514.2 600.7 320.8 C
AT	2011-01-01	03:52:46	1m	289.2	512.7	611.3	315.4	C
								AT 2011-01-01 04:20:46 1m 324.7 511.7 598.2 321.3 C
AT	2011-01-01	03:53:46	1m	288.2	514.0	613.9	312.9	C
								AT 2011-01-01 04:21:46 1m 326.9 509.4 596.5 322.8 C
AT	2011-01-01	03:54:46	1m	286.2	512.6	615.3	309.9	C
								AT 2011-01-01 04:22:46 1m 328.6 508.3 592.9 323.9 C
AT	2011-01-01	03:55:46	1m	286.7	510.2	616.9	308.1	C
								AT 2011-01-01 04:23:46 1m 331.1 508.7 592.3 324.3 C
AT	2011-01-01	03:56:46	1m	288.2	508.7	614.9	307.4	C
								AT 2011-01-01 04:24:46 1m 331.8 511.4 593.6 326.4 C
AT	2011-01-01	03:57:46	1m	289.7	508.4	614.2	306.3	C
								AT 2011-01-01 04:25:46 1m 331.6 513.8 595.1 327.8 C
AT	2011-01-01	03:58:46	1m	291.8	509.6	612.2	305.6	C
								AT 2011-01-01 04:26:46 1m 331.7 511.7 594.4 329.4 C
AT	2011-01-01	03:59:46	1m	293.3	510.4	607.4	304.9	C
								AT 2011-01-01 04:27:46 1m 331.2 510.7 593.9 332.6 C
AT	2011-01-01	04:00:46	1m	295.6	514.3	603.2	305.1	C
								AT 2011-01-01 04:28:46 1m 330.1 508.1 595.7 334.4 C
AT	2011-01-01	04:01:46	1m	297.8	519.6	599.7	305.3	C
								AT 2011-01-01 04:29:46 1m 330.1 505.1 597.3 335.2 C
AT	2011-01-01	04:02:46	1m	296.8	519.8	598.2	305.1	C
								AT 2011-01-01 04:30:46 1m 331.3 502.7 597.5 335.6 C
AT	2011-01-01	04:03:46	1m	295.6	516.9	599.2	304.5	C
								AT 2011-01-01 04:31:46 1m 332.0 500.6 598.3 335.9 C
AT	2011-01-01	04:04:46	1m	296.4	518.2	601.8	304.6	C
								AT 2011-01-01 04:32:46 1m 331.4 499.1 597.7 344.6 C
AT	2011-01-01	04:05:46	1m	297.7	518.4	599.1	306.0	C
								AT 2011-01-01 04:33:46 1m 331.6 499.9 600.4 345.2 C
AT	2011-01-01	04:06:46	1m	298.4	521.3	595.9	308.8	C
								AT 2011-01-01 04:34:46 1m 333.0 502.3 603.1 345.5 C
AT	2011-01-01	04:07:46	1m	296.8	522.8	595.2	310.8	C
								AT 2011-01-01 04:35:46 1m 332.8 503.5 604.5 345.3 C
AT	2011-01-01	04:08:46	1m	296.2	523.7	596.3	312.8	C
								AT 2011-01-01 04:36:46 1m 332.8 503.4 603.7 344.4 C
AT	2011-01-01	04:09:46	1m	297.1	524.7	597.2	313.8	C
								AT 2011-01-01 04:37:46 1m 333.8 501.0 603.3 343.9 C
AT	2011-01-01	04:10:46	1m	299.8	526.2	596.9	313.7	C
AT	2011-01-01	04:11:46	1m	304.4	530.2	595.3	313.4	C
AT	2011-01-01	04:12:46	1m	310.5	532.8	595.9	313.5	C
AT	2011-01-01	04:13:46	1m	315.1	531.7	596.8	314.7	C

April 27, 2021, Long Term Firing Event

MN/AT	date	time	int	1ch	2ch	3ch	4ch	unit
								AT 2011-01-01 05:05:46 1m 361.4 487.9 683.4 345.7 C
AT	2011-01-01	04:38:46	1m	335.6	498.5	600.4	343.5	C
								AT 2011-01-01 05:06:46 1m 362.7 486.8 684.9 344.8 C
AT	2011-01-01	04:39:46	1m	336.0	493.9	599.8	343.7	C
								AT 2011-01-01 05:07:46 1m 363.1 486.4 690.9 344.1 C
AT	2011-01-01	04:40:46	1m	336.4	489.1	599.8	343.8	C
								AT 2011-01-01 05:08:46 1m 361.7 486.2 700.2 344.4 C
AT	2011-01-01	04:41:46	1m	336.9	484.3	600.6	344.4	C
								AT 2011-01-01 05:09:46 1m 361.8 485.8 700.8 343.9 C
AT	2011-01-01	04:42:46	1m	336.7	480.8	602.3	345.4	C
								AT 2011-01-01 05:10:46 1m 360.2 484.7 706.2 343.5 C
AT	2011-01-01	04:43:46	1m	336.2	476.0	605.6	346.8	C
								AT 2011-01-01 05:11:46 1m 359.3 483.0 711.0 343.0 C
AT	2011-01-01	04:44:46	1m	338.6	470.8	604.8	347.7	C
								AT 2011-01-01 05:12:46 1m 358.2 481.3 712.5 342.8 C
AT	2011-01-01	04:45:46	1m	339.2	468.6	602.7	347.3	C
								AT 2011-01-01 05:13:46 1m 357.7 478.5 710.4 342.4 C
AT	2011-01-01	04:46:46	1m	341.7	469.7	607.2	344.8	C
								AT 2011-01-01 05:14:46 1m 355.6 475.4 714.0 343.0 C
AT	2011-01-01	04:47:46	1m	343.7	472.6	614.9	344.6	C
								AT 2011-01-01 05:15:46 1m 353.5 471.9 722.9 343.8 C
AT	2011-01-01	04:48:46	1m	345.2	475.3	620.9	345.2	C
								AT 2011-01-01 05:16:46 1m 352.9 462.6 728.2 344.4 C
AT	2011-01-01	04:49:46	1m	345.6	477.1	629.7	346.4	C
								AT 2011-01-01 05:17:46 1m 351.9 453.9 725.1 344.4 C
AT	2011-01-01	04:50:46	1m	347.5	479.6	641.2	347.8	C
								AT 2011-01-01 05:18:46 1m 350.3 446.4 736.8 345.3 C
AT	2011-01-01	04:51:46	1m	349.0	481.5	646.3	348.3	C
								AT 2011-01-01 05:19:46 1m 349.3 439.7 742.6 346.3 C
AT	2011-01-01	04:52:46	1m	350.2	482.3	647.4	348.7	C
								AT 2011-01-01 05:20:46 1m 348.6 433.3 741.9 346.6 C
AT	2011-01-01	04:53:46	1m	351.3	482.6	647.3	349.4	C
								AT 2011-01-01 05:21:46 1m 345.9 427.0 740.3 346.4 C
AT	2011-01-01	04:54:46	1m	354.3	483.1	651.4	349.5	C
								AT 2011-01-01 05:22:46 1m 343.4 421.3 746.7 346.6 C
AT	2011-01-01	04:55:46	1m	355.5	484.7	656.3	349.5	C
								AT 2011-01-01 05:23:46 1m 342.3 416.8 748.9 346.6 C
AT	2011-01-01	04:56:46	1m	356.3	486.2	663.0	349.6	C
								AT 2011-01-01 05:24:46 1m 342.4 413.7 763.8 347.0 C
AT	2011-01-01	04:57:46	1m	356.6	490.3	670.0	349.6	C
								AT 2011-01-01 05:25:46 1m 342.5 414.4 774.6 348.2 C
AT	2011-01-01	04:58:46	1m	358.9	491.4	670.8	348.3	C
								AT 2011-01-01 05:26:46 1m 342.8 394.7 765.5 350.1 C
AT	2011-01-01	04:59:46	1m	361.8	492.2	667.8	346.9	C
								AT 2011-01-01 05:27:46 1m 342.3 398.7 751.6 351.7 C
AT	2011-01-01	05:00:46	1m	363.3	493.2	662.8	346.7	C
								AT 2011-01-01 05:28:46 1m 343.2 402.4 750.1 353.2 C
AT	2011-01-01	05:01:46	1m	361.9	493.3	662.2	346.9	C
AT	2011-01-01	05:02:46	1m	360.2	492.9	676.5	347.3	C
AT	2011-01-01	05:03:46	1m	360.5	490.9	685.3	346.9	C
AT	2011-01-01	05:04:46	1m	361.0	489.4	684.3	346.6	C

April 27, 2021, Long Term Firing Event

MN/AT	date	time	int	1ch	2ch	3ch	4ch	unit
								AT 2011-01-01 05:56:46 1m 344.8 605.4 702.2 357.8 C
AT	2011-01-01	05:29:46	1m	345.6	404.3	707.5	353.6	C
								AT 2011-01-01 05:57:46 1m 344.8 611.9 691.2 359.1 C
AT	2011-01-01	05:30:46	1m	345.4	412.9	680.2	355.7	C
								AT 2011-01-01 05:58:46 1m 344.6 608.4 676.2 359.7 C
AT	2011-01-01	05:31:46	1m	344.6	418.7	677.2	358.1	C
								AT 2011-01-01 05:59:46 1m 344.2 612.7 664.9 359.8 C
AT	2011-01-01	05:32:46	1m	344.1	421.3	673.6	359.9	C
								AT 2011-01-01 06:00:46 1m 343.2 621.3 657.9 360.1 C
AT	2011-01-01	05:33:46	1m	343.3	423.2	674.6	361.6	C
								AT 2011-01-01 06:01:46 1m 342.1 625.4 655.2 360.7 C
AT	2011-01-01	05:34:46	1m	342.9	425.8	666.7	362.3	C
								AT 2011-01-01 06:02:46 1m 340.4 629.5 654.3 361.1 C
AT	2011-01-01	05:35:46	1m	342.8	430.8	646.7	362.3	C
								AT 2011-01-01 06:03:46 1m 339.2 629.3 652.7 361.7 C
AT	2011-01-01	05:36:46	1m	342.8	433.2	644.7	362.3	C
								AT 2011-01-01 06:04:46 1m 337.7 630.4 650.1 362.1 C
AT	2011-01-01	05:37:46	1m	342.7	434.2	644.7	362.2	C
								AT 2011-01-01 06:05:46 1m 335.3 613.3 650.5 362.3 C
AT	2011-01-01	05:38:46	1m	340.9	433.7	657.8	362.2	C
								AT 2011-01-01 06:06:46 1m 334.2 595.6 647.6 362.0 C
AT	2011-01-01	05:39:46	1m	340.3	431.6	674.4	361.9	C
								AT 2011-01-01 06:07:46 1m 333.4 574.3 644.2 361.6 C
AT	2011-01-01	05:40:46	1m	340.2	430.9	681.7	361.3	C
								AT 2011-01-01 06:08:46 1m 332.7 555.7 642.6 361.3 C
AT	2011-01-01	05:41:46	1m	339.7	428.7	691.5	360.9	C
								AT 2011-01-01 06:09:46 1m 332.1 542.7 641.9 360.9 C
AT	2011-01-01	05:42:46	1m	338.9	426.8	702.3	360.8	C
								AT 2011-01-01 06:10:46 1m 330.9 534.6 641.1 361.2 C
AT	2011-01-01	05:43:46	1m	338.7	423.2	715.4	361.2	C
								AT 2011-01-01 06:11:46 1m 330.4 528.4 637.9 361.1 C
AT	2011-01-01	05:44:46	1m	340.4	422.7	716.3	361.3	C
								AT 2011-01-01 06:12:46 1m 330.7 522.7 638.9 360.6 C
AT	2011-01-01	05:45:46	1m	342.4	424.5	720.7	361.4	C
								AT 2011-01-01 06:13:46 1m 334.9 535.8 640.7 359.9 C
AT	2011-01-01	05:46:46	1m	344.1	427.5	731.3	361.2	C
								AT 2011-01-01 06:14:46 1m 337.4 561.8 635.1 359.4 C
AT	2011-01-01	05:47:46	1m	344.6	432.8	733.8	360.2	C
								AT 2011-01-01 06:15:46 1m 339.3 574.8 625.8 359.2 C
AT	2011-01-01	05:48:46	1m	344.7	430.0	727.9	358.2	C
								AT 2011-01-01 06:16:46 1m 342.2 584.4 616.4 358.6 C
AT	2011-01-01	05:49:46	1m	344.3	458.4	716.4	357.6	C
								AT 2011-01-01 06:17:46 1m 346.1 593.0 608.4 356.8 C
AT	2011-01-01	05:50:46	1m	344.2	478.1	707.3	357.2	C
								AT 2011-01-01 06:18:46 1m 351.3 597.9 602.8 356.3 C
AT	2011-01-01	05:51:46	1m	344.2	497.7	699.9	357.4	C
								AT 2011-01-01 06:19:46 1m 356.5 598.4 597.4 354.3 C
AT	2011-01-01	05:52:46	1m	344.3	514.4	698.4	357.6	C
AT	2011-01-01	05:53:46	1m	343.8	531.2	698.2	358.1	C
AT	2011-01-01	05:54:46	1m	344.0	545.6	700.4	358.3	C
AT	2011-01-01	05:55:46	1m	344.5	553.9	702.8	357.9	C
								AT 2011-01-01 06:20:46 1m 361.6 598.2 592.7 353.1 C

April 27, 2021, Long Term Firing Event

MN/AT	date	time	int	1ch	2ch	3ch	4ch	unit
AT	2011-01-01	06:21:46	1m	366.2	596.5	588.7	351.7	C
AT	2011-01-01	06:22:46	1m	373.1	602.1	588.1	352.0	C
AT	2011-01-01	06:23:46	1m	377.9	577.8	586.9	350.6	C
AT	2011-01-01	06:24:46	1m	381.4	566.7	583.2	350.4	C
AT	2011-01-01	06:25:46	1m	383.6	556.9	578.8	348.7	C
AT	2011-01-01	06:26:46	1m	385.4	548.1	573.7	347.7	C
AT	2011-01-01	06:27:46	1m	386.4	541.3	571.1	345.1	C
AT	2011-01-01	06:28:46	1m	387.6	535.2	568.4	343.8	C
AT	2011-01-01	06:29:46	1m	389.4	530.2	565.9	342.9	C
AT	2011-01-01	06:30:46	1m	390.8	526.2	564.9	342.0	C
AT	2011-01-01	06:31:46	1m	393.1	522.9	564.6	341.1	C
AT	2011-01-01	06:32:46	1m	395.4	519.9	564.8	340.5	C
AT	2011-01-01	06:33:46	1m	411.6	504.0	637.7	342.3	C
AT	2011-01-01	06:34:46	1m	422.7	500.8	726.5	341.3	C
AT	2011-01-01	06:35:46	1m	427.1	503.6	740.8	340.9	C
AT	2011-01-01	06:36:46	1m	430.6	506.9	703.5	338.4	C
AT	2011-01-01	06:37:46	1m	440.3	505.7	672.9	338.9	C

AT	2011-01-01	06:38:46	1m	448.5	503.7	679.4	340.2	C
AT	2011-01-01	06:39:46	1m	450.4	502.1	681.2	338.7	C
AT	2011-01-01	06:40:46	1m	449.3	500.1	689.8	338.1	C
AT	2011-01-01	06:41:46	1m	446.3	497.3	666.3	335.8	C
AT	2011-01-01	06:42:46	1m	444.8	495.0	672.3	334.9	C
AT	2011-01-01	06:43:46	1m	442.8	491.7	667.3	333.7	C
AT	2011-01-01	06:44:46	1m	439.9	487.8	666.9	333.1	C
AT	2011-01-01	06:45:46	1m	436.3	483.3	659.5	331.5	C
AT	2011-01-01	06:46:46	1m	432.7	479.1	637.8	329.7	C
AT	2011-01-01	06:47:46	1m	429.9	475.5	615.2	327.7	C
AT	2011-01-01	06:48:46	1m	428.7	471.4	611.9	327.3	C
AT	2011-01-01	06:49:46	1m	429.2	466.9	614.1	327.5	C
AT	2011-01-01	06:50:46	1m	425.3	462.3	607.8	343.3	C
AT	2011-01-01	06:51:46	1m	418.2	460.8	578.8	349.4	C
AT	2011-01-01	06:52:46	1m	415.3	462.0	562.1	354.2	C
AT	2011-01-01	06:53:46	1m	414.0	465.1	551.1	357.3	C
AT	2011-01-01	06:54:46	1m	413.2	467.6	544.4	360.3	C
AT	2011-01-01	06:55:46	1m	412.3	468.8	538.8	363.2	C
AT	2011-01-01	06:56:46	1m	411.7	466.5	532.8	365.9	C

April 30th, 2021. Short Terming Firing Event

MN/AT	date	time	int	1ch	2ch	3ch	4ch	unit									
									AT	2011-01-31	00:30:48	1m	289.1	18.0	17.6	363.4	C
AT	2011-01-31	00:04:48	1m	5.4	1.9	4.9	9.2	C	AT	2011-01-31	00:31:48	1m	298.2	20.8	25.5	427.6	C
AT	2011-01-31	00:05:48	1m	4.7	2.1	4.8	67.7	C	AT	2011-01-31	00:32:48	1m	325.6	22.3	29.3	435.3	C
AT	2011-01-31	00:06:48	1m	5.4	2.2	4.6	87.6	C	AT	2011-01-31	00:33:48	1m	326.4	22.7	38.2	431.2	C
AT	2011-01-31	00:07:48	1m	8.9	3.4	5.6	126.8	C	AT	2011-01-31	00:34:48	1m	320.2	21.6	37.0	436.4	C
AT	2011-01-31	00:08:48	1m	21.1	5.2	9.0	162.0	C	AT	2011-01-31	00:35:48	1m	298.7	22.1	34.3	676.1	C
AT	2011-01-31	00:09:48	1m	35.1	5.8	10.6	179.0	C	AT	2011-01-31	00:36:48	1m	285.7	31.2	43.7	678.9	C
AT	2011-01-31	00:10:48	1m	63.7	19.7	16.6	159.9	C	AT	2011-01-31	00:37:48	1m	276.4	25.1	41.9	673.7	C
AT	2011-01-31	00:11:48	1m	92.8	9.4	19.2	175.5	C	AT	2011-01-31	00:38:48	1m	247.3	18.3	34.9	688.9	C
AT	2011-01-31	00:12:48	1m	118.3	9.3	21.5	201.2	C	AT	2011-01-31	00:39:48	1m	238.8	19.0	29.6	666.6	C
AT	2011-01-31	00:13:48	1m	131.3	6.3	23.4	186.0	C	AT	2011-01-31	00:40:48	1m	233.6	16.3	27.1	671.7	C
AT	2011-01-31	00:14:48	1m	121.9	4.5	19.1	167.7	C	AT	2011-01-31	00:41:48	1m	240.2	17.3	28.3	701.0	C
AT	2011-01-31	00:15:48	1m	140.7	3.3	14.9	169.5	C	AT	2011-01-31	00:42:48	1m	271.6	15.9	35.9	679.6	C
AT	2011-01-31	00:16:48	1m	126.4	3.3	11.8	149.8	C	AT	2011-01-31	00:43:48	1m	307.3	17.2	41.7	692.1	C
AT	2011-01-31	00:17:48	1m	138.5	3.4	10.7	154.8	C	AT	2011-01-31	00:44:48	1m	333.8	21.9	48.4	687.1	C
AT	2011-01-31	00:18:48	1m	181.4	4.3	11.1	164.2	C	AT	2011-01-31	00:45:48	1m	358.8	22.8	55.3	702.9	C
AT	2011-01-31	00:19:48	1m	177.0	7.9	11.1	187.4	C	AT	2011-01-31	00:46:48	1m	485.8	23.8	64.1	717.2	C
AT	2011-01-31	00:20:48	1m	187.7	5.3	13.4	183.3	C	AT	2011-01-31	00:47:48	1m	464.2	24.4	70.3	737.2	C
AT	2011-01-31	00:21:48	1m	208.4	4.8	14.4	206.6	C	AT	2011-01-31	00:48:48	1m	416.6	24.3	69.3	792.6	C
AT	2011-01-31	00:22:48	1m	214.1	7.9	15.9	226.8	C	AT	2011-01-31	00:49:48	1m	399.1	24.4	67.7	744.3	C
AT	2011-01-31	00:23:48	1m	205.6	6.1	18.0	239.7	C	AT	2011-01-31	00:50:48	1m	413.6	22.0	63.4	762.6	C
AT	2011-01-31	00:24:48	1m	241.1	5.7	19.8	280.9	C	AT	2011-01-31	00:51:48	1m	394.4	26.2	63.2	773.2	C
AT	2011-01-31	00:25:48	1m	246.3	11.8	19.3	307.1	C	AT	2011-01-31	00:52:48	1m	394.1	26.0	65.0	787.7	C
AT	2011-01-31	00:26:48	1m	232.9	6.6	15.6	304.2	C	AT	2011-01-31	00:53:48	1m	403.8	20.9	64.3	793.7	C
AT	2011-01-31	00:27:48	1m	223.2	6.1	13.6	324.5	C	AT	2011-01-31	00:54:48	1m	451.5	18.1	65.4	802.6	C
AT	2011-01-31	00:28:48	1m	215.7	7.4	12.2	317.4	C									
AT	2011-01-31	00:29:48	1m	237.8	7.4	12.3	326.1	C									

April 30th, 2021. Short Tarming Firing Event

MN/AT	date	time	int	1ch	2ch	3ch	4ch	unit
AT	2011-01-31	00:55:48	1m	463.1	17.4	71.7	809.0	C
AT	2011-01-31	00:56:48	1m	462.5	17.9	85.6	796.9	C
AT	2011-01-31	00:57:48	1m	475.1	29.4	120.6	804.9	C
AT	2011-01-31	00:58:48	1m	486.8	30.1	166.3	822.2	C
AT	2011-01-31	00:59:48	1m	522.2	36.3	336.4	788.1	C
AT	2011-01-31	01:00:48	1m	653.5	32.1	438.3	777.8	C
AT	2011-01-31	01:01:48	1m	693.2	218.3	561.5	767.1	C
AT	2011-01-31	01:02:48	1m	629.4	44.5	560.5	783.9	C
AT	2011-01-31	01:03:48	1m	577.6	50.2	625.9	772.6	C
AT	2011-01-31	01:04:48	1m	576.3	71.2	634.6	793.6	C
AT	2011-01-31	01:05:48	1m	632.8	59.4	641.6	773.8	C
AT	2011-01-31	01:06:48	1m	599.7	78.1	566.1	748.4	C
AT	2011-01-31	01:07:48	1m	605.2	45.8	554.0	754.2	C
AT	2011-01-31	01:08:48	1m	615.4	80.2	569.0	785.4	C
AT	2011-01-31	01:09:48	1m	602.1	49.7	564.3	816.3	C
AT	2011-01-31	01:10:48	1m	596.7	75.6	577.2	817.4	C
AT	2011-01-31	01:11:48	1m	603.9	69.4	561.2	830.6	C
AT	2011-01-31	01:12:48	1m	610.6	58.7	566.3	798.4	C
AT	2011-01-31	01:13:48	1m	678.1	53.1	569.9	807.3	C
AT	2011-01-31	01:14:48	1m	726.4	53.8	620.5	817.7	C
AT	2011-01-31	01:15:48	1m	746.9	54.1	582.9	790.9	C
AT	2011-01-31	01:16:48	1m	775.2	114.1	529.4	817.0	C
AT	2011-01-31	01:17:48	1m	787.4	106.4	613.9	836.4	C
AT	2011-01-31	01:18:48	1m	802.4	97.1	613.3	810.1	C
AT	2011-01-31	01:19:48	1m	806.9	94.4	658.5	814.3	C
AT	2011-01-31	01:46:48	1m	859.7	246.3	814.1	981.9	C
AT	2011-01-31	01:47:48	1m	798.3	702.9	821.4	952.1	C

AT	2011-01-31	01:20:48	1m	808.6	94.3	674.6	819.6	C
AT	2011-01-31	01:21:48	1m	833.3	96.3	690.1	845.6	C
AT	2011-01-31	01:22:48	1m	850.4	110.1	644.7	856.9	C
AT	2011-01-31	01:23:48	1m	863.8	112.6	671.0	817.3	C
AT	2011-01-31	01:24:48	1m	868.7	107.3	663.2	810.9	C
AT	2011-01-31	01:25:48	1m	875.6	112.6	682.3	812.6	C
AT	2011-01-31	01:26:48	1m	866.4	115.4	698.0	839.2	C
AT	2011-01-31	01:27:48	1m	857.8	122.1	685.3	817.4	C
AT	2011-01-31	01:28:48	1m	856.8	127.9	670.2	826.0	C
AT	2011-01-31	01:29:48	1m	854.2	132.9	655.8	838.6	C
AT	2011-01-31	01:30:48	1m	853.3	121.4	708.9	903.3	C
AT	2011-01-31	01:31:48	1m	854.8	124.5	701.6	900.0	C
AT	2011-01-31	01:32:48	1m	852.8	103.5	718.8	912.0	C
AT	2011-01-31	01:33:48	1m	849.4	132.4	703.4	914.7	C
AT	2011-01-31	01:34:48	1m	856.2	124.1	709.2	864.3	C
AT	2011-01-31	01:35:48	1m	858.0	138.3	705.7	913.2	C
AT	2011-01-31	01:36:48	1m	869.6	109.5	695.7	867.6	C
AT	2011-01-31	01:37:48	1m	874.6	117.1	691.7	865.6	C
AT	2011-01-31	01:38:48	1m	879.1	318.3	736.6	911.5	C
AT	2011-01-31	01:39:48	1m	878.3	179.0	719.2	891.3	C
AT	2011-01-31	01:40:48	1m	866.9	170.0	717.3	952.6	C
AT	2011-01-31	01:41:48	1m	853.6	137.7	796.6	856.9	C
AT	2011-01-31	01:42:48	1m	854.3	264.3	809.8	932.4	C
AT	2011-01-31	01:43:48	1m	858.8	134.1	800.5	928.4	C
AT	2011-01-31	01:44:48	1m	878.4	179.6	795.3	948.9	C
AT	2011-01-31	01:45:48	1m	880.7	274.4	811.2	984.2	C
AT	2011-01-31	01:48:48	1m	788.1	495.6	829.5	964.7	C

April 30th, 2021. Short Terming Firing Event

MN/AT	date	time	int	1ch	2ch	3ch	4ch	unit
AT	2011-01-31	01:49:48	1m	785.8	292.5	830.8	961.4	C
AT	2011-01-31	01:50:48	1m	780.9	349.2	831.2	950.3	C
AT	2011-01-31	01:51:48	1m	778.9	266.6	828.3	966.2	C
AT	2011-01-31	01:52:48	1m	784.1	269.1	830.4	969.1	C
AT	2011-01-31	01:53:48	1m	789.8	263.3	839.1	1001	C
AT	2011-01-31	01:54:48	1m	788.7	287.6	836.3	971.3	C
AT	2011-01-31	01:55:48	1m	780.8	146.7	797.8	949.8	C
AT	2011-01-31	01:56:48	1m	757.1	118.3	757.8	936.4	C
AT	2011-01-31	01:57:48	1m	747.2	112.3	749.8	934.9	C
AT	2011-01-31	01:58:48	1m	737.9	177.6	754.4	905.5	C
AT	2011-01-31	01:59:48	1m	736.4	149.1	759.5	902.6	C
AT	2011-01-31	02:00:48	1m	736.6	117.8	761.2	915.0	C
AT	2011-01-31	02:01:48	1m	737.2	137.4	766.2	932.7	C
AT	2011-01-31	02:02:48	1m	739.9	140.2	775.4	943.9	C
AT	2011-01-31	02:03:48	1m	740.3	183.1	785.2	973.1	C
AT	2011-01-31	02:04:48	1m	744.7	145.0	791.7	982.9	C
AT	2011-01-31	02:05:48	1m	752.9	200.7	800.6	981.9	C
AT	2011-01-31	02:06:48	1m	763.0	176.4	805.7	962.1	C
AT	2011-01-31	02:07:48	1m	746.0	208.6	811.7	924.1	C
AT	2011-01-31	02:08:48	1m	749.7	155.2	810.1	910.3	C
AT	2011-01-31	02:09:48	1m	753.4	209.1	814.1	919.4	C
AT	2011-01-31	02:10:48	1m	770.5	178.3	813.4	936.0	C
AT	2011-01-31	02:11:48	1m	772.6	186.8	810.4	925.9	C
AT	2011-01-31	02:37:48	1m	672.2		822.9	809.2	C
AT	2011-01-31	02:38:48	1m	673.0		804.4	807.8	C
AT	2011-01-31	02:39:48	1m	674.1		796.6	806.7	C
AT	2011-01-31	02:40:48	1m	677.9		785.2	801.1	C

AT	2011-01-31	02:12:48	1m	777.9	192.3	810.2	911.6	C
AT	2011-01-31	02:13:48	1m	779.6	196.9	808.2	933.4	C
AT	2011-01-31	02:14:48	1m	775.6	198.3	765.3	934.8	C
AT	2011-01-31	02:15:48	1m	771.6	189.1	750.3	934.5	C
AT	2011-01-31	02:16:48	1m	774.6	244.4	753.2	936.1	C
AT	2011-01-31	02:17:48	1m	756.9	137.2	744.2	920.3	C
AT	2011-01-31	02:18:48	1m	743.7	155.6	744.7	905.4	C
AT	2011-01-31	02:19:48	1m	733.1	119.2	744.6	918.1	C
AT	2011-01-31	02:20:48	1m	722.8	143.9	747.5	927.2	C
AT	2011-01-31	02:21:48	1m	720.1	170.5	748.2	924.8	C
AT	2011-01-31	02:22:48	1m	722.7	186.2	748.6	922.1	C
AT	2011-01-31	02:23:48	1m	721.9	164.4	747.8	935.6	C
AT	2011-01-31	02:24:48	1m	718.6	192.1	746.4	919.6	C
AT	2011-01-31	02:25:48	1m	717.3	208.1	745.5	921.9	C
AT	2011-01-31	02:26:48	1m	722.8	316.6	741.9	849.6	C
AT	2011-01-31	02:27:48	1m	718.5	257.6	731.2	825.2	C
AT	2011-01-31	02:28:48	1m	710.1	248.9	726.4	813.2	C
AT	2011-01-31	02:29:48	1m	699.5	249.9	725.4	810.8	C
AT	2011-01-31	02:30:48	1m	690.3	262.8	723.4	808.8	C
AT	2011-01-31	02:31:48	1m	682.4	301.2	733.3	818.4	C
AT	2011-01-31	02:32:48	1m	675.9	330.3	741.0	813.0	C
AT	2011-01-31	02:33:48	1m	672.0	365.2	742.1	807.6	C
AT	2011-01-31	02:34:48	1m	670.4	394.3	737.7	804.9	C
AT	2011-01-31	02:35:48	1m	670.1	420.8	763.6	798.4	C
AT	2011-01-31	02:36:48	1m	671.0	445.3	810.4	805.2	C
AT	2011-01-31	02:41:48	1m	678.8		788.5	790.4	C
AT	2011-01-31	02:42:48	1m	677.1	E03	794.4	778.1	C
AT	2011-01-31	02:43:48	1m	676.8		786.0	765.2	C
AT	2011-01-31	02:44:48	1m	670.5		766.2	751.9	C

April 30th, 2021. Short Terming Firing Event

MN/AT	date	time	int	1ch	2ch	3ch	4ch	unit
AT	2011-01-31	02:45:48	1m	663.9		753.6	740.3	C
AT	2011-01-31	02:46:48	1m	658.9		744.1	733.2	C
AT	2011-01-31	02:47:48	1m	652.8		737.9	735.8	C
AT	2011-01-31	02:48:48	1m	647.4		730.4	741.7	C
AT	2011-01-31	02:49:48	1m	641.8		726.6	741.6	C
AT	2011-01-31	02:50:48	1m	636.0		725.4	741.8	C
AT	2011-01-31	02:51:48	1m	630.1		723.5	741.2	C
AT	2011-01-31	02:52:48	1m	623.9		722.9	736.5	C
AT	2011-01-31	02:53:48	1m	619.1		719.4	733.9	C
AT	2011-01-31	02:54:48	1m	615.0		717.6	730.9	C
AT	2011-01-31	02:55:48	1m	612.2		710.5	725.2	C
AT	2011-01-31	02:56:48	1m	609.8		705.4	720.0	C
AT	2011-01-31	02:57:48	1m	607.4		717.3	714.1	C
AT	2011-01-31	02:58:48	1m	606.0		730.7	708.8	C
AT	2011-01-31	02:59:48	1m	604.6		743.8	704.2	C
AT	2011-01-31	03:00:48	1m	602.9		752.9	700.2	C
AT	2011-01-31	03:01:48	1m	601.8		763.3	696.4	C
AT	2011-01-31	03:02:48	1m	600.5		774.4	695.8	C
AT	2011-01-31	03:03:48	1m	599.2		773.6	695.2	C
AT	2011-01-31	03:04:48	1m	597.7		772.9	689.0	C
AT	2011-01-31	03:05:48	1m	596.6		766.8	683.6	C
AT	2011-01-31	03:06:48	1m	595.4		761.6	677.0	C
AT	2011-01-31	03:30:48	1m	562.6		724.9	610.1	C
AT	2011-01-31	03:31:48	1m	560.6		714.7	608.2	C
AT	2011-01-31	03:32:48	1m	559.2		710.7	606.6	C
AT	2011-01-31	03:33:48	1m	557.6		700.9	605.6	C
AT	2011-01-31	03:34:48	1m	555.8		688.5	604.1	C
AT	2011-01-31	03:07:48	1m	592.6		753.8	669.5	C
AT	2011-01-31	03:08:48	1m	592.1		748.4	664.7	C
AT	2011-01-31	03:09:48	1m	591.6		754.7	659.2	C
AT	2011-01-31	03:10:48	1m	590.6		763.9	654.4	C
AT	2011-01-31	03:11:48	1m	590.1		771.8	651.2	C
AT	2011-01-31	03:12:48	1m	589.4		778.5	648.7	C
AT	2011-01-31	03:13:48	1m	588.9		784.4	647.4	C
AT	2011-01-31	03:14:48	1m	588.3		786.4	646.7	C
AT	2011-01-31	03:15:48	1m	587.2		789.4	645.8	C
AT	2011-01-31	03:16:48	1m	586.4		791.7	644.7	C
AT	2011-01-31	03:17:48	1m	586.3		793.2	643.6	C
AT	2011-01-31	03:18:48	1m	586.0		795.0	643.1	C
AT	2011-01-31	03:19:48	1m	585.8		793.7	642.8	C
AT	2011-01-31	03:20:48	1m	585.1		790.1	641.4	C
AT	2011-01-31	03:21:48	1m	584.0		773.0	638.2	C
AT	2011-01-31	03:22:48	1m	583.1		758.6	634.2	C
AT	2011-01-31	03:23:48	1m	581.8		750.8	629.5	C
AT	2011-01-31	03:24:48	1m	579.3		750.3	624.9	C
AT	2011-01-31	03:25:48	1m	576.6		751.9	621.3	C
AT	2011-01-31	03:26:48	1m	574.0		747.1	618.6	C
AT	2011-01-31	03:27:48	1m	570.4		740.4	616.6	C
AT	2011-01-31	03:28:48	1m	567.6		733.1	613.8	C
AT	2011-01-31	03:29:48	1m	565.1		734.1	611.7	C
AT	2011-01-31	03:35:48	1m	554.8		678.6	602.3	C
AT	2011-01-31	03:36:48	1m	553.4		670.0	600.6	C
AT	2011-01-31	03:37:48	1m	551.8		662.8	599.2	C
AT	2011-01-31	03:38:48	1m	550.5		657.3	598.2	C
AT	2011-01-31	03:39:48	1m	549.5		652.6	597.8	C

April 30th, 2021. Short Terming Firing Event

MN/AT	date	time	int	1ch	2ch	3ch	4ch	unit
AT	2011-01-31	04:07:48	1m	547.8		671.4	561.3	C
AT	2011-01-31	04:08:48	1m	546.5		671.7	560.6	C
AT	2011-01-31	04:09:48	1m	544.8		672.8	559.8	C
AT	2011-01-31	04:10:48	1m	542.7		673.3	559.1	C
AT	2011-01-31	04:11:48	1m	541.1		673.9	558.8	C
AT	2011-01-31	04:12:48	1m	539.1		674.9	558.6	C
AT	2011-01-31	04:13:48	1m	537.7		681.7	558.6	C
AT	2011-01-31	04:14:48	1m	536.3		682.5	558.8	C
AT	2011-01-31	04:15:48	1m	535.0		682.1	558.8	C
AT	2011-01-31	04:16:48	1m	533.0		681.1	558.6	C
AT	2011-01-31	04:17:48	1m	531.4		681.8	558.1	C
AT	2011-01-31	04:18:48	1m	531.2		683.9	557.0	C
AT	2011-01-31	04:19:48	1m	530.8		687.2	555.6	C
AT	2011-01-31	04:20:48	1m	529.4		689.4	553.8	C
AT	2011-01-31	04:21:48	1m	529.2		690.7	552.2	C
AT	2011-01-31	04:22:48	1m	528.7		691.8	550.8	C
AT	2011-01-31	04:23:48	1m	528.4		692.6	549.9	C
AT	2011-01-31	04:24:48	1m	527.5		692.6	548.8	C
AT	2011-01-31	04:25:48	1m	525.6		690.9	548.1	C
AT	2011-01-31	04:26:48	1m	524.6		688.1	547.3	C
AT	2011-01-31	04:27:48	1m	524.1		684.2	546.8	C
AT	2011-01-31	04:28:48	1m	523.7		680.5	546.2	C
AT	2011-01-31	04:29:48	1m	523.0		677.0	545.5	C
AT	2011-01-31	04:30:48	1m	522.6		673.6	544.7	C
AT	2011-01-31	04:31:48	1m	522.2		672.7	543.8	C
AT	2011-01-31	04:32:48	1m	521.4		670.6	542.9	C
AT	2011-01-31	04:33:48	1m	520.6		668.3	542.3	C
AT	2011-01-31	04:34:48	1m	519.9		668.0	542.0	C
AT	2011-01-31	04:35:48	1m	519.4		671.7	542.1	C
AT	2011-01-31	03:40:48	1m	548.3	650.8	597.6		C
AT	2011-01-31	03:41:48	1m	547.3	649.3	597.3		C
AT	2011-01-31	03:42:48	1m	546.2	649.4	597.2		C
AT	2011-01-31	03:43:48	1m	545.2	651.4	597.8		C
AT	2011-01-31	03:44:48	1m	543.1	654.1	597.1		C
AT	2011-01-31	03:45:48	1m	542.3	660.1	596.9		C
AT	2011-01-31	03:46:48	1m	542.0	668.2	597.3		C
AT	2011-01-31	03:47:48	1m	542.0	674.7	597.9		C
AT	2011-01-31	03:48:48	1m	542.2	681.2	597.3		C
AT	2011-01-31	03:49:48	1m	542.7	688.1	596.1		C
AT	2011-01-31	03:50:48	1m	543.1	695.2	593.6		C
AT	2011-01-31	03:51:48	1m	542.4	699.8	590.6		C
AT	2011-01-31	03:52:48	1m	541.4	699.2	586.2		C
AT	2011-01-31	03:53:48	1m	540.6	696.7	580.4		C
AT	2011-01-31	03:54:48	1m	540.4	694.8	576.4		C
AT	2011-01-31	03:55:48	1m	541.3	694.7	573.2		C
AT	2011-01-31	03:56:48	1m	542.9	699.1	571.9		C
AT	2011-01-31	03:57:48	1m	544.7	705.9	569.9		C
AT	2011-01-31	03:58:48	1m	546.6	707.9	568.6		C
AT	2011-01-31	03:59:48	1m	548.4	704.1	568.2		C
AT	2011-01-31	04:00:48	1m	550.1	698.8	567.3		C
AT	2011-01-31	04:01:48	1m	551.4	694.4	566.6		C
AT	2011-01-31	04:02:48	1m	551.8	688.4	565.7		C
AT	2011-01-31	04:03:48	1m	551.7	684.8	564.6		C
AT	2011-01-31	04:04:48	1m	550.8	683.2	563.7		C
AT	2011-01-31	04:05:48	1m	549.8	678.9	563.1		C
AT	2011-01-31	04:06:48	1m	548.7	673.9	562.3		C

April 30th, 2021. Short Terming Firing Event

MN/AT	date	time	int	1ch	2ch	3ch	4ch	unit								
									AT	2011-01-31	05:03:48	1m	486.0	622.3	522.8	C
AT	2011-01-31	04:36:48	1m	519.0		675.6	542.1	C	AT	2011-01-31	05:04:48	1m	486.9	617.8	520.5	C
AT	2011-01-31	04:37:48	1m	518.6		679.9	542.3	C	AT	2011-01-31	05:05:48	1m	487.0	612.8	517.4	C
AT	2011-01-31	04:38:48	1m	518.1		683.2	542.4	C	AT	2011-01-31	05:06:48	1m	486.1	606.8	515.0	C
AT	2011-01-31	04:39:48	1m	517.6		682.8	542.9	C	AT	2011-01-31	05:07:48	1m	485.3	600.7	511.6	C
AT	2011-01-31	04:40:48	1m	516.9		676.6	543.8	C	AT	2011-01-31	05:08:48	1m	484.4	596.1	508.6	C
AT	2011-01-31	04:41:48	1m	516.1		670.2	544.0	C	AT	2011-01-31	05:09:48	1m	483.2	591.7	504.8	C
AT	2011-01-31	04:42:48	1m	515.4		667.7	543.8	C	AT	2011-01-31	05:10:48	1m	481.8	588.3	501.2	C
AT	2011-01-31	04:43:48	1m	514.4		665.6	544.0	C	AT	2011-01-31	05:11:48	1m	481.1	586.6	498.2	C
AT	2011-01-31	04:44:48	1m	513.7		663.0	544.9	C	AT	2011-01-31	05:12:48	1m	480.6	584.2	496.1	C
AT	2011-01-31	04:45:48	1m	512.3		663.1	545.7	C	AT	2011-01-31	05:13:48	1m	480.0	582.7	493.2	C
AT	2011-01-31	04:46:48	1m	511.2		661.2	546.1	C	AT	2011-01-31	05:14:48	1m	479.7	581.9	491.6	C
AT	2011-01-31	04:47:48	1m	508.0		657.0	546.0	C	AT	2011-01-31	05:15:48	1m	479.1	581.3	489.6	C
AT	2011-01-31	04:48:48	1m	505.6		650.9	544.6	C	AT	2011-01-31	05:16:48	1m	478.3	579.5	487.6	C
AT	2011-01-31	04:49:48	1m	503.9		647.1	542.8	C	AT	2011-01-31	05:17:48	1m	477.3	577.6	484.7	C
AT	2011-01-31	04:50:48	1m	502.4		644.9	540.7	C	AT	2011-01-31	05:18:48	1m	475.6	574.3	481.7	C
AT	2011-01-31	04:51:48	1m	501.0		644.2	538.4	C	AT	2011-01-31	05:19:48	1m	474.2	571.9	479.2	C
AT	2011-01-31	04:52:48	1m	499.6		644.4	536.5	C	AT	2011-01-31	05:20:48	1m	473.4	570.2	477.7	C
AT	2011-01-31	04:53:48	1m	498.3		644.7	535.3	C	AT	2011-01-31	05:21:48	1m	472.8	568.8	476.9	C
AT	2011-01-31	04:54:48	1m	496.8		644.1	533.0	C	AT	2011-01-31	05:22:48	1m	472.2	567.9	476.1	C
AT	2011-01-31	04:55:48	1m	494.6		643.5	531.4	C	AT	2011-01-31	05:23:48	1m	470.9	566.6	474.6	C
AT	2011-01-31	04:56:48	1m	493.2		642.9	530.2	C	AT	2011-01-31	05:24:48	1m	469.5	565.1	473.2	C
AT	2011-01-31	04:57:48	1m	492.0		642.9	529.0	C	AT	2011-01-31	05:25:48	1m	468.1	562.9	471.8	C
AT	2011-01-31	04:58:48	1m	490.8		642.1	528.0	C	AT	2011-01-31	05:26:48	1m	467.0	560.2	470.8	C
AT	2011-01-31	04:59:48	1m	489.6		641.4	527.2	C	AT	2011-01-31	05:27:48	1m	465.7	557.1	470.4	C
AT	2011-01-31	05:00:48	1m	488.3		640.5	526.3	C	AT	2011-01-31	05:28:48	1m	464.4	553.3	470.7	C
AT	2011-01-31	05:01:48	1m	487.3		634.9	525.3	C	AT	2011-01-31	05:29:48	1m	463.4	549.8	471.2	C
AT	2011-01-31	05:02:48	1m	486.7		627.7	524.2	C	AT	2011-01-31	05:30:48	1m	462.3	546.9	471.7	C

April 30th, 2021. Short Terming Firing Event

MN/AT	date	time	int	1ch	2ch	3ch	4ch	unit								
									AT	2011-01-31	05:44:48	1m	445.9	538.4	482.3	C
AT	2011-01-31	05:31:48	1m	461.1		543.2	471.4	C	AT	2011-01-31	05:45:48	1m	444.5	515.5	488.6	C
AT	2011-01-31	05:32:48	1m	460.3		539.8	471.2	C	AT	2011-01-31	05:46:48	1m	443.2	493.4	494.9	C
AT	2011-01-31	05:33:48	1m	459.2		536.7	470.5	C	AT	2011-01-31	05:47:48	1m	442.1	468.1	500.1	C
AT	2011-01-31	05:34:48	1m	458.2		533.9	469.2	C	AT	2011-01-31	05:48:48	1m	440.9	444.1	504.4	C
AT	2011-01-31	05:35:48	1m	457.2		531.0	468.3	C	AT	2011-01-31	05:49:48	1m	173.2	420.1	507.1	C
AT	2011-01-31	05:36:48	1m	456.3		527.9	467.7	C	AT	2011-01-31	05:50:48	1m	70.6	400.6	508.8	C
AT	2011-01-31	05:37:48	1m	455.1		524.1	466.6	C	AT	2011-01-31	05:51:48	1m	37.9	379.3	429.8	C
AT	2011-01-31	05:38:48	1m	454.2		521.2	465.4	C								
AT	2011-01-31	05:39:48	1m	453.2		517.7	464.5	C								
AT	2011-01-31	05:40:48	1m	452.1		514.5	463.3	C								
AT	2011-01-31	05:41:48	1m	450.9		510.9	462.3	C								
AT	2011-01-31	05:42:48	1m	448.7		510.8	474.3	C								
AT	2011-01-31	05:43:48	1m	447.4		511.3	477.0	C								

May 1st, 2021. Short Term Firing Event

MN/AT	date	time	int	1ch	2ch	3ch	4ch	unit
AT	2011-02-03	01:12:59	1m	6.4	4.8	9.8	7.4	C
AT	2011-02-03	01:13:59	1m	5.4	4.1	7.3	5.7	C
AT	2011-02-03	01:14:59	1m	5.1	3.8	6.2	5.2	C
AT	2011-02-03	01:15:59	1m	4.8	3.6	5.6	4.7	C
AT	2011-02-03	01:16:59	1m	4.6	3.8	5.2	4.4	C
AT	2011-02-03	01:17:59	1m	9.0	4.3	4.9	4.4	C
AT	2011-02-03	01:18:59	1m	29.0	4.1	4.7	8.4	C
AT	2011-02-03	01:19:59	1m	25.3	5.0	4.9	10.9	C
AT	2011-02-03	01:20:59	1m	24.0	4.4	7.8	11.4	C
AT	2011-02-03	01:21:59	1m	96.4	8.7	9.4	17.1	C
AT	2011-02-03	01:22:59	1m	109.8	13.4	29.1	32.1	C
AT	2011-02-03	01:23:59	1m	411.1	14.8	76.4	91.0	C
AT	2011-02-03	01:24:59	1m	418.3	17.8	302.0	125.8	C
AT	2011-02-03	01:25:59	1m	510.9	21.2	481.8	243.9	C
AT	2011-02-03	01:26:59	1m	493.2	24.1	515.9	458.7	C
AT	2011-02-03	01:27:59	1m	471.4	82.1	497.2	474.9	C
AT	2011-02-03	01:28:59	1m	504.4	36.7	462.4	473.3	C
AT	2011-02-03	01:29:59	1m	479.9	21.9	402.6	449.7	C
AT	2011-02-03	01:30:59	1m	481.0	26.0	400.1	406.1	C
AT	2011-02-03	01:31:59	1m	560.8	28.3	396.3	447.3	C
AT	2011-02-03	01:32:59	1m	643.9	26.9	389.0	450.0	C
AT	2011-02-03	01:33:59	1m	627.8	28.3	400.8	456.7	C
AT	2011-02-03	01:34:59	1m	650.8	32.7	436.4	463.2	C
AT	2011-02-03	01:35:59	1m	710.4	40.2	511.4	472.1	C
AT	2011-02-03	01:36:59	1m	694.2	42.3	558.3	500.5	C
AT	2011-02-03	01:37:59	1m	647.8	50.9	574.4	461.1	C
AT	2011-02-03	01:38:59	1m	661.0	53.6	613.2	337.2	C

AT	2011-02-03	01:39:59	1m	723.6	64.8	658.4	317.8	C
AT	2011-02-03	01:40:59	1m	715.7	39.5	673.7	331.1	C
AT	2011-02-03	01:41:59	1m	752.2	76.4	703.9	372.7	C
AT	2011-02-03	01:42:59	1m	763.4	106.6	720.6	448.2	C
AT	2011-02-03	01:43:59	1m	766.6	113.6	724.8	527.9	C
AT	2011-02-03	01:44:59	1m	756.7	112.2	738.2	481.8	C
AT	2011-02-03	01:45:59	1m	766.7	121.9	753.4	621.3	C
AT	2011-02-03	01:46:59	1m	774.1	121.4	750.2	640.1	C
AT	2011-02-03	01:47:59	1m	776.1	116.0	758.8	606.9	C
AT	2011-02-03	01:48:59	1m	775.9	122.8	764.4	649.7	C
AT	2011-02-03	01:49:59	1m	779.2	120.7	745.4	609.8	C
AT	2011-02-03	01:50:59	1m	781.7	122.6	745.7	617.5	C
AT	2011-02-03	01:51:59	1m	765.4	124.1	744.6	619.3	C
AT	2011-02-03	01:52:59	1m	820.5	148.2	757.1	614.1	C
AT	2011-02-03	01:53:59	1m	815.9	148.2	762.2	622.6	C
AT	2011-02-03	01:54:59	1m	806.9	174.7	761.5	640.1	C
AT	2011-02-03	01:55:59	1m	800.9	77.2	760.7	660.2	C
AT	2011-02-03	01:56:59	1m	805.9	63.4	771.7	677.2	C
AT	2011-02-03	01:57:59	1m	840.9	128.1	778.1	671.6	C
AT	2011-02-03	01:58:59	1m	843.1	97.1	752.7	679.3	C
AT	2011-02-03	01:59:59	1m	830.9	89.3	805.6	656.9	C
AT	2011-02-03	02:00:59	1m	848.6	94.8	825.5	663.2	C
AT	2011-02-03	02:01:59	1m	869.9	123.1	810.2	682.2	C
AT	2011-02-03	02:02:59	1m	818.1	106.4	803.2	674.4	C
AT	2011-02-03	02:03:59	1m	836.3	139.6	795.3	712.5	C
AT	2011-02-03	02:04:59	1m	830.1	148.4	778.3	715.9	C
AT	2011-02-03	02:05:59	1m	842.8	183.7	776.1	740.4	C
AT	2011-02-03	02:06:59	1m	815.8	178.4	767.9	752.8	C
AT	2011-02-03	02:07:59	1m	814.4	165.9	758.4	744.8	C

May 1st, 2021. Short Term Firing Event

MN/AT	date	time	int	1ch	2ch	3ch	4ch	unit
AT	2011-02-03	02:08:59	1m	801.3	194.7	776.4	757.3	C
AT	2011-02-03	02:09:59	1m	809.0	169.8	799.1	756.8	C
AT	2011-02-03	02:10:59	1m	756.2	133.7	792.2	784.8	C
AT	2011-02-03	02:11:59	1m	715.8	122.6	756.0	775.1	C
AT	2011-02-03	02:12:59	1m	698.2	100.7	740.9	785.8	C
AT	2011-02-03	02:13:59	1m	695.8	92.4	721.7	789.0	C
AT	2011-02-03	02:14:59	1m	692.9	68.5	697.6	784.4	C
AT	2011-02-03	02:15:59	1m	696.2	91.7	681.9	782.3	C
AT	2011-02-03	02:16:59	1m	702.0	74.9	672.1	784.4	C
AT	2011-02-03	02:17:59	1m	683.2	112.9	666.9	769.0	C
AT	2011-02-03	02:18:59	1m	675.1	148.2	656.5	771.6	C
AT	2011-02-03	02:19:59	1m	680.2	172.8	645.9	783.4	C
AT	2011-02-03	02:20:59	1m	678.8	98.6	639.1	788.9	C
AT	2011-02-03	02:21:59	1m	674.1	110.1	637.2	799.9	C
AT	2011-02-03	02:22:59	1m	656.9	112.2	639.7	773.6	C
AT	2011-02-03	02:23:59	1m	648.8	129.0	625.2	702.7	C
AT	2011-02-03	02:24:59	1m	637.9	114.6	609.2	659.0	C
AT	2011-02-03	02:25:59	1m	633.7	97.4	593.9	634.9	C
AT	2011-02-03	02:26:59	1m	629.9	112.4	583.4	626.5	C
AT	2011-02-03	02:27:59	1m	625.6	144.9	575.2	617.8	C
AT	2011-02-03	02:28:59	1m	620.4	106.2	568.2	609.9	C
AT	2011-02-03	02:29:59	1m	617.3	169.1	559.4	605.1	C
AT	2011-02-03	02:30:59	1m	617.3	176.7	553.4	599.5	C
AT	2011-02-03	02:31:59	1m	617.6	203.4	549.0	590.4	C
AT	2011-02-03	02:32:59	1m	615.5	203.2	547.8	583.1	C
AT	2011-02-03	02:33:59	1m	616.2	245.3	542.7	578.3	C
AT	2011-02-03	02:34:59	1m	615.5	392.2	541.9	576.5	C

AT	2011-02-03	02:35:59	1m	617.7	204.7	539.9	575.8	C
AT	2011-02-03	02:36:59	1m	618.6	135.6	539.9	577.9	C
AT	2011-02-03	02:37:59	1m	619.8	112.2	539.9	580.1	C
AT	2011-02-03	02:38:59	1m	619.3	136.1	539.6	582.4	C
AT	2011-02-03	02:39:59	1m	619.1	150.4	540.2	584.4	C
AT	2011-02-03	02:40:59	1m	621.9	129.9	543.2	585.8	C
AT	2011-02-03	02:41:59	1m	628.1	109.4	544.6	589.3	C
AT	2011-02-03	02:42:59	1m	630.8	95.9	549.9	594.8	C
AT	2011-02-03	02:43:59	1m	631.7	220.5	556.8	600.3	C
AT	2011-02-03	02:44:59	1m	634.1	141.3	562.9	604.7	C
AT	2011-02-03	02:45:59	1m	635.8	110.7	569.2	607.7	C
AT	2011-02-03	02:46:59	1m	630.1	157.7	574.2	605.2	C
AT	2011-02-03	02:47:59	1m	623.3	100.8	574.1	599.1	C
AT	2011-02-03	02:48:59	1m	619.8	110.8	573.1	592.8	C
AT	2011-02-03	02:49:59	1m	619.1	175.7	571.9	588.9	C
AT	2011-02-03	02:50:59	1m	618.1	145.7	570.4	587.9	C
AT	2011-02-03	02:51:59	1m	617.2	110.3	573.1	590.4	C
AT	2011-02-03	02:52:59	1m	619.8	92.8	574.8	590.8	C
AT	2011-02-03	02:53:59	1m	625.4	105.3	575.1	590.9	C
AT	2011-02-03	02:54:59	1m	629.8	123.0	574.1	591.0	C
AT	2011-02-03	02:55:59	1m	637.2	129.6	573.4	591.8	C
AT	2011-02-03	02:56:59	1m	643.2	129.3	571.2	593.2	C
AT	2011-02-03	02:57:59	1m	650.3	108.7	569.9	596.0	C
AT	2011-02-03	02:58:59	1m	657.9	89.7	569.4	600.8	C
AT	2011-02-03	02:59:59	1m	655.2	105.1	567.7	599.3	C
AT	2011-02-03	03:00:59	1m	643.8	108.4	564.9	603.2	C
AT	2011-02-03	03:01:59	1m	627.7	133.2	561.1	587.7	C
AT	2011-02-03	03:02:59	1m	618.3	116.6	557.7	574.3	C
AT	2011-02-03	03:03:59	1m	611.3	120.5	555.1	564.3	C

May 1st, 2021. Short Term Firing Event

MN/AT	date	time	int	1ch	2ch	3ch	4ch	unit
AT	2011-02-03	03:31:59	1m	565.9	81.3	521.2	533.9	C
AT	2011-02-03	03:32:59	1m	560.8	71.3	515.2	529.7	C
AT	2011-02-03	03:04:59	1m	617.8	125.2	553.1	561.8	C
AT	2011-02-03	03:05:59	1m	618.0	107.6	552.2	561.6	C
AT	2011-02-03	03:06:59	1m	613.7	124.3	552.4	559.1	C
AT	2011-02-03	03:07:59	1m	608.4	138.1	553.4	554.6	C
AT	2011-02-03	03:08:59	1m	602.1	123.6	555.2	549.7	C
AT	2011-02-03	03:09:59	1m	597.5	69.8	557.4	546.5	C
AT	2011-02-03	03:10:59	1m	596.2	75.9	559.2	540.0	C
AT	2011-02-03	03:11:59	1m	590.1	98.6	559.8	535.0	C
AT	2011-02-03	03:12:59	1m	582.8	104.0	559.3	533.4	C
AT	2011-02-03	03:13:59	1m	587.7	96.3	558.6	532.1	C
AT	2011-02-03	03:14:59	1m	588.1	66.4	557.9	532.6	C
AT	2011-02-03	03:15:59	1m	593.1	60.5	555.7	531.9	C
AT	2011-02-03	03:16:59	1m	601.1	63.9	553.0	529.4	C
AT	2011-02-03	03:17:59	1m	612.8	52.2	548.4	529.5	C
AT	2011-02-03	03:18:59	1m	616.9	63.4	545.5	535.2	C
AT	2011-02-03	03:19:59	1m	622.8	58.4	543.2	542.3	C
AT	2011-02-03	03:20:59	1m	631.9	63.5	542.3	547.1	C
AT	2011-02-03	03:21:59	1m	631.1	51.1	542.7	550.0	C
AT	2011-02-03	03:22:59	1m	617.7	70.6	544.6	550.4	C
AT	2011-02-03	03:23:59	1m	609.6	74.2	545.1	549.8	C
AT	2011-02-03	03:24:59	1m	608.8	47.9	545.5	552.0	C
AT	2011-02-03	03:25:59	1m	612.9	88.3	545.6	553.6	C
AT	2011-02-03	03:26:59	1m	619.2	68.1	546.9	554.8	C
AT	2011-02-03	03:27:59	1m	620.1	74.1	548.4	554.2	C
AT	2011-02-03	03:28:59	1m	605.9	85.6	544.4	551.9	C
AT	2011-02-03	03:29:59	1m	587.3	78.4	536.7	546.4	C
AT	2011-02-03	03:30:59	1m	575.2	77.2	528.9	539.6	C
AT	2011-02-03	03:31:59	1m	565.9	81.3	521.2	533.9	C
AT	2011-02-03	03:32:59	1m	560.8	71.3	515.2	529.7	C
AT	2011-02-03	03:33:59	1m	558.8	96.0	508.9	527.4	C
AT	2011-02-03	03:34:59	1m	557.2	94.3	504.0	526.1	C
AT	2011-02-03	03:35:59	1m	555.5	80.6	499.4	522.9	C
AT	2011-02-03	03:36:59	1m	551.9	81.1	496.3	519.7	C
AT	2011-02-03	03:37:59	1m	547.3	78.2	493.2	516.1	C
AT	2011-02-03	03:38:59	1m	539.9	75.4	487.3	512.7	C
AT	2011-02-03	03:39:59	1m	535.1	81.7	481.9	509.7	C
AT	2011-02-03	03:40:59	1m	530.3	68.9	477.6	506.8	C
AT	2011-02-03	03:41:59	1m	538.0	518.2	453.4	410.0	C
AT	2011-02-03	03:42:59	1m	565.4	334.1	457.8	384.9	C
AT	2011-02-03	03:43:59	1m	567.3	308.0	442.4	376.7	C
AT	2011-02-03	03:44:59	1m	563.9	176.2	479.8	390.2	C
AT	2011-02-03	03:45:59	1m	567.2	207.2	528.5	392.2	C
AT	2011-02-03	03:46:59	1m	610.6	506.3	607.0	401.3	C
AT	2011-02-03	03:47:59	1m	657.3	242.2	614.8	417.6	C
AT	2011-02-03	03:48:59	1m	666.0	467.4	608.9	431.4	C
AT	2011-02-03	03:49:59	1m	660.8	227.3	645.8	435.9	C
AT	2011-02-03	03:50:59	1m	649.1	286.8	648.1	437.2	C
AT	2011-02-03	03:51:59	1m	657.0	220.4	624.8	435.2	C
AT	2011-02-03	03:52:59	1m	643.3	248.0	610.3	437.7	C
AT	2011-02-03	03:53:59	1m	633.6	517.1	603.0	437.7	C
AT	2011-02-03	03:54:59	1m	629.3	700.3	625.1	438.8	C
AT	2011-02-03	03:55:59	1m	629.8	553.8	605.8	440.1	C
AT	2011-02-03	03:56:59	1m	639.2	452.7	594.9	441.4	C
AT	2011-02-03	03:57:59	1m	643.7	-0.4	601.0	445.2	C
AT	2011-02-03	03:58:59	1m	637.6	290.6	584.4	447.6	C
AT	2011-02-03	03:59:59	1m	633.2	E03	569.0	447.8	C

May 1st, 2021. Short Term Firing Event

MN/AT	date	time	int	1ch	2ch	3ch	4ch	unit
AT	2011-02-03	04:00:59	1m	624.7	625.9	556.0	448.4	C
AT	2011-02-03	04:01:59	1m	613.8	589.2	541.7	448.2	C
AT	2011-02-03	04:02:59	1m	608.4	569.5	530.7	447.6	C
AT	2011-02-03	04:03:59	1m	609.4	551.9	520.9	447.9	C
AT	2011-02-03	04:04:59	1m	610.0	567.8	511.5	448.5	C
AT	2011-02-03	04:05:59	1m	606.5	574.3	504.8	448.9	C
AT	2011-02-03	04:06:59	1m	592.9	557.9	499.2	448.9	C
AT	2011-02-03	04:07:59	1m	582.6	545.1	493.5	448.4	C
AT	2011-02-03	04:08:59	1m	575.7	532.9	491.3	449.6	C
AT	2011-02-03	04:09:59	1m	569.5	523.6	489.6	450.3	C
AT	2011-02-03	04:10:59	1m	564.9	512.1	486.9	450.6	C
AT	2011-02-03	04:11:59	1m	560.3	495.3	484.1	450.0	C
AT	2011-02-03	04:12:59	1m	557.7	482.0	479.1	448.8	C
AT	2011-02-03	04:13:59	1m	559.2	473.8	478.2	449.4	C
AT	2011-02-03	04:14:59	1m	560.4	465.8	478.4	450.2	C
AT	2011-02-03	04:15:59	1m	563.7	458.5	480.7	459.8	C
AT	2011-02-03	04:16:59	1m	535.6	453.4	484.0	454.6	C
AT	2011-02-03	04:17:59	1m	479.0	447.0	488.2	434.4	C
AT	2011-02-03	04:18:59	1m	448.4	442.4	488.8	408.1	C
AT	2011-02-03	04:19:59	1m	304.8	437.7	488.0	392.4	C
AT	2011-02-03	04:20:59	1m	307.7	432.3	487.4	373.7	C
AT	2011-02-03	04:21:59	1m	312.2	427.6	487.4	359.2	C
AT	2011-02-03	04:22:59	1m	409.7	422.8	486.1	348.9	C
AT	2011-02-03	04:23:59	1m	539.8	417.9	486.3	340.4	C
AT	2011-02-03	04:24:59	1m	638.5	413.7	485.4	332.2	C
AT	2011-02-03	04:25:59	1m	484.3	409.4	484.1	323.6	C
AT	2011-02-03	04:26:59	1m	400.7	406.0	483.6	315.7	C
AT	2011-02-03	04:27:59	1m	342.8	402.2	483.6	309.0	C
AT	2011-02-03	04:28:59	1m	302.9	398.8	483.7	302.8	C
AT	2011-02-03	04:29:59	1m	282.5	396.4	484.3	295.2	C
AT	2011-02-03	04:30:59	1m	264.2	393.6	476.8	287.6	C
AT	2011-02-03	04:31:59	1m	240.4	391.7	468.2	275.3	C
AT	2011-02-03	04:32:59	1m	219.8	389.8	487.5	265.1	C
AT	2011-02-03	04:33:59	1m	218.5	388.1	518.7	259.7	C
AT	2011-02-03	04:34:59	1m	230.7	386.7	519.3	249.7	C
AT	2011-02-03	04:35:59	1m	327.6	384.3	517.9	267.6	C
AT	2011-02-03	04:36:59	1m	395.2	382.4	525.3	349.7	C
AT	2011-02-03	04:37:59	1m	380.8	380.4	533.2	424.1	C
AT	2011-02-03	04:38:59	1m	346.8	376.8	536.7	430.7	C
AT	2011-02-03	04:39:59	1m	305.7	374.5	538.0	463.9	C
AT	2011-02-03	04:40:59	1m	297.8	371.4	543.7	511.0	C
AT	2011-02-03	04:41:59	1m	283.6	370.2	552.5	532.9	C
AT	2011-02-03	04:42:59	1m	275.8	368.4	563.6	545.3	C
AT	2011-02-03	04:43:59	1m	260.9	366.7	567.6	548.7	C
AT	2011-02-03	04:44:59	1m	267.1	364.9	577.0	551.3	C
AT	2011-02-03	04:45:59	1m	256.2	363.4	585.1	550.9	C
AT	2011-02-03	04:46:59	1m	250.1	362.2	592.2	550.4	C
AT	2011-02-03	04:47:59	1m	242.7	361.0	587.4	562.2	C
AT	2011-02-03	04:48:59	1m	444.3	470.1	587.9	546.4	C
AT	2011-02-03	04:49:59	1m	495.9	478.5	574.6	531.4	C
AT	2011-02-03	04:50:59	1m	514.6	528.3	561.4	520.9	C
AT	2011-02-03	04:51:59	1m	519.3	501.2	550.2	473.7	C
AT	2011-02-03	04:52:59	1m	573.6	475.4	527.5	441.9	C
AT	2011-02-03	04:53:59	1m	647.8	496.9	510.1	441.1	C
AT	2011-02-03	04:54:59	1m	647.7	634.8	500.1	449.0	C
AT	2011-02-03	04:55:59	1m	626.5	663.6	492.8	422.9	C

May 1st, 2021. Short Term Firing Event

MN/AT	date	time	int	1ch	2ch	3ch	4ch	unit
AT	2011-02-03	04:56:59	1m	623.2	607.1	488.4	422.9	C
AT	2011-02-03	04:57:59	1m	571.4	606.3	483.0	427.3	C
AT	2011-02-03	04:58:59	1m	757.8	545.9	476.6	433.8	C
AT	2011-02-03	04:59:59	1m	789.2	645.4	467.6	439.2	C
AT	2011-02-03	05:00:59	1m	797.2	652.7	459.2	443.7	C
AT	2011-02-03	05:01:59	1m	770.1	595.8	452.3	447.7	C
AT	2011-02-03	05:02:59	1m	691.6	576.3	450.9	451.1	C
AT	2011-02-03	05:03:59	1m	785.4	580.2	452.3	454.6	C
AT	2011-02-03	05:04:59	1m	710.2	565.1	453.3	456.9	C
AT	2011-02-03	05:05:59	1m	620.3	587.0	453.6	458.3	C
AT	2011-02-03	05:06:59	1m	601.7	560.8	452.7	458.8	C
AT	2011-02-03	05:07:59	1m	698.4	539.4	450.5	458.6	C
AT	2011-02-03	05:08:59	1m	745.8	604.3	448.5	457.4	C
AT	2011-02-03	05:09:59	1m	828.5	646.3	447.2	455.8	C
AT	2011-02-03	05:10:59	1m	714.2	668.9	445.2	453.3	C
AT	2011-02-03	05:11:59	1m	667.6	710.3	443.9	452.1	C
AT	2011-02-03	05:12:59	1m	633.4	709.7	442.7	450.8	C
AT	2011-02-03	05:13:59	1m	606.3	687.6	439.7	449.1	C
AT	2011-02-03	05:14:59	1m	560.9	680.6	437.9	448.3	C
AT	2011-02-03	05:15:59	1m	559.9	653.9	436.4	447.6	C
AT	2011-02-03	05:16:59	1m	641.0	652.0	435.5	447.0	C
AT	2011-02-03	05:17:59	1m	644.8	621.8	434.5	446.5	C
AT	2011-02-03	05:18:59	1m	625.8	607.2	433.4	445.9	C
AT	2011-02-03	05:19:59	1m	620.7	466.3	432.2	445.9	C
AT	2011-02-03	05:20:59	1m	616.2	436.2	432.3	443.4	C
AT	2011-02-03	05:21:59	1m	612.1	443.8	429.7	440.7	C

AT	2011-02-03	05:22:59	1m	590.3	430.6	432.9	438.5	C
AT	2011-02-03	05:23:59	1m	584.3	417.9	435.7	439.6	C
AT	2011-02-03	05:24:59	1m	586.7	411.3	437.9	438.3	C
AT	2011-02-03	05:25:59	1m	591.6	381.2	440.1	436.2	C
AT	2011-02-03	05:26:59	1m	587.2	364.1	443.3	434.7	C
AT	2011-02-03	05:27:59	1m	579.4	358.1	441.8	431.8	C
AT	2011-02-03	05:28:59	1m	577.2	349.8	438.9	430.2	C
AT	2011-02-03	05:29:59	1m	571.2	488.8	436.0	428.2	C
AT	2011-02-03	05:30:59	1m	560.5	483.1	434.1	425.6	C
AT	2011-02-03	05:31:59	1m	557.1	473.1	432.6	426.5	C
AT	2011-02-03	05:32:59	1m	555.6	462.1	420.1	426.7	C
AT	2011-02-03	05:33:59	1m	539.1	455.8	416.1	426.4	C
AT	2011-02-03	05:34:59	1m	599.2	469.7	419.5	434.0	C
AT	2011-02-03	05:35:59	1m	572.6	475.1	425.9	423.7	C
AT	2011-02-03	05:36:59	1m	590.9	508.8	421.3	421.2	C
AT	2011-02-03	05:37:59	1m	573.7	421.8	425.3	C	
AT	2011-02-03	05:38:59	1m	563.6	423.2	432.7	C	
AT	2011-02-03	05:39:59	1m	551.2	422.7	436.9	C	
AT	2011-02-03	05:40:59	1m	549.5	423.8	440.9	C	
AT	2011-02-03	05:41:59	1m	414.6	427.7	368.4	C	
AT	2011-02-03	05:42:59	1m	381.9	424.6	332.0	C	
AT	2011-02-03	05:43:59	1m	260.4	427.4	369.1	C	
AT	2011-02-03	05:44:59	1m	344.0	413.2	436.1	C	
AT	2011-02-03	05:45:59	1m	327.4	397.2	375.2	C	
AT	2011-02-03	05:46:59	1m	308.3	364.7	343.6	C	
AT	2011-02-03	05:47:59	1m	266.7	330.2	311.4	C	

May 22nd, 2021. Short Term Firing Event

MN/AT	date	time	int	1ch	2ch	3ch	4ch	unit
AT	2011-02-12	02:09:34	1m	336.2	47.3	508.0	420.7	C
AT	2011-02-12	02:10:34	1m	337.3	40.1	518.1	418.6	C
AT	2011-02-12	01:45:34	1m	453.1	-31.2	542.5	471.4	C
AT	2011-02-12	02:11:34	1m	340.6	51.1	524.5	426.5	C
AT	2011-02-12	01:46:34	1m	459.5	177.5	547.2	462.2	C
AT	2011-02-12	02:12:34	1m	343.8	50.7	527.7	435.5	C
AT	2011-02-12	01:47:34	1m	463.6	542.4	553.4	498.4	C
AT	2011-02-12	02:13:34	1m	346.2	49.5	528.6	443.5	C
AT	2011-02-12	01:48:34	1m	460.7	188.3	561.2	494.3	C
AT	2011-02-12	02:14:34	1m	349.8	58.9	526.5	443.2	C
AT	2011-02-12	01:49:34	1m	465.7	143.7	570.2	495.7	C
AT	2011-02-12	02:15:34	1m	354.4	59.1	526.8	444.1	C
AT	2011-02-12	01:50:34	1m	479.4	174.9	578.8	505.3	C
AT	2011-02-12	02:16:34	1m	358.4	42.5	530.8	447.6	C
AT	2011-02-12	01:51:34	1m	487.0	162.8	592.3	504.9	C
AT	2011-02-12	02:17:34	1m	362.6	23.4	537.4	452.2	C
AT	2011-02-12	01:52:34	1m	490.8	185.1	592.0	486.1	C
AT	2011-02-12	02:18:34	1m	367.1	16.7	546.1	459.7	C
AT	2011-02-12	01:53:34	1m	493.2	265.4	597.1	487.9	C
AT	2011-02-12	02:19:34	1m	372.6	33.9	554.4	467.7	C
AT	2011-02-12	01:54:34	1m	495.3	142.2	598.1	429.9	C
AT	2011-02-12	02:20:34	1m	378.8	20.7	560.8	468.8	C
AT	2011-02-12	01:55:34	1m	497.2	123.2	592.2	518.3	C
AT	2011-02-12	02:21:34	1m	382.8	2.9	571.8	479.4	C
AT	2011-02-12	01:56:34	1m	480.9	49.8	652.1	521.6	C
AT	2011-02-12	02:22:34	1m	385.6	7.8	582.1	484.7	C
AT	2011-02-12	01:57:34	1m	445.2	69.8	583.3	487.9	C
AT	2011-02-12	02:23:34	1m	386.3	4.5	593.2	493.5	C
AT	2011-02-12	01:58:34	1m	418.4	48.7	547.4	443.3	C
AT	2011-02-12	02:24:34	1m	387.2	10.9	600.9	500.0	C
AT	2011-02-12	01:59:34	1m	398.3	34.3	520.1	417.8	C
AT	2011-02-12	02:25:34	1m	388.6	7.5	604.1	502.9	C
AT	2011-02-12	02:00:34	1m	382.9	44.6	497.7	403.8	C
AT	2011-02-12	02:26:34	1m	390.9	8.8	608.3	506.1	C
AT	2011-02-12	02:01:34	1m	370.9	18.2	489.4	394.9	C
AT	2011-02-12	02:27:34	1m	393.3	14.4	612.4	508.1	C
AT	2011-02-12	02:02:34	1m	363.2	45.9	487.4	391.8	C
AT	2011-02-12	02:28:34	1m	397.9	22.2	614.1	507.8	C
AT	2011-02-12	02:03:34	1m	356.5	23.3	486.1	419.7	C
AT	2011-02-12	02:29:34	1m	402.3	19.3	608.8	503.6	C
AT	2011-02-12	02:04:34	1m	350.8	28.2	485.5	413.4	C
AT	2011-02-12	02:30:34	1m	411.6	15.4	601.8	496.1	C
AT	2011-02-12	02:05:34	1m	345.3	46.2	487.8	413.1	C
AT	2011-02-12	02:31:34	1m	417.7	18.9	597.0	489.6	C
AT	2011-02-12	02:06:34	1m	341.4	44.6	488.5	416.2	C
AT	2011-02-12	02:32:34	1m	422.6	21.6	592.9	487.7	C
AT	2011-02-12	02:07:34	1m	339.0	48.8	493.8	418.4	C
AT	2011-02-12	02:33:34	1m	426.6	26.9	590.5	486.3	C
AT	2011-02-12	02:08:34	1m	337.0	49.9	500.9	417.4	C
AT	2011-02-12	02:34:34	1m	429.2	21.3	584.3	480.1	C
AT	2011-02-12	02:35:34	1m	431.9	19.3	580.4	473.2	C
AT	2011-02-12	02:36:34	1m	434.4	19.0	567.2	463.3	C
AT	2011-02-12	02:39:34	1m	440.0	9.3	540.9	460.3	C

May 22nd, 2021. Short Term Firing Event

MN/AT	date	time	int	1ch	2ch	3ch	4ch	unit
AT	2011-02-12	02:40:34	1m	442.1	15.4	545.8	463.4	C
AT	2011-02-12	02:41:34	1m	442.2	10.8	557.0	465.3	C
AT	2011-02-12	02:42:34	1m	442.7	11.6	554.4	462.6	C
AT	2011-02-12	02:43:34	1m	443.5	10.6	554.4	461.1	C
AT	2011-02-12	02:44:34	1m	443.3	13.4	558.3	462.2	C
AT	2011-02-12	02:45:34	1m	443.1	12.3	564.0	464.2	C
AT	2011-02-12	02:46:34	1m	443.4	11.1	572.3	468.8	C
AT	2011-02-12	02:47:34	1m	444.2	8.9	581.2	475.8	C
AT	2011-02-12	02:48:34	1m	444.8	10.6	585.4	481.4	C
AT	2011-02-12	02:49:34	1m	445.2	12.9	590.3	483.4	C
AT	2011-02-12	02:50:34	1m	444.4	10.3	593.6	490.2	C
AT	2011-02-12	02:51:34	1m	440.2	8.9	593.3	487.1	C
AT	2011-02-12	02:52:34	1m	437.9	10.1	595.2	489.3	C
AT	2011-02-12	02:53:34	1m	437.5	12.7	598.5	493.8	C
AT	2011-02-12	02:54:34	1m	435.6	14.9	586.1	484.8	C
AT	2011-02-12	02:55:34	1m	433.0	10.7	578.8	479.5	C
AT	2011-02-12	02:56:34	1m	430.7	13.2	575.8	482.3	C
AT	2011-02-12	02:57:34	1m	428.8	8.4	570.5	474.8	C
AT	2011-02-12	02:58:34	1m	427.2	-15.2	562.2	470.0	C
AT	2011-02-12	02:59:34	1m	426.4	-11.8	535.7	450.4	C
AT	2011-02-12	03:00:34	1m	424.1	-13.6	516.2	440.7	C
AT	2011-02-12	03:01:34	1m	421.4	-19.2	502.2	429.7	C
AT	2011-02-12	03:25:34	1m	365.1	9.0	405.6	454.1	C
AT	2011-02-12	03:26:34	1m	363.3	9.1	401.2	465.4	C
AT	2011-02-12	03:27:34	1m	359.8	7.7	395.6	457.3	C
AT	2011-02-12	03:28:34	1m	357.2	10.1	390.6	489.9	C
AT	2011-02-12	03:29:34	1m	354.5	9.4	384.8	493.3	C

AT	2011-02-12	03:02:34	1m	418.2	-11.9	492.3	423.4	C
AT	2011-02-12	03:03:34	1m	414.8	-14.7	484.3	418.3	C
AT	2011-02-12	03:04:34	1m	412.1	-11.0	478.0	409.3	C
AT	2011-02-12	03:05:34	1m	407.4	-14.8	473.6	401.7	C
AT	2011-02-12	03:06:34	1m	401.4	-12.7	472.6	399.0	C
AT	2011-02-12	03:07:34	1m	397.8	-13.1	468.8	408.4	C
AT	2011-02-12	03:08:34	1m	395.2	-13.9	464.8	409.6	C
AT	2011-02-12	03:09:34	1m	393.7	-18.5	460.8	421.9	C
AT	2011-02-12	03:10:34	1m	393.3	-17.7	456.1	408.4	C
AT	2011-02-12	03:11:34	1m	391.7	-13.8	452.3	406.7	C
AT	2011-02-12	03:12:34	1m	389.5	-12.2	449.8	403.8	C
AT	2011-02-12	03:13:34	1m	388.3	-15.8	446.6	396.5	C
AT	2011-02-12	03:14:34	1m	388.0	-17.8	444.2	395.3	C
AT	2011-02-12	03:15:34	1m	387.0	-13.6	440.8	395.9	C
AT	2011-02-12	03:16:34	1m	383.4	-16.3	437.9	403.9	C
AT	2011-02-12	03:17:34	1m	379.9	-11.9	436.6	412.6	C
AT	2011-02-12	03:18:34	1m	376.6	-12.7	435.0	416.9	C
AT	2011-02-12	03:19:34	1m	373.8	7.0	432.6	438.6	C
AT	2011-02-12	03:20:34	1m	371.5	7.4	429.4	430.5	C
AT	2011-02-12	03:21:34	1m	370.0	12.1	425.1	445.4	C
AT	2011-02-12	03:22:34	1m	369.6	12.8	422.9	438.5	C
AT	2011-02-12	03:23:34	1m	368.6	6.2	417.5	500.1	C
AT	2011-02-12	03:24:34	1m	366.6	5.9	411.8	470.9	C
AT	2011-02-12	03:30:34	1m	350.9	6.6	379.4	469.4	C
AT	2011-02-12	03:31:34	1m	346.3	6.9	375.4	490.9	C
AT	2011-02-12	03:32:34	1m	341.8	8.8	371.9	456.1	C
AT	2011-02-12	03:33:34	1m	335.7	8.5	368.9	439.9	C
AT	2011-02-12	03:34:34	1m	329.4	6.0	367.2	449.4	C

May 22nd, 2021. Short Term Firing Event

MN/AT	date	time	int	1ch	2ch	3ch	4ch	unit
AT	2011-02-12	03:56:34	1m	216.6	6.2	174.4	541.2	C
AT	2011-02-12	03:57:34	1m	214.0	9.2	168.6	549.0	C
AT	2011-02-12	03:58:34	1m	211.1	7.6	162.6	599.6	C
AT	2011-02-12	03:59:34	1m	208.6	6.1	156.3	575.5	C
AT	2011-02-12	04:00:34	1m	205.8	9.3	150.7	566.4	C
AT	2011-02-12	04:01:34	1m	203.0	7.0	146.0	592.6	C
AT	2011-02-12	04:02:34	1m	200.1	11.2	141.3	578.6	C
AT	2011-02-12	04:03:34	1m	197.6	7.3	137.6	602.8	C
AT	2011-02-12	04:04:34	1m	195.3	8.3	133.0	607.6	C
AT	2011-02-12	04:05:34	1m	192.7	7.6	129.3	634.7	C
AT	2011-02-12	04:06:34	1m	190.2	5.9	126.2	620.2	C
AT	2011-02-12	04:07:34	1m	186.8	5.5	123.1	541.3	C
AT	2011-02-12	04:08:34	1m	184.2	6.7	120.6	559.4	C
AT	2011-02-12	04:09:34	1m	181.4	6.3	118.0	563.3	C
AT	2011-02-12	04:10:34	1m	178.6	6.6	115.7	573.6	C
AT	2011-02-12	04:11:34	1m	176.3	6.3	112.9	603.7	C
AT	2011-02-12	04:12:34	1m	174.2	9.1	110.6	545.9	C
AT	2011-02-12	04:13:34	1m	172.1	8.3	107.9	590.4	C
AT	2011-02-12	04:14:34	1m	169.8	7.3	106.1	562.3	C
AT	2011-02-12	04:15:34	1m	167.1	7.1	103.9	554.8	C
AT	2011-02-12	04:16:34	1m	164.6	5.8	101.9	538.3	C
AT	2011-02-12	04:17:34	1m	162.2	7.6	100.1	513.6	C
AT	2011-02-12	04:18:34	1m	159.6	7.5	98.7	491.2	C
AT	2011-02-12	04:19:34	1m	157.6	5.9	96.9	482.4	C
AT	2011-02-12	04:20:34	1m	155.3	7.0	95.3	472.4	C
AT	2011-02-12	04:21:34	1m	152.6	7.2	93.8	470.0	C
AT	2011-02-12	04:22:34	1m	150.8	6.6	92.4	493.4	C
AT	2011-02-12	04:23:34	1m	148.7	7.6	90.9	483.6	C

May 22nd, 2021. Short Term Firing Event

MN/AT	date	time	int	1ch	2ch	3ch	4ch	unit
AT	2011-02-12	04:49:34	1m	60.4	7.4	33.3	1103	C
AT	2011-02-12	04:50:34	1m	52.9	5.9	26.3	1108	C
AT	2011-02-12	04:51:34	1m	49.1	8.4	22.5	1182	C
AT	2011-02-12	04:52:34	1m	46.4	4.8	21.1	1177	C
AT	2011-02-12	04:53:34	1m	44.2	7.0	19.8	1180	C
AT	2011-02-12	04:54:34	1m	43.6	6.5	19.5	1175	C
AT	2011-02-12	04:55:34	1m	43.1	7.1	19.5	1188	C
AT	2011-02-12	04:56:34	1m	42.2	5.7	19.0	1268	C
AT	2011-02-12	04:57:34	1m	41.4	6.6	19.3	1264	C
AT	2011-02-12	04:58:34	1m	41.4	5.4	19.3	1257	C
AT	2011-02-12	04:59:34	1m	40.2	5.8	18.9	1310	C
AT	2011-02-12	05:00:34	1m	39.9	6.8	18.9	1317	C
AT	2011-02-12	05:01:34	1m	40.0	6.3	18.3	1358	C
AT	2011-02-12	05:02:34	1m	39.6	7.7	18.4	1353	C
AT	2011-02-12	05:03:34	1m	38.2	6.1	17.7	1308	C
AT	2011-02-12	05:04:34	1m	37.6	6.1	17.3	1243	C
AT	2011-02-12	05:05:34	1m	37.8	6.9	17.3	1224	C
AT	2011-02-12	05:06:34	1m	37.3	7.8	17.1	1138	C
AT	2011-02-12	05:07:34	1m	37.4	6.2	16.4	1070	C
AT	2011-02-12	05:08:34	1m	37.6	4.6	17.2	1082	C
AT	2011-02-12	05:09:34	1m	36.7	5.0	17.1	1090	C
AT	2011-02-12	05:10:34	1m	35.7	4.8	17.3	1096	C
AT	2011-02-12	05:11:34	1m	35.2	7.6	17.3	1096	C
AT	2011-02-12	05:12:34	1m	35.8	7.1	17.2	1111	C
AT	2011-02-12	05:13:34	1m	36.4	7.2	16.9	1081	C
AT	2011-02-12	05:14:34	1m	35.3	7.0	15.8	1092	C
AT	2011-02-12	05:15:34	1m	35.4	7.4	15.8	1077	C
AT	2011-02-12	05:16:34	1m	34.8	5.1	15.8	1108	C
AT	2011-02-12	05:17:34	1m	34.3	5.2	16.6	1104	C
AT	2011-02-12	05:18:34	1m	33.4	6.0	16.3	1111	C
AT	2011-02-12	05:19:34	1m	32.9	5.4	16.0	1096	C
AT	2011-02-12	05:20:34	1m	31.9	5.3	15.6	1149	C
AT	2011-02-12	05:21:34	1m	31.7	4.1	15.5	1160	C
AT	2011-02-12	05:22:34	1m	31.6	5.3	15.4	1136	C
AT	2011-02-12	05:23:34	1m	31.3	4.6	15.3	1135	C
AT	2011-02-12	05:24:34	1m	31.3	4.6	15.4	1136	C

May 22nd, 2021. Short Term Firing Event

MN/AT	date	time	int	1ch	2ch	3ch	4ch	unit
AT	2011-02-12	05:25:34	1m	31.0	5.0	15.7	1131	C
AT	2011-02-12	05:28:34	1m	29.8	4.3	15.0		C
AT	2011-02-12	05:26:34	1m	31.5	5.7	15.7	1133	C
AT	2011-02-12	05:27:34	1m	30.2	4.6	15.4	1136	C

May 23, 2021. Short Term Firing Event

MN/AT	date	time	int	1ch	2ch	3ch	4ch	unit	
									AT 2011-07-16 23:11:26 1m 125.2 44.9 147.6 66.7 C
AT	2011-07-16	22:46:26	1m	22.6	9.3	102.4	11.3	C	AT 2011-07-16 23:12:26 1m 192.1 18.6 154.9 74.8 C
AT	2011-07-16	22:47:26	1m	22.4	10.4	89.3	12.2	C	AT 2011-07-16 23:13:26 1m 198.2 24.9 162.8 72.1 C
AT	2011-07-16	22:48:26	1m	22.1	12.4	82.3	13.2	C	AT 2011-07-16 23:14:26 1m 103.3 25.1 164.0 68.6 C
AT	2011-07-16	22:49:26	1m	22.8	12.4	81.3	16.7	C	AT 2011-07-16 23:15:26 1m 181.7 29.7 160.4 68.4 C
AT	2011-07-16	22:50:26	1m	24.3	16.5	75.3	13.4	C	AT 2011-07-16 23:16:26 1m 159.6 25.3 156.4 71.4 C
AT	2011-07-16	22:51:26	1m	30.1	15.3	79.5	11.3	C	AT 2011-07-16 23:17:26 1m 113.1 30.3 151.9 76.0 C
AT	2011-07-16	22:52:26	1m	25.7	14.1	119.1	9.1	C	AT 2011-07-16 23:18:26 1m 92.9 28.2 146.9 78.8 C
AT	2011-07-16	22:53:26	1m	25.9	15.2	118.8	10.6	C	AT 2011-07-16 23:19:26 1m 92.8 36.7 144.6 104.8 C
AT	2011-07-16	22:54:26	1m	27.3	16.4	119.4	12.9	C	AT 2011-07-16 23:20:26 1m 81.4 27.8 144.9 130.8 C
AT	2011-07-16	22:55:26	1m	29.7	17.6	122.9	15.8	C	AT 2011-07-16 23:21:26 1m 77.1 37.1 146.6 136.7 C
AT	2011-07-16	22:56:26	1m	43.3	18.8	170.8	13.3	C	AT 2011-07-16 23:22:26 1m 98.7 27.1 148.8 139.1 C
AT	2011-07-16	22:57:26	1m	39.9	20.4	191.9	11.3	C	AT 2011-07-16 23:23:26 1m 126.3 25.2 150.3 141.3 C
AT	2011-07-16	22:58:26	1m	41.8	17.4	190.8	13.9	C	AT 2011-07-16 23:24:26 1m 129.5 32.4 149.5 148.8 C
AT	2011-07-16	22:59:26	1m	41.2	30.6	197.9	14.1	C	AT 2011-07-16 23:25:26 1m 123.8 39.4 147.2 161.8 C
AT	2011-07-16	23:00:26	1m	44.0	40.3	215.8	14.9	C	AT 2011-07-16 23:26:26 1m 138.2 29.7 144.4 179.8 C
AT	2011-07-16	23:01:26	1m	57.9	39.1	262.7	20.8	C	AT 2011-07-16 23:27:26 1m 144.6 37.8 143.4 184.4 C
AT	2011-07-16	23:02:26	1m	63.1	39.8	233.1	60.5	C	AT 2011-07-16 23:28:26 1m 131.2 37.3 142.7 183.2 C
AT	2011-07-16	23:03:26	1m	75.5	47.2	322.2	31.7	C	AT 2011-07-16 23:29:26 1m 117.5 34.1 141.2 183.8 C
AT	2011-07-16	23:04:26	1m	83.4	31.3	334.3	24.7	C	AT 2011-07-16 23:30:26 1m 131.2 47.0 140.9 199.2 C
AT	2011-07-16	23:05:26	1m	93.4	41.9	294.1	47.2	C	AT 2011-07-16 23:31:26 1m 151.1 38.1 140.9 237.2 C
AT	2011-07-16	23:06:26	1m	103.1	42.7	232.2	56.4	C	AT 2011-07-16 23:32:26 1m 142.2 32.6 141.3 235.8 C
AT	2011-07-16	23:07:26	1m	158.5	41.7	191.6	65.3	C	AT 2011-07-16 23:33:26 1m 140.7 34.2 141.8 239.7 C
AT	2011-07-16	23:08:26	1m	188.9	38.4	169.4	54.7	C	AT 2011-07-16 23:34:26 1m 150.7 33.0 143.1 243.6 C
AT	2011-07-16	23:09:26	1m	195.1	49.4	157.3	43.9	C	AT 2011-07-16 23:35:26 1m 160.4 41.6 144.6 255.9 C
AT	2011-07-16	23:10:26	1m	20.2	51.6	148.1	69.3	C	AT 2011-07-16 23:36:26 1m 174.3 41.8 145.6 281.8 C
AT	2011-07-16	23:37:26	1m	177.3	42.8	149.2	321.5	C	AT 2011-07-16 23:39:26 1m 181.9 48.7 155.8 356.0 C
AT	2011-07-16	23:38:26	1m	178.7	54.3	151.8	339.4	C	AT 2011-07-16 23:40:26 1m 194.2 48.2 159.2 384.6 C

May 23, 2021. Short Term Firing Event

MN/AT	date	time	int	1ch	2ch	3ch	4ch	unit
AT	2011-07-16	23:41:26	1m	194.7	58.1	163.0	410.7	C
AT	2011-07-16	23:42:26	1m	199.9	66.1	168.8	468.3	C
AT	2011-07-16	23:43:26	1m	182.9	45.2	173.8	441.3	C
AT	2011-07-16	23:44:26	1m	176.6	55.1	177.6	435.2	C
AT	2011-07-16	23:45:26	1m	177.8	61.9	183.4	469.1	C
AT	2011-07-16	23:46:26	1m	178.0	67.6	190.0	478.0	C
AT	2011-07-16	23:47:26	1m	179.7	57.9	196.7	487.3	C
AT	2011-07-16	23:48:26	1m	182.3	67.7	204.3	499.9	C
AT	2011-07-16	23:49:26	1m	183.9	74.7	213.2	518.8	C
AT	2011-07-16	23:50:26	1m	182.6	59.3	221.5	510.3	C
AT	2011-07-16	23:51:26	1m	199.7	56.4	227.4	526.9	C
AT	2011-07-16	23:52:26	1m	199.5	65.8	234.7	528.3	C
AT	2011-07-16	23:53:26	1m	197.2	94.1	242.9	518.7	C
AT	2011-07-16	23:54:26	1m	192.2	65.9	248.4	526.4	C
AT	2011-07-16	23:55:26	1m	194.8	72.4	252.0	522.7	C
AT	2011-07-16	23:56:26	1m	197.0	84.8	255.1	518.1	C
AT	2011-07-16	23:57:26	1m	203.0	68.9	257.7	507.9	C
AT	2011-07-16	23:58:26	1m	203.4	69.6	258.5	511.5	C
AT	2011-07-16	23:59:26	1m	194.5	61.9	259.2	537.1	C
AT	2011-07-17	00:00:26	1m	184.1	49.7	263.5	538.4	C
AT	2011-07-17	00:01:26	1m	168.9	51.8	270.5	548.1	C
AT	2011-07-17	00:02:26	1m	168.7	61.3	276.9	538.6	C
AT	2011-07-17	00:03:26	1m	164.6	66.0	283.4	535.8	C
AT	2011-07-17	00:04:26	1m	161.5	42.4	290.0	543.3	C
AT	2011-07-17	00:30:26	1m	80.4	44.2	308.8	213.6	C
AT	2011-07-17	00:31:26	1m	75.9	41.1	302.4	211.8	C
AT	2011-07-17	00:32:26	1m	77.4	46.8	297.6	210.9	C

AT	2011-07-17	00:05:26	1m	152.9	60.7	294.1	528.6	C
AT	2011-07-17	00:06:26	1m	145.2	66.6	297.8	523.3	C
AT	2011-07-17	00:07:26	1m	133.9	49.3	302.1	507.9	C
AT	2011-07-17	00:08:26	1m	132.7	51.1	305.6	519.8	C
AT	2011-07-17	00:09:26	1m	127.6	84.8	308.3	527.4	C
AT	2011-07-17	00:10:26	1m	138.4	76.1	311.6	489.6	C
AT	2011-07-17	00:11:26	1m	133.0	95.3	313.2	490.6	C
AT	2011-07-17	00:12:26	1m	125.7	53.7	315.2	473.9	C
AT	2011-07-17	00:13:26	1m	119.0	56.6	316.9	479.2	C
AT	2011-07-17	00:14:26	1m	120.6	68.7	319.8	487.7	C
AT	2011-07-17	00:15:26	1m	118.0	44.4	322.0	499.0	C
AT	2011-07-17	00:16:26	1m	112.9	43.2	325.6	514.8	C
AT	2011-07-17	00:17:26	1m	114.0	61.8	329.4	521.9	C
AT	2011-07-17	00:18:26	1m	109.1	51.7	333.7	537.4	C
AT	2011-07-17	00:19:26	1m	106.9	70.9	348.4	493.6	C
AT	2011-07-17	00:20:26	1m	103.0	79.9	355.0	433.8	C
AT	2011-07-17	00:21:26	1m	91.0	104.6	359.4	386.3	C
AT	2011-07-17	00:22:26	1m	84.3	41.0	365.8	338.9	C
AT	2011-07-17	00:23:26	1m	81.0	43.8	364.6	304.1	C
AT	2011-07-17	00:24:26	1m	85.1	71.3	357.4	275.8	C
AT	2011-07-17	00:25:26	1m	89.0	107.7	347.9	253.2	C
AT	2011-07-17	00:26:26	1m	87.7	83.5	338.4	236.5	C
AT	2011-07-17	00:27:26	1m	85.8	78.0	329.7	224.2	C
AT	2011-07-17	00:28:26	1m	84.5	102.6	322.7	218.7	C
AT	2011-07-17	00:29:26	1m	81.9	63.1	316.0	215.3	C
AT	2011-07-17	00:33:26	1m	80.6	49.3	295.0	212.6	C
AT	2011-07-17	00:34:26	1m	79.9	50.8	292.7	215.1	C
AT	2011-07-17	00:35:26	1m	78.3	56.6	290.1	218.3	C

May 23, 2021. Short Term Firing Event

MN/AT	date	time	int	1ch	2ch	3ch	4ch	unit
AT	2011-07-17	00:36:26	1m	80.2	50.6	287.4	222.3	C
AT	2011-07-17	00:37:26	1m	76.9	49.0	285.3	226.6	C
AT	2011-07-17	00:38:26	1m	83.3	47.4	283.2	230.9	C
AT	2011-07-17	00:39:26	1m	81.9	55.1	282.7	236.6	C
AT	2011-07-17	00:40:26	1m	84.8	48.5	283.2	242.4	C
AT	2011-07-17	00:41:26	1m	91.7	54.7	284.7	247.9	C
AT	2011-07-17	00:42:26	1m	78.1	54.4	286.4	253.2	C
AT	2011-07-17	00:43:26	1m	75.8	41.8	287.1	256.9	C
AT	2011-07-17	00:44:26	1m	76.2	70.1	286.6	258.9	C
AT	2011-07-17	00:45:26	1m	75.4	57.6	285.5	260.7	C
AT	2011-07-17	00:46:26	1m	75.4	43.9	289.9	243.7	C
AT	2011-07-17	00:47:26	1m	80.4	89.6	295.4	231.8	C
AT	2011-07-17	00:48:26	1m	82.7	97.1	297.1	236.5	C
AT	2011-07-17	00:49:26	1m	81.6	50.7	296.7	250.8	C
AT	2011-07-17	00:50:26	1m	81.0	87.7	296.9	266.4	C
AT	2011-07-17	00:51:26	1m	81.1	59.3	299.4	281.4	C
AT	2011-07-17	00:52:26	1m	78.7	58.6	302.7	292.3	C
AT	2011-07-17	00:53:26	1m	77.7	52.1	307.6	298.8	C
AT	2011-07-17	00:54:26	1m	82.3	76.4	312.4	303.7	C
AT	2011-07-17	00:55:26	1m	81.1	81.3	317.7	309.6	C
AT	2011-07-17	00:56:26	1m	82.3	63.5	323.4	319.3	C
AT	2011-07-17	00:57:26	1m	85.1	56.8	329.2	328.3	C
AT	2011-07-17	00:58:26	1m	84.9	61.8	336.7	335.9	C
AT	2011-07-17	00:59:26	1m	86.2	52.2	342.9	341.1	C
AT	2011-07-17	01:00:26	1m	88.9	58.2	342.7	344.4	C
AT	2011-07-17	01:01:26	1m	85.4	61.5	344.6	342.1	C
AT	2011-07-17	01:02:26	1m	83.6	63.7	351.4	344.4	C

AT	2011-07-17	01:03:26	1m	81.1	70.1	361.6	350.1	C
AT	2011-07-17	01:04:26	1m	78.8	58.8	374.2	356.8	C
AT	2011-07-17	01:05:26	1m	79.0	62.6	388.2	363.3	C
AT	2011-07-17	01:06:26	1m	78.1	66.2	402.4	369.1	C
AT	2011-07-17	01:07:26	1m	79.2	67.1	416.1	373.4	C
AT	2011-07-17	01:08:26	1m	78.8	59.1	429.3	374.8	C
AT	2011-07-17	01:09:26	1m	80.0	68.5	443.3	376.3	C
AT	2011-07-17	01:10:26	1m	79.7	50.1	456.7	378.8	C
AT	2011-07-17	01:11:26	1m	82.5	72.2	468.2	378.5	C
AT	2011-07-17	01:12:26	1m	84.3	72.2	478.2	378.4	C
AT	2011-07-17	01:13:26	1m	95.1	78.0	504.0	382.6	C
AT	2011-07-17	01:14:26	1m	103.3	39.3	521.2	368.9	C
AT	2011-07-17	01:15:26	1m	106.6	41.9	518.9	351.4	C
AT	2011-07-17	01:16:26	1m	110.3	57.7	511.3	336.1	C
AT	2011-07-17	01:17:26	1m	107.9	60.3	516.2	325.7	C
AT	2011-07-17	01:18:26	1m	109.0	37.1	517.6	323.4	C
AT	2011-07-17	01:19:26	1m	107.9	37.4	530.2	323.6	C
AT	2011-07-17	01:20:26	1m	104.6	34.3	539.6	327.9	C
AT	2011-07-17	01:21:26	1m	105.7	58.2	554.0	331.9	C
AT	2011-07-17	01:22:26	1m	109.4	36.5	562.6	336.6	C
AT	2011-07-17	01:23:26	1m	108.9	45.9	564.1	338.9	C
AT	2011-07-17	01:24:26	1m	105.5	43.1	567.8	337.8	C
AT	2011-07-17	01:25:26	1m	109.2	49.1	567.1	334.1	C
AT	2011-07-17	01:26:26	1m	110.3	53.1	570.8	329.8	C
AT	2011-07-17	01:27:26	1m	107.6	44.2	581.3	324.3	C
AT	2011-07-17	01:28:26	1m	101.9	35.3	592.2	319.3	C
AT	2011-07-17	01:29:26	1m	103.4	59.2	598.9	315.8	C
AT	2011-07-17	01:30:26	1m	106.3	53.6	609.8	314.4	C

May 23, 2021. Short Term Firing Event

AT 2011-07-17 01:31:26 1m 92.6 34.3 595.3 312.8 C

MN/AT date time int 1ch 2ch 3ch 4ch unit

AT 2011-07-17 01:32:26 1m 88.4 35.2 573.4 315.6 C

AT 2011-07-17 01:38:26 1m 27.3 60.1 510.2 249.3 C

AT 2011-07-17 01:33:26 1m 84.7 46.5 555.1 323.6 C

AT 2011-07-17 01:39:26 1m 25.3 47.1 529.8 116.6 C

AT 2011-07-17 01:34:26 1m 78.4 45.2 538.7 312.9 C

AT 2011-07-17 01:40:26 1m 18.1 35.4 534.9 59.5 C

AT 2011-07-17 01:35:26 1m 77.9 49.9 528.2 307.4 C

AT 2011-07-17 01:41:26 1m 21.6 38.9 277.3 42.4 C

AT 2011-07-17 01:36:26 1m 76.7 46.6 522.4 308.9 C

AT 2011-07-17 01:42:26 1m 26.9 20.2 136.1 35.9 C

AT 2011-07-17 01:37:26 1m 73.6 35.4 517.9 309.8 C

May 25, 2021. Short Term Firing Event

MN/AT	date	time	int	1ch	2ch	3ch	4ch	unit
AT	2011-07-21	22:49:57	1m	10.9	12.6	11.6	14.4	C
AT	2011-07-21	22:50:57	1m	12.0	14.2	11.9	12.2	C
AT	2011-07-21	22:51:57	1m	11.4	12.9	11.6	10.6	C
AT	2011-07-21	22:52:57	1m	10.4	12.4	11.9	10.8	C
AT	2011-07-21	22:53:57	1m	10.0	13.4	11.8	11.2	C
AT	2011-07-21	22:54:57	1m	8.2	9.8	10.8	9.7	C
AT	2011-07-21	22:55:57	1m	6.6	10.8	9.9	8.4	C
AT	2011-07-21	22:56:57	1m	5.6	10.4	9.4	7.3	C
AT	2011-07-21	22:57:57	1m	5.6	12.3	9.1	7.1	C
AT	2011-07-21	22:58:57	1m	6.4	12.5	9.5	8.3	C
AT	2011-07-21	22:59:57	1m	8.2	11.6	10.4	10.4	C
AT	2011-07-21	23:00:57	1m	9.2	11.7	11.2	11.1	C
AT	2011-07-21	23:01:57	1m	9.3	13.0	10.9	11.9	C
AT	2011-07-21	23:02:57	1m	9.6	12.0	10.9	11.3	C
AT	2011-07-21	23:03:57	1m	11.5	13.9	11.7	12.0	C
AT	2011-07-21	23:04:57	1m	12.9	13.7	12.6	14.1	C
AT	2011-07-21	23:05:57	1m	12.4	11.3	11.9	13.6	C
AT	2011-07-21	23:06:57	1m	11.2	15.0	11.2	12.4	C
AT	2011-07-21	23:07:57	1m	11.1	18.0	11.6	11.2	C
AT	2011-07-21	23:08:57	1m	11.2	15.9	12.4	10.3	C
AT	2011-07-21	23:09:57	1m	11.3	14.3	13.7	8.8	C
AT	2011-07-21	23:10:57	1m	12.1	14.7	12.9	8.6	C
AT	2011-07-21	23:11:57	1m	13.0	15.3	13.6	8.5	C
AT	2011-07-21	23:12:57	1m	13.9	17.1	14.9	8.3	C
AT	2011-07-21	23:13:57	1m	14.2	17.2	17.4	8.4	C
AT	2011-07-21	23:40:57	1m	26.2	39.4	451.6	61.2	C
AT	2011-07-21	23:41:57	1m	24.9	49.5	463.3	59.7	C
AT	2011-07-21	23:14:57	1m	14.3	18.6	21.1	8.6	C
AT	2011-07-21	23:15:57	1m	14.1	19.6	22.4	8.2	C
AT	2011-07-21	23:16:57	1m	14.3	17.2	66.4	8.3	C
AT	2011-07-21	23:17:57	1m	15.0	17.9	38.3	8.6	C
AT	2011-07-21	23:18:57	1m	15.2	19.9	26.7	8.4	C
AT	2011-07-21	23:19:57	1m	15.3	18.8	21.0	7.7	C
AT	2011-07-21	23:20:57	1m	15.6	18.9	17.6	7.4	C
AT	2011-07-21	23:21:57	1m	15.9	16.2	15.7	7.6	C
AT	2011-07-21	23:22:57	1m	17.4	19.6	15.6	8.9	C
AT	2011-07-21	23:23:57	1m	18.7	161.9	25.3	13.1	C
AT	2011-07-21	23:24:57	1m	20.1	104.2	85.9	32.3	C
AT	2011-07-21	23:25:57	1m	19.9	53.9	95.1	27.1	C
AT	2011-07-21	23:26:57	1m	20.2	298.0	194.0	45.6	C
AT	2011-07-21	23:27:57	1m	21.4	343.1	402.3	100.2	C
AT	2011-07-21	23:28:57	1m	22.1	202.3	452.4	97.7	C
AT	2011-07-21	23:29:57	1m	22.2	114.9	458.1	126.3	C
AT	2011-07-21	23:30:57	1m	23.3	125.1	436.7	106.7	C
AT	2011-07-21	23:31:57	1m	24.8	409.7	529.9	169.7	C
AT	2011-07-21	23:32:57	1m	25.8	148.9	554.0	170.4	C
AT	2011-07-21	23:33:57	1m	23.7	51.5	472.8	116.3	C
AT	2011-07-21	23:34:57	1m	22.9	53.4	470.7	81.6	C
AT	2011-07-21	23:35:57	1m	22.3	35.6	425.6	69.1	C
AT	2011-07-21	23:36:57	1m	21.7	41.3	450.0	60.7	C
AT	2011-07-21	23:37:57	1m	24.3	53.4	448.3	58.3	C
AT	2011-07-21	23:38:57	1m	25.6	39.5	440.7	58.5	C
AT	2011-07-21	23:39:57	1m	26.2	52.1	436.1	59.8	C
AT	2011-07-21	23:42:57	1m	22.8	70.3	471.3	58.7	C
AT	2011-07-21	23:43:57	1m	20.9	65.6	478.8	59.3	C

May 25, 2021. Short Term Firing Event

MN/AT	date	time	int	1ch	2ch	3ch	4ch	unit
AT	2011-07-21	23:44:57	1m	20.1	53.1	484.9	56.9	C
AT	2011-07-21	23:45:57	1m	20.6	51.2	492.8	59.8	C
AT	2011-07-21	23:46:57	1m	22.5	74.3	509.1	63.9	C
AT	2011-07-21	23:47:57	1m	23.1	50.6	528.1	66.1	C
AT	2011-07-21	23:48:57	1m	24.4	65.3	544.1	66.2	C
AT	2011-07-21	23:49:57	1m	25.3	82.3	559.3	76.0	C
AT	2011-07-21	23:50:57	1m	26.7	79.5	557.7	76.8	C
AT	2011-07-21	23:51:57	1m	27.6	92.7	576.4	83.6	C
AT	2011-07-21	23:52:57	1m	27.9	81.7	592.8	93.3	C
AT	2011-07-21	23:53:57	1m	27.8	90.5	615.6	104.3	C
AT	2011-07-21	23:54:57	1m	27.4	77.3	600.8	103.3	C
AT	2011-07-21	23:55:57	1m	27.1	54.6	570.8	98.9	C
AT	2011-07-21	23:56:57	1m	24.7	89.3	594.3	96.7	C
AT	2011-07-21	23:57:57	1m	22.2	94.8	659.6	97.4	C
AT	2011-07-21	23:58:57	1m	20.9	81.1	637.7	97.8	C
AT	2011-07-21	23:59:57	1m	20.2	101.1	634.9	100.6	C
AT	2011-07-22	00:00:57	1m	19.7	54.6	616.7	101.0	C
AT	2011-07-22	00:01:57	1m	19.7	61.7	586.2	103.5	C
AT	2011-07-22	00:02:57	1m	20.1	49.9	571.3	106.2	C
AT	2011-07-22	00:03:57	1m	21.4	45.4	568.6	110.9	C
AT	2011-07-22	00:04:57	1m	22.3	59.8	557.8	115.5	C
AT	2011-07-22	00:05:57	1m	22.8	38.7	562.1	120.2	C
AT	2011-07-22	00:06:57	1m	23.4	73.6	526.1	124.3	C
AT	2011-07-22	00:07:57	1m	25.5	83.6	563.4	130.4	C
AT	2011-07-22	00:33:57	1m	29.4	63.8	579.2	316.3	C
AT	2011-07-22	00:34:57	1m	29.9	85.8	564.1	327.2	C
AT	2011-07-22	00:35:57	1m	31.4	83.3	555.7	335.2	C
AT	2011-07-22	00:08:57	1m	25.7	87.3	581.0	135.8	C
AT	2011-07-22	00:09:57	1m	25.3	125.8	566.7	142.2	C
AT	2011-07-22	00:10:57	1m	26.2	131.2	567.3	152.1	C
AT	2011-07-22	00:11:57	1m	26.8	248.6	585.3	165.2	C
AT	2011-07-22	00:12:57	1m	26.3	135.9	591.1	172.7	C
AT	2011-07-22	00:13:57	1m	27.5	117.8	590.8	180.2	C
AT	2011-07-22	00:14:57	1m	29.4	231.7	592.2	196.9	C
AT	2011-07-22	00:15:57	1m	31.5	585.8	606.3	212.6	C
AT	2011-07-22	00:16:57	1m	32.4	668.8	643.0	221.6	C
AT	2011-07-22	00:17:57	1m	33.3	342.8	650.2	233.7	C
AT	2011-07-22	00:18:57	1m	32.1	151.5	618.6	243.6	C
AT	2011-07-22	00:19:57	1m	29.7	75.3	651.2	255.8	C
AT	2011-07-22	00:20:57	1m	28.2	114.3	662.3	265.9	C
AT	2011-07-22	00:21:57	1m	27.6	85.9	670.3	276.4	C
AT	2011-07-22	00:22:57	1m	26.7	101.9	659.9	282.2	C
AT	2011-07-22	00:23:57	1m	26.5	86.2	669.2	283.9	C
AT	2011-07-22	00:24:57	1m	26.7	85.7	668.0	283.4	C
AT	2011-07-22	00:25:57	1m	26.4	113.0	680.6	281.5	C
AT	2011-07-22	00:26:57	1m	26.1	70.9	683.8	281.2	C
AT	2011-07-22	00:27:57	1m	25.9	62.9	705.6	283.0	C
AT	2011-07-22	00:28:57	1m	25.7	91.3	708.2	284.2	C
AT	2011-07-22	00:29:57	1m	25.6	84.5	706.2	285.0	C
AT	2011-07-22	00:30:57	1m	26.7	104.1	701.3	288.4	C
AT	2011-07-22	00:31:57	1m	27.8	84.0	630.7	296.1	C
AT	2011-07-22	00:32:57	1m	28.7	75.8	594.9	305.8	C
AT	2011-07-22	00:36:57	1m	31.3	75.5	556.7	338.7	C
AT	2011-07-22	00:37:57	1m	31.9	71.6	547.2	367.6	C
AT	2011-07-22	00:38:57	1m	31.2	56.2	519.2	353.3	C

May 25, 2021. Short Term Firing Event

MN/AT	date	time	int	1ch	2ch	3ch	4ch	unit
AT	2011-07-22	01:01:57	1m	33.5	55.1	394.5	236.6	C
AT	2011-07-22	01:02:57	1m	34.9	46.2	380.4	245.6	C
AT	2011-07-22	01:03:57	1m	35.1	47.1	364.2	253.7	C
AT	2011-07-22	01:04:57	1m	34.5	48.3	350.3	261.0	C
AT	2011-07-22	01:05:57	1m	33.7	42.7	337.9	265.1	C
AT	2011-07-22	01:06:57	1m	33.4	38.8	329.4	269.2	C
AT	2011-07-22	01:07:57	1m	33.4	53.3	326.7	273.3	C
AT	2011-07-22	01:08:57	1m	33.9	68.9	337.7	275.4	C
AT	2011-07-22	01:09:57	1m	35.0	55.5	355.6	276.3	C
AT	2011-07-22	01:10:57	1m	35.8	108.3	371.9	278.8	C
AT	2011-07-22	01:11:57	1m	36.0	36.7	381.4	282.9	C
AT	2011-07-22	01:12:57	1m	35.0	58.4	390.8	286.7	C
AT	2011-07-22	01:13:57	1m	34.6	48.1	401.7	291.8	C
AT	2011-07-22	01:14:57	1m	33.9	41.3	404.7	297.6	C
AT	2011-07-22	01:15:57	1m	37.2	62.3	412.6	302.7	C
AT	2011-07-22	01:16:57	1m	38.5	38.9	435.4	306.8	C
AT	2011-07-22	01:17:57	1m	39.0	45.6	449.3	310.2	C
AT	2011-07-22	01:18:57	1m	40.3	59.4	465.7	314.1	C
AT	2011-07-22	01:19:57	1m	40.1	46.1	478.9	316.9	C
AT	2011-07-22	01:20:57	1m	39.3	53.0	490.4	320.1	C
AT	2011-07-22	01:21:57	1m	39.0	52.8	498.1	324.1	C
AT	2011-07-22	01:22:57	1m	38.9	57.2	510.5	327.2	C
AT	2011-07-22	01:23:57	1m	38.9	61.7	527.7	330.9	C
AT	2011-07-22	01:24:57	1m	39.0	61.0	538.9	336.0	C
AT	2011-07-22	01:25:57	1m	39.3	60.6	540.3	341.7	C
AT	2011-07-22	01:26:57	1m	38.2	28.1	539.7	346.8	C
AT	2011-07-22	01:27:57	1m	37.9	37.9	545.3	368.9	C
AT	2011-07-22	01:28:57	1m	37.2	58.1	510.1	367.0	C
AT	2011-07-22	01:29:57	1m	37.6	47.3	501.1	372.4	C
AT	2011-07-22	01:30:57	1m	38.2	48.7	498.7	380.9	C
AT	2011-07-22	01:31:57	1m	38.8	52.9	498.7	388.2	C
AT	2011-07-22	01:32:57	1m	38.4	42.9	485.4	392.1	C
AT	2011-07-22	01:33:57	1m	37.6	48.2	473.9	390.6	C

May 25, 2021. Short Term Firing Event

MN/AT	date	time	int	1ch	2ch	3ch	4ch	unit
AT	2011-07-22	01:34:57	1m	37.4	43.1	471.4	391.8	C
AT	2011-07-22	01:35:57	1m	37.3	46.3	460.7	389.0	C
AT	2011-07-22	01:36:57	1m	36.5	41.7	447.8	386.0	C
AT	2011-07-22	01:37:57	1m	36.1	41.8	434.6	383.8	C
AT	2011-07-22	01:38:57	1m	36.3	36.9	430.2	375.7	C
AT	2011-07-22	01:39:57	1m	36.5	30.7	414.0	369.7	C
AT	2011-07-22	01:40:57	1m	35.9	31.1	400.8	364.8	C
AT	2011-07-22	01:41:57	1m	36.4	32.2	403.0	360.3	C
AT	2011-07-22	01:42:57	1m	36.9	38.7	409.3	356.7	C
AT	2011-07-22	01:43:57	1m	36.6	39.2	424.2	360.1	C
AT	2011-07-22	01:44:57	1m	37.4	38.7	425.5	363.6	C
AT	2011-07-22	01:45:57	1m	37.5	41.1	338.6	369.6	C
AT	2011-07-22	01:46:57	1m	36.1	33.4	267.4	354.7	C
AT	2011-07-22	01:47:57	1m	35.3	36.2	258.9	343.1	C
AT	2011-07-22	01:48:57	1m	35.1	38.2	240.8	337.2	C
AT	2011-07-22	01:49:57	1m	34.9	33.6	264.4	336.6	C
AT	2011-07-22	01:50:57	1m	34.9	32.8	266.7	338.4	C
AT	2011-07-22	01:51:57	1m	34.8	29.2	262.4	341.0	C

AT	2011-07-22	01:52:57	1m	33.9	35.7	268.2	342.2	C
AT	2011-07-22	01:53:57	1m	34.0	35.7	252.3	341.8	C
AT	2011-07-22	01:54:57	1m	34.6	31.1	346.3	343.9	C
AT	2011-07-22	01:55:57	1m	34.8	32.9	353.1	341.1	C
AT	2011-07-22	01:56:57	1m	34.1	33.6	359.4	338.5	C
AT	2011-07-22	01:57:57	1m	32.6	41.2	364.0	335.8	C
AT	2011-07-22	01:58:57	1m	31.4	30.7	368.5	333.8	C
AT	2011-07-22	01:59:57	1m	30.4	27.7	375.7	333.4	C
AT	2011-07-22	02:00:57	1m	29.8	26.1	379.1	333.3	C
AT	2011-07-22	02:01:57	1m	29.7	34.1	387.9	334.3	C
AT	2011-07-22	02:02:57	1m	29.6	31.7	395.4	335.4	C
AT	2011-07-22	02:03:57	1m	29.2	29.4	406.5	335.6	C
AT	2011-07-22	02:04:57	1m	29.1	28.4	417.9	336.2	C
AT	2011-07-22	02:05:57	1m	29.2	50.1	414.3	328.2	C
AT	2011-07-22	02:06:57	1m	26.4	36.5	219.4	217.6	C
AT	2011-07-22	02:07:57	1m	29.4	36.1	144.4	164.4	C
AT	2011-07-22	02:08:57	1m	32.6	35.6	112.8	134.6	C
AT	2011-07-22	02:09:57	1m	33.1	29.9	96.9	118.3	C
AT	2011-07-22	02:10:57	1m	35.2	30.4	84.2	106.4	C
AT	2011-07-22	02:11:57	1m	35.7	39.3	77.4	99.9	C

May 29, 2021. Short Term Firing Event

MN/AT	date	time	int	1ch	2ch	3ch	4ch	unit
AT	2011-07-23	00:10:06	1m	56.6	197.4	178.7	393.9	C
AT	2011-07-23	00:11:06	1m	56.9	234.7	178.8	383.3	C
AT	2011-07-23	00:12:06	1m	57.4	265.1	179.1	385.4	C
AT	2011-07-23	00:13:06	1m	58.2	266.7	180.2	393.9	C
AT	2011-07-23	00:14:06	1m	59.1	864.1	186.6	397.9	C
AT	2011-07-23	00:15:06	1m	60.5	816.8	193.7	399.8	C
AT	2011-07-23	00:16:06	1m	62.2	712.6	199.6	401.2	C
AT	2011-07-23	00:17:06	1m	64.4	717.6	202.3	405.1	C
AT	2011-07-23	00:18:06	1m	67.0	402.8	205.4	407.7	C
AT	2011-07-23	00:19:06	1m	68.5	547.0	207.9	408.1	C
AT	2011-07-23	00:20:06	1m	69.8	320.3	211.4	416.4	C
AT	2011-07-23	00:21:06	1m	70.7	442.7	215.9	445.7	C
AT	2011-07-23	00:22:06	1m	71.6	411.8	224.0	463.7	C
AT	2011-07-23	00:23:06	1m	72.1	382.1	230.1	497.4	C
AT	2011-07-23	00:24:06	1m	72.7	396.8	237.4	518.3	C
AT	2011-07-23	00:25:06	1m	73.2	681.5	248.3	525.5	C
AT	2011-07-23	00:26:06	1m	73.5	651.7	262.9	543.7	C
AT	2011-07-23	00:27:06	1m	74.1	297.8	282.7	543.4	C
AT	2011-07-23	00:28:06	1m	74.6	283.9	290.5	514.7	C
AT	2011-07-23	00:29:06	1m	74.5	306.6	289.9	505.6	C
AT	2011-07-23	00:30:06	1m	74.8	424.1	292.0	512.5	C
AT	2011-07-23	00:31:06	1m	75.7	360.7	300.1	532.3	C
AT	2011-07-23	00:32:06	1m	75.8	252.6	305.3	527.7	C
AT	2011-07-23	00:33:06	1m	75.6	314.7	303.7	519.0	C
AT	2011-07-23	00:59:06	1m	68.9	209.6	376.2	482.8	C
AT	2011-07-23	01:00:06	1m	68.8	188.0	389.9	499.0	C
AT	2011-07-23	01:01:06	1m	68.7	219.6	390.2	505.5	C
AT	2011-07-23	00:34:06	1m	75.2	256.3	303.0	522.8	C
AT	2011-07-23	00:35:06	1m	74.9	285.9	304.2	520.4	C
AT	2011-07-23	00:36:06	1m	74.1	298.1	307.8	532.9	C
AT	2011-07-23	00:37:06	1m	73.8	328.7	309.6	521.4	C
AT	2011-07-23	00:38:06	1m	73.4	272.9	315.8	535.4	C
AT	2011-07-23	00:39:06	1m	73.1	327.3	323.3	538.0	C
AT	2011-07-23	00:40:06	1m	72.6	279.6	331.3	563.7	C
AT	2011-07-23	00:41:06	1m	72.0	312.2	335.8	558.9	C
AT	2011-07-23	00:42:06	1m	71.7	329.9	342.9	564.6	C
AT	2011-07-23	00:43:06	1m	71.3	193.4	350.5	581.9	C
AT	2011-07-23	00:44:06	1m	70.8	269.8	347.1	546.9	C
AT	2011-07-23	00:45:06	1m	70.8	188.4	340.6	530.0	C
AT	2011-07-23	00:46:06	1m	70.4	317.5	338.7	509.5	C
AT	2011-07-23	00:47:06	1m	70.3	250.3	346.3	503.7	C
AT	2011-07-23	00:48:06	1m	70.3	231.8	351.5	501.2	C
AT	2011-07-23	00:49:06	1m	70.3	248.5	357.3	506.3	C
AT	2011-07-23	00:50:06	1m	70.2	236.7	365.1	511.1	C
AT	2011-07-23	00:51:06	1m	70.1	250.8	360.7	502.3	C
AT	2011-07-23	00:52:06	1m	70.2	231.6	353.7	495.3	C
AT	2011-07-23	00:53:06	1m	70.4	217.2	350.1	489.9	C
AT	2011-07-23	00:54:06	1m	70.2	200.6	350.6	483.3	C
AT	2011-07-23	00:55:06	1m	70.0	143.9	350.2	480.3	C
AT	2011-07-23	00:56:06	1m	69.4	232.6	349.3	479.4	C
AT	2011-07-23	00:57:06	1m	68.8	178.1	348.7	474.5	C
AT	2011-07-23	00:58:06	1m	68.8	231.4	356.6	470.5	C
AT	2011-07-23	01:02:06	1m	68.5	145.2	367.2	508.0	C
AT	2011-07-23	01:03:06	1m	68.3	167.7	370.1	494.8	C
AT	2011-07-23	01:04:06	1m	68.4	186.3	373.4	489.7	C

May 29, 2021. Short Term Firing Event

MN/AT	date	time	int	1ch	2ch	3ch	4ch	unit
AT	2011-07-23	01:05:06	1m	68.8	148.9	378.7	488.2	C
AT	2011-07-23	01:06:06	1m	69.2	146.1	384.6	489.0	C
AT	2011-07-23	01:07:06	1m	69.1	107.2	387.6	495.7	C
AT	2011-07-23	01:08:06	1m	68.3	103.2	388.6	507.5	C
AT	2011-07-23	01:09:06	1m	67.4	124.4	388.6	516.1	C
AT	2011-07-23	01:10:06	1m	67.2	129.1	389.4	508.1	C
AT	2011-07-23	01:11:06	1m	67.4	136.9	392.5	509.9	C
AT	2011-07-23	01:12:06	1m	67.8	122.1	395.9	514.8	C
AT	2011-07-23	01:13:06	1m	67.9	196.1	399.7	512.4	C
AT	2011-07-23	01:14:06	1m	67.6	108.9	397.4	510.9	C
AT	2011-07-23	01:15:06	1m	66.8	133.1	395.8	504.8	C
AT	2011-07-23	01:16:06	1m	66.6	165.6	397.7	500.2	C
AT	2011-07-23	01:17:06	1m	66.8	239.9	402.8	523.1	C
AT	2011-07-23	01:18:06	1m	66.4	207.6	393.9	513.4	C
AT	2011-07-23	01:19:06	1m	65.6	195.1	383.4	495.5	C
AT	2011-07-23	01:20:06	1m	64.9	239.0	377.3	484.3	C
AT	2011-07-23	01:21:06	1m	64.2	200.4	368.9	475.8	C
AT	2011-07-23	01:22:06	1m	63.4	240.0	362.5	465.9	C
AT	2011-07-23	01:23:06	1m	62.5	182.1	358.3	462.5	C
AT	2011-07-23	01:24:06	1m	61.9	152.2	354.4	462.3	C
AT	2011-07-23	01:25:06	1m	61.3	195.2	351.2	466.3	C
AT	2011-07-23	01:26:06	1m	60.5	136.9	349.3	471.9	C
AT	2011-07-23	01:50:06	1m	63.9	504.6	368.1	438.1	C
AT	2011-07-23	01:51:06	1m	64.3	519.3	367.1	440.8	C
AT	2011-07-23	01:52:06	1m	64.4	521.6	368.3	444.2	C
AT	2011-07-23	01:53:06	1m	64.8	516.0	368.9	448.6	C
AT	2011-07-23	01:54:06	1m	64.9	520.0	366.1	454.3	C

AT	2011-07-23	01:27:06	1m	59.9	241.2	348.1	478.2	C
AT	2011-07-23	01:28:06	1m	59.2	225.3	347.9	478.2	C
AT	2011-07-23	01:29:06	1m	58.9	254.9	351.1	478.0	C
AT	2011-07-23	01:30:06	1m	58.6	407.1	355.7	477.1	C
AT	2011-07-23	01:31:06	1m	58.0	321.8	359.6	475.9	C
AT	2011-07-23	01:32:06	1m	58.6	189.6	358.1	476.4	C
AT	2011-07-23	01:33:06	1m	58.7	177.0	354.3	475.2	C
AT	2011-07-23	01:34:06	1m	59.1	182.4	351.9	469.9	C
AT	2011-07-23	01:35:06	1m	59.6	177.2	348.3	463.8	C
AT	2011-07-23	01:36:06	1m	60.1	216.7	345.8	458.8	C
AT	2011-07-23	01:37:06	1m	60.6	484.3	345.6	456.1	C
AT	2011-07-23	01:38:06	1m	60.9	453.2	349.9	455.3	C
AT	2011-07-23	01:39:06	1m	60.9	506.2	349.3	452.4	C
AT	2011-07-23	01:40:06	1m	60.6	497.8	348.1	449.2	C
AT	2011-07-23	01:41:06	1m	60.5	499.2	348.3	446.0	C
AT	2011-07-23	01:42:06	1m	61.9	581.0	349.5	442.7	C
AT	2011-07-23	01:43:06	1m	63.1	515.6	354.5	442.3	C
AT	2011-07-23	01:44:06	1m	63.6	548.1	360.0	444.8	C
AT	2011-07-23	01:45:06	1m	64.5	559.8	365.7	447.7	C
AT	2011-07-23	01:46:06	1m	64.5	543.7	367.6	446.3	C
AT	2011-07-23	01:47:06	1m	63.8	519.8	368.3	443.3	C
AT	2011-07-23	01:48:06	1m	63.5	524.8	368.7	439.0	C
AT	2011-07-23	01:49:06	1m	63.7	499.1	368.5	437.8	C
AT	2011-07-23	01:55:06	1m	64.9	520.8	366.0	460.7	C
AT	2011-07-23	01:56:06	1m	65.0	109.0	366.2	463.5	C
AT	2011-07-23	01:57:06	1m	65.3	65.0	366.2	460.9	C
AT	2011-07-23	01:58:06	1m	66.1	84.1	368.6	460.3	C
AT	2011-07-23	01:59:06	1m	66.1	100.5	370.4	461.0	C

May 29, 2021. Short Term Firing Event

MN/AT	date	time	int	1ch	2ch	3ch	4ch	unit
AT	2011-07-23	02:21:06	1m	61.9	43.4	359.9	404.6	C
AT	2011-07-23	02:22:06	1m	61.6	59.2	360.8	404.4	C
AT	2011-07-23	02:23:06	1m	61.4	68.1	358.1	402.5	C
AT	2011-07-23	02:24:06	1m	61.7	33.4	353.3	402.7	C
AT	2011-07-23	02:25:06	1m	60.9	27.4	349.2	401.9	C
AT	2011-07-23	02:26:06	1m	60.6	71.0	343.9	399.9	C
AT	2011-07-23	02:27:06	1m	60.6	43.8	338.8	399.2	C
AT	2011-07-23	02:28:06	1m	60.6	35.6	333.6	401.2	C
AT	2011-07-23	02:29:06	1m	59.7	40.7	325.9	402.0	C
AT	2011-07-23	02:30:06	1m	58.8	54.8	321.7	399.7	C
AT	2011-07-23	02:31:06	1m	58.7	37.5	315.5	397.4	C
AT	2011-07-23	02:32:06	1m	58.3	45.4	310.8	395.6	C
AT	2011-07-23	02:33:06	1m	58.6	52.8	308.1	395.2	C
AT	2011-07-23	02:34:06	1m	58.6	58.7	306.6	396.0	C
AT	2011-07-23	02:35:06	1m	58.3	54.3	300.5	395.9	C
AT	2011-07-23	02:36:06	1m	58.4	45.0	292.1	396.7	C
AT	2011-07-23	02:37:06	1m	57.2	38.3	279.6	393.9	C
AT	2011-07-23	02:38:06	1m	56.2	38.7	271.1	389.2	C
AT	2011-07-23	02:39:06	1m	55.7	47.8	263.2	384.1	C
AT	2011-07-23	02:40:06	1m	55.8	51.4	254.4	381.3	C
AT	2011-07-23	02:41:06	1m	55.9	54.2	249.2	380.7	C
AT	2011-07-23	02:42:06	1m	55.8	56.2	243.9	380.4	C
AT	2011-07-23	02:43:06	1m	55.7	56.7	237.3	380.6	C
AT	2011-07-23	02:44:06	1m	55.6	31.9	232.6	379.4	C
AT	2011-07-23	02:45:06	1m	55.3	38.9	227.7	377.3	C
AT	2011-07-23	02:46:06	1m	55.1	35.9	223.7	375.4	C
AT	2011-07-23	02:47:06	1m	54.8	31.0	220.0	374.2	C
AT	2011-07-23	02:48:06	1m	54.7	50.4	216.3	372.2	C
AT	2011-07-23	02:21:06	1m	61.9	43.4	359.9	404.6	C

May 29, 2021. Short Term Firing Event

MN/AT	date	time	int	1ch	2ch	3ch	4ch	unit
AT	2011-07-23	03:14:06	1m	50.1	37.1	124.7	371.3	C
AT	2011-07-23	03:15:06	1m	50.3	29.3	122.7	370.1	C
AT	2011-07-23	02:55:06	1m	52.6	47.9	190.2	356.8	C
AT	2011-07-23	03:16:06	1m	50.3	28.9	121.0	367.2	C
AT	2011-07-23	02:56:06	1m	52.2	45.7	186.8	354.2	C
AT	2011-07-23	03:17:06	1m	50.0	30.8	118.3	362.7	C
AT	2011-07-23	02:57:06	1m	52.1	39.4	183.7	351.8	C
AT	2011-07-23	03:18:06	1m	49.6	32.4	116.2	360.1	C
AT	2011-07-23	02:58:06	1m	51.1	37.3	179.9	347.3	C
AT	2011-07-23	03:19:06	1m	49.5	36.2	114.2	357.7	C
AT	2011-07-23	02:59:06	1m	50.2	40.8	176.1	342.4	C
AT	2011-07-23	03:20:06	1m	49.4	28.9	112.5	354.8	C
AT	2011-07-23	03:00:06	1m	49.8	32.2	173.7	338.4	C
AT	2011-07-23	03:21:06	1m	48.9	34.1	110.7	350.2	C
AT	2011-07-23	03:01:06	1m	49.6	31.8	170.8	334.9	C
AT	2011-07-23	03:22:06	1m	48.8	34.6	109.1	346.1	C
AT	2011-07-23	03:02:06	1m	50.0	43.6	168.6	333.9	C
AT	2011-07-23	03:23:06	1m	48.6	32.5	108.2	341.8	C
AT	2011-07-23	03:03:06	1m	50.4	40.1	166.2	332.3	C
AT	2011-07-23	03:24:06	1m	48.1	31.0	106.4	335.2	C
AT	2011-07-23	03:04:06	1m	50.1	47.6	163.5	331.4	C
AT	2011-07-23	03:25:06	1m	47.8	28.7	105.5	329.3	C
AT	2011-07-23	03:05:06	1m	50.3	36.3	161.6	330.7	C
AT	2011-07-23	03:26:06	1m	47.8	29.0	103.6	323.6	C
AT	2011-07-23	03:06:06	1m	50.6	35.8	150.6	330.6	C
AT	2011-07-23	03:27:06	1m	47.7	33.4	102.8	317.8	C
AT	2011-07-23	03:07:06	1m	50.8	37.4	145.7	338.5	C
AT	2011-07-23	03:28:06	1m	47.8	32.6	101.6	310.2	C
AT	2011-07-23	03:08:06	1m	50.6	29.9	141.9	346.2	C
AT	2011-07-23	03:29:06	1m	47.4	32.4	100.2	294.3	C
AT	2011-07-23	03:09:06	1m	50.3	31.5	138.3	353.6	C
AT	2011-07-23	03:30:06	1m	47.1	38.7	99.2	283.3	C
AT	2011-07-23	03:10:06	1m	50.3	34.0	135.7	362.7	C
AT	2011-07-23	03:31:06	1m	47.1	27.1	98.3	276.4	C
AT	2011-07-23	03:11:06	1m	50.4	38.9	132.5	370.3	C
AT	2011-07-23	03:32:06	1m	46.9	29.2	97.2	271.1	C
AT	2011-07-23	03:12:06	1m	50.4	39.8	129.7	373.2	C
AT	2011-07-23	03:33:06	1m	46.8	33.8	96.1	266.4	C
AT	2011-07-23	03:13:06	1m	50.2	30.5	126.9	371.7	C
AT	2011-07-23	03:34:06	1m	47.6	31.9	95.7	263.2	C
AT	2011-07-23	03:35:06	1m	48.1	35.6	94.9	259.6	C
AT	2011-07-23	03:36:06	1m	47.7	28.5	93.4	255.8	C
AT	2011-07-23	03:37:06	1m	47.2	30.9	92.6	251.8	C
AT	2011-07-23	03:38:06	1m	46.8	24.6	90.9	248.8	C
AT	2011-07-23	03:39:06	1m	46.3	25.7	90.2	245.5	C
AT	2011-07-23	03:40:06	1m	45.9	29.7	88.9	241.9	C
AT	2011-07-23	03:41:06	1m	45.6	30.7	87.7	238.6	C
AT	2011-07-23	03:42:06	1m	45.3	28.5	86.8	235.2	C
AT	2011-07-23	03:43:06	1m	44.7	25.9	85.8	232.1	C
AT	2011-07-23	03:44:06	1m	44.4	27.2	85.1	229.5	C
AT	2011-07-23	03:45:06	1m	43.8	25.4	84.3	225.7	C
AT	2011-07-23	03:46:06	1m	43.4	27.9	83.6	222.8	C
AT	2011-07-23	03:47:06	1m	43.3	29.1	82.9	219.5	C
AT	2011-07-23	03:48:06	1m	43.3	24.9	82.4	216.8	C
AT	2011-07-23	03:49:06	1m	43.4	28.4	81.9	212.8	C

May 29, 2021. Short Term Firing Event

AT 2011-07-23 03:50:06 1m 43.6 26.5 81.4 208.0 C

MN/AT date time int 1ch 2ch 3ch 4ch unit

AT 2011-07-23 03:53:06 1m 43.6 29.8 79.1 194.4 C

AT 2011-07-23 03:54:06 1m 43.4 21.2 78.7 191.7 C

AT 2011-07-23 03:55:06 1m 37.4 25.9 60.4 189.7 C

AT 2011-07-23 03:56:06 1m 33.4 24.3 48.7 188.0 C

AT 2011-07-23 03:51:06 1m 43.8 24.9 80.7 202.9 C

AT 2011-07-23 03:52:06 1m 43.8 26.4 80.1 198.4 C

October 22-2021. Long Term Firing Event

MN/AT	date	time	int	1ch	2ch	3ch	4ch	unit
AT	2011-08-19	21:04:55	1m	19.2	17.1	15.7	12.1	C
AT	2011-08-19	21:05:55	1m	19.9	29.4	16.3	12.1	C
AT	2011-08-19	21:06:55	1m	20.6	15.6	16.3	11.8	C
AT	2011-08-19	21:07:55	1m	20.9	16.0	16.4	11.4	C
AT	2011-08-19	21:08:55	1m	22.7	15.4	17.0	11.7	C
AT	2011-08-19	21:09:55	1m	24.1	56.3	17.8	12.0	C
AT	2011-08-19	21:10:55	1m	23.7	60.1	18.4	11.9	C
AT	2011-08-19	21:11:55	1m	23.9	41.1	18.9	11.7	C
AT	2011-08-19	21:12:55	1m	24.1	63.3	19.1	11.6	C
AT	2011-08-19	21:13:55	1m	23.9	39.0	19.5	12.0	C
AT	2011-08-19	21:14:55	1m	24.7	125.1	21.3	13.4	C
AT	2011-08-19	21:15:55	1m	25.3	238.3	22.7	14.9	C
AT	2011-08-19	21:16:55	1m	25.9	43.4	24.2	16.3	C
AT	2011-08-19	21:17:55	1m	26.5	38.2	24.7	17.4	C
AT	2011-08-19	21:18:55	1m	27.3	54.2	24.3	18.1	C
AT	2011-08-19	21:19:55	1m	29.6	38.2	25.2	20.9	C
AT	2011-08-19	21:20:55	1m	32.2	56.2	27.5	24.2	C
AT	2011-08-19	21:21:55	1m	34.0	341.0	30.2	25.3	C
AT	2011-08-19	21:22:55	1m	35.8	139.2	31.2	25.4	C
AT	2011-08-19	21:23:55	1m	39.2	30.3	31.4	24.6	C
AT	2011-08-19	21:24:55	1m	40.9	43.1	31.4	25.1	C
AT	2011-08-19	21:25:55	1m	43.2	407.1	33.2	24.3	C
AT	2011-08-19	21:26:55	1m	44.9	137.6	38.4	23.6	C
AT	2011-08-19	21:27:55	1m	50.1	42.5	36.0	23.9	C
AT	2011-08-19	21:28:55	1m	53.3	217.2	36.3	24.4	C
AT	2011-08-19	21:29:55	1m	56.6	54.5	38.0	26.4	C
AT	2011-08-19	21:30:55	1m	59.1	96.2	40.1	28.1	C
AT	2011-08-19	21:31:55	1m	62.4	192.1	40.6	28.3	C
AT	2011-08-19	21:32:55	1m	63.2	37.3	41.2	28.7	C
AT	2011-08-19	21:33:55	1m	65.3	38.8	41.9	29.2	C
AT	2011-08-19	21:34:55	1m	67.9	40.9	42.4	30.6	C
AT	2011-08-19	21:35:55	1m	70.6	105.8	44.4	32.2	C
AT	2011-08-19	21:36:55	1m	71.6	33.9	44.6	33.2	C
AT	2011-08-19	21:37:55	1m	73.4	57.7	43.6	34.3	C
AT	2011-08-19	21:38:55	1m	74.3	202.4	43.7	34.5	C
AT	2011-08-19	21:39:55	1m	75.2	114.9	45.5	34.7	C
AT	2011-08-19	21:40:55	1m	75.4	107.8	46.3	35.4	C
AT	2011-08-19	21:41:55	1m	76.6	47.8	46.4	36.2	C
AT	2011-08-19	21:42:55	1m	77.4	93.8	45.8	36.0	C
AT	2011-08-19	21:43:55	1m	78.2	127.8	46.3	35.7	C
AT	2011-08-19	21:44:55	1m	78.2	373.5	46.9	35.6	C
AT	2011-08-19	21:45:55	1m	78.5	49.9	47.5	35.3	C
AT	2011-08-19	21:46:55	1m	78.8	99.9	47.7	35.1	C
AT	2011-08-19	21:47:55	1m	80.4	233.9	48.4	35.3	C
AT	2011-08-19	21:48:55	1m	81.6	158.7	48.7	35.5	C
AT	2011-08-19	21:49:55	1m	83.2	407.9	50.0	35.7	C
AT	2011-08-19	21:50:55	1m	86.1	45.4	51.7	36.2	C
AT	2011-08-19	21:51:55	1m	89.4	133.9	50.5	36.9	C
AT	2011-08-19	21:52:55	1m	92.3	50.4	50.2	37.2	C
AT	2011-08-19	21:53:55	1m	94.9	160.4	50.3	37.6	C
AT	2011-08-19	21:54:55	1m	97.3	46.6	50.4	38.4	C
AT	2011-08-19	21:55:55	1m	100.3	43.2	50.8	39.4	C
AT	2011-08-19	21:56:55	1m	102.4	107.9	50.7	40.0	C
AT	2011-08-19	21:57:55	1m	105.2	145.2	51.8	40.4	C
AT	2011-08-19	21:58:55	1m	108.0	50.8	52.0	41.8	C
AT	2011-08-19	21:59:55	1m	111.4	123.5	52.5	43.2	C

October 22 2021. Long Term Firing Event

MN/AT	date	time	int	1ch	2ch	3ch	4ch	unit
AT	2011-08-19	22:00:55	1m	114.4	206.9	52.6	44.7	C
AT	2011-08-19	22:01:55	1m	117.3	90.4	52.4	45.4	C
AT	2011-08-19	22:02:55	1m	119.0	72.2	53.0	46.0	C
AT	2011-08-19	22:03:55	1m	121.0	155.0	53.0	46.5	C
AT	2011-08-19	22:04:55	1m	123.6	96.0	53.8	46.7	C
AT	2011-08-19	22:05:55	1m	124.9	197.4	53.4	46.7	C
AT	2011-08-19	22:06:55	1m	126.6	101.9	53.7	46.8	C
AT	2011-08-19	22:07:55	1m	127.9	49.1	53.3	46.9	C
AT	2011-08-19	22:08:55	1m	128.8	82.3	53.1	47.3	C
AT	2011-08-19	22:09:55	1m	130.0	57.8	53.2	47.6	C
AT	2011-08-19	22:10:55	1m	130.6	49.2	53.4	47.8	C
AT	2011-08-19	22:11:55	1m	131.6	128.8	53.7	48.1	C
AT	2011-08-19	22:12:55	1m	132.6	68.2	53.3	48.2	C
AT	2011-08-19	22:13:55	1m	134.8	43.3	53.8	48.2	C
AT	2011-08-19	22:14:55	1m	134.4	178.8	53.8	48.3	C
AT	2011-08-19	22:15:55	1m	135.1	56.4	54.1	48.4	C
AT	2011-08-19	22:16:55	1m	135.7	704.9	54.4	48.2	C
AT	2011-08-19	22:17:55	1m	136.1	270.1	56.1	47.9	C
AT	2011-08-19	22:18:55	1m	136.6	302.4	58.6	48.2	C
AT	2011-08-19	22:19:55	1m	138.3	170.8	58.6	49.5	C
AT	2011-08-19	22:20:55	1m	141.3	191.4	58.2	52.7	C
AT	2011-08-19	22:21:55	1m	145.1	138.6	57.8	54.8	C
AT	2011-08-19	22:22:55	1m	148.7	307.8	58.4	56.4	C
AT	2011-08-19	22:23:55	1m	152.2	166.0	58.7	57.6	C
AT	2011-08-19	22:24:55	1m	156.8	333.1	59.6	59.3	C
AT	2011-08-19	22:25:55	1m	161.4	392.2	60.2	60.9	C
AT	2011-08-19	22:26:55	1m	168.2	125.8	60.5	62.4	C
AT	2011-08-19	22:27:55	1m	171.2	138.4	61.0	64.1	C
AT	2011-08-19	22:28:55	1m	175.7	222.2	60.9	65.6	C
AT	2011-08-19	22:29:55	1m	180.0	141.2	61.7	66.9	C
AT	2011-08-19	22:30:55	1m	182.6	521.2	62.3	68.4	C
AT	2011-08-19	22:31:55	1m	187.9	392.8	63.8	71.1	C
AT	2011-08-19	22:32:55	1m	191.7	372.8	63.0	73.1	C
AT	2011-08-19	22:33:55	1m	191.7	316.2	62.4	73.7	C
AT	2011-08-19	22:34:55	1m	190.6	351.7	62.1	73.4	C
AT	2011-08-19	22:35:55	1m	190.8	334.6	62.4	73.7	C
AT	2011-08-19	22:36:55	1m	191.5	341.1	61.4	73.2	C
AT	2011-08-19	22:37:55	1m	191.9	312.5	60.6	72.6	C
AT	2011-08-19	22:38:55	1m	191.7	245.1	60.7	72.3	C
AT	2011-08-19	22:39:55	1m	191.5	257.9	59.3	71.8	C
AT	2011-08-19	22:40:55	1m	191.4	225.3	59.2	71.6	C
AT	2011-08-19	22:41:55	1m	191.6	306.1	59.4	71.3	C
AT	2011-08-19	22:42:55	1m	192.1	294.6	59.1	70.4	C
AT	2011-08-19	22:43:55	1m	192.7	84.6	58.7	73.1	C
AT	2011-08-19	22:44:55	1m	195.5	127.7	59.3	72.1	C
AT	2011-08-19	22:45:55	1m	197.2	95.4	59.7	71.1	C
AT	2011-08-19	22:46:55	1m	211.3	98.5	60.9	71.1	C
AT	2011-08-19	22:47:55	1m	214.7	112.7	61.4	69.2	C
AT	2011-08-19	22:48:55	1m	215.9	223.1	60.1	66.7	C
AT	2011-08-19	22:49:55	1m	210.7	218.7	67.3	64.2	C
AT	2011-08-19	22:50:55	1m	191.3	158.3	64.9	62.4	C
AT	2011-08-19	22:51:55	1m	180.1	155.1	63.0	63.1	C
AT	2011-08-19	22:52:55	1m	174.3	186.5	61.9	63.6	C
AT	2011-08-19	22:53:55	1m	168.4	157.3	62.4	63.4	C
AT	2011-08-19	22:54:55	1m	163.3	148.3	63.4	63.3	C
AT	2011-08-19	22:55:55	1m	158.7	159.3	66.1	62.4	C

October 22 2021. Long Term Firing Event

MN/AT	date	time	int	1ch	2ch	3ch	4ch	unit
AT	2011-08-19	22:56:55	1m	153.9	91.7	65.2	61.2	C
AT	2011-08-19	22:57:55	1m	149.3	160.4	64.6	60.3	C
AT	2011-08-19	22:58:55	1m	145.3	96.8	66.7	58.2	C
AT	2011-08-19	22:59:55	1m	141.7	164.7	65.9	56.7	C
AT	2011-08-19	23:00:55	1m	135.8	704.3	71.2	52.4	C
AT	2011-08-19	23:01:55	1m	128.3	117.6	72.7	61.6	C
AT	2011-08-19	23:02:55	1m	127.9	265.1	70.1	64.9	C
AT	2011-08-19	23:03:55	1m	128.7	128.2	69.3	67.0	C
AT	2011-08-19	23:04:55	1m	129.1	156.5	70.2	71.9	C
AT	2011-08-19	23:05:55	1m	128.8	98.6	72.0	82.9	C
AT	2011-08-19	23:06:55	1m	129.6	643.8	73.6	88.4	C
AT	2011-08-19	23:07:55	1m	132.1	304.2	76.3	95.2	C
AT	2011-08-19	23:08:55	1m	131.9	194.2	84.4	97.2	C
AT	2011-08-19	23:09:55	1m	132.3	321.6	86.8	101.5	C
AT	2011-08-19	23:10:55	1m	373.4	304.1	90.3	99.3	C
AT	2011-08-19	23:11:55	1m	525.1	287.1	97.3	101.4	C
AT	2011-08-19	23:12:55	1m	527.4	296.6	107.7	103.0	C
AT	2011-08-19	23:13:55	1m	565.3	397.9	107.2	103.1	C
AT	2011-08-19	23:14:55	1m	514.8	238.4	106.9	106.0	C
AT	2011-08-19	23:15:55	1m	302.9	332.9	129.1	107.7	C
AT	2011-08-19	23:16:55	1m	268.4	223.3	117.2	106.5	C
AT	2011-08-19	23:17:55	1m	275.3	193.8	114.1	106.2	C
AT	2011-08-19	23:18:55	1m	298.6	534.3	118.2	105.9	C
AT	2011-08-19	23:19:55	1m	303.8	559.5	122.8	107.0	C
AT	2011-08-19	23:20:55	1m	328.4	305.3	121.2	108.9	C
AT	2011-08-19	23:21:55	1m	310.0	556.1	122.6	104.6	C
AT	2011-08-19	23:22:55	1m	286.4	279.1	119.4	111.0	C
AT	2011-08-19	23:23:55	1m	292.5	302.1	121.3	113.2	C
AT	2011-08-19	23:24:55	1m	265.0	150.2	122.2	112.3	C
AT	2011-08-19	23:25:55	1m	226.1	229.0	120.6	110.3	C
AT	2011-08-19	23:26:55	1m	189.9	146.3	121.7	112.8	C
AT	2011-08-19	23:27:55	1m	189.9	155.3	120.9	111.9	C
AT	2011-08-19	23:28:55	1m	187.0	181.1	122.6	115.6	C
AT	2011-08-19	23:29:55	1m	180.5	153.8	121.7	113.1	C
AT	2011-08-19	23:30:55	1m	181.2	266.9	120.7	111.1	C
AT	2011-08-19	23:31:55	1m	178.6	215.7	122.2	111.3	C
AT	2011-08-19	23:32:55	1m	182.1	172.4	120.8	112.2	C
AT	2011-08-19	23:33:55	1m	186.3	368.1	124.6	112.9	C
AT	2011-08-19	23:34:55	1m	195.3	181.6	126.6	116.1	C
AT	2011-08-19	23:35:55	1m	195.0	183.6	125.7	117.2	C
AT	2011-08-19	23:36:55	1m	203.3	178.6	125.6	135.1	C
AT	2011-08-19	23:37:55	1m	153.0	178.2	129.8	146.4	C
AT	2011-08-19	23:38:55	1m	131.6	116.9	127.3	159.9	C
AT	2011-08-19	23:39:55	1m	126.9	171.2	121.1	159.3	C
AT	2011-08-19	23:40:55	1m	134.2	120.2	120.9	154.4	C
AT	2011-08-19	23:41:55	1m	135.6	144.0	119.3	151.1	C
AT	2011-08-19	23:42:55	1m	126.3	160.6	118.8	147.3	C
AT	2011-08-19	23:43:55	1m	141.8	159.3	118.5	141.6	C
AT	2011-08-19	23:44:55	1m	132.6	127.3	118.0	140.1	C
AT	2011-08-19	23:45:55	1m	145.2	92.2	117.1	139.1	C
AT	2011-08-19	23:46:55	1m	150.9	115.4	115.5	135.6	C
AT	2011-08-19	23:47:55	1m	138.9	126.1	116.8	134.4	C
AT	2011-08-19	23:48:55	1m	143.3	115.6	117.1	134.1	C
AT	2011-08-19	23:49:55	1m	154.4	123.8	117.6	132.0	C
AT	2011-08-19	23:50:55	1m	142.8	110.7	117.7	131.6	C
AT	2011-08-19	23:51:55	1m	146.6	103.9	116.9	128.2	C

October 22 2021. Long Term Firing Event

MN/AT	date	time	int	1ch	2ch	3ch	4ch	unit
AT	2011-08-19	23:52:55	1m	144.1	86.8	116.8	121.3	C
AT	2011-08-19	23:53:55	1m	134.2	64.9	117.4	116.9	C
AT	2011-08-19	23:54:55	1m	122.3	69.9	118.6	111.8	C
AT	2011-08-19	23:55:55	1m	142.4	76.4	119.1	114.3	C
AT	2011-08-19	23:56:55	1m	129.1	72.6	118.8	115.2	C
AT	2011-08-19	23:57:55	1m	121.6	79.9	118.1	116.3	C
AT	2011-08-19	23:58:55	1m	133.4	173.1	118.1	115.8	C
AT	2011-08-19	23:59:55	1m	145.7	89.6	119.2	115.2	C
AT	2011-08-20	00:00:55	1m	131.3	93.4	119.5	115.1	C
AT	2011-08-20	00:01:55	1m	133.1	100.6	120.5	111.9	C
AT	2011-08-20	00:02:55	1m	149.7	79.6	120.1	115.5	C
AT	2011-08-20	00:03:55	1m	134.1	70.7	119.7	112.5	C
AT	2011-08-20	00:04:55	1m	151.7	104.3	119.3	111.1	C
AT	2011-08-20	00:05:55	1m	147.1	63.5	120.7	110.7	C
AT	2011-08-20	00:06:55	1m	140.4	89.3	120.8	106.5	C
AT	2011-08-20	00:07:55	1m	145.7	83.0	120.2	107.2	C
AT	2011-08-20	00:08:55	1m	140.4	125.1	120.2	105.2	C
AT	2011-08-20	00:09:55	1m	150.9	112.2	120.6	104.1	C
AT	2011-08-20	00:10:55	1m	147.9	100.1	120.1	101.5	C
AT	2011-08-20	00:11:55	1m	153.0	90.9	118.8	101.8	C
AT	2011-08-20	00:12:55	1m	148.5	97.2	118.0	101.4	C
AT	2011-08-20	00:13:55	1m	140.2	107.7	118.4	98.6	C
AT	2011-08-20	00:14:55	1m	153.0	102.3	119.1	100.4	C
AT	2011-08-20	00:15:55	1m	136.0	99.2	117.7	98.5	C
AT	2011-08-20	00:16:55	1m	139.4	197.1	119.9	96.1	C
AT	2011-08-20	00:17:55	1m	151.1	108.6	118.3	96.4	C
AT	2011-08-20	00:18:55	1m	142.7	104.4	121.7	98.4	C
AT	2011-08-20	00:19:55	1m	146.1	148.8	119.8	94.3	C
AT	2011-08-20	00:20:55	1m	144.3	148.0	122.6	91.2	C
AT	2011-08-20	00:21:55	1m	158.9	201.3	121.4	89.3	C
AT	2011-08-20	00:22:55	1m	144.4	123.4	124.8	91.6	C
AT	2011-08-20	00:23:55	1m	130.4	151.4	127.7	96.7	C
AT	2011-08-20	00:24:55	1m	127.0	278.0	135.4	97.3	C
AT	2011-08-20	00:25:55	1m	141.7	221.6	131.6	100.1	C
AT	2011-08-20	00:26:55	1m	133.0	133.0	132.8	105.9	C
AT	2011-08-20	00:27:55	1m	141.9	146.9	132.4	100.9	C
AT	2011-08-20	00:28:55	1m	138.4	123.6	129.5	98.3	C
AT	2011-08-20	00:29:55	1m	128.6	127.9	132.3	97.2	C
AT	2011-08-20	00:30:55	1m	128.6	223.5	134.2	97.7	C
AT	2011-08-20	00:31:55	1m	144.8	164.7	132.9	97.3	C
AT	2011-08-20	00:32:55	1m	122.6	178.1	134.7	97.4	C
AT	2011-08-20	00:33:55	1m	120.1	173.3	135.6	98.3	C
AT	2011-08-20	00:34:55	1m	133.1	241.0	132.9	98.2	C
AT	2011-08-20	00:35:55	1m	121.7	180.3	130.8	97.7	C
AT	2011-08-20	00:36:55	1m	116.6	188.3	131.3	95.7	C
AT	2011-08-20	00:37:55	1m	113.4	185.4	132.8	97.6	C
AT	2011-08-20	00:38:55	1m	111.2	146.2	131.6	95.4	C
AT	2011-08-20	00:39:55	1m	101.3	131.1	130.9	92.8	C
AT	2011-08-20	00:40:55	1m	104.3	130.3	132.2	95.6	C
AT	2011-08-20	00:41:55	1m	108.1	112.3	132.2	102.8	C
AT	2011-08-20	00:42:55	1m	101.2	128.7	130.7	106.9	C
AT	2011-08-20	00:43:55	1m	106.9	118.0	130.6	110.1	C
AT	2011-08-20	00:44:55	1m	100.6	95.1	130.2	113.2	C
AT	2011-08-20	00:45:55	1m	94.6	141.8	130.6	118.0	C
AT	2011-08-20	00:46:55	1m	90.8	152.7	129.4	126.2	C
AT	2011-08-20	00:47:55	1m	91.8	156.8	131.1	132.1	C

October 22, 2021. Long Term Firing Event

MN/AT	date	time	int	1ch	2ch	3ch	4ch	unit
AT	2011-08-20	01:15:55	1m	83.6	233.2	157.2	254.7	C
AT	2011-08-20	01:16:55	1m	86.2	225.8	161.9	257.6	C
AT	2011-08-20	01:17:55	1m	83.8	211.6	171.7	262.7	C
AT	2011-08-20	01:18:55	1m	89.3	209.4	167.7	264.7	C
AT	2011-08-20	01:19:55	1m	91.3	246.7	170.9	267.9	C
AT	2011-08-20	01:20:55	1m	84.3	247.8	182.9	274.2	C
AT	2011-08-20	01:21:55	1m	83.7	270.1	172.4	295.0	C
AT	2011-08-20	01:22:55	1m	78.6	256.7	170.6	334.4	C
AT	2011-08-20	01:23:55	1m	89.9	200.8	176.0	321.7	C
AT	2011-08-20	01:24:55	1m	91.3	230.6	177.4	293.8	C
AT	2011-08-20	01:25:55	1m	99.0	220.4	182.1	263.2	C
AT	2011-08-20	01:26:55	1m	92.7	241.8	183.9	251.6	C
AT	2011-08-20	01:27:55	1m	94.3	254.6	182.9	248.1	C
AT	2011-08-20	01:28:55	1m	107.6	299.3	200.3	230.1	C
AT	2011-08-20	01:29:55	1m	108.9	264.7	189.2	239.0	C
AT	2011-08-20	01:30:55	1m	98.9	293.8	187.2	235.4	C
AT	2011-08-20	01:31:55	1m	96.9	190.7	184.8	232.8	C
AT	2011-08-20	01:32:55	1m	93.6	179.6	186.9	228.1	C
AT	2011-08-20	01:33:55	1m	96.6	217.4	187.2	225.2	C
AT	2011-08-20	01:34:55	1m	97.6	202.7	178.8	229.7	C
AT	2011-08-20	01:35:55	1m	100.6	226.9	178.1	226.7	C
AT	2011-08-20	01:36:55	1m	104.7	209.3	175.9	223.2	C
AT	2011-08-20	01:37:55	1m	102.1	232.1	174.7	218.7	C
AT	2011-08-20	01:38:55	1m	98.6	197.5	174.2	212.8	C
AT	2011-08-20	01:39:55	1m	100.5	276.6	175.1	217.9	C
AT	2011-08-20	01:40:55	1m	100.1	256.3	172.7	180.4	C
AT	2011-08-20	01:41:55	1m	100.9	281.3	172.7	213.2	C
AT	2011-08-20	01:42:55	1m	110.3	395.5	169.3	373.1	C
AT	2011-08-20	01:43:55	1m	114.4	392.1	167.6	442.9	C

October 22 2021. Long Term Firing Event

MN/AT	date	time	int	1ch	2ch	3ch	4ch	unit
AT	2011-08-20	02:11:55	1m	84.4	254.6	132.7	172.9	C
AT	2011-08-20	02:12:55	1m	91.2	129.9	131.6	175.4	C
AT	2011-08-20	02:13:55	1m	85.7	123.0	127.7	170.6	C
AT	2011-08-20	02:14:55	1m	87.2	132.1	126.1	167.1	C
AT	2011-08-20	02:15:55	1m	86.7	112.8	124.3	165.1	C
AT	2011-08-20	02:16:55	1m	84.8	96.9	122.9	146.5	C
AT	2011-08-20	02:17:55	1m	88.3	115.2	122.4	151.4	C
AT	2011-08-20	02:18:55	1m	85.8	101.3	122.0	151.0	C
AT	2011-08-20	02:19:55	1m	89.1	95.7	119.3	150.3	C
AT	2011-08-20	02:20:55	1m	87.8	112.9	118.9	151.9	C
AT	2011-08-20	02:21:55	1m	87.8	105.0	118.6	152.3	C
AT	2011-08-20	02:22:55	1m	87.0	96.6	116.8	147.2	C
AT	2011-08-20	02:23:55	1m	82.7	87.8	115.4	144.3	C
AT	2011-08-20	02:24:55	1m	82.1	87.3	114.6	143.4	C
AT	2011-08-20	02:25:55	1m	80.3	89.6	114.3	147.8	C
AT	2011-08-20	02:26:55	1m	80.9	115.8	114.1	140.3	C
AT	2011-08-20	02:27:55	1m	77.8	87.3	113.3	145.0	C
AT	2011-08-20	02:28:55	1m	79.9	68.6	111.7	143.1	C
AT	2011-08-20	02:29:55	1m	78.4	84.1	110.1	143.3	C
AT	2011-08-20	02:30:55	1m	80.3	79.3	109.9	142.0	C
AT	2011-08-20	02:31:55	1m	81.1	83.9	108.1	130.4	C
AT	2011-08-20	02:32:55	1m	83.1	90.1	108.4	132.5	C
AT	2011-08-20	02:33:55	1m	91.4	101.4	112.9	137.9	C
AT	2011-08-20	02:34:55	1m	91.8	88.7	111.7	140.4	C
AT	2011-08-20	02:35:55	1m	90.9	93.8	112.7	139.5	C
AT	2011-08-20	02:36:55	1m	93.3	86.9	112.5	142.3	C
AT	2011-08-20	02:37:55	1m	75.7	148.0	112.1	135.3	C
AT	2011-08-20	02:38:55	1m	44.7	56.1	109.7	135.5	C
AT	2011-08-20	02:39:55	1m	38.3	66.6	108.6	130.3	C

October 22-2021. Long Term Firing Event

MN/AT	date	time	int	1ch	2ch	3ch	4ch	unit
AT	2011-08-20	02:40:55	1m	36.6	60.3	109.0	131.7	C
AT	2011-08-20	02:41:55	1m	38.3	74.4	109.6	140.6	C
AT	2011-08-20	02:42:55	1m	39.6	73.2	110.8	149.9	C
AT	2011-08-20	02:43:55	1m	37.6	68.6	110.8	153.7	C
AT	2011-08-20	02:44:55	1m	37.0	96.9	109.6	150.7	C
AT	2011-08-20	02:45:55	1m	37.2	55.8	111.7	145.1	C
AT	2011-08-20	02:46:55	1m	35.7	51.7	108.8	141.4	C
AT	2011-08-20	02:47:55	1m	36.6	55.4	108.6	145.6	C
AT	2011-08-20	02:48:55	1m	35.7	52.2	108.2	145.3	C
AT	2011-08-20	02:49:55	1m	35.4	42.9	107.7	147.8	C
AT	2011-08-20	02:50:55	1m	35.9	53.1	107.6	145.5	C
AT	2011-08-20	02:51:55	1m	39.1	84.0	108.3	143.7	C
AT	2011-08-20	02:52:55	1m	40.0	41.4	108.3	139.5	C
AT	2011-08-20	02:53:55	1m	36.1	57.2	106.0	135.7	C
AT	2011-08-20	02:54:55	1m	36.8	74.3	105.0	137.4	C

AT	2011-08-20	02:55:55	1m	34.4	55.8	103.6	137.1	C
AT	2011-08-20	02:56:55	1m	37.1	71.8	103.8	134.7	C
AT	2011-08-20	02:57:55	1m	40.6	75.3	104.3	124.9	C
AT	2011-08-20	02:58:55	1m	40.3	65.8	105.2	121.1	C
AT	2011-08-20	02:59:55	1m	37.8	68.1	102.8	113.3	C
AT	2011-08-20	03:00:55	1m	39.1	71.9	102.2	116.7	C
AT	2011-08-20	03:01:55	1m	36.9	49.2	101.8	119.8	C
AT	2011-08-20	03:02:55	1m	37.2	53.9	100.8	118.2	C
AT	2011-08-20	03:03:55	1m	36.6	72.4	99.5	113.1	C
AT	2011-08-20	03:04:55	1m	36.7	49.9	99.6	110.8	C
AT	2011-08-20	03:05:55	1m	36.2	44.7	98.0	106.8	C
AT	2011-08-20	03:06:55	1m	35.9	62.9	97.2	108.0	C
AT	2011-08-20	03:07:55	1m	35.5	46.5	96.9	110.1	C
AT	2011-08-20	03:08:55	1m	35.9	43.7	96.7	104.9	C

October 25, 2021. Long Term Firing Event

MN/AT	date	time	int	1ch	2ch	3ch	4ch	unit
AT	2011-12-06	21:03:39	1m	307.4	65.4	105.0	417.3	C
AT	2011-12-06	21:04:39	1m	300.2	63.3	111.8	435.4	C
AT	2011-12-06	21:05:39	1m	549.7	62.1	117.2	488.6	C
AT	2011-12-06	21:06:39	1m	471.9	72.2	120.6	505.4	C
AT	2011-12-06	21:07:39	1m	455.7	74.8	123.9	529.1	C
AT	2011-12-06	21:08:39	1m	527.1	58.5	126.7	525.5	C
AT	2011-12-06	21:09:39	1m	482.3	69.4	143.8	522.3	C
AT	2011-12-06	21:10:39	1m	438.5	76.6	174.7	541.9	C
AT	2011-12-06	21:11:39	1m	434.2	66.1	190.2	632.1	C
AT	2011-12-06	21:12:39	1m	440.6	59.7	181.1	609.3	C
AT	2011-12-06	21:13:39	1m	485.4	83.4	200.8	380.4	C
AT	2011-12-06	21:14:39	1m	509.8	91.1	210.1	276.5	C
AT	2011-12-06	21:15:39	1m	502.8	82.3	204.2	257.3	C
AT	2011-12-06	21:16:39	1m	488.4	120.9	200.7	264.8	C
AT	2011-12-06	21:17:39	1m	488.1	80.2	209.3	223.3	C
AT	2011-12-06	21:18:39	1m	492.2	74.3	214.7	237.4	C
AT	2011-12-06	21:19:39	1m	484.3	79.6	230.3	294.4	C
AT	2011-12-06	21:20:39	1m	471.3	72.9	233.9	394.2	C
AT	2011-12-06	21:21:39	1m	466.8	223.0	258.3	474.9	C
AT	2011-12-06	21:22:39	1m	475.0	89.7	288.3	580.1	C
AT	2011-12-06	21:23:39	1m	498.5	59.5	377.1	623.5	C
AT	2011-12-06	21:24:39	1m	544.6	68.1	414.4	703.5	C
AT	2011-12-06	21:25:39	1m	591.7	73.5	364.2	652.6	C
AT	2011-12-06	21:26:39	1m	693.3	74.2	362.2	670.4	C
AT	2011-12-06	21:27:39	1m	702.8	79.6	367.9	726.4	C
AT	2011-12-06	21:28:39	1m	607.1	77.5	400.7	650.3	C
AT	2011-12-06	21:29:39	1m	587.9	69.2	421.4	665.9	C
AT	2011-12-06	21:30:39	1m	595.5	82.4	410.1	723.7	C
AT	2011-12-06	21:31:39	1m	606.8	76.9	390.6	679.8	C

October 25, 2021. Long Term Firing Event

MN/AT	date	time	int	1ch	2ch	3ch	4ch	unit
AT	2011-12-06	21:32:39	1m	621.3	86.2	357.7	637.6	C
AT	2011-12-06	21:33:39	1m	639.4	88.3	356.2	613.5	C
AT	2011-12-06	21:34:39	1m	629.7	109.7	364.5	591.2	C
AT	2011-12-06	21:35:39	1m	620.9	88.4	363.6	645.2	C
AT	2011-12-06	21:36:39	1m	608.3	109.3	360.0	649.3	C
AT	2011-12-06	21:37:39	1m	611.0	86.2	377.1	636.7	C
AT	2011-12-06	21:38:39	1m	621.5	95.4	369.8	633.2	C
AT	2011-12-06	21:39:39	1m	629.3	99.3	370.1	621.8	C
AT	2011-12-06	21:40:39	1m	671.2	103.7	384.9	595.2	C
AT	2011-12-06	21:41:39	1m	676.6	87.8	395.8	606.2	C
AT	2011-12-06	21:42:39	1m	581.6	112.6	371.8	627.1	C
AT	2011-12-06	21:43:39	1m	568.9	109.4	343.3	625.3	C
AT	2011-12-06	21:44:39	1m	663.2	108.6	374.9	626.3	C
AT	2011-12-06	21:45:39	1m	625.6	93.2	409.6	617.9	C
AT	2011-12-06	21:46:39	1m	665.8	115.1	460.0	608.0	C
AT	2011-12-06	21:47:39	1m	725.8	95.4	652.8	582.8	C
AT	2011-12-06	21:48:39	1m	748.5	133.0	688.2	566.3	C
AT	2011-12-06	21:49:39	1m	764.4	102.0	705.4	552.6	C
AT	2011-12-06	21:50:39	1m	772.6	104.5	688.4	586.8	C
AT	2011-12-06	21:51:39	1m	776.1	101.8	664.0	637.2	C
AT	2011-12-06	21:52:39	1m	776.9	97.3	657.7	656.1	C
AT	2011-12-06	21:53:39	1m	769.3	105.7	652.7	655.4	C
AT	2011-12-06	21:54:39	1m	760.7	107.1	636.7	658.7	C
AT	2011-12-06	21:55:39	1m	755.2	103.0	626.2	670.6	C
AT	2011-12-06	21:56:39	1m	734.2	120.3	632.2	688.1	C
AT	2011-12-06	21:57:39	1m	791.2	123.0	634.2	686.4	C
AT	2011-12-06	21:58:39	1m	818.7	124.5	619.4	696.4	C
AT	2011-12-06	21:59:39	1m	790.9	128.2	603.2	711.0	C
AT	2011-12-06	22:00:39	1m	760.4	118.6	595.0	724.7	C
AT	2011-12-06	22:01:39	1m	765.9	144.5	609.4	748.0	C
AT	2011-12-06	22:02:39	1m	750.8	88.9	621.3	766.2	C
AT	2011-12-06	22:03:39	1m	727.9	100.2	627.6	770.3	C
AT	2011-12-06	22:04:39	1m	743.6	101.0	630.7	774.6	C
AT	2011-12-06	22:05:39	1m	694.0	146.7	627.7	776.6	C
AT	2011-12-06	22:06:39	1m	705.2	145.1	630.4	777.1	C
AT	2011-12-06	22:07:39	1m	714.3	143.1	618.7	769.0	C
AT	2011-12-06	22:08:39	1m	753.9	142.8	616.5	778.7	C
AT	2011-12-06	22:09:39	1m	755.9	117.9	616.2	778.1	C
AT	2011-12-06	22:10:39	1m	706.2	130.3	620.6	789.3	C
AT	2011-12-06	22:11:39	1m	697.6	109.6	622.4	798.7	C
AT	2011-12-06	22:12:39	1m	697.1	103.0	624.4	810.3	C
AT	2011-12-06	22:13:39	1m	731.8	143.0	622.8	805.0	C
AT	2011-12-06	22:14:39	1m	690.5	191.2	629.6	804.9	C
AT	2011-12-06	22:15:39	1m	744.4	198.9	632.3	804.3	C
AT	2011-12-06	22:16:39	1m	748.1	153.8	651.3	707.8	C
AT	2011-12-06	22:17:39	1m	715.8	144.3	662.2	697.7	C
AT	2011-12-06	22:18:39	1m	700.1	175.0	685.6	705.2	C
AT	2011-12-06	22:19:39	1m	700.6	161.8	695.8	716.0	C
AT	2011-12-06	22:20:39	1m	708.1	142.6	706.8	710.1	C
AT	2011-12-06	22:21:39	1m	704.9	160.0	710.8	650.9	C
AT	2011-12-06	22:22:39	1m	697.0	163.2	711.9	631.2	C
AT	2011-12-06	22:23:39	1m	685.3	140.4	724.5	610.9	C
AT	2011-12-06	22:24:39	1m	680.4	149.7	742.5	609.4	C
AT	2011-12-06	22:25:39	1m	699.2	111.9	755.3	619.6	C
AT	2011-12-06	22:26:39	1m	699.3	121.3	771.0	622.4	C
AT	2011-12-06	22:27:39	1m	651.9	145.6	784.3	626.9	C

October 25, 2021. Long Term Firing Event

MN/AT	date	time	int	1ch	2ch	3ch	4ch	unit
AT	2011-12-06	22:55:39	1m	597.4	187.2	655.3	585.4	C
AT	2011-12-06	22:56:39	1m	594.3	103.6	643.7	577.3	C
AT	2011-12-06	22:57:39	1m	598.9	141.3	635.4	565.7	C
AT	2011-12-06	22:58:39	1m	612.7	252.8	627.9	560.1	C
AT	2011-12-06	22:59:39	1m	615.4	200.4	622.9	558.8	C
AT	2011-12-06	23:00:39	1m	613.9	141.4	603.7	557.7	C
AT	2011-12-06	23:01:39	1m	596.5	542.3	599.3	560.5	C
AT	2011-12-06	23:02:39	1m	595.0	445.4	597.3	561.4	C
AT	2011-12-06	23:03:39	1m	614.7	327.3	595.8	571.9	C
AT	2011-12-06	23:04:39	1m	615.3	265.7	598.8	594.7	C
AT	2011-12-06	23:05:39	1m	605.6	272.7	601.1	612.9	C
AT	2011-12-06	23:06:39	1m	604.7	371.4	603.7	621.9	C
AT	2011-12-06	23:07:39	1m	598.5	261.3	605.0	630.7	C
AT	2011-12-06	23:08:39	1m	640.4	260.5	608.2	625.1	C
AT	2011-12-06	23:09:39	1m	659.6	195.1	612.3	618.4	C
AT	2011-12-06	23:10:39	1m	687.4	202.6	622.2	611.4	C
AT	2011-12-06	23:11:39	1m	709.8	224.8	631.9	607.3	C
AT	2011-12-06	23:12:39	1m	711.9	349.2	644.6	597.7	C
AT	2011-12-06	23:13:39	1m	690.3	382.6	658.4	594.2	C
AT	2011-12-06	23:14:39	1m	687.5	598.1	661.0	604.3	C
AT	2011-12-06	23:15:39	1m	687.3	647.4	667.9	614.9	C
AT	2011-12-06	23:16:39	1m	710.3	479.9	674.2	622.7	C
AT	2011-12-06	23:17:39	1m	706.8	525.1	679.2	632.2	C
AT	2011-12-06	23:18:39	1m	716.0	349.8	680.2	641.2	C
AT	2011-12-06	23:19:39	1m	733.9	388.4	682.4	640.3	C
AT	2011-12-06	23:20:39	1m	739.5	415.2	685.1	639.2	C
AT	2011-12-06	23:21:39	1m	740.6	353.3	687.1	639.9	C
AT	2011-12-06	23:22:39	1m	779.0	353.2	689.9	644.2	C
AT	2011-12-06	23:23:39	1m	773.1	681.7	689.6	660.8	C

October 25, 2021. Long Term Firing Event

MN/AT	date	time	int	1ch	2ch	3ch	4ch	unit
AT	2011-12-06	23:51:39	1m	715.9	178.3	660.7	718.5	C
AT	2011-12-06	23:52:39	1m	717.4	172.9	653.1	708.1	C
AT	2011-12-06	23:24:39	1m	783.7	708.2	683.7	679.7	C
AT	2011-12-06	23:25:39	1m	767.9	596.6	680.8	701.9	C
AT	2011-12-06	23:26:39	1m	620.8	407.3	680.3	696.9	C
AT	2011-12-06	23:27:39	1m	678.0	603.7	679.3	697.1	C
AT	2011-12-06	23:28:39	1m	699.8	437.9	678.9	697.4	C
AT	2011-12-06	23:29:39	1m	715.1	264.3	681.8	693.4	C
AT	2011-12-06	23:30:39	1m	722.4	332.0	687.4	694.4	C
AT	2011-12-06	23:31:39	1m	722.2	623.2	688.8	697.2	C
AT	2011-12-06	23:32:39	1m	721.7	361.6	689.3	699.5	C
AT	2011-12-06	23:33:39	1m	720.6	501.1	687.8	703.7	C
AT	2011-12-06	23:34:39	1m	714.1	375.3	679.9	714.7	C
AT	2011-12-06	23:35:39	1m	709.2	593.9	675.5	710.6	C
AT	2011-12-06	23:36:39	1m	705.3	536.8	669.6	721.4	C
AT	2011-12-06	23:37:39	1m	701.9	536.3	664.1	717.4	C
AT	2011-12-06	23:38:39	1m	697.1	582.0	658.9	718.1	C
AT	2011-12-06	23:39:39	1m	695.4	257.2	667.1	713.7	C
AT	2011-12-06	23:40:39	1m	693.7	643.9	674.2	723.4	C
AT	2011-12-06	23:41:39	1m	692.5	463.1	668.1	723.6	C
AT	2011-12-06	23:42:39	1m	693.1	666.6	669.6	721.8	C
AT	2011-12-06	23:43:39	1m	692.2	794.4	665.4	720.3	C
AT	2011-12-06	23:44:39	1m	693.8	832.6	670.2	719.5	C
AT	2011-12-06	23:45:39	1m	703.5	697.4	674.8	721.9	C
AT	2011-12-06	23:46:39	1m	707.2	620.1	677.2	732.2	C
AT	2011-12-06	23:47:39	1m	709.6	593.2	680.0	749.7	C
AT	2011-12-06	23:48:39	1m	712.4	577.4	683.4	754.7	C
AT	2011-12-06	23:49:39	1m	713.6	294.8	678.8	739.3	C
AT	2011-12-06	23:50:39	1m	716.5	191.1	669.3	727.2	C
AT	2011-12-07	00:00:39	1m	760.3	179.9	645.9	727.7	C
AT	2011-12-07	00:01:39	1m	763.9	184.6	647.7	735.5	C
AT	2011-12-07	00:02:39	1m	757.8	189.8	650.4	739.2	C
AT	2011-12-07	00:03:39	1m	745.4	196.9	653.2	746.6	C
AT	2011-12-07	00:04:39	1m	736.3	203.3	656.6	751.4	C
AT	2011-12-07	00:05:39	1m	730.8	211.4	659.9	747.3	C
AT	2011-12-07	00:06:39	1m	699.6	201.2	660.5	743.8	C
AT	2011-12-07	00:07:39	1m	674.8	210.2	656.6	729.1	C
AT	2011-12-07	00:08:39	1m	657.1	228.1	652.8	722.2	C
AT	2011-12-07	00:09:39	1m	643.6	238.4	650.5	718.3	C
AT	2011-12-07	00:10:39	1m	631.8	241.9	649.1	710.1	C
AT	2011-12-07	00:11:39	1m	622.5	243.7	648.7	707.7	C
AT	2011-12-07	00:12:39	1m	615.0	248.5	649.2	704.7	C
AT	2011-12-07	00:13:39	1m	607.5	255.0	649.2	699.9	C
AT	2011-12-07	00:14:39	1m	601.9	261.8	648.2	700.1	C
AT	2011-12-07	00:15:39	1m	596.4	348.9	647.9	703.7	C
AT	2011-12-07	00:16:39	1m	592.8	445.6	648.6	700.1	C
AT	2011-12-07	00:17:39	1m	586.3	94.1	647.8	696.7	C
AT	2011-12-07	00:18:39	1m	581.4	112.3	643.4	692.8	C
AT	2011-12-07	00:19:39	1m	576.3	108.3	637.1	689.9	C

October 25, 2021. Long Term Firing Event

MN/AT	date	time	int	1ch	2ch	3ch	4ch	unit
AT	2011-12-07	00:20:39	1m	572.4	120.3	632.9	689.5	C
AT	2011-12-07	00:21:39	1m	568.6	101.3	629.0	690.1	C
AT	2011-12-07	00:22:39	1m	565.7	102.2	626.1	687.9	C
AT	2011-12-07	00:23:39	1m	562.7	72.1	625.4	686.3	C
AT	2011-12-07	00:24:39	1m	559.3	70.9	620.6	685.3	C
AT	2011-12-07	00:25:39	1m	556.4	70.2	615.6	683.3	C
AT	2011-12-07	00:26:39	1m	552.2	259.9	609.3	682.2	C
AT	2011-12-07	00:27:39	1m	548.1	91.3	600.3	681.1	C
AT	2011-12-07	00:28:39	1m	545.5	78.9	590.8	682.9	C
AT	2011-12-07	00:29:39	1m	542.5	114.2	585.3	684.3	C
AT	2011-12-07	00:30:39	1m	541.0	83.1	581.5	685.6	C
AT	2011-12-07	00:31:39	1m	539.1	97.5	577.8	686.3	C
AT	2011-12-07	00:32:39	1m	536.9	104.7	574.9	689.0	C
AT	2011-12-07	00:33:39	1m	535.1	113.0	572.6	694.6	C
AT	2011-12-07	00:34:39	1m	532.3	93.3	571.7	697.7	C
AT	2011-12-07	00:35:39	1m	530.2	102.2	570.3	699.5	C
AT	2011-12-07	00:36:39	1m	529.0	104.2	569.1	702.7	C
AT	2011-12-07	00:37:39	1m	527.8	99.0	568.3	705.5	C
AT	2011-12-07	00:38:39	1m	527.0	126.9	567.9	704.1	C
AT	2011-12-07	00:39:39	1m	526.6	106.9	569.3	711.2	C
AT	2011-12-07	00:40:39	1m	526.3	116.5	569.1	705.2	C
AT	2011-12-07	00:41:39	1m	526.3	118.9	567.8	696.5	C
AT	2011-12-07	00:42:39	1m	525.9	107.6	566.9	691.4	C
AT	2011-12-07	00:43:39	1m	525.5	97.9	567.6	686.6	C
AT	2011-12-07	00:44:39	1m	524.4	116.9	565.7	681.6	C
AT	2011-12-07	00:45:39	1m	524.0	134.7	564.8	682.1	C
AT	2011-12-07	00:46:39	1m	524.3	99.9	564.2	682.6	C
AT	2011-12-07	00:47:39	1m	524.3	96.8	564.0	685.7	C
AT	2011-12-07	00:48:39	1m	524.1	111.9	564.7	690.1	C
AT	2011-12-07	00:49:39	1m	523.6	124.3	565.1	691.8	C
AT	2011-12-07	00:50:39	1m	523.4	144.1	564.7	694.6	C
AT	2011-12-07	00:51:39	1m	523.8	116.2	564.0	701.1	C
AT	2011-12-07	00:52:39	1m	524.5	105.5	563.4	707.9	C
AT	2011-12-07	00:53:39	1m	525.2	102.0	561.1	712.1	C
AT	2011-12-07	00:54:39	1m	525.3	101.7	561.3	713.2	C
AT	2011-12-07	00:55:39	1m	524.9	134.8	559.6	716.8	C
AT	2011-12-07	00:56:39	1m	523.2	103.6	556.0	712.8	C
AT	2011-12-07	00:57:39	1m	522.6	124.5	553.5	698.6	C
AT	2011-12-07	00:58:39	1m	523.0	123.9	550.1	695.3	C
AT	2011-12-07	00:59:39	1m	523.8	144.7	547.6	693.7	C
AT	2011-12-07	01:00:39	1m	523.5	130.1	544.2	681.7	C
AT	2011-12-07	01:01:39	1m	522.2	136.2	540.9	670.8	C
AT	2011-12-07	01:02:39	1m	519.9	139.2	537.3	662.6	C
AT	2011-12-07	01:03:39	1m	516.9	142.5	534.0	657.6	C
AT	2011-12-07	01:04:39	1m	513.7	155.9	531.3	654.6	C
AT	2011-12-07	01:05:39	1m	511.1	147.3	529.2	653.1	C
AT	2011-12-07	01:06:39	1m	508.1	126.5	526.5	653.3	C
AT	2011-12-07	01:07:39	1m	506.0	140.1	525.2	654.7	C
AT	2011-12-07	01:08:39	1m	504.1	117.7	524.1	655.9	C
AT	2011-12-07	01:09:39	1m	501.9	115.3	522.8	660.3	C
AT	2011-12-07	01:10:39	1m	499.7	120.5	520.9	662.6	C
AT	2011-12-07	01:11:39	1m	498.1	121.9	519.6	662.7	C
AT	2011-12-07	01:12:39	1m	496.1	121.8	518.3	663.3	C
AT	2011-12-07	01:13:39	1m	494.5	171.3	517.0	663.3	C
AT	2011-12-07	01:14:39	1m	492.8	137.1	515.7	666.2	C
AT	2011-12-07	01:15:39	1m	491.1	114.7	512.9	668.2	C

October 25, 2021. Long Term Firing Event

MN/AT	date	time	int	1ch	2ch	3ch	4ch	unit	
AT	2011-12-07	01:16:39	1m	489.8	124.1	512.3	665.6	C	AT 2011-12-07 01:43:39 1m 463.4 105.8 513.8 602.7 C
AT	2011-12-07	01:17:39	1m	488.6	130.2	511.7	668.1	C	AT 2011-12-07 01:44:39 1m 462.2 103.8 514.1 600.7 C
AT	2011-12-07	01:18:39	1m	487.6	153.1	511.2	668.6	C	AT 2011-12-07 01:45:39 1m 460.9 98.0 514.6 598.9 C
AT	2011-12-07	01:19:39	1m	486.2	139.4	510.6	665.0	C	AT 2011-12-07 01:46:39 1m 459.9 120.9 515.1 597.4 C
AT	2011-12-07	01:20:39	1m	484.8	141.7	509.9	659.6	C	AT 2011-12-07 01:47:39 1m 458.7 106.4 515.3 596.4 C
AT	2011-12-07	01:21:39	1m	483.9	137.0	509.5	656.4	C	AT 2011-12-07 01:48:39 1m 457.6 102.9 515.4 595.4 C
AT	2011-12-07	01:22:39	1m	483.4	141.7	509.3	653.8	C	AT 2011-12-07 01:49:39 1m 456.6 110.8 515.8 594.2 C
AT	2011-12-07	01:23:39	1m	483.0	131.7	509.4	652.6	C	AT 2011-12-07 01:50:39 1m 455.8 110.6 516.6 592.8 C
AT	2011-12-07	01:24:39	1m	482.5	203.3	509.7	650.6	C	AT 2011-12-07 01:51:39 1m 455.1 144.2 516.5 592.9 C
AT	2011-12-07	01:25:39	1m	482.1	258.4	509.9	641.1	C	AT 2011-12-07 01:52:39 1m 454.4 123.4 516.6 593.2 C
AT	2011-12-07	01:26:39	1m	482.0	140.3	509.8	633.5	C	AT 2011-12-07 01:53:39 1m 453.1 114.7 516.7 591.4 C
AT	2011-12-07	01:27:39	1m	482.3	116.4	510.0	629.1	C	AT 2011-12-07 01:54:39 1m 452.3 98.6 516.7 587.9 C
AT	2011-12-07	01:28:39	1m	482.7	131.4	510.2	625.8	C	AT 2011-12-07 01:55:39 1m 450.8 132.3 515.8 584.1 C
AT	2011-12-07	01:29:39	1m	483.2	124.4	510.6	623.2	C	AT 2011-12-07 01:56:39 1m 449.3 150.4 513.6 579.7 C
AT	2011-12-07	01:30:39	1m	483.4	117.3	511.2	621.3	C	AT 2011-12-07 01:57:39 1m 448.2 105.5 512.2 576.4 C
AT	2011-12-07	01:31:39	1m	482.4	151.1	511.7	620.8	C	AT 2011-12-07 01:58:39 1m 446.5 136.3 510.4 573.2 C
AT	2011-12-07	01:32:39	1m	480.7	112.2	511.9	620.5	C	AT 2011-12-07 01:59:39 1m 444.2 110.4 508.2 569.7 C
AT	2011-12-07	01:33:39	1m	479.6	110.1	511.9	620.8	C	AT 2011-12-07 02:00:39 1m 442.9 94.9 506.2 566.8 C
AT	2011-12-07	01:34:39	1m	478.3	111.6	512.2	619.1	C	AT 2011-12-07 02:01:39 1m 441.6 98.7 505.3 564.2 C
AT	2011-12-07	01:35:39	1m	476.8	124.7	512.3	616.3	C	AT 2011-12-07 02:02:39 1m 440.2 105.7 504.6 561.7 C
AT	2011-12-07	01:36:39	1m	474.5	113.1	512.2	612.9	C	AT 2011-12-07 02:03:39 1m 438.4 97.1 503.2 560.2 C
AT	2011-12-07	01:37:39	1m	473.1	100.3	512.1	611.4	C	AT 2011-12-07 02:04:39 1m 436.8 94.2 501.4 559.0 C
AT	2011-12-07	01:38:39	1m	471.1	106.8	511.9	610.1	C	AT 2011-12-07 02:05:39 1m 433.9 94.2 499.7 556.3 C
AT	2011-12-07	01:39:39	1m	469.3	103.9	512.3	609.3	C	AT 2011-12-07 02:06:39 1m 430.3 94.8 496.8 553.3 C
AT	2011-12-07	01:40:39	1m	467.6	104.3	512.8	608.4	C	AT 2011-12-07 02:07:39 1m 427.4 106.7 494.2 551.1 C
AT	2011-12-07	01:41:39	1m	466.2	99.8	513.3	606.5	C	AT 2011-12-07 02:08:39 1m 424.7 104.2 492.1 549.1 C
AT	2011-12-07	01:42:39	1m	464.7	102.5	513.6	604.7	C	AT 2011-12-07 02:09:39 1m 422.4 91.6 490.3 547.3 C
									AT 2011-12-07 02:10:39 1m 421.0 110.5 489.6 545.4 C
									AT 2011-12-07 02:11:39 1m 419.3 93.2 487.8 543.1 C

October 25, 2021. Long Term Firing Event

MN/AT	date	time	int	1ch	2ch	3ch	4ch	unit
AT	2011-12-07	02:12:39	1m	418.3	82.2	487.0	541.8	C
AT	2011-12-07	02:13:39	1m	417.6	102.4	485.6	540.1	C
AT	2011-12-07	02:14:39	1m	417.0	103.5	485.3	546.1	C
AT	2011-12-07	02:15:39	1m	416.4	92.9	484.8	548.9	C
AT	2011-12-07	02:16:39	1m	415.9	83.7	483.8	550.3	C
AT	2011-12-07	02:17:39	1m	415.1	87.9	481.4	551.4	C
AT	2011-12-07	02:18:39	1m	414.7	104.3	479.9	551.9	C
AT	2011-12-07	02:19:39	1m	414.4	99.1	476.6	551.0	C
AT	2011-12-07	02:20:39	1m	414.0	80.6	474.3	549.3	C
AT	2011-12-07	02:21:39	1m	413.7	90.4	471.1	547.0	C
AT	2011-12-07	02:22:39	1m	413.2	86.2	468.3	545.2	C
AT	2011-12-07	02:23:39	1m	412.8	109.3	465.6	543.1	C
AT	2011-12-07	02:24:39	1m	412.3	75.7	463.3	541.8	C
AT	2011-12-07	02:25:39	1m	411.7	78.8	460.1	540.6	C
AT	2011-12-07	02:26:39	1m	411.2	71.3	457.9	539.7	C
AT	2011-12-07	02:27:39	1m	410.4	66.0	454.7	539.2	C
AT	2011-12-07	02:28:39	1m	409.4	96.1	452.6	539.5	C
AT	2011-12-07	02:29:39	1m	408.1	78.7	449.1	539.5	C
AT	2011-12-07	02:30:39	1m	405.8	97.0	445.3	537.9	C
AT	2011-12-07	02:31:39	1m	404.1	84.6	441.9	535.2	C
AT	2011-12-07	02:32:39	1m	403.4	81.9	439.4	533.5	C
AT	2011-12-07	02:33:39	1m	401.7	74.0	436.7	530.3	C
AT	2011-12-07	02:34:39	1m	400.3	80.6	433.3	527.7	C
AT	2011-12-07	02:35:39	1m	398.4	83.7	430.4	525.7	C
AT	2011-12-07	02:36:39	1m	397.1	63.5	427.3	521.7	C
AT	2011-12-07	02:37:39	1m	395.9	92.1	425.1	521.4	C
AT	2011-12-07	02:38:39	1m	394.7	72.1	422.1	522.3	C
AT	2011-12-07	02:39:39	1m	394.9	70.3	421.4	524.5	C
AT	2011-12-07	02:40:39	1m	395.8	63.1	420.3	526.5	C
AT	2011-12-07	02:41:39	1m	396.7	63.1	420.1	528.1	C
AT	2011-12-07	02:42:39	1m	397.0	58.7	418.4	528.7	C
AT	2011-12-07	02:43:39	1m	397.1	58.8	417.7	527.8	C
AT	2011-12-07	02:44:39	1m	397.0	58.4	416.3	526.2	C
AT	2011-12-07	02:45:39	1m	396.4	58.3	414.6	523.4	C
AT	2011-12-07	02:46:39	1m	395.7	51.4	412.6	519.7	C
AT	2011-12-07	02:47:39	1m	394.6	52.7	410.7	516.1	C
AT	2011-12-07	02:48:39	1m	393.5	57.8	408.7	512.1	C
AT	2011-12-07	02:49:39	1m	392.4	67.7	406.0	508.8	C
AT	2011-12-07	02:50:39	1m	390.9	45.5	403.8	504.7	C
AT	2011-12-07	02:51:39	1m	389.5	55.1	401.5	501.7	C
AT	2011-12-07	02:52:39	1m	388.0	50.2	399.3	498.2	C
AT	2011-12-07	02:53:39	1m	386.5	45.3	397.6	495.4	C
AT	2011-12-07	02:54:39	1m	384.9	40.8	395.3	492.2	C
AT	2011-12-07	02:55:39	1m	383.4	40.3	393.1	489.8	C
AT	2011-12-07	02:56:39	1m	381.8	49.4	391.0	487.2	C
AT	2011-12-07	02:57:39	1m	380.3	49.8	388.9	484.8	C
AT	2011-12-07	02:58:39	1m	378.6	51.8	385.8	481.4	C
AT	2011-12-07	02:59:39	1m	376.1	50.8	383.3	479.0	C
AT	2011-12-07	03:00:39	1m	374.8	50.1	380.9	476.7	C
AT	2011-12-07	03:01:39	1m	373.5	56.7	378.9	474.2	C
AT	2011-12-07	03:02:39	1m	372.5	45.8	377.2	472.4	C
AT	2011-12-07	03:03:39	1m	370.4	61.1	374.8	470.2	C
AT	2011-12-07	03:04:39	1m	368.1	47.4	371.7	467.5	C
AT	2011-12-07	03:05:39	1m	366.3	52.4	369.3	464.6	C
AT	2011-12-07	03:06:39	1m	364.9	42.8	367.1	462.8	C
AT	2011-12-07	03:07:39	1m	362.8	47.8	364.8	461.0	C

October 25, 2021. Long Term Firing Event

MN/AT	date	time	int	1ch	2ch	3ch	4ch	unit
AT	2011-12-07	03:08:39	1m	361.4	54.8	362.2	459.2	C
AT	2011-12-07	03:09:39	1m	359.8	44.7	359.7	457.7	C
AT	2011-12-07	03:10:39	1m	358.7	42.6	358.6	456.7	C
AT	2011-12-07	03:11:39	1m	357.9	54.0	356.7	456.0	C
AT	2011-12-07	03:12:39	1m	357.4	53.6	355.2	454.3	C
AT	2011-12-07	03:13:39	1m	356.5	44.4	353.7	453.1	C

AT 2011-12-07 03:14:39 1m 355.8 36.9 352.9 452.6 C

AT 2011-12-07 03:15:39 1m 355.2 51.2 351.1 451.3 C

AT 2011-12-07 03:16:39 1m 162.7 31.0 204.7 199.6 C

AT 2011-12-07 03:17:39 1m 77.8 30.6 88.7 102.9 C

Appendix B: Magnetic Susceptibility Data

Baseline Magnetic Susceptibility

Location	Measurement Number	Mag sus (Translated)	Location	Measurement Number	Mag sus (Translated)	Location	Measurement Number	Mag sus (Translated)
A	1	0.0036	BD	151	0.00639	A	301	0.00579
B	2	0.005	BE	152	0.00436	B	302	0.00581
C	3	0.00513	BF	153	0.00523	C	303	0.00431
D	4	0.00544	BG	154	0.00478	D	304	0.00561
E	5	0.00735	BH	155	0.00534	E	305	0.00792
J	6	0.00637	BC	156	0.00465	F	306	0.006
I	7	0.00676	BB	157	0.00529	G	307	0.00562
H	8	0.00679	BA	158	0.00422	H	308	0.00374
G	9	0.00632	AZ	159	0.00649	I	309	0.00422
F	10	0.0069	AY	160	0.00436	J	310	0.00462
K	11	0.00628	AT	161	0.00417	K	311	0.00443
L	12	0.00667	AU	162	0.00702	L	312	0.00618
M	13	0.00625	AV	163	0.00467	M	313	0.00678
N	14	0.00593	AW	164	0.00571	N	314	0.00539
O	15	0.00789	AX	165	0.00636	O	315	0.00537
T	16	0.00736	AS	166	0.00755	P	316	0.00601
S	17	0.00644	AR	167	0.0057	Q	317	0.00569
R	18	0.00496	AQ	168	0.00526	R	318	0.00456
Q	19	0.0059	AP	169	0.00318	S	319	0.0069
P	20	0.00504	AO	170	0.00303	T	320	0.0056
U	21	0.00641	AJ	171	0.00436	U	321	0.00302
V	22	0.00596	AK	172	0.00538	V	322	0.0022
W	23	0.00632	AL	173	0.00633	W	323	0.00359
X	24	0.00506	AM	174	0.00489	X	324	0.00446
Y	25	0.00629	AN	175	0.00487	Y	325	0.00501
Z	26	0.00654	AI	176	0.00305	Z	326	0.00422
AA	27	0.00698	AH	177	0.00536	AA	327	0.00494
AB	28	0.00633	AG	178	0.00456	AB	328	0.00511
AC	29	0.00621	AF	179	0.00434	AC	329	0.00502
AD	30	0.00613	AE	180	0.00274	AD	330	0.00577
AD	31	0.00612	A	181	0.00415	BD	331	0.00594
AC	32	0.00581	B	182	0.00603	BE	332	0.00544
AB	33	0.00538	C	183	0.00598	BC	333	0.0064
AA	34	0.00571	D	184	0.00699	4N 0E, NWQ	334	0.00445
Z	35	0.00595	E	185	0.0067	4N 0E, NEQ	335	0.00615
U	36	0.00527	J	186	0.00575	4N 0E, SEQ	336	0.0064

Location	Measurement Number	Mag sus (Translated)	Location	Measurement Number	Mag sus (Translated)	Location	Measurement Number	Mag sus (Translated)
V	37	0.00543	I	187	0.00504	4N 0E, SWQ	337	0.00687
W	38	0.00512	H	188	0.00391	3N 0E, NWQ	338	0.00648
X	39	0.00567	G	189	0.00466	3N 0E, NEQ	339	0.00671
Y	40	0.00532	F	190	0.0044	3N 0E, SEQ	340	0.00636
T	41	0.00643	K	191	0.00673	3N 0E, SWQ	341	0.00596
S	42	0.00597	L	192	0.00721	2N 0E, NWQ	342	0.0063
R	43	0.00614	M	193	0.00691	2N 0E, NEQ	343	0.00641
Q	44	0.00463	N	194	0.00642	2N 0E, SEQ	344	0.00655
P	45	0.00674	O	195	0.0071	2N 0E, SWQ	345	0.00627
K	46	0.00567	T	196	0.00591	1N 0E, NWQ	346	0.00666
L	47	0.00705	S	197	0.00589	1N 0E, NEQ	347	0.00747
M	48	0.00651	R	198	0.00737	1N 0E, SEQ	348	0.00781
N	49	0.00741	Q	199	0.00646	1N 0E, SWQ	349	0.00728
O	50	0.0073	P	200	0.00625	0N 0E, NWQ	350	0.00505
J	51	0.00674	U	201	0.00567	0N 0E, NEQ	351	0.00571
I	52	0.00756	V	202	0.00564	0N 0E, SEQ	352	0.00595
H	53	0.00614	W	203	0.00606	0N 0E, SWQ	353	0.00588
G	54	0.00571	X	204	0.00695	0N 0E, Center	354	0.00632
F	55	0.00655	Y	205	0.00687	1N 3E, NWQ	355	0.00581
E	56	0.00608	Z	206	0.00573	1N 3E, NEQ	356	0.00345
D	57	0.00632	AA	207	0.00671	1N 3E, SEQ	357	0.00597
C	58	0.00596	AB	208	0.0056	1N 3E, SWQ	358	0.00536
B	59	0.00609	AC	209	0.00508	1N 3E, Center	359	0.00596
A	60	0.00594	AD	210	0.00651	2N 2E, NWQ	360	0.00583
AE	61	0.0059	BD	211	0.00619	2N 2E, NEQ	361	0.00628
AF	62	0.00589	BE	212	0.00678	2N 2E, SEQ	362	0.00949
AG	63	0.00582	BF	213	0.00715	2N 2E, SWQ	363	0.00558
AH	64	0.00546	BG	214	0.00697	0N 2E, NWQ	364	0.00737
AI	65	0.00952	BH	215	0.0058	0N 2E, NEQ	365	0.00864
AN	66	0.00767	BC	216	0.00641	0N 2E, SEQ	366	0.00529
AM	67	0.0077	BB	217	0.00675	0N 2E, SWQ	367	0.00696
AL	68	0.00689	BA	218	0.00743	0N 2E, Center	368	0.00767
AK	69	0.00573	AZ	219	0.008			
AJ	70	0.00583	AV	220	0.00699			
AO	71	0.00597	AT	221	0.00806			
AP	72	0.00571	AU	222	0.00696			
AQ	73	0.00601	AV	223	0.00715			
AR	74	0.00494	AW	224	0.005			
AS	75	0.00628	AX	225	0.0041			
AX	76	0.00458	AS	226	0.00465			

Location	Measurement Number	Mag sus (Translated)	Location	Measurement Number	Mag sus (Translated)			
AW	77	0.00558	AR	227	0.00502			
AV	78	0.0057	AQ	228	0.00508			
AU	79	0.00595	AP	229	0.00485			
AT	80	0.00527	AO	230	0.00463			
AY	81	0.00664	AJ	231	0.00577			
AZ	82	0.00535	AK	232	0.00333			
BA	83	0.00643	AL	233	0.00402			
BB	84	0.00479	AM	234	0.00312			
BC	85	0.00532	AN	235	0.00369			
BH	86	0.00675	AI	236	0.00652			
BG	87	0.00625	AH	237	0.00432			
BF	88	0.00485	AG	238	0.00531			
BE	89	0.00618	AF	239	0.00428			
BD	90	0.00576	AE	240	0.00381			
Z	91	0.00603	AE	241	0.00352			
AA	92	0.00618	AF	242	0.00362			
AB	93	0.00613	AG	243	0.00436			
AC	94	0.00645	AH	244	0.00468			
AD	95	0.00698	AI	245	0.00437			
Y	96	0.00791	AN	246	0.00557			
X	97	0.0062	AM	247	0.00612			
W	98	0.00763	AL	248	0.00593			
V	99	0.00602	AK	249	0.00647			
U	100	0.00516	AJ	250	0.0047			
P	101	0.00607	AO	251	0.00634			
Q	102	0.00512	AP	252	0.00621			
R	103	0.00653	AQ	253	0.00521			
S	104	0.00685	AR	254	0.00663			
T	105	0.00537	AS	255	0.00561			
O	106	0.00612	AX	256	0.00533			
N	107	0.0046	AW	257	0.00554			
M	108	0.00625	AV	258	0.00593			
L	109	0.00641	AU	259	0.00695			
K	110	0.00644	AT	260	0.00544			
F	111	0.00459	AY	261	0.0058			
G	112	0.00603	AZ	262	0.00684			
H	113	0.00602	BA	263	0.00558			
I	114	0.00606	BB	264	0.00541			
J	115	0.00522	BC	265	0.00463			
E	116	0.00625	BH	266	0.00578			

Location	Measurement Number	Mag sus (Translated)	Location	Measurement Number	Mag sus (Translated)			
D	117	0.00539	BG	267	0.00643			
C	118	0.00545	BF	268	0.0059			
B	119	0.00603	BE	269	0.00554			
A	120	0.00613	BD	270	0.00721			
A	121	0.00678	Z	271	0.00541			
B	122	0.00692	AA	272	0.00613			
C	123	0.00628	AB	273	0.00479			
D	124	0.0058	AC	274	0.00665			
E	125	0.00558	AD	275	0.00684			
J	126	0.00311	Y	276	0.00722			
I	127	0.00475	X	277	0.00747			
H	128	0.00378	W	278	0.007			
G	129	0.00237	V	279	0.00711			
F	130	0.00603	U	280	0.00751			
K	131	0.00647	P	281	0.00769			
L	132	0.00415	Q	282	0.00633			
M	133	0.00523	R	283	0.00609			
N	134	0.0028	S	284	0.00665			
O	135	0.00398	T	285	0.00476			
T	136	0.00606	O	286	0.0057			
S	137	0.00531	N	287	0.00737			
R	138	0.0043	M	288	0.00701			
Q	139	0.00713	L	289	0.00653			
P	140	0.00572	K	290	0.00603			
U	141	0.00299	F	291	0.00632			
V	142	0.00555	G	292	0.00463			
W	143	0.00409	H	293	0.00531			
X	144	0.0042	I	294	0.00596			
Y	145	0.00391	J	295	0.00571			
AD	146	0.006	E	296	0.00673			
AC	147	0.00537	D	297	0.00669			
AB	148	0.00579	C	298	0.00525			
AA	149	0.00563	B	299	0.00517			
Z	150	0.00433	A	300	0.00627			

Fired Magnetic Susceptibility

Northing	Easting	Location of measurement	Pre-burn measurement	Pre-burn measurement	Post Burn 1 Measurement 1	Post Burn 1 Measurement 1	
4	0	NWQ	4.45*10 ⁻³	0.00445	4.87*10 ⁻³	0.00487	
4	0	NEQ	6.15*10 ⁻³	0.00615	3.81*10 ⁻³	0.00381	
4	0	SEQ	6.40*10 ⁻³	0.0064	6.86*10 ⁻³	0.00686	
4	0	SWQ	6.87*10 ⁻³	0.00687	5.11*10 ⁻³	0.00511	
4	0	Center					
3	0	NWQ	6.48*10 ⁻³	0.00648	6.28*10 ⁻³	0.00628	
3	0	NEQ	6.71*10 ⁻³	0.00671	6.41*10 ⁻³	0.00641	
3	0	SEQ	6.36*10 ⁻³	0.00636	6.55*10 ⁻³	0.00655	
3	0	SWQ	5.96*10 ⁻³	0.00596	6.27*10 ⁻³	0.00627	
		Center					
2	0	NWQ	6.30*10 ⁻³	0.0063	7.09*10 ⁻³	0.00709	
2	0	NEQ	6.41*10 ⁻³	0.00641	6.27*10 ⁻³	0.00627	
2	0	SEQ	6.55*10 ⁻³	0.00655	5.08*10 ⁻³	0.00508	
2	0	SWQ	6.27*10 ⁻³	0.00627	6.75*10 ⁻³	0.00675	
		Center					
1	0	NWQ	6.66*10 ⁻³	0.00666	6.75*10 ⁻³	0.00675	
1	0	NEQ	7.47*10 ⁻³	0.00747	6.38*10 ⁻³	0.00638	
1	0	SEQ	7.81*10 ⁻³	0.00781	4.95*10 ⁻³	0.00495	
1	0	SWQ	7.28*10 ⁻³	0.00728	7.03*10 ⁻³	0.00703	
		Center			7.05*10 ⁻³	0.00705	
0	0	NWQ	5.05*10 ⁻³	0.00505	7.18*10 ⁻³	0.00718	
0	0	NEQ	5.71*10 ⁻³	0.00571	7.43*10 ⁻³	0.00743	
0	0	SEQ	5.95*10 ⁻³	0.00595	4.99*10 ⁻³	0.00499	
0	0	SWQ	5.88*10 ⁻³	0.00588	7.03*10 ⁻³	0.00703	
0	0	Center	6.32*10 ⁻³	0.00632	6.72*10 ⁻³	0.00672	
1	3	NWQ	5.81*10 ⁻³	0.00581	7.01*10 ⁻³	0.00701	
1	3	NEQ	3.45*10 ⁻³	0.00345	6.90*10 ⁻³	0.0069	
1	3	SEQ	5.97*10 ⁻³	0.00597	9.57*10 ⁻³	0.00957	
1	3	SWQ	5.36*10 ⁻³	0.00536	7.66*10 ⁻³	0.00766	
1	3	Center	5.96*10 ⁻³	0.00596	6.21*10 ⁻³	0.00621	
2	2	NWQ	5.83*10 ⁻³	0.00583	6.45*10 ⁻³	0.00645	
2	2	NEQ	6.28*10 ⁻³	0.00628	7.05*10 ⁻³	0.00705	
2	2	SEQ	9.49*10 ⁻³	0.00949	7.54*10 ⁻³	0.00754	
2	2	SWQ	5.58*10 ⁻³	0.00558	7.76*10 ⁻³	0.00776	
2	2	Center			6.90*10 ⁻³	0.0069	
0	2	NWQ	7.37*10 ⁻³	0.00737			
0	2	NEQ	8.64*10 ⁻³	0.00864			
0	2	SEQ	5.29*10 ⁻³	0.00529			

Northing	Easting	Location of measurement	Pre-burn measurement	Pre-burn measurement	Post Burn 1 Measurement 1	Post Burn 1 Measurement 1	
0	2	SWQ	6.96*10 ⁻³	0.00696			
0	2	Center	7.67*10 ⁻³	0.00767			
Northing	Easting	Location of measurement	Post Burn 2	Post Burn 2	Post Burn 3	Post Burn 3	
4	0	NWQ	5.14*10 ⁻³	0.00514	4.93*10 ⁻³	0.00493	
4	0	NEQ	4.66*10 ⁻³	0.00466	6.13*10 ⁻³	0.00613	
4	0	SEQ	5.10*10 ⁻³	0.0051	6.56*10 ⁻³	0.00656	
4	0	SWQ	5.50*10 ⁻³	0.0055	5.49*10 ⁻³	0.00549	
4	0	Center					
3	0	NWQ	6.89*10 ⁻³	0.00689			
3	0	NEQ	8.83*10 ⁻³	0.00883			
3	0	SEQ	7.29*10 ⁻³	0.00729			
3	0	SWQ	10.2*10 ⁻³	0.0102			
		Center					
2	0	NWQ	5.84*10 ⁻³	0.00584	6.89*10 ⁻³	0.00689	
2	0	NEQ	4.22*10 ⁻³	0.00422	5.23*10 ⁻³	0.00523	
2	0	SEQ	4.86*10 ⁻³	0.00486	2.42*10 ⁻³	0.00242	
2	0	SWQ	5.65*10 ⁻³	0.00565	7.33*10 ⁻³	0.00733	
		Center			7.84*10 ⁻³	0.00784	
1	0	NWQ					
1	0	NEQ					
1	0	SEQ					
1	0	SWQ					
		Center					
0	0	NWQ					
0	0	NEQ					
0	0	SEQ					
0	0	SWQ					
0	0	Center					
1	3	NWQ			4.19*10 ⁻³	0.00419	
1	3	NEQ			4.98*10 ⁻³	0.00498	
1	3	SEQ			6.06*10 ⁻³	0.00606	
1	3	SWQ			4.47*10 ⁻³	0.00447	
1	3	Center			4.45*10 ⁻³	0.00445	
2	2	NWQ	6.76*10 ⁻³	0.00676	7.77*10 ⁻³	0.00777	
2	2	NEQ	6.30*10 ⁻³	0.0063	9.29*10 ⁻³	0.00929	
2	2	SEQ	6.17*10 ⁻³	0.00617	9.74*10 ⁻³	0.00974	
2	2	SWQ	6.17*10 ⁻³	0.00617	8.76*10 ⁻³	0.00876	
2	2	Center	8.08*10 ⁻³	0.00808	7.05*10 ⁻³	0.00705	
0	2	NWQ					

Northing	Easting	Location of measurement	Post Burn 2	Post Burn 2	Post Burn 3	Post Burn 3	Northing
0	2	NEQ					
0	2	SEQ					
0	2	SWQ					
0	2	Center					
Northing	Easting	Location of measurement	post burn 4	post burn 4	Post burn 4	Post burn4	
4	0	NWQ	5.12*10 ⁻³	0.00512	4.75*10 ⁻³	0.00475	
4	0	NEQ	4.15*10 ⁻³	0.00415	5.55*10 ⁻³	0.00555	
4	0	SEQ	4.93*10 ⁻³	0.00493	6.27*10 ⁻³	0.00627	
4	0	SWQ	5.01*10 ⁻³	0.00501	6.14*10 ⁻³	0.00614	
4	0	Center	4.93*10 ⁻³	0.00493	6.88*10 ⁻³	0.00688	
3	0	NWQ	6.11*10 ⁻³	0.00611	6.75*10 ⁻³	0.00675	
3	0	NEQ	5.52*10 ⁻³	0.00552	7.64*10 ⁻³	0.00764	
3	0	SEQ	5.91*10 ⁻³	0.00591	8.09*10 ⁻³	0.00809	
3	0	SWQ	5.73*10 ⁻³	0.00573	6.97*10 ⁻³	0.00697	
		Center	5.73*10 ⁻³	0.00573	7.90*10 ⁻³	0.0079	
Northing	Easting	Location of measurement	August 6th measurements	August 6th measurements	October 15 measurements	October 15 measurements (Post burn 5)	November 9 measurements
4	0	NWQ	4.17*10 ⁻³	0.00417	7.12*10 ⁻³	0.00712	0.0103
4	0	NEQ	5.26*10 ⁻³	0.00526	7.02*10 ⁻³	0.00702	0.00733
4	0	SEQ	5.15*10 ⁻³	0.00515	6.37*10 ⁻³	0.00637	0.00853
4	0	SWQ	6.03*10 ⁻³	0.00603	7.89*10 ⁻³	0.00789	0.00839
4	0	Center	7.26*10 ⁻³	0.00726	6.79*10 ⁻³	0.00679	0.00728
3	0	NWQ	6.61*10 ⁻³	0.00661	6.58*10 ⁻³	0.00658	0.00706
3	0	NEQ	7.63*10 ⁻³	0.00763	7.44*10 ⁻³	0.00744	0.00679
3	0	SEQ	8.40*10 ⁻³	0.0084	9.80*10 ⁻³	0.0098	0.00726
3	0	SWQ	7.08*10 ⁻³	0.00708	7.73*10 ⁻³	0.00773	0.00776
		Center	6.21*10 ⁻³	0.00621	7.23*10 ⁻³	0.00723	0.00684
2	0	NWQ	7.10*10 ⁻³	0.0071	7.52*10 ⁻³	0.00752	0.00718
2	0	NEQ	6.47*10 ⁻³	0.00647	8.04*10 ⁻³	0.00804	0.00743
2	0	SEQ	6.04*10 ⁻³	0.00604	6.58*10 ⁻³	0.00658	0.00599
2	0	SWQ	6.35*10 ⁻³	0.00635	6.22*10 ⁻³	0.00622	0.00699
		Center	8.57*10 ⁻³	0.00857	8.69*10 ⁻³	0.00869	0.00805
1	0	NWQ	5.14*10 ⁻³	0.00514	6.23*10 ⁻³	0.00623	0.00685
1	0	NEQ	5.60*10 ⁻³	0.0056	6.23*10 ⁻³	0.00623	0.00622
1	0	SEQ	7.28*10 ⁻³	0.00728	7.39*10 ⁻³	0.00739	0.00738
1	0	SWQ	7.94*10 ⁻³	0.00794	7.09*10 ⁻³	0.00709	0.0074
		Center	8.31*10 ⁻³	0.00831	7.19*10 ⁻³	0.00719	0.00729
0	0	NWQ	7.38*10 ⁻³	0.00738	6.73*10 ⁻³	0.00673	0.00625
0	0	NEQ	7.07*10 ⁻³	0.00707	8.36*10 ⁻³	0.00836	0.00821
0	0	SEQ	5.86*10 ⁻³	0.00586	6.43*10 ⁻³	0.00643	0.00741

Northing	Easting	Location of measurement	August 6th measurements	August 6th measurements	October 15 measurements	October 15 measurements (Post burn 5)	November 9 measurements
0	0	SWQ	7.03*10 ⁻³	0.00703	7.16*10 ⁻³	0.00716	0.00677
0	0	Center	8.35*10 ⁻³	0.00835	7.41*10 ⁻³	0.00741	0.00746
1	3	NWQ	6.23*10 ⁻³	0.00623	6.60*10 ⁻³	0.0066	0.00863
1	3	NEQ	6.62*10 ⁻³	0.00662	7.01*10 ⁻³	0.00701	0.0082
1	3	SEQ	5.82*10 ⁻³	0.00582	6.16*10 ⁻³	0.00616	0.00636
1	3	SWQ	6.86*10 ⁻³	0.00686	6.99*10 ⁻³	0.00699	0.00822
1	3	Center	6.00*10 ⁻³	0.006	6.51*10 ⁻³	0.00651	0.00677
2	2	NWQ	6.27*10 ⁻³	0.00627	7.23*10 ⁻³	0.00723	0.0069
2	2	NEQ	10.1*10 ⁻³	0.0101	7.99*10 ⁻³	0.00799	0.00912
2	2	SEQ	8.88*10 ⁻³	0.00888	7.15*10 ⁻³	0.0071	0.00702
2	2	SWQ	10.2*10 ⁻³	0.0102	6.98*10 ⁻³	0.00698	0.0079
2	2	Center	9.48*10 ⁻³	0.00948	7.59*10 ⁻³	0.00759	0.0074
0	2	NWQ			6.81*10 ⁻³	0.00681	0.0069
0	2	NEQ			6.21*10 ⁻³	0.00621	0.00655
0	2	SEQ			7.83*10 ⁻³	0.00783	0.00776
0	2	SWQ			6.99*10 ⁻³	0.00699	0.00709
0	2	Center			6.51*10 ⁻³	0.00651	0.00637